031651 5061 / COOK
Chicago / USX Southworks
Superfund / Tech. Reports

EPA Region 5 Records Ctr.
367063

McLaren Hart
ENVIRONMENTAL ENGINEERING CORPORATION

HUMAN HEALTH
RISK ASSESSMENT
FOR
THE SOUTH WORKS SITE
CHICAGO, ILLINOIS

August 25, 1995

Prepared for:

U.S. Steel Group
USX Corporation
600 Grant Street
Pittsburgh, Pennsylvania 15219-2749

Prepared by:

ChemRisk® Division
McLaren/Hart Environmental Engineering Corporation
8500 Brooktree Road
Pittsburgh, Pennsylvania 15090

This report is confidential and may not be copied, shared or publicly disclosed without the permission of USX Realty Department.

1.0 INTRODUCTION

In December of 1993, U.S. Steel voluntarily entered the former U.S. Steel South Works steel making site in the Illinois Pre-Notice Site Cleanup Program. The program provides the guidance, assistance, and the oversight to the Illinois Environmental Protection Agency (IEPA) to owners/operators of industrial/commercial property in Illinois, performing environmental site assessments and/or remediation for the purpose of selling or redeveloping the property. To facilitate property redevelopment as part of the Pre-Notice Site Cleanup Program, this Health Risk Assessment (HRA) was prepared by ChemRisk, a Division of McLaren/Hart Environmental Engineering, on behalf of USX Corporation for the former U.S. Steel South Works steel making site located in Chicago, Illinois. This HRA follows the technical and conceptual risk assessment approach identified in the Preliminary Human Health and Ecological Risk Assessment (PRA) that was prepared by ChemRisk and approved by the Illinois Environmental Protection Agency (IEPA) on March 29, 1995 (ChemRisk, 1995). In the PRA, the potential for terrestrial and aquatic ecological effects at South Works was determined to be insignificant based on analytical and background data for the site. Therefore, this HRA is focused on the potential human health risks associated with future land use conditions at South Works. The objective of this HRA is to provide site-specific remediation goals (RGs), which are concentrations of chemicals in soil that are protective of human health. The RGs developed in the HRA will provide the basis for identifying the nature and extent of remedial activities required at the South Works site, if any, to protect public health. The RGs presented in the HRA will also be used to evaluate analytical data from confirmatory sampling in areas that are currently undergoing demolition, remediation (sewers), and sediment removal. The HRA is consistent with the following USEPA and IEPA risk assessment guidance documents, as well as on going discussions between IEPA and USX:

- U.S. Environmental Protection Agency. (1989). *Risk Assessment Guidelines for Superfund, Volume I. Human Health Evaluation Manual (Part A).* Interim Final. Office of Emergency and Remedial Response, Washington, D.C. EPA/540/1-89/002.

- U.S. Environmental Protection Agency. (1991). *Risk Assessment Guidance for Superfund; Volume I, Part B, Development of Risk-Based Preliminary Remediation Goals.* Interim. Office of Emergency and Remedial Response, Washington, D.C.

- U.S. Environmental Protection Agency. (1995). *Risk-Based Concentration Table, January-June, 1995.* Memorandum from Roy L. Smith, Senior Toxicologist, Region III.

- U.S. Environmental Protection Agency. (1988). *Guidance for Establishing Target Cleanup Levels at Hazardous Waste Sites.* Washington, D.C.

- U.S. Environmental Protection Agency. (1989). *Exposure Factors Handbook.* Office of Health and Environmental Assessment. Washington, D.C. EPA/600/8-89/043

- Illinois Environmental Protection Agency. (1992). *Guidance for Developing a Site-Specific Soil Cleanup Level Proposal for RCRA Clean Closures.* Springfield, IL.

- Illinois Environmental Protection Agency. (1994). *Interim Default Values for the Estimation of the Dermal Absorption of Chemicals from Soil.* Memorandum from T. Hornshaw.

The above referenced documents are available from the IEPA or the USEPA.

1.1 HEALTH RISK ASSESSMENT ORGANIZATION

The HRA is organized in the following chapters:

2.0 ***Hazard Identification*** - In this section, a general overview is provided for the site, including operational history, key site characteristics, and a summary of analytical data. In addition, the chemicals and media of interest for the HRA are identified.

3.0 ***Dose-Response Assessment*** - In this section, the method for identifying reference doses and slope factors for the chemicals of interest is

presented. Additionally, the approach for evaluating the carcinogenic polynuclear aromatic hydrocarbons (PAHs) in soil is discussed.

4.0 *Exposure Assessment* - This section identifies the potentially exposed populations, exposure pathways, and the exposure parameters used for calculating the RGs, as well as the algorithms for calculating the RGs. In addition, a description of the methodology used for determining an RG for lead is also provided in this section.

5.0 *Risk Characterization* - This section presents the calculated RGs for each future land use scenario and compares them to on-site soil concentrations of the chemicals of interest. A discussion of the meaning of health risk estimates and risk levels that have been deemed acceptable at other sites is provided, in addition to a qualitative uncertainty analysis.

6.0 *Conclusions* - This section summarizes the findings of the assessment and discusses what remedial actions, if any, are required for each scenario to protect human health.

7.0 *References* - This section presents the literature cited throughout the HRA.

TABLE OF CONTENTS

EXECUTIVE SUMMARY

1.0 INTRODUCTION 1-1

1.1 HEALTH RISK ASSESSMENT ORGANIZATION 1-2

2.0 HAZARD IDENTIFICATION 2-1

2.1 SITE LOCATION 2-1
2.2 HISTORY 2-1
2.3 SITE CONDITIONS 2-2
2.4 CHEMICALS OF INTEREST 2-4

2.4.1 Soil 2-4

2.4.1.1 Organic Constituents 2-4
2.4.1.2 Inorganic Constituents 2-6
2.4.1.3 Data Summary for the COIs in Soil 2-10

2.4.2 Sediments 2-11
2.4.3 Groundwater 2-13

2.5 CHEMICAL-SPECIFIC HALF-LIVES 2-14

3.0 DOSE RESPONSE ASSESSMENT 3-1

3.1 NONCARCINOGENIC DOSE RESPONSE ASSESSMENT 3-2
3.2 CARCINOGENIC DOSE RESPONSE ASSESSMENT 3-5

4.0 EXPOSURE ASSESSMENT 4-1

4.1 EXPOSURE PATHWAYS 4-2
4.2 IDENTIFICATION OF APPROPRIATE EXPOSURE SCENARIOS 4-3
4.3 EXPOSURE PARAMETERS 4-6

4.3.1 General Exposure Parameters 4-7
4.3.2 Soil Ingestion Pathway 4-11
4.3.3 Inhalation of Particulates Pathway 4-15
4.3.4 Dermal Contact Pathway 4-17

4.4 CALCULATION OF REMEDIATION GOALS (RGS) 4-20
4.5 NONCANCER ASSESSMENT FOR LEAD 4-26

4.5.1 USEPA IEUBK Model for Lead 4-31
4.5.2 PBPK Model 4-33
4.5.3 Bowers *et al.* Model for Lead 4-35

5.0 RISK CHARACTERIZATION 5-1

5.1 REMEDIATION GOALS 5-1
5.2 UNCERTAINTY ANALYSIS 5-4

5.2.1 Uncertainties Associated with Site Sampling 5-5
5.2.2 Uncertainties Associated with the Dose-Response Assessment 5-6
5.2.3 Uncertainties Associated with the Exposure Parameters 5-9
5.2.4 Uncertainties Associated with Risk Characterization 5-10

5.3 CANCER RISK CRITERIA AND REGULATORY POLICY 5-10

6.0 CONCLUSIONS 6-1

7.0 REFERENCE 7-1

EXECUTIVE SUMMARY

In December of 1993, U.S. Steel voluntarily entered the former U.S. Steel South Works steel making site into the Illinois Pre-Notice Site Cleanup Program. The program provides the guidance, assistance and the oversight of the Illinois Environmental Protection Agency (IEPA) to owners/operators of industrial/commercial property in Illinois, performing environmental site assessments and/or remediation, for the purpose of selling or redeveloping the property. To facilitate property redevelopment as part of the Pre-Notice Site Cleanup Program, this Health Risk Assessment (HRA) was prepared by ChemRisk, a Division of McLaren/Hart Environmental Engineering, on behalf of USX Corporation for the former U.S. Steel South Works steel making site located in Chicago, Illinois. This HRA was based upon the Preliminary Human Health and Ecological Risk Assessment (PRA; March, 1995) approved by the IEPA on March 29, 1995. In the PRA, the potential for terrestrial and aquatic ecological effects at South Works was determined to be insignificant. Therefore, this HRA addresses only the potential human health effects associated with future land use conditions at South Works. The objective of this HRA was to provide site-specific remediation goals (RGs) that are protective of human health for chemicals of interest (COIs) in soil or slag fill at the site. The concentrations of the COIs measured in site soil were then compared to the calculated RGs to determine if and where remediation may be necessary to protect future site users based on the current analytical data generated thus far for the site. Analytical data from confirmatory sampling in areas currently undergoing demolition, remediation (sewers) and/or sediment removal will be compared to the RGs calculated in this HRA. Additional areas of remediation may be identified in the future and are not shown in this report.

The COIs in soil at the South Works site were determined from three environmental assessments that were performed by Waste Technology Incorporated (WTI) and are antimony, beryllium, cadmium, lead, manganese, benzo(a)pyrene, benzo(a)anthracene, benzo(b)fluoranthene, dibenz(a,h)anthracene, and indeno(1,2,3-cd)pyrene. These COIs were selected based on a comparison of the maximum measured concentration of each chemical in soil with the USEPA Region III Risk-Based Concentrations (RBCs) for residential sites (USEPA, 1995a). The inorganics were further compared by statistical analysis to naturally occurring background concentrations of each in Illinois soil or soil of the conterminous U.S. (Dragun and Chiasson), 1991). Those chemicals measured at levels higher than the RBCs and naturally occurring background levels in soil were considered COIs for this HRA. It is important to recognize that the inorganic COIs are bound tightly to the slag fill material at the site because of their physical properties and the nature of the slag fill. For this reason, bioavailability (*i.e.* bioaccessibility) of the inorganics is most likely very low.

Two levels of exposure were addressed in this HRA: a maximally exposed individual (MEI) and a most likely exposed individual (MLEI). The MEI represents the "worst-case" or highest exposure for a given population, while the MLEI describes the average or median exposure in a given population. For these two levels of exposure, this HRA evaluated the following exposure scenarios:

- Residential
- Recreational
- Industrial/Commercial
- Construction

For each exposure scenario, the following pathways and media were investigated:

RESIDENTIAL SCENARIO	RECREATIONAL SCENARIO	INDUSTRIAL/COMMERCIAL SCENARIO	CONSTRUCTION SCENARIO
EXPOSURE PATHWAY	EXPOSURE PATHWAY	EXPOSURE PATHWAY	EXPOSURE PATHWAY
Incidental Ingestion (surface soil) Dermal Contact (surface soil)	Incidental Ingestion (surface soil) Dermal Contact (surface soil)	Incidental Ingestion (surface soil) Dermal Contact (surface soil)	Incidental Ingestion (surface/subsurface soil) Dermal Contact (surface/subsurface soil) Inhalation of Suspended Particulates (surface/subsurface soil)

RGs calculated for the residential, recreational and industrial/commercial scenarios are applicable to surface soil (0 - 2 feet). RGs calculated for the construction scenario are applicable to surface and subsurface soils (>2 feet).

Individual RGs were calculated for each COI for each exposure scenario based upon an acceptable hazard index of one and/or a target theoretical cancer risk range of 1×10^{-5} to 1×10^{-6}. For carcinogenic COIs, RGs were developed based only on potential carcinogenic effects and not for noncarcinogenic effects. This approach is conservative as the USEPA toxicity criteria protective of carcinogenic effects are generally much lower than those protective of noncarcinogenic effects. For all scenarios, RGs for lead were calculated using a physiologically-based pharmacokinetic (PBPK) model for blood lead developed by Dr. O'Flaherty of the University of Cincinnati. At the request of the IEPA, the USEPA modified Bowers *et al.* (1994) model for long term adult exposure scenarios and the USEPA Integrated Exposure Uptake Biokinetic (IEUBK) model for children were presented for comparison and to show that all available blood-lead modeling approaches were considered. However, the PBPK model was deemed the most appropriate for determining RGs as it is the only model that is: 1) capable of

evaluating both adults and children, 2) physiologically based, 3) validated for a variety of short and long term exposures, and 4) published in the peer-reviewed scientific literature.

Results

The RGs calculated for the COIs at the South Works site are presented in Tables ES-1 through ES-4 along with the maximum concentrations of each COI in surface soil and in the entire soil column. The concentrations of the COIs in soil at each sampling location were compared to the RGs for each scenario, and exceedences are summarized below.

RGs Protective of	Number of Sampling Locations Where Concentrations in Soil Exceed Calculated RGs							
	Residential		Recreational		Industrial/Commercial		Construction	
	MEI	MLEI	MEI	MLEI	MEI	MLEI	MEI	MLEI
10^{-6} Cancer Risk Level	23[a]	2[a]	8[a]	None	None	None	1[b]	None
10^{-5} Cancer Risk Level	None	None	None	None	None	None	None	None
Noncancer Effects	3[c]	None	None	None	None	None	1[d]	None

a Only the RG for beryllium at a 10^{-6} increased cancer risk level was exceeded at all but one sampling location (total number of sampling locations = 24).

b One sample exceeded the RG for cadmium at a 10^{-6} increased cancer risk level.

c The RG for lead calculated using the O'Flaherty model, which is protective of children in a residential setting, was exceeded at three sample locations.

d The RG for lead, which is protective of a female construction worker of child-bearing age, was exceeded at one sampling location.

Based on a comparison of RGs to the analytical data at individual soil sampling locations from the environmental assessments, the following conclusions can be drawn:

- The RGs calculated for the industrial/commercial land use scenario at both the 10^{-5} and 10^{-6} risk levels and/or a hazard index of one were all higher than the measured levels of COIs in site soil. Therefore, remediation of soils for future industrial/commercial land use is not deemed necessary.

- The RG calculated for cadmium at the 10^{-6} risk level for the MEI construction scenario (53 mg/kg) was exceeded at one sampling location (SB-39-2, 89.1 mg/kg). All other construction scenario RGs were higher than their measured levels in site soils. This single exceedence of the cadmium RG is driven by the inhalation of particles during future construction activities. Because the total mass of soil particulates in the air would be from a large part of the site during construction activities, rather than a single location, remediation of this single sampling location is not deemed necessary.

- As shown in the above table, at a 10^{-6} risk level, 23 of 24 surface soil samples had concentrations of beryllium above the residential MEI RG of 1.1 mg/kg, and 2 had concentrations of beryllium above the residential MLEI RG of 6.2 mg/kg. The 10^{-6} RG calculated for beryllium for the MEI recreational scenario of 3.7 mg/kg was exceeded by concentrations of beryllium at 8 sampling locations.

- The RG for beryllium for the residential MEI and MLEI and recreational MEI scenarios at the 10^{-6} risk level are within the range of naturally occurring background concentrations. Therefore, these RGs are not meaningful because remediation below naturally occurring background concentrations is neither feasible nor reasonable. Further, because no animal or human study in the scientific literature has ever demonstrated an increased incidence of cancer following oral exposure to beryllium, the evaluation of beryllium as an oral carcinogen is highly questionable.

- Concentrations of the COIs, including beryllium, did not exceed the RGs for any scenario at the 10^{-5} risk level.

- The residential MEI RG for lead of 932 mg/kg (child scenario), calculated using O'Flaherty PBPK model, was exceeded by the concentrations of lead at three sampling locations. This RG is consistent with the USEPA recommended range of cleanup levels for lead at Superfund sites of 500 to 1,000 mg/kg. Because future residential children could be exposed to these areas, these lead levels should be addressed prior to residential development.

- The MEI short- and long-term construction worker RGs were exceeded by the maximum concentration of lead (3,200 mg/kg) measured at one sampling location (SS-9-01). This area also exceeds the MEI residential RG and should be addressed prior to site redevelopment.

- The total additive theoretical cancer risk associated with multiple chemical exposures does not exceed the USEPA acceptable risk range of 10^{-4} to 10^{-6} for Superfund sites (USEPA, 1990). Additionally, the acceptable hazard index associated with multiple chemical exposures does not exceed one except in the three locations where lead exceeds 932 mg/kg. With the exception of beryllium, the total cancer risk marginally exceeds the 10^{-6} risk level at one location (SB-37-

1) where benzo(a)pyrene and dibenz(a,h)anthracene both occur at their maximum concentrations. At this location, the total cancer risk does not exceed the 10^{-5} risk level.

Based on the blood-lead modeling analysis, it may be necessary to remediate lead in three areas identified in this HRA, should these areas be developed for residential use in the future. One area, with the maximum concentration of lead in soil, should be addressed prior to site redevelopment to protect future construction workers. As stated previously, analytical data from confirmatory sampling in areas currently undergoing demolition, remediation (sewers) and/or sediment removal will be compared to the RGs calculated in this HRA.

At a 10^{-5} risk level, it should not be necessary to remediate soils at the South Works site for beryllium (or any other COI) in the areas evaluated in this HRA. At all but one sampling location, the 10^{-6} RG for beryllium for the residential MEI scenario (*i.e.*, the "maximally exposed individual") was exceeded. This is due to a combination of the highly conservative nature of the residential MEI scenario evaluated in this HRA and the highly conservative USEPA oral cancer slope factor for beryllium. For example, for the MEI scenario, this assessment used the USEPA default soil ingestion rates of 200 mg/day for a child and 50 mg/day for an adult. If more realistic soil ingestion rates presented in recent scientific literature of 25 mg/day and 10 mg/day were used for children and adults, respectively, an RG for the MEI residential scenario would be 10 mg/kg at a 10^{-6} risk level. The concentrations of beryllium in site soil (maximum concentration = 9.8 mg/kg) do not exceed this RG. These soil ingestion rates have been used to describe the MEI scenario in another IEPA-approved HRA (ChemRisk, 1989).

Finally, it is noteworthy that only the RGs protective of a 1 x 10^{-6} increased risk level for beryllium are exceeded by site concentrations. These beryllium RGs for a 10^{-6} risk level should not be used to guide remedial efforts because: 1) they are within the range of naturally occurring background levels of beryllium in soil, 2) beryllium has never been shown to cause cancer in animals or humans following oral exposure, 3) the bioavailability of metals in slag material on the site is very low, and 4) the RGs were calculated using very conservative assumptions regarding the level, frequency and duration of exposure. For these reasons, the RGs for

beryllium protective of a 1 x 10^{-5} increased cancer risk level, which were not exceeded by concentrations of beryllium in site soil, should be protective of human health.

TABLE ES-1
REMEDIATION GOALS BASED ON A 1 x 10^{-5} CANCER RISK AND HAZARD INDEX OF ONE FOR THE RESIDENTIAL, RECREATIONAL, AND INDUSTRIAL/COMMERCIAL SCENARIOS
(mg/kg)

Chemical	Maximum Surface Soil Concentration (mg/kg)	Residential Scenario				Recreational Scenario				Industrial/Commercial Scenario	
		MEI		MLEI		MEI		MLEI			
		Adult	Child	Adult	Child	Adult	Child	Adult	Child	MEI	MLEI
Antimony	7.6	601	46	1,960	158	2,020	153	12,100	745	841	5,020
Beryllium	9.3	11[a]		62[a]		37[a]		210[a]		83.3[b]	2,760[b]
Cadmium	89.1	1,500	114	4,890	394	5,060	383	30,200	1,860	2,100	12,500
Lead	3,200	NC[c]	932	NC[c]	932	NC[c]	3,790	NC[c]	3,790	6,150	72,800
Manganese	29,900	$> 10^6$	75,000	$> 10^6$	355,000	$> 10^6$	253,000	$> 10^6$	$> 10^6$	$> 10^6$	$> 10^6$
Benzo(a)anthracene	1.3	185[a]		1,050[a]		624[a]		3,530[a]		1,180[b]	39,000[b]
Benzo(a)pyrene	1.7	23.8[a]		135[a]		80[a]		453[a]		151[b]	5,000[b]
Benzo(b)fluoranthene	1.6	207[a]		1,170[a]		695[a]		3,930[a]		1,310[b]	43,400[b]
Dibenz(a,h)anthracene	0.57	134[a]		75.9[a]		45.1[a]		255[a]		85.2[b]	2,820[b]
Indeno(1,2,3-cd)pyrene	1.3	173[a]		977[a]		581[a]		3,290[a]		1,100[b]	36,300[b]

a Value is for adult and child exposure combined based on carcinogenic effects.
b Based on carcinogenic effects for adults only.
c RG for child exposure is also protective for adult exposures.
NC Not Calculated

L:\USS\SWORKS\RA\TABLES\TBLES-1

TABLE ES - 2
REMEDIATION GOALS BASED ON A 1 x 10^{-5} CANCER RISK
AND A HAZARD INDEX OF ONE
FOR THE CONSTRUCTION SCENARIO
(mg/kg)

Chemical	Maximum Soil Concentration[b] (mg/kg)	Construction Scenario		Short-Term Construction Scenario	
		MEI	MLEI	MEI	MLEI
Antimony	64.7	241	558	NC	NC
Beryllium	9.8	224[a]	1,900[a]	NC	NC
Cadmium	89.1	534	1,390	NC	NC
Lead	3,200	3,750	15,600	2,080	18,650
Manganese	35,900	443,000	$> 10^6$	NC	NC
Benzo(a)anthracene	1.7	805[a]	3,650[a]	NC	NC
Benzo(a)pyrene	1.7	84.6[a]	383[a]	NC	NC
Benzo(b)fluoranthene	1.6	821[a]	3,720[a]	NC	NC
Dibenz(a,h)anthracene	0.57	76.7[a]	347[a]	NC	NC
Indeno(1,2,3-cd)pyrene	1.3	796[a]	3,600[a]	NC	NC

a Based on carcinogenic effects for adults only.
b Soil concentrations for both surface and subsurface soils.
NC Not Calculated

TABLE ES - 3
REMEDIATION GOALS BASED ON A 1 x 10^{-6} CANCER RISK AND HAZARD INDEX OF ONE FOR THE RESIDENTIAL, RECREATIONAL, AND INDUSTRIAL/COMMERCIAL SCENARIOS
(mg/kg)

Chemical	Maximum Surface Soil Concentration (mg/kg)	Residential Scenario				Recreational Scenario				*Industrial/Commercial Scenario*	
		MEI		MLEI		MEI		MLEI			
		Adult	Child	Adult	Child	Adult	Child	Adult	Child	MEI	MLEI
Antimony	7.6	601	46	1,960	158	2,020	153	12,100	745	841	5,020
Beryllium	9.3	1.1[a]		6.2[a]		3.7[a]		21[a]		8.3[b]	276[b]
Cadmium	89.1	1,500	114	4,890	394	5,060	383	30,200	1,860	2,100	12,500
Lead	3,200	NC[c]	932	NC[c]	932	NC[c]	3,790	NC[c]	3,790	6,150	72,800
Manganese	29,900	> 10^6	75,000	> 10^6	355,000	> 10^6	253,000	> 10^6	> 10^6	> 10^6	> 10^6
Benzo(a)anthracene	1.3	18.5[a]		105[a]		62.4[a]		353[a]		118[b]	3900[b]
Benzo(a)pyrene	1.7	2.38[a]		13.5[a]		8.0[a]		45.3[a]		15.1[b]	500[b]
Benzo(b)fluoranthene	1.6	20.7[a]		117[a]		69.5[a]		393[a]		131[b]	4340[b]
Dibenz(a,h)anthracene	0.57	13.4[a]		7.59[a]		4.51[a]		25.5[a]		8.5[b]	282[b]
Indeno(1,2,3-cd)pyrene	1.3	17.3[a]		97.7[a]		58.1[a]		329[a]		110[b]	3630[b]

a Value is for adult and child exposure combined based on carcinogenic effects.
b Based on carcinogenic effects for adults only.
c RG for child exposure is also protective for adult exposures.
NC Not Calculated

L:\USS\SWORKS\RA\TABLES\TBLES-3

TABLE ES - 4
REMEDIATION GOALS BASED ON A 1 x 10^{-6} CANCER RISK
AND A HAZARD INDEX OF ONE
FOR THE CONSTRUCTION SCENARIO
(mg/kg)

Chemical	Maximum Soil Concentration[b] (mg/kg)	Construction Scenario		Short-Term Construction Scenario	
		MEI	MLEI	MEI	MLEI
Antimony	64.7	241	558	NC	NC
Beryllium	9.8	22.4[a]	190[a]	NC	NC
Cadmium	89.1	53.4	1,390	NC	NC
Lead	3,200	3,750	15,600	2,080	18,650
Manganese	35,900	443,000	$> 10^6$	NC	NC
Benzo(a)anthracene	1.7	80.5[a]	365[a]	NC	NC
Benzo(a)pyrene	1.7	8.46[a]	38.3[a]	NC	NC
Benzo(b)fluoranthene	1.6	82.1[a]	372[a]	NC	NC
Dibenz(a,h)anthracene	0.57	7.7[a]	34.7[a]	NC	NC
Indeno(1,2,3-cd)pyrene	1.3	80[a]	360[a]	NC	NC

a Based on carcinogenic effects for adults only.
b Soil concentrations for both surface and subsurface soils.
NC Not Calculated

2.0 HAZARD IDENTIFICATION

This section summarizes the soil and sediment data from the previous environmental assessments conducted at the site (WTI, 1993a,b; 1994), and describes site location, history, and conditions. More detailed discussions of site conditions and history are provided in the site investigation reports (WTI, 1993a,b; 1994). Additionally, this section provides the basis for determining the chemicals of interest (COIs) to be quantitatively evaluated in the HRA.

2.1 SITE LOCATION

The South Works site, covering approximately 567 acres, is located in the southeast side of the City of Chicago and is bordered by Lake Michigan to the north and east, the Calumet River to the south, and by a residential area to the west (Figure 2-1). The North and South Vessel Slips, used for shipping and receiving when the site was active, are located adjacent to the North Ore Yard leading into Lake Michigan and adjacent to the South Ore Yard leading into the Calumet River, respectively.

2.2 HISTORY

The North Chicago Railway Mill Company began construction of a primary steel plant at the site in March of 1880; once completed, it encompassed 73 acres. In March of 1881, the first blast furnace went into production and steel shipments began. Since this time, the site has been owned and operated by the Illinois Steel Company, the Carnegie-Illinois Steel Company, and finally U.S. Steel Corporation in 1901. The byproduct of operations, molten slag, was used as

fill material during the course of plant operations to increase the plant area so that future expansion could occur (WTI, 1993a).

U.S. Steel began operations at the South Work site in 1901 producing steel products such as stainless steel, and special alloy grade steel (WTI, 1994). Coking was not part of the steel making process at the South Works facility. In 1982, decreased annual trade shipments resulted in the progressive shut down of all but two major operations at the site. Approximately two-thirds of the plant facilities were demolished by 1991, and the facility ceased all operations on April 10, 1992. A more complete site operational history is presented in the three investigation reports by WTI (WTI, 1993a,b; 1994).

2.3 SITE CONDITIONS

The stratigraphy of the South Works site is variable, consisting of fill material underlain by very fine and silty sand. The fill consisted of cinders and molten slag, a by-product of the steel making process. As stated previously, the molten slag was deposited along the lake front to increase the plant area for future expansion. Heavy metals are tightly bound constituents of the molten slag matrix and are not readily released from the matrix.

The thickness of the slag/fill material varies from 4-12 feet in the southwestern region of the site, to 25-35 feet at the eastern and northern regions. The fine sand reaches 11-16 feet below Lake Michigan where a region of clay is met and extends 70 feet to a region of limestone (WTI, 1993a, b; 1994).

Soil from the South Works site, sediments from the North and South Vessel Slips, and groundwater beneath the site were sampled in three phases of a site investigation (WTI, 1993a,b; 1994) to characterize the extent of chemical impacts that may have occurred at the site. All of the Phase III Investigation data, that were validated by Contract Laboratory Program (CLP) standards, are used in the HRA. In addition, the Phase I and II data for lead were used because lead was detected above an IEPA screening level of 700 mg/kg in these data (Section 2.4.1.2).

Lead was the only chemical that was found above its screening level in the Phase I and II data but not in the Phase III data (Section 2.4).

A total of 23 surface soil samples and 25 subsurface samples were collected as part of the Phase III investigation (WTI, 1994) from a grid sampling pattern designed to evenly and uniformly characterize the concentrations of chemicals in soil across the site. The Phase I and II investigations targeted areas thought to be impacted by previous site activities. Therefore, these data were biased towards sampling locations that most likely exhibited higher concentrations of the COIs. For this reason, the Phase III data were deemed to be the most appropriate for characterizing potential future exposure at the site.

All surficial soil samples were analyzed for the following chemical constituents:

TCL[a] Total Metals	11-TCLP[b] Metals
Chloride	Total Cyanide
Ammonia (NH_3-N)	Phenols
Sulfate	Total Sulfide
pH	

a Target compound list
b Toxicity characteristic leaching potential

Selected samples were also analyzed for TCL volatile organic compounds (VOCs), TCL semi-volatile organic compounds (SVOCs), and polychlorinated biphenyls (PCBs) (WTI, 1994).

All subsurface soil samples were analyzed for the following compounds:

TCL Total Metals	11-TCLP Metals
Chloride	Total Cyanide
Ammonia (NH_3-N)	Phenols
Sulfate	Total Sulfide
pH	

Selected samples were also analyzed for TCL VOCs, TCL SVOCs, and PCBs (WTI, 1994).

2.4 CHEMICALS OF INTEREST

Chemicals of Interest (COIs) were identified in this HRA, consistent with USEPA risk assessment guidance to focus the assessment on only those chemicals that may pose a significant risk at the site. Only COIs are quantitatively evaluated in this HRA as per the IEPA-approved PRA. The selection criteria used to identify COIs in soil and sediment are described below.

2.4.1 Soil

The preliminary inorganic and organic COIs for soil were initially identified for the site based on a comparison of the maximum measured concentrations of each chemical in soil with the USEPA Region III Risk-Based Concentrations (RBCs) for direct contact exposures at residential sites (USEPA, 1995a). The Region III RBCs are "screening" levels of individual chemical constituents in soil, groundwater, and air that were calculated by USEPA Region III using conservative, standard default exposure assumptions for direct contact exposures. The RBCs are concentrations of chemicals below which adverse effects to human health are not likely to occur. The residential RBCs are designed to protect individuals residing at the site, including children and are considered protective of all land uses for direct contact exposures. This is because residential exposure scenarios are the most conservative (*i.e.*, longest exposure duration and frequency). The RBCs are appropriate screening levels for this site because potential impacts to groundwater will be dealt with separately, as discussed in Section 2.4.3. Those chemicals measured above their RBCs were mutually agreed upon by IEPA and USX to be the COIs for the site (Kubala and Pilja, 1994). Inorganic constituents which exceeded their respective RBCs were further evaluated to determine if constituent levels in on-site soils were statistically greater than regional background concentrations, as discussed further in this section.

2.4.1.1 Organic Constituents

Five polynuclear aromatic hydrocarbon (PAH) compounds were detected in site soils at concentrations in exceedence of the Region III RBCs: benzo(a)anthracene, benzo(a)pyrene,

benzo(b)fluoranthene, dibenz(a,h)anthracene, and indeno(1,2,3-cd)pyrene. Therefore, they were considered the organic COIs for soil in this HRA. All other organic constituents were detected in site soils at levels below their respective RBCs. The analytical limits of detection (LOD) for those organic constituents not detected in site soil were also compared with their respective RBCs, and were found to be below their respective RBCs. Because PAHs are generally found as a chemical mixture of more than one chemical constituent, the analytical LODs for those PAHs not detected in site soil were also compared with the RBCs for each PAH. The LODs for all PAHs, except benzo(a)pyrene and dibenz(a,h)anthracene, were below their respective RBCs. These two chemicals were also measured above the LOD in some site soil samples. The PAHs will be considered to be present in soil at one-half their LODs for the purposes of this evaluation (USEPA, 1989a).

It is important to note that PAHs are found naturally in the environment. The Agency for Toxic Substances and Disease Registry (ATSDR) states that PAHs are ubiquitous in soil because of the incomplete combustion of organic materials (*i.e.*, forest fires, burning of fossil fuels) (ATSDR, 1993). PAHs have even been detected in Arctic soils (Thomas, 1986). PAHs have been measured at concentrations up to 1.3 mg/kg in rural soils, 0.9 mg/kg in agricultural soils, and 166 mg/kg in urban soils from non-specific natural and anthropogenic sources (ATSDR, 1993).

A study by Berggreen *et al.* (1991) reports concentrations of 18 different PAHs from a survey of several sites (number not specified) in the Chicago area. A total of 26 samples were collected and analyzed, and the results indicate that PAHs are widespread in Chicago fill soils. Specifically, benzo(a)pyrene was detected in 3 of 26 samples at a maximum concentration of 5 mg/kg, and chrysene was detected in all but six samples at concentrations up to 55 mg/kg. Total PAH concentrations ranged from nondetect to 512 mg/kg. The authors theorized that historically, garbage, cinders, ashes, and clay were used as fill material throughout Chicago to facilitate land development especially near the Lake Michigan waterfront, and that numerous fires contributed to the elevated PAH levels. Although it is recognized that there are background levels of PAHs in the area from natural and anthropogenic sources not related to the South

Works site, this HRA does not account for any contribution to the site from background concentrations as the background contribution cannot be quantitatively estimated.

2.4.1.2 Inorganic Constituents

Six inorganic constituents were detected in one or more soil samples from the Phase III analytical data at concentrations exceeding Region III RBCs. These are antimony, arsenic, beryllium, cadmium, manganese, and vanadium. Region III does not provide an RBC for inorganic lead; therefore, IEPA and USX mutually agreed to a screening level for lead of 700 mg/kg (Kubala and Pilja, 1994). Although lead was not detected at levels above 700 mg/kg in the Phase III Investigation, soil samples collected in Phase I and Phase II contained lead levels above 700 mg/kg. Therefore, lead was included as a potential COI in this HRA. Lead was the only constituent that exceeded it's RBC in the Phase I and Phase II investigations but not in the Phase III investigation.

These above referenced seven inorganic constituents (including lead) were further screened by comparing the site analytical data to background levels of these inorganic constituents in soils which is consistent with USEPA and IEPA guidance. Sufficient background data (mean and standard deviation) for arsenic, beryllium, lead and vanadium in Illinois soils were available (Dragun and Chiasson, 1991). Because background data specific to Illinois were not available for the other inorganic constituents, background data for antimony and manganese reported for eastern U.S. soils were used, and background data reported for Michigan were used for cadmium (Dragun and Chiasson, 1991).

A Behrens-Fisher *t*-test (discussed below) was used to determine if there is a statistically significant difference between the on-site concentrations of inorganic chemicals and regional background concentrations. If it was determined that an inorganic constituent was present on-site at levels not exceeding background concentrations, that constituent was eliminated as a COI. It is important to note that, because of the conservative assumptions used to derive the RBCs (*i.e.*, 200 mg/day soil ingestion rate, 350 days/year exposure frequency), some RBCs for

inorganic constituents (*i.e.*, arsenic and beryllium) are much lower than natural background concentrations.

Behrens-Fisher *t*-Test

The Behrens-Fisher *t*-test is valid for comparing the means from two populations that are unequal in size and in variance (Guttman *et al.*, 1965). Both populations must also have normal (Gaussian) distributions (Guttman *et al.*, 1965). The null hypothesis for the background comparison is that the mean on-site soil concentration for a constituent is less than or equal to the corresponding mean background soil concentration. A right-sided, one-tailed, two sample test was used to evaluate the alternative hypothesis. The alternative hypothesis for this comparison is that the mean on-site soil concentration for a constituent is greater than the corresponding mean background soil concentration. If the null hypothesis is shown to be false (also referred to as rejecting the null hypothesis), the alternative hypothesis is accepted as being true, and the mean soil concentration of a constituent is considered to be significantly greater than the mean background soil concentration.

Since the B-F *t*-test requires that the datasets being tested have normal distributions, all datasets were tested using Lilliefors modification of the Kolmogorov-Smirnov test (Lilliefors, 1965) to determine whether the on-site and background soil datasets have normal or lognormal distributions. This test indicated that arsenic, beryllium, cadmium, lead, and manganese are lognormally distributed and antimony and vanadium are either normally distributed or do not fit either distribution. The B-F *t*-test was performed using the geometric mean and standard deviations for all of the metals. This is done since, by definition, the natural logarithms of data from a lognormal distribution will have a normal distribution. For those datasets that did fit a lognormal or normal distribution, the B-F *t*-test was performed on the natural logarithms of the data. This was done to ensure that any statistical differences between a dataset with a large variance and a dataset with a small variance was detectable. Otherwise, by assuming a normal distribution for the datasets, two datasets that truly have different means may not be seen as statistically different because of the larger variance of one dataset encompassing the mean and variance of the other dataset.

The B-F t-test compares the calculated statistic (defined as a function of a random variable) to a tabulated value of the standard student's t distribution table. The statistic used by the test is:

$$T = \frac{(\mu_1 - \mu_2)}{[(\frac{S_1^2}{n_1}) + (\frac{S_2^2}{n_2})]^{\frac{1}{2}}}$$

where:

T	=	The computed statistic which is compared to the critical value of the student's t distribution for the specified confidence level. The null hypothesis is rejected for large values of T, specifically when $T > t_{crit}$, (obtained from a standard t distribution table). The value of t_{crit} is determined by the level of confidence ($1-\alpha$) and the degrees of freedom (df)
μ_1	=	The mean of the on-site soil sample data (or natural logarithms) for a specific inorganic constituent
μ_2	=	The mean of the background soil data (or natural logarithms) for a specific inorganic constituent
S_1	=	The sample variance of the on-site soil sample data (or natural logarithms) for a specific inorganic constituent
S_2	=	The sample variance of the background soil sample data (or natural logarithms) for a specific inorganic constituent
n_1	=	The number of on-site soil samples collected for a specific inorganic constituent
n_2	=	The number of on-site background samples collected for a specific inorganic constituent

The degrees of freedom, df, needed to determine t_{crit} was calculated by solving the following two equations:

$$\frac{1}{df} = \frac{c^2}{n_1 - 1} + \frac{(1 - c)^2}{n_2 - 1}$$

where:

$$c = \frac{\left(\frac{S_1^2}{n_1}\right)}{\left[\left(\frac{S_1^2}{n_1}\right) + \left(\frac{S_2^2}{n_2}\right)\right]}$$

To perform the B-F *t*-test, the value for T is calculated for each inorganic constituent and compared to the tabulated t_{crit} value for the given confidence level and degrees of freedom (Guttman *et al.*, 1965; Abramowitz and Stegun, 1972). If the calculated T value is greater than the t_{crit}, the null hypothesis is rejected and the inorganic COI is considered statistically different (greater) than background and retained in the HRA. A confidence level of 95%, was used which is equal to the power of the background soil sampling data set (USEPA, 1989a,b).

For the purposes of this HRA, mean background concentrations for the seven inorganic constituents were taken from Dragun and Chiasson (1991). These means were compared to the mean concentrations derived from all of the surface and subsurface soil samples collected in Phase III, and for all phases for lead. The results of the *t*-test (Table 2-1) indicate that concentrations of antimony, beryllium, cadmium, lead, and manganese exceed naturally-occurring background concentrations. Therefore, these metals were retained as inorganic COIs in this HRA. Concentrations of vanadium and arsenic in site soils were found below regional background concentrations and are not evaluated further in this assessment. In summary, based upon the comparison with the RBCs and the results of the B-F *t*-test, the COIs for soil are the following:

Organic COIs	Inorganic COIs
Benzo(a)anthracene	Antimony
Benzo(a)pyrene	Beryllium
Benzo(b)fluoranthene	Cadmium
Dibenz(a,h)anthracene	Manganese
Indeno(1,2,3-cd)pyrene	Lead

2.4.1.3 Data Summary for the COIs in Soil

Tables 2-2 and 2-3 present statistical summaries of the analytical data for the COIs in the entire soil column and in surface soil respectively, from the South Works site. The arithmetic mean concentration, frequency of detection, and concentration range are presented. The arithmetic mean provides a measure of central tendency for a normally distributed dataset. With the exception of lead, these statistics are based upon the Phase III analytical data. Samples for which the detection limit was greater than the maximum detected concentration were not included. One-half the limit of detection was used for those samples with detection limits less than the maximum concentration per USEPA guidance (USEPA, 1989c). The lead summary statistics are based on data from all three site investigations (WTI, 1993a, b; 1994). The inorganic COIs are present above detection limits in nearly all samples as would be expected because these chemicals occur naturally in most soils and in fill material derived from molten slag. The exception is antimony which was detected in only two Phase III samples above the detection limit.

For surface and subsurface soils combined (Table 2-2), the arithmetic mean concentrations for the PAHs are all below 0.5 mg/kg. The PAHs range in concentration from a low of 0.022 mg/kg for dibenz(a,h)anthracene to a high of 1.7 mg/kg for benzo(a)pyrene and benzo(a)anthracene. Lead and manganese were detected within a wide range of concentrations from 0.05 to 3,200 mg/kg for lead and 30.1 to 35,900 mg/kg for manganese. Beryllium,

antimony, and cadmium were detected at concentrations ranging from 0.14 to 9.8 mg/kg, 1.35 to 64.7 mg/kg, and 0.135 mg/kg to 89.1 mg/kg, respectively. The concentration range for beryllium in South Works soil is within the range of naturally occurring background in the U.S. (1-15 mg/kg) (Dragun and Chiasson, 1991).

The arithmetic mean concentrations of the PAHs in surface soil were only slightly higher than the arithmetic mean concentrations for surface and subsurface soils combined (Table 2-2 and 2-3), but the PAHs were detected in at least half of the surface soil samples collected (Table 2-3). As referenced above, concentrations of beryllium in surface soil (0.14 to 9.8 mg/kg) ranged within naturally occurring background levels in the U.S. (1 to 15 mg/kg) (Dragun and Chiasson, 1991). The same is true for cadmium, measured at concentrations ranging from 1.1 to 9.3 mg/kg with background concentrations ranging from non-detectable to 11 mg/kg (Dragun and Chiasson, 1991). Conversely, lead and manganese were measured at concentrations significantly higher than their naturally occurring background concentrations of less than 10 to 700 mg/kg and less than 2.0 to 7,000 mg/kg, respectively (Dragun and Chiasson, 1991). Lead and manganese were detected at concentrations ranging from 0.05 to 3,200 mg/kg and 378 to 29,900 mg/kg, respectively, in surface soils.

In the Risk Characterization Section (Section 5.0), concentrations of COIs measured at individual sampling locations were compared to the RGs for each future land use scenario.

2.4.2 Sediments

A total of five sediment samples were collected from the North and South Vessel Slips during the environmental assessments conducted at the South Works site (WTI, 1994). Only two chemical constituents, beryllium, and manganese, exceeded Region III RBCs for soil (USEPA, 1995a). Because these screening values are more appropriate for soil samples than sediment, further information on regional and local sediment quality was sought. The regional and local sediment data also provide an indication of the sediment quality upgradient or "background" to the site.

Similar to the screening comparisons conducted for soils, it is important to determine if the measured levels of these constituents exceed regional background levels. USX obtained background data for sediments from Lake Michigan and the Calumet River, located upgradient of the Slips, via Freedom of Information Act (FOIA) requests. These requests yielded sediment analytical data from the USEPA (1992a) and the U.S. Army Corps of Engineers (1978, 1980, 1981). Other information was obtained from the published scientific literature on background concentrations of inorganic constituents in soil and sediment throughout the United States (Dragun and Chiasson, 1991). Additionally, USX contacted the USEPA Assessment and Remediation of Contaminated Sediments (ARCS) working group for information that might be applicable to the South Works site (1990, 1991, 1993, 1994). The ARCS group is currently studying sediments in all five of the Great Lakes. These requests resulted in receipt of an extensive amount of sediment data generated over the past 20 years.

Because the Calumet River, which is located adjacent to the southern boundary of the South Works site, flows from Lake Michigan to the Cal-Sag Channel, Lake Michigan sediments in the Calumet Harbor are most representative of upgradient, background sediments for the South Works site. The Calumet River flows from Lake Michigan eventually to the Mississippi River. This condition, coupled with other industrial and municipal wastewater treatment plant discharges to Lake Michigan, both present and past, have created a set of unique conditions in the sediments from this area of Lake Michigan.

These conditions limit the applicability of the large amount of sediment data generated by the above referenced agencies to represent background sediment conditions for the South Works site. The use of Lake Michigan sediment data collected offshore of the states of Wisconsin, Illinois, Indiana, or Michigan do not appropriately represent upgradient background conditions for the North and South Vessel Slips.

Sediment data, obtained from the USEPA, U.S. Army Corps of Engineers, and from the ARCS program are the most current data available. The 1984 Corps of Engineers sediment data are the most recent data collected from the Calumet Harbor which, as referenced earlier, most

appropriately represents upgradient sediments for the North and South Vessel Slips. The Corps of Engineers has conducted only limited dredging in the headwaters of the Calumet River adjacent to the southern boundary of the site and in the Calumet Harbor adjacent to the eastern boundary of the site. Therefore, sediment samples obtained by the Corps in 1984 should still represent sediment conditions today. In addition, by 1984, approximately 50% to 75% of the steel production facilities at the South Works site had ceased operation and, therefore, no longer had the potential to impact sediments in the North and South Vessel Slips.

The concentrations of inorganic constituents detected in the North and South Vessel Slip sediments are consistent with the above referenced background sediment and soil data representative for background conditions at the site (Table 2-4). Beryllium, while only slightly exceeding regional background levels for sediments in one sample, was well within the range of background soil concentrations from which sediment is derived (Dragun and Chiasson, 1991). Data from both Lake Calumet and the Calumet River have been included in Table 2-4 to show the significantly higher levels of inorganic constituents within a short distance of the South Works site. Because sediments in the North and South Vessel Slips are consistent with regional background soil and sediment data, they will not be evaluated further in this HRA

2.4.3 Groundwater

The Phase III investigation results showed that eight chemicals were detected in one or more samples at levels exceeding Class I groundwater standards but, in most cases, were below Class II standards. It is important to recognize that groundwater beneath the South Works site is not currently used for drinking water or other residential/industrial uses, nor is it likely to be in the future. In addition, it is highly unlikely that a domestic use well would be installed in the City of Chicago as municipal water is available. Therefore, groundwater was not evaluated in this HRA as per discussions with IEPA and as stated in the approved PRA (ChemRisk®, 1995).

2.5 CHEMICAL-SPECIFIC HALF-LIVES

Organic chemicals are naturally degraded in the environment by a variety of processes (*i.e.*, photodegradation, microbial activity, hydrolysis, etc.). This HRA incorporates chemical-specific degradation (*i.e.*, environmental half-lives) to evaluate the environmental degradation of the organic COIs in soil for the calculation of RGs (Section 4.4). Environmental half-lives are a chemical-specific measure of the amount of time necessary for the chemical concentration to decrease by one half. Half-lives vary for specific chemicals based on environmental conditions (*i.e.*, presence of bacteria, pH, exposure to sunlight and oxygen).

The chemical-specific half-lives of the organic COIs are presented in Table 2-5. Literature reported (Howard *et al.*, 1991) and USEPA (1986) values are both presented for comparison purposes. The "high" value represents the longest (slowest) half-life reported for a specific chemical while the "low" value represents the shortest half-life. The high value from Howard *et al.* (1991) for each PAH was used in this HRA to ensure that the degradation rate was not over-estimated. The half-lives were used to calculate the time-averaged concentrations of the PAHs, and are incorporated into the RG calculation (Section 4.4).

Toxicity of PAHs To Soil Microbes

Because this HRA derives RGs for soil based on chemical-specific environmental half-lives for PAHs, it follows that an evaluation of the microbial toxicity of PAHs to microbes should be addressed. Biological transformation, or breakdown of chemicals by microscopic organisms, is the primary process affecting the degradation of PAHs in environmental systems (Sims and Overcash, 1983). However, many other processes occur as well including low levels of volatilization, photodegradation, and abiotic loss (ATSDR, 1993). Because microorganisms provide the primary degradation process for the PAHs, inhibition of this action was investigated. PAHs are degraded by microorganisms by the transformation of the aromatic nucleus (Cerniglia, 1981; Gibson, 1977; Park *et al.*, 1990). First, bacteria oxidize PAHs by the incorporation of two atoms of oxygen into the substrate to form a *cis*-configuration dihydrodiol (Dagley, 1971; Gibson, 1977; Park *et al.*, 1990). This *cis*-dihydrodiol is further oxidized to a catechol which

is ultimately the substrate for transformation by dioxygenase that causes the fission of the aromatic rings (Dagley, 1971; Gibson, 1977; Park *et al.*, 1990). Fungi work via a different mechanism. Specifically, fungi oxidize PAHs via cytochrome p-450 catalyzed monooxygenase and epoxide hydrolase reactions to *trans*-dihydrodiols (Cerniglia, 1981).

While many researchers have studied the rate of microbial and bacterial degradation of the PAHs, very few have investigated the tolerable loading of PAHs in soil systems that will preclude microbial degradation due to overt toxicity. One study was located in the literature which determined maximum loading rates that would result in limited toxicity to soil microorganisms and not inhibit active degradation (Matthews and Hasting, 1987). This research utilized wood preserving wastes of creosote (WPC), pentachlorophenol (WPP) and technical grade creosote (TGC) (Matthews and Hastings, 1987). Using the Microtox™ system of measuring bacterial bioluminescence as the indicator of toxicity, these researchers determined a maximum loading rate for each mixture. The authors relied upon two separate laboratories to determine the precision of their results and to evaluate interlaboratory variation. The results reported indicate that 10,000 - 20,000 mg/kg and 9,000 - 18,000 mg/kg, reported by the two laboratories, is the maximum loading rate for WPC wastes. For TGC, 700 - 1,400 mg/kg and 600 - 1,200 mg/kg were reported by the two laboratories.

It is important to note that no chemical-specific analyses were conducted on the WPC or TGC, and as a consequence, the PAH concentration in these mixtures is not known. Despite this, the results may still be used in this HRA as a semi-quantitative indicator of potential degradation impairment at the South Works site. Even considering the lowest reported loading rate (600 mg/kg for TGC), it may be concluded that the concentrations of PAHs detected at the South Works site would not be expected to be toxic to the soil microorganisms responsible for the degradation of PAHs because maximum measured levels of PAHs are more than 100 times lower than this concentration. Therefore, the incorporation of environmental half-lives for the PAHs in this HRA is appropriate.

TABLE 2-1

t-TEST COMPARISON OF MEANS OF PRELIMINARY INORGANIC CONSTITUENTS OF INTEREST VS. MEAN REGIONAL BACKGROUND CONCENTRATIONS SOUTH WORKS SITE

Chemical	Background Arithmetic Mean ± Standard Deviation (mg/kg)	Degrees of Freedom	Calculated *t* Value	Table *t* Value	Above Background (Chemical of Interest)
Antimony	0.52 ± 0.67[b]	45	1.85	1.68	YES
Arsenic	7.4 ± 2.5[c]	65	-2.92	1.67	NO
Beryllium	0.36 ± 0.59[c]	54	7.10	1.67	YES
Cadmium	0.45 ± 0.39[d]	45	2.73	1.68	YES
Lead	38 ± 60[c]	149	3.65	1.66	YES
Manganese	640 ± 1,431[b]	45	4.66	1.68	YES
Vanadium	62 ± 22[c]	49	0.15	1.68	NO

a Table is based on a 95% confidence limit and the indicated degrees of freedom; if the calculated *t* value is greater than the Table T value, then the site concentration exceeds background.

b Background reported for eastern US soils (Dragun and Chiasson, 1991).

c Background reported for Illinois soils (Dragun and Chiasson, 1991).

d Background reported for Michigan soils (Dragun and Chiasson, 1991).

L:\USS\SWORKS\RA\TABLES\TBL2-1

TABLE 2-2

STATISTICAL SUMMARY OF SURFACE AND SUBSURFACE SOIL DATA FOR THE CHEMICALS OF INTEREST AT THE SOUTH WORKS SITE

Chemical of Interest	Concentration Range (mg/kg)	Detection Frequency	Arithmetic Mean Concentration (mg/kg)
INORGANIC CONSTITUENTS			
Antimony	1.35 - 64.7	2/48	3.23
Beryllium	0.14 - 9.8	46/48	3.25
Cadmium	0.135 - 89.1	34/48	5.72
Lead	0.005 - 3,200	131/131	163
Manganese	30.1 - 35,900	46/48	6,400
ORGANIC CONSTITUENTS			
Benzo(a)pyrene	0.115 - 1.7	11/48	0.42
Benzo(a)anthracene	0.12 - 1.7	9/48	0.38
Benzo(b)flouranthene	0.12 - 1.6	12/48	0.44
Dibenz(ah)anthracene	0.022 - 0.57	7/48	0.22
Indeno(1,2,3-cd)pyrene	0.12 - 1.3	11/48	0.34

TABLE 2-3

STATISTICAL SUMMARY OF SURFACE SOIL DATA FOR THE CHEMICALS OF INTEREST AT THE SOUTH WORKS SITE

Chemical of Interest	Concentration Range (mg/kg)	Detection Frequency	Mean Concentration (mg/kg)
INORGANIC CONSTITUENTS			
Beryllium	0.14 - 9.3	23/23	3.48
Cadmium	1.1 - 89.1	18/23	7.80
Lead	0.05 - 3,200	63/63	267
Manganese	378 - 29,900	23/23	6,140
ORGANIC CONSTITUENTS			
Benzo(a)pyrene	0.12 - 1.7	10/12	0.520
Benzo(a)anthracene	0.12 - 1.3	7/12	0.403
Benzo(b)flouranthene	0.15 - 1.6	8/12	0.55
Dibenz(ah)anthracene	0.022 - 0.57	6/12	0.224
Indeno(1,2,3-cd)pyrene	0.12 - 1.3	9/12	0.403

Note: Antimony is not presented on this table as it was not detected in surface soils above the limit of detection.

TABLE 2-4

SOUTH WORKS SEDIMENT DATA AND BACKGROUND SEDIMENT AND SOIL DATA

Parameters	Average South Works Sediment Concentration (mg/kg)	Maximum South Works Sediment Concentration (mg/kg)	Lake Calumet and Grand Calumet Sediment Quality Concentration Range [a] (mg/kg)	Chicago Harbor and Calumet Harbor Sediment Quality Concentration Range [b] (mg/kg)	Background Soils [c]	
					Range	Mean
Aluminum	5,618	7,210	60,100 - 115,600	NA	700 - >100,000	72,000
Arsenic	9.3	11.5	11.4 - 37.0	0.4 - 46.0	<1.0 - 97	7.2
Barium	44.12	60.4	<20 - 490	23.0 - 168.0	10 - 5,000	580
Beryllium	1.82	2.1	<1.0 - 1.2	NA	<1.0 - 15	0.92
Calcium	50,540	56,600	56,000 - 123,000	NA	100 - 320,000	24,000
Cadmium	4.2	7.2	1.0 - 6.0	0.9 - 13.0	n.d. - 11	---
Cobalt	12.1	14.5	9.0 - 21.0	NA	<3.0 - 70	9.1
Chromium	42.5	70.1	6.6 - 1,330	23.0 - 133	1.0 - 2,000	54
Copper	56.8	73.2	23.0 - 220	34.0 - 100	<1.0 - 700	25
Iron	28,800	47,100	10,000 - 68,500	22,000 - 54,000	100 - 100,000	26,000
Mercury	0.21	0.56	0.10 - 0.31	<0.01 - 0.66	<0.01 - 4.6	0.09
Potassium	1039	1,210	19,200 - 32,900	NA	50 - 63,000	15,000
Magnesium	23,280	26,600	35,500 - 57,720	NA	50 - >100,000	9,000
Manganese	958	1,200	70,000 - 150,000	600 - 2,100	<2.0 - 7,000	550
Sodium	194	225	5,000 - 10,600	NA	<500 - 100,000	12,000
Nickel	20.9	27.6	7.0 - 90.0	15.0 - 50.0	<5.0 - 700	19
Lead	122	272	64.0 - 308	50.0 - 656	<10 - 700	19
Thallium	0.32	0.43	4.0 - 40.0	NA	<0.25 - <3.4	---
Vanadium	22	34.2	12.0 - 60.0	NA	<7.0 - 500	80
Zinc	339	478	84.0 - 1,025	280 - 2,300	<5.0 - 2,900	60

[a] U.S. Environmental Protection Agency, Region V, Inventory of Contaminated Sediment Sites (Interim Version 7/31/92).

[b] U.S. Army Corps. of Engineers (1984) (Contract No. DACW23-84-0-0012) Water Quality Monitoring Chicago Area Confined Disposal Facility. Final Report on Operations.

[c] Dragun and Chiasson, 1991. Values are for soils of the conterminous USA.

NA Not available.

n.d. Non-detect.

--- Not evaluated.

TABLE 2-5

ENVIRONMENTAL HALF LIVES FOR THE ORGANIC CHEMICALS OF INTEREST IN SOILS SOUTH WORKS SITE

Chemicals of Interest	Howard *et al.* (1991) [a]		U.S. EPA (1986a) [b]	
	High (days)	Low (days)	High (days)	Low (days)
Benzo(a)anthracene	680	102	5.5	1
Benzo(a)pyrene	530	57	480	420
Benzo(b)fluoranthene	610	360	5.5	1
Dibenz(a,h)anthracene	940	361	5.5	0.0208
Indeno(1,2,3-cd)pyrene	730	600	5.5	0.0208

a. Data for soils only.
b. Data for air, soil, and water combined.

FIGURE 2-1

South Works Facility
WTI, 1993a

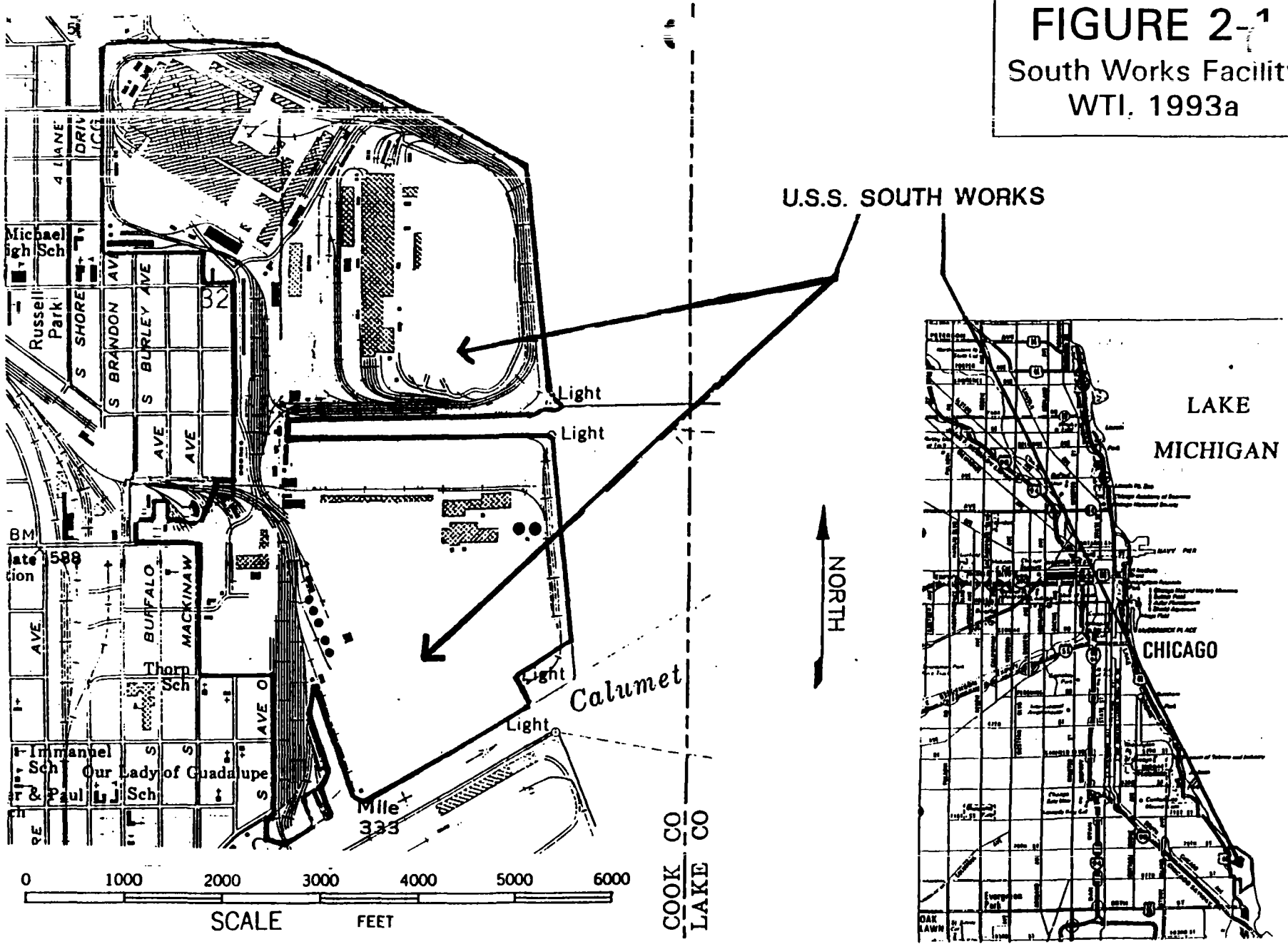

WTI WASTE TECHNOLOGY, INC.

3.0 DOSE RESPONSE ASSESSMENT

Dose response assessment is the process of characterizing the relationship between the dose of a chemical agent and the frequency of an adverse health effect in an exposed population. The dose is the quantity of the chemical that enters the body through a specific exposure route. The dose response relationship is often established under controlled conditions to minimize responses due to confounding variables. Mathematical models are used to extrapolate the relatively high doses administered to animals to predict potential human responses at levels far below those tested in animals. Humans are typically exposed to environmental contaminants at levels much lower than those tested in animals. Such doses may be detoxified or rendered inactive by the myriad of protective mechanisms that are present in humans (Ames, 1987). Consequently, the results of standard bioassays are of limited use in accurately predicting a dose response relationship in humans. In addition, the human population is likely to have a wider range of responses to toxic agents than the small groups of well controlled, genetically homogenous animals used in exposure studies. As discussed further in this section, to correct for the wider range of intraspecies variability among humans, the USEPA incorporates uncertainty or safety factors when setting toxicity criteria.

Dose-response information or toxicity criteria for the noncarcinogenic effects and carcinogenic effects of each COI evaluated at this site have been obtained from: The *Integrated Risk Information System* (IRIS) (USEPA, 1995b); the *Health Effects Assessment Summary Tables* (HEAST) (USEPA, 1993a) and the *Threshold Limit Values* (TLVs) *for Chemical Substances and Physical Agents* (ACGIH, 1994). Complete toxicity profiles for the COIs are provided in Appendix C.

The TLVs are nonpromulgated standards developed by the American Council of Governmental Industrial Hygienists (ACGIH) for the protection of workers in occupational settings. The TLVs will only be used to evaluate short-term exposure to workers (*i.e.*, a construction worker scenario) and their use is discussed in detail in Section 3.1. The appropriate chemical specific dose-response criteria will be combined with the uptake or exposure rates in the Exposure Assessment (Section 4.0) to derive the RGs.

Based on USEPA toxicity criteria, the COIs at the South Works site that were evaluated as noncarcinogens are:

- antimony,
- cadmium,
- lead, and
- manganese.

COIs at the South Works site that were evaluated as carcinogens are:

- benzo(a)pyrene,
- benzo(a)anthracene,
- dibenz(a,h)anthracene,
- indeno(1,2,3-cd)pyrene.
- beryllium, and
- cadmium (for inhalation exposures only).

3.1 NONCARCINOGENIC DOSE-RESPONSE ASSESSMENT

The potential noncarcinogenic health effects associated with exposure to the COIs were evaluated using acceptable daily intake levels established by the USEPA (1993a, 1995a) and ACGIH (1994). It is widely accepted that most noncarcinogenic effects of chemicals occur only after a threshold dose is exceeded (Klaassen *et al.*, 1986; Paustenbach, 1989a). For the purposes of establishing noncarcinogenic health criteria, this threshold dose is usually estimated from the no-observed adverse effect level (NOAEL) or lowest-observed adverse effect level (LOAEL) determined in chronic animal or human studies. The NOAEL is defined as the highest dose at which no adverse effects appear, while the LOAEL is the lowest dose at which adverse effects begin to appear (Klaassen *et al.*, 1986). The LOAEL or NOAEL from the most sensitive animal

or human study is used by the USEPA to establish long-term health criteria, termed reference doses (RfDs). The RfD is a daily uptake level (mg/kg-day) for the human population, including sensitive subpopulations, that is not expected to cause adverse health effects over a lifetime of exposure (USEPA, 1989a).

The oral RfD is developed from a NOAEL for the most sensitive or critical adverse health effect based in part on the assumption that if the most critical effect is prevented, then all toxic effects are prevented (USEPA, 1989a). Derivation of the inhalation RfD is similar to that of the oral RfD. However, the actual analysis is more complex than for oral exposures due to the dynamics of the respiratory system and its diversity across species (USEPA, 1989a).

In an attempt to account for limitations in the quality or quantity of available toxicological data, uncertainty factors are used with NOAELs (or LOAELs) to set RfDs for noncarcinogenic effects. Generally, an experimental NOAEL is divided by an uncertainty factor ranging from ten to ten thousand. A factor of ten is used to account for uncertainties in extrapolating animal data to human health effects; another ten-fold factor accounts for differences in sensitivity within the human population; a third ten-fold factor is used if the available data base is incomplete and a fourth ten-fold factor is used if the exposures were for a partial lifetime (*i.e.*, subchronic). In cases where the data do not meet all the conditions for one of these categories and appear to fall between requirements for two categories, an intermediate uncertainty factor (usually three) is used. It should be noted that RfDs are generally very conservative, *i.e.*, health protective, because of the use of large uncertainty (safety) factors.

The RfDs established by the USEPA and TLVs established by ACGIH for the COIs at the South Works site are presented in Table 3-1. Table 3-2 presents the critical effect that serves as the basis for the toxicity criteria developed by the USEPA. Currently, there are no promulgated RfD criteria for the five PAHs that are COIs at the South Works site because noncarcinogenic effects are only observed at dose levels higher than those that ultimately result in a carcinogenic response. These PAHs will be evaluated on the basis of carcinogenic effects only using USEPA carcinogenic health criteria for these constituents. This approach is conservative (*i.e.*, health

protective) since RGs protective of carcinogenic responses will also be protective of noncarcinogenic responses.

The inhalation of particulates from suspended soil is addressed in this HRA for a construction scenario since construction activities during redevelopment of the site may generate dust (Section 4.3.3). Consequently, the potential health effects due to worker exposure (eight hours per day; five days per week) were evaluated using acceptable exposure levels, TLVs, established by ACGIH for the noncarcinogenic COIs. TLVs are airborne concentrations of chemicals and represent conditions under which it is believed that nearly all workers may be repeatedly exposed day after day without adverse health effects (ACGIH, 1994).

TLVs for manganese and antimony were used in this assessment to evaluate potential effects to construction workers (Table 3-1). The TLV for manganese dust and compounds (5 mg/m^3 as a ceiling value) is considered protective of the potential acute and chronic effects of manganese on the pulmonary and central nervous systems (ACGIH, 1991). This conclusion was reached by ACGIH after review of case and epidemiological studies involving workers exposed to manganese at high concentrations (approximately 100 mg/m^3). Workers exposed continuously to average concentrations of 5 mg/m^3 or less showed no signs of manganese poisoning (Finn *et al.*, 1940; Davies, 1946; Tanaka and Lieben, 1969). Additionally, the TLV for manganese is consistent with the Occupational Safety and Health Administration's (OSHA) permissible exposure limit (PEL) which is a promulgated standard for the protection of worker health from the chronic health effects such as manganese fume poisoning, lung damage, and pneumonia (ACGIH, 1991). The USEPA inhalation RfD for manganese is considered questionable and is currently being reevaluated by USEPA (Valesquez, *pers. comm.*, 1995). Therefore, the TLV and PEL were deemed the most appropriate regulatory standards for manganese for the evaluation of short-term construction worker exposure.

The TLV and PEL for antimony of 0.5 mg/m^3 were developed to be protective of chronic heart disease, high blood pressure and ulcers observed among workers exposed to high levels of antimony. However, the toxicological evaluation on which the antimony standards were set is

quite limited, and the data were influenced by exposures to chemicals other than antimony. An inhalation RfD for antimony has not been developed by USEPA.

It should be recognized that the inhalation RfD represents the dose to which even a sensitive individual may receive continuously for a lifetime without risk of deleterious health effects, while the TLVs and PELs are designed to be protective of long-term exposure to workers for a 40 hour work-week. For this reason, TLVs are only applicable in this HRA for the short-term (1 year) construction worker exposure scenario evaluated. An inhalation RfD for antimony has not been developed, and inhalation RfDs are not available for beryllium or cadmium. However, the USEPA has verified carcinogenic health criteria for beryllium and cadmium which are used in this HRA for all scenarios.

USEPA has not verified toxicity criteria (RfDs or slope factors) for lead, and as a consequence, blood lead concentration modeling was performed to evaluate the potential hazard to lead in site soil and to set RGs. Three modeling approaches were evaluated: the physiologically-based pharmacokinetic model developed by Dr. Ellen O'Flaherty (O'Flaherty, 1991a,b,c; 1993, 1995), the USEPA Integrated Exposure Uptake Biokinetic (IEUBK) model for children (USEPA, 1994a), and a USEPA-modified version Bowers *et al.*, (1994) model for adults. These modeling approaches and results are discussed in Section 4.5.

3.2 CARCINOGENIC DOSE-RESPONSE ASSESSMENT

The accepted regulatory approach generally assumes that potentially carcinogenic chemicals should be treated as if they have no threshold of activity (Paustenbach, 1989a). To estimate theoretically plausible responses at low doses, various mathematical models, which describe the expected quantitative relationship between risk and dose, can be used (Paustenbach, 1989a,b). The mathematical model currently used by the USEPA for low-dose extrapolation is the linearized multistage model (LMS). This model is based on the multistage theory of the carcinogenic process. This suggests that a cell may go through a sequence of specific changes (stages) before reaching a malignant state. The LMS model is used in USEPA carcinogen

assessments to estimate the dose response characteristics of carcinogens at low exposure levels typically encountered in the environment because it assumes linearity between dose and effect (the most conservative assumption) to zero dose (*i.e.*, no threshold for carcinogenicity). The slope of the dose-response curve at low doses, the "slope factor," is used as a measure of the carcinogenic potential of a chemical; the higher the slope factor, the greater the carcinogenic potential.

Health risks for exposures to carcinogens are defined in terms of probabilities. These probabilities identify the likelihood of a carcinogenic response in an individual that receives a given dose of a particular constituent. The slope factor (SF), expressed in units of $(mg/kg\text{-}day)^{-1}$, multiplied by the daily human intake (dose) of the chemical, provides an estimate of the theoretical excess risk of developing cancer.

The following USEPA Weight of Evidence Classification was used to determine which COIs will be evaluated for potential carcinogenic effects:

Group A	Human Carcinogen (sufficient evidence of carcinogenicity in humans)
Group B1	Probable Human Carcinogen (limited evidence of carcinogenicity in humans)
Group B2	Probable Human Carcinogen (sufficient evidence of carcinogenicity in animals with inadequate or lack of evidence in humans)
Group C	Possible Human Carcinogen (limited evidence of carcinogenicity in animals or lack of human data)
Group D	Not Classifiable as to Human Carcinogenicity (inadequate or no evidence)
Group E	Evidence of Noncarcinogenicity for Humans (no evidence of carcinogenicity in adequate studies)

The COIs are presented with their ratings in Table 3-1. According to USEPA guidance (1989a), only those chemicals with a Group A, B (B1 or B2), or C ranking were addressed for possible

carcinogenic effects. For this HRA, the COIs addressed for possible carcinogenic effects are: benzo(a)anthracene, benzo(a)pyrene, benzo(b)fluoranthene, dibenz(a,h)anthracene, indeno(1,2,3-cd)pyrene, beryllium, and cadmium (for the inhalation pathway only).

Carcinogenic Evaluation of the PAHs

The current USEPA approach for addressing potential relative carcinogenic potency was used for evaluating the PAHs in this assessment. In July 1993, the USEPA Office of Research and Development issued *Provisional Guidance for Quantitative Risk Assessment of Polycyclic Aromatic Hydrocarbons* (USEPA, 1993d). This publication provided guidance for assigning a relative carcinogenic potency (RCP) to specific PAH compounds based on the potency of benzo(a)pyrene. RCPs have been derived for six PAH compounds: benzo(a)anthracene, benzo(b)fluoranthene, benzo(k)fluoranthene, chrysene, dibenz(ah)anthracene, and indeno(1,2,3-cd)pyrene. The relative carcinogenic potencies of these PAHs were estimated from the potency of benzo(a)pyrene [7.3 (mg/kg-day^{-1})]. The table below presents the RCPs used in this assessment for the Group B2 PAHs that are COIs at the South Works site. It is important to note that the resulting slope factors from the RCP approach are the same as those used in USEPA Region III's *Risk-Based Concentrations* (USEPA, 1995a).

Chemical	Relative Carcinogenic Potency
Benzo(a)pyrene	1.0
Benzo(a)anthracene	0.1
Benzo(b)fluoranthene	0.1
Dibenz(a,h)anthracene	1.0
Indeno(1,2,3-cd)pyrene	0.1

These relative potencies were used in this HRA to calculate remediation goals for the PAHs present at the South Works site.

TABLE 3-1

HEALTH CRITERIA FOR THE CHEMICALS OF INTEREST

Chemical of Interest	Oral		Inhalation			USEPA Group Classification
	RfD[a] (mg/kg-day)	SF[b] $(mg/kg\text{-}day)^{-1}$	RfD[a] (mg/kg-day)	SF[b] $(mg/kg\text{-}day)^{-1}$	ACGIH TLV[c] (mg/m^3)	
Benzo(a)anthracene	NI	7.3×10^{-1}	NI	NI	NA	B2
Benzo(a)pyrene	NI	7.3×10^{0}	NI	NI	NA	B2
Benzo(b)fluoranthene	NI	7.3×10^{-2}	NI	NI	NA	B2
Dibenz(a,h)anthracene	NI	7.3×10^{0}	NI	NI	NA	B2
Indeno(1,2,3-cd)pyrene	NI	7.3×10^{-1}	NI	NI	NA	B2
Antimony	4.0×10^{-4}	NA	NI	NI	0.5	NS
Beryllium	5.0×10^{-3}	4.3×10^{0}	NI	8.4×10^{0}	---	B2
Cadmium	5.0×10^{-4}	NA	NI	6.3×10^{0}	---	B1
Manganese	1.4×10^{-1}	NA	1.43×10^{-5}	NA	5	NS

a Reference dose, USEPA, 1995a; 1995b.
b Slope factor; USEPA, 1995a; 1995b.
c American Conference of Governmental Industrial Hygienists Threshold Limit Values (ACGIH, 1994).
NI Not issued by the USEPA.
NA Not available, chemical not carcinogenic by this pathway.
NS Not stated.
--- Chemical evaluated on the basis of carcinogenic effects.

TABLE 3-2
BASIS OF USEPA TOXICITY CRITERIA

Chemical of Interest	Primary Toxic Effect[a]	
	Inhalation	Oral
INORGANIC CONSTITUENTS		
Antimony	NA	Myocardial damage
Beryllium	Lung and bone cancer	Bone cancer
Cadmium	Lung cancer	Kidney damage
Lead	Neurological impairment	Neurological impairment in children
Manganese	CNS damage in older adults	CNS damage in older adults
ORGANIC CONSTITUENTS		
Benzo(a)pyrene	Lung & liver cancer	Liver cancer
Benzo(a)anthracene	Lung & liver cancer	Liver cancer
Benzo(b)flouranthene	Lung & liver cancer	Liver cancer
Dibenz(a,h)anthracene	Lung & liver cancer	Liver cancer
Indeno(1,2,3-cd)pyrene	Lung & liver cancer	Liver cancer

a All toxic effects reported from USEPA, 1995b.
NA Not available, no adverse health effect reported (USEPA, 1995b).
CNS Central Nervous System.

4.0 EXPOSURE ASSESSMENT

Exposure assessment is the process through which the exposure of biological receptors to substances present in the environment is estimated and/or measured. Exposure assessment generally involves analysis of the following variables: 1) magnitude, duration and route of exposure; 2) nature and size of potential receptor populations; and 3) uncertainties associated with each variable (NAS, 1983). Exposure assessment is useful in identifying the optimal remedial alternative by estimating the likely human exposures associated with future land use scenarios or remedial alternatives (Paustenbach *et al.*, 1990). For this HRA, the exposure assessment relies upon the exposure pathways, scenarios, and parameters that were provided in the Preliminary Risk Assessment (PRA) and the results of the site-specific bioavailability studies, both of which were approved by the IEPA.

Exposure pathways are determined by environmental conditions (*e.g.*, location of surface waters, groundwater, vegetative cover, prevailing wind direction, meteorological factors), by the potential for chemical migration from one environmental medium (*e.g.*, soil, water, or air) to another, and by the general activities of the potentially exposed populations (*e.g.*, time spent inside or outside, level of work activity). Each pathway describes a unique mechanism by which a population or an individual may be exposed to a chemical. Although several potential pathways may exist, not all may be complete. For a pathway to be complete, the following conditions must exist:

- a source and mechanism of chemical release to the environment;
- an environmental transport medium (*e.g.*, air, water, soil);

- a point of potential human contact with the medium; and
- a human exposure route at the contact point (*e.g.*, inhalation, ingestion, dermal contact).

The potential for the occurrence of an adverse health effect associated with exposure to a chemical depends on the degree of systemic uptake (amount absorbed into the blood and tissues). For any route of exposure, the uptake (U) is the product of exposure (E) and the absorption efficiency or bioavailability (B):

$$Uptake = E * B$$

Although a number of different factors are used to quantify exposure, the mathematical relationship shown above holds true for all exposure routes and is expressed as mass of chemical per mass of body weight per day (mg/kg-day).

4.1 EXPOSURE PATHWAYS

In this HRA, chemical uptake (or dose) was not quantified. Rather, RGs were calculated based on the acceptable level of risk (theoretical excess cancer risk range of 1×10^{-5} to 1×10^{-6} for carcinogens and a hazard index of one for noncarcinogens as discussed further in this section), USEPA toxicity criteria (Section 3.0), and measures of exposure and bioavailability. In essence, the calculation of RGs is risk assessment in reverse where one starts with the acceptable level of risk and, through traditional risk assessment methodology and equations, derives the soil concentration associated with the acceptable level of risk, which are the RGs.

Because the COIs are present in surface and subsurface soil at the South Works site, direct contact exposure pathways are considered potentially complete and were evaluated in this assessment. These are incidental soil ingestion, and dermal contact with soil.

As discussed in the PRA (ChemRisk®, 1995), ingestion of home grown vegetables was not evaluated because the type of residential dwellings planned (condominiums, apartments, etc.) are unlikely to support significant home gardening activities in the future. Also, the suspension of surface soils to ambient air and subsequent inhalation exposure was not evaluated for future use scenarios (residential, industrial, etc.) since this pathway is unlikely to be significant (greater than 1 % of the total dose) when compared to the direct contact pathways (Sheehan et *al.*, 1991). Further, land cover associated with site development (buildings, pavement and landscaping) is expected to prevent significant erosion of surface soil. However, the suspension of surface and subsurface soils could occur for a site construction scenario as construction activities (excavation, movement of heavy equipment) are known to generate considerable dust unless suppressants are used. Therefore, the inhalation of locally suspended soil was evaluated as an exposure pathway for the construction worker scenario.

Volatilization of chemicals from the soil into ambient air was not addressed since none of the COIs have a Henry's Law Constant greater than 1×10^{-5} atm-m^3/mole and a molecular weight less than 200 g/mole and, therefore by definition, are not likely to volatilize (USEPA, 1991a; IEPA, 1992).

Finally, direct contact with and ingestion of groundwater were considered incomplete pathways of exposure because the groundwater is not potable and the installation of a domestic use well in the City of Chicago is highly unlikely as municipal water is available. Therefore, groundwater was not a media of concern for this risk assessment.

4.2 Identification Of Appropriate Exposure Scenarios

This section identifies the applicable exposure scenarios for potentially exposed individuals in the future based on proposed land uses for the South Works site once redeveloped. The potential for contact with site soils was determined based on site-specific conditions and anticipated land uses for the site.

Redevelopment of the South Works site could include residential, industrial/commercial, and recreational uses although specific plans have not yet been defined. Therefore, industrial/commercial, residential, and recreational scenarios were evaluated in this HRA. In addition, construction workers may be exposed to site surface and subsurface soils during redevelopment of the site and their potential exposure, although short-term, was quantitatively addressed. The industrial/commercial scenario accounts for common activities associated with individuals working at the site five days per week. The recreational scenario accounts for infrequent visitation to facilities such as playgrounds, and the construction worker scenario accounts for exposure for one construction season (assumed to be eight months). The residential scenario addresses the highest exposure possible as it assumes that an individual spends all of his or her time at the site. The residential land use scenario also incorporates very conservative (*i.e.*, health-protective) exposure assumptions.

The calculated RGs for the future residential, industrial/commercial, and recreational exposure scenarios will be applicable to surface soils (0-2 feet) only because these populations are unlikely to come into contact with subsurface soils (more than 2 feet below the ground surface) on a regular basis. However, the RGs protective of potential exposures to construction workers during site redevelopment were applied to both surface and subsurface soils because these workers are more likely to contact subsurface soils during site redevelopment activities which could include soil excavation. If subsurface soils are excavated and brought to the surface during site construction, the RGs applicable to surface soil (those for the residential, recreational and/or industrial/commercial scenario, as appropriate) should be applied to the excavated soil.

Only adult exposure (individuals 18 to 70 years old) was quantified for the industrial/commercial and construction scenarios because children are not expected to be present at an operating industrial/commercial facility or at an active construction site on a regular basis. For the residential and recreational scenarios, exposures to all age groups (0 to 70 years) were evaluated (USEPA, 1989a). It is important to note that the USEPA has provided sufficient guidance for conducting exposure evaluations for the industrial/commercial and residential scenarios.

However, very little guidance exists for quantifying either the recreational or construction worker exposure scenarios. Therefore, these scenarios were quantified using "best professional judgement," site-specific exposure parameters (where available) and conservative estimates of exposure potential. RGs were calculated for the residential, industrial/commercial, recreational, and construction worker scenarios for two exposure levels as described below.

Maximally Exposed Individual

The maximally exposed individual (MEI) is the single individual with the highest potential exposure in a given population. This term has historically been defined in various ways (including the definition above) and is synonymous with the "reasonable maximum exposure" (RME) or "upper bound" estimate (USEPA, 1992b). The MEI was determined by using upper bound estimates for key exposure parameters, such as the 95th percentile estimates for exposure duration, frequency and intake rates. The MEI was calculated based on a combination of upper-bound and median exposure parameters from the USEPA risk assessment guidance (USEPA, 1989a; 1991b).

Most Likely Exposed Individual

The most likely exposed individual (MLEI) is the individual with the median (50th percentile) or average exposure in a given population. The MLEI is synonymous with the central tendency (CT) estimate, and was calculated using the median or average values of the exposure parameter distributions to represent a probable or more likely exposure scenario. The exposure parameters used for the MLEI were taken from both regulatory guidance and the scientific literature.

The advantage of using the MEI and MLEI scenarios in the exposure assessment is that the resulting range of RGs provide some measure of the uncertainty associated with the worst case estimates. This type of approach, where the range of risk estimates is determined, is recommended in IEPA risk assessment guidance (IEPA, 1992). Additionally, by developing cleanup levels for the two exposure levels, it may not be necessary to apply the worst-case

cleanup levels (those based on the MEI) to any "hot spot" areas of the site when cleanup levels based on the expected average exposure levels for these isolated areas may be more reasonable.

The exposure scenarios, pathways and media evaluated in this HRA are summarized below:

RESIDENTIAL SCENARIO	RECREATIONAL SCENARIO	INDUSTRIAL/COMMERCIAL SCENARIO	CONSTRUCTION SCENARIO
EXPOSURE PATHWAY	EXPOSURE PATHWAY	EXPOSURE PATHWAY	EXPOSURE PATHWAY
Incidental Ingestion (surface soil) Dermal Contact (surface soil)	Incidental Ingestion (surface soil) Dermal Contact (surface soil)	Incidental Ingestion (surface soil) Dermal Contact (surface soil)	Incidental Ingestion (surface/subsurface soil) Dermal Contact (surface/subsurface soil) Inhalation of Suspended Particulates (surface/subsurface soil)

The RG calculations and parameters used to quantify potential chemical uptake from each complete exposure pathway are presented in more detail in the following sections.

4.3 EXPOSURE PARAMETERS

In this section, the exposure parameters used for each complete exposure pathway [*i.e.*, soil ingestion, dermal contact and inhalation of locally suspended soil (construction scenario only)] are described. The exposure parameters were used to calculate the level of uptake of soil using the exposure rate equations described in Section 4.4. The rate of soil uptake is used with the acceptable or safe daily doses established by the USEPA to determine the RGs. The exposure

parameters used in the assessment are presented in Table 4-1. A discussion of each of the parameters is provided in this section.

4.3.1 General Exposure Parameters

Exposure Duration

The exposure duration for the residential scenario is the fraction of a lifetime an individual might spend at one's home. The USEPA uses a default value of 30 years to represent the upper bound of residential tenure (USEPA, 1989a; 1991b). This value was used as the exposure duration for the MEI adult residential and recreational evaluations since residents are also likely to participate in recreational activities. This period is divided into two categories: 6 years as a child and 24 years as an adult. An exposure duration of 9.3 years was used for the MLEI. This value is the median residence time based on national census data of actual single-family housing statistics (USEPA, 1989d). It is most conservative to assume that 6 years of the 9.3 years is spent as a child, and the remaining 3.3 years as an adult because the intake or dose by the soil ingestion and dermal contact pathways (in milligrams of chemical per kilogram body weight per day) is higher for a child than an adult.

The exposure duration for the industrial/commercial scenario is the amount of time (years) an adult individual works at one job. The Bureau of Labor Statistics (1990) has described the distribution of worker tenure in the United States. Because there is no reason to believe that worker tenure will be significantly different for those industries and commercial establishments to be developed on-site as compared to national statistics, the data from the Bureau of Labor Statistics was used in the assessment. The exposure duration for the MLEI in this assessment is the 50th percentile of the occupational tenure distribution (4.5 years). For the MEI, the USEPA default value of 25 years, representing the 90th percentile of the distribution, was used (USEPA, 1989a; 1991b).

The exposure duration for the construction worker scenario was one year representing one construction season. While construction and redevelopment of the site may take more than one season, direct contact with soil is likely to be limited to one year as an upper-bound estimate based on professional judgement. This value was used for both the MEI and MLEI.

Exposure Frequency

Exposure frequency accounts for time spent away from the site (*i.e.*, outside of the exposure realm). For the industrial/commercial and construction worker scenarios, it was conservatively assumed that an adult worker will spend five days per week at the site. For industrial/commercial workers, exposure is expected to occur for 50 weeks per year at the site (250 days/year) for both the MEI and MLEI evaluations (USEPA, 1989a; 1991b). For construction workers for both the MEI and MLEI evaluations, the exposure frequency accounts for five days per week at the site for a construction season of eight months (160 days/year). For the MEI and MLEI residential scenario, the USEPA default value of 350 days/year, accounting for approximately two weeks away from the site per year, was used for both children and adults (USEPA, 1989a; 1991b).

No guidance has been issued by the USEPA or the IEPA on the exposure frequency that should be used for a recreational scenario, and no guidance was located in the scientific literature. Therefore, it was necessary to rely upon best professional judgement to determine this parameter. An exposure frequency of 104 days/year was determined to be reasonable for the South Works site assuming both adults and children might frequent the area designated for recreational use 2 days per week. It follows that this value may underestimate the amount of time spent in the recreational area during the summer months. However, it more than likely overestimates the time spent at the site during the winter months. Therefore, it is concluded that this value is conservative enough not to underestimate the total number of days an adult or child might visit the recreational areas. This value was used for both the MEI and MLEI recreational evaluations.

Meteorological Factor

A meteorological factor was used to account for that fraction of the year during which exposure to chemicals in soils may occur (Sheehan *et al.*, 1991; USEPA, 1989a). Since most individuals would not be expected to directly contact soil when it is raining, when there is snow on the ground or when the ground is frozen, the frequency of contact with potentially impacted soil was adjusted for site-specific meteorological conditions (USEPA, 1989a). This factor was used for both the MEI and MLEI evaluations for the residential, industrial/commercial, and recreational scenarios, but not for the construction scenario as construction workers are known to work through reasonably bad weather and since the exposure frequency is limited to eight months.

Climatic data for Chicago was reviewed to determine the number of days on which a tenth of an inch or greater of precipitation fell and the high temperature did not exceed 32°F. Based on ten years of meteorological data (1970-1979) provided by USEPA (1995c), on average, 73 days/year receive 0.1 inches or more of precipitation, and there are typically 77 days/year with a mean temperature of 32°F. Accounting for days when both events occur (10 days/year) a meteorological factor of 62% (73 + 77 - 10 = 140; 365 - 140 = 225; 225 ÷ 365 = 0.62 x 100%) was derived. Thus for the MEI evaluations, it was assumed that exposure to the future resident, industrial/commercial worker, and recreator will only occur 62% of the time due to weather restrictions.

For the MLEI evaluations, the same climatic data was reviewed for the number of days on which a hundredth of an inch or greater of precipitation fell and the high temperature did not exceed 32°F. Using the same approach as presented above, on average 118 days/year receive 0.01 inches of precipitation or more, 77 days/year with a mean temperature of 32°F, and 21 days/year when both events occur. Therefore, a meteorological factor of 52% (118 + 77 - 21 = 174, 365 - 174 = 191; 191 ÷ 365 = 0.52 x 100%) was derived.

Body Weight

Seventy kilograms is the standard body weight for adults (USEPA, 1989a; 1991a), and is the value used for calculating USEPA toxicity criteria (reference doses and cancer slope factors). Therefore, it was used for the MEI and MLEI values for all adult exposure scenarios (18 to 70 years). A standard body weight of 15 kg was used for the child (1-6 years) residential and recreational MEI and MLEI evaluations (USEPA, 1989a; 1991b).

Averaging Time

The averaging time for exposure to carcinogens is assumed to be a lifetime (70 years or 25,550 days) (USEPA, 1989a) and was used for both the MEI and MLEI analyses. Because the dose for carcinogens is considered to be a lifetime average daily dose, the child dose is added to the adult dose and that sum is averaged over an entire lifetime (USEPA, 1989a). Hence, the averaging time for exposure to carcinogens for both children and adults was 25,550 days (70 years).

For noncarcinogens, the averaging time is equal to the exposure duration or the time period over which exposure is assumed to occur. Therefore, the dose is an average daily dose derived separately for an adult and a child (not averaged over a lifetime). The averaging time of 9,125 days (25 years) was used for the industrial/commercial MEI, and the averaging time of 1,643 days (4.5 years) for the industrial/commercial MLEI. For the construction worker scenario, the averaging time for noncarcinogens was one year (365 days) for both the MEI and MLEI scenarios. Averaging times for the residential and recreational scenarios are different for children and adults since exposure duration is different for each (see page 4-7; Exposure Duration). For the MLEI, exposure was assumed to occur for a total of 9.3 years. Therefore, 2,190 days (6 years) was the averaging time for a child, and 1,205 days (3.3 years) was the averaging time for an adult. For the MEI, exposure was assumed to occur for a total of 30 years. Therefore, 2,190 days (6 years) was the averaging time for a child, and 8,760 days (24 years) was the averaging time for an adult.

4.3.2 Soil Ingestion Pathway

Soil Ingestion Rate

Incidental soil ingestion occurs at all ages as a result of hand-to-mouth activities. It is widely believed that children approximately two to five years old are the only age group that consumes a potentially significant amount of soil (Calabrese *et al.*, 1989; van Wijnen *et al.*, 1990). As a result, numerous studies of soil ingestion rates in children have been conducted. The most thorough and rigorous studies to date are those by Calabrese *et al.*, (1989), Davis *et al.* (1990), and van Wijnen *et al.* (1990). In the Calabrese study, eight different tracer elements (aluminum, barium, manganese, silicon, titanium, vanadium, yttrium, and zirconium) were quantitatively evaluated in the stools of 65 children, age one to four years old. In a subsequent validation study, Calabrese and Stanek (Calabrese *et al.*, 1991; Calabrese and Stanek 1991) developed a model to measure the precision of the soil ingestion rates calculated for each of the tracers used in their 1989 study and those used by Davis *et al.* The model validated the results for only two of the tracers (zirconium and titanium) in the Calabrese *et al.* study and none of the tracers used in the Davis *et al.* study. Since the confidence interval for zirconium was narrower than that for titanium, Calabrese and Stanek (1991b) concluded that the soil ingestion estimates calculated for zirconium were the most accurate. The median soil ingestion rates for zirconium and titanium were 16 and 55 mg/day, respectively.

It should be noted that the population of 40 children studied by Calabrese contained one child that displayed *pica* behavior (ingestion of greater than 5 grams of soil per day) ingesting 13 grams of soil per day for one week. Therefore, the Calabrese soil ingestion estimates are likely to overestimate the actual soil ingestion rate because *pica* is a very rare condition affecting less than 0.2 percent of the population (Calabrese *et. al.*, 1991). Based on these data, it is reasonable to assume that children normally ingest less than 25 mg of soil per day, and this soil ingestion rate has been used in another IEPA-approved risk assessment for the MEI scenario (ChemRisk, 1989). This soil ingestion rate (25 mg/day) is considerably less than the value of 200 mg/day currently recommended by the USEPA (USEPA, 1989a). However, the Agency

value predates the work of Calabrese *et al.* and van Wijnen *et al.*, which is currently under review within the USEPA. To maintain consistency with current USEPA guidance, a soil ingestion rate of 50 mg/day was used in this assessment for children (ages 1 to 6) for the recreational and residential MLEI evaluations, and 200 mg/day was used for the MEI evaluations (USEPA, 1989a; 1991b). However, as discussed above and in the uncertainty analysis (Section 5.2.3), these soil ingestion rates are thought to significantly overestimate actual soil ingestion rates among children based on data presented in the recent scientific literature.

There are little or no reliable quantitative data available for estimating adult soil ingestion rates. USEPA risk assessment guidance suggests a soil ingestion rate of 100 mg/day for adults in a residential scenario, based primarily on Hawley's published estimate of 65 mg/day (1985). However, Hawley's estimate was not based on quantitative tracer data. Current USEPA risk assessment guidance (USEPA, 1991b) also suggests a soil ingestion rate of 50 mg/work day for adults in commercial/industrial settings, based on the results reported in Calabrese's preliminary adult soil ingestion study (Calabrese *et al.*, 1990). However, Calabrese and Stanek (1991) have since determined that the soil ingestion rates reported in their preliminary adult study were invalid, and that the 50 mg/day value is likely to be an overestimate (Calabrese and Stanek; 1991, Calabrese *et al.*, 1991). Therefore, neither of the Agency recommended estimates of adult soil ingestion rates are strongly supported by the literature.

Because the validated median soil ingestion rates determined for children in the Calabrese study are 16 mg/day and 55 mg/day for zirconium and titanium, respectively, it is reasonable to expect that adult soil ingestion rates are less than 10 mg/day, as suggested by Paustenbach (1987) and Calabrese *et al.* (1991). Accordingly, for all scenarios in this evaluation except the construction worker, a value of 10 mg/day was used to represent the adult (all individuals older than 6 years) soil ingestion rate for the MLEI evaluations, and an upper-bound of 50 mg/day was used for the MEI. For the construction worker scenario, 50 mg/day was used for the MLEI evaluation and 200 mg/day for the MEI. The latter is used to account for the possible increased rate of soil

ingestion for construction workers in direct contact with surface and subsurface soil during construction activities (*i.e.*, excavation).

Oral Bioavailability

Oral bioavailability is a measure of the degree to which a chemical may be systemically absorbed following ingestion. Some chemicals are absorbed almost completely (100% bioavailability) when ingested in pure form. Other chemicals may pass through the body largely unabsorbed. In general, as the lipophilicity of a chemical increases, its absorption across the gastrointestinal tract increases.

Oral bioavailability of soil-bound chemicals is also dependent upon the rate at which chemicals dissociate from the soil or slag matrix in the gut. Soil-bound chemicals, particularly inorganics, are usually absorbed to a lesser degree than chemicals in pure form (Paustenbach, 1987; Goon, 1990; 1991; Sheehan *et al.*, 1991; 1992). The reduced absorption is a result of hydrophobic attraction between the chemical and soil matrix. The greater the degree of affinity between a chemical and soil, the less likely that a soil-bound chemical will be absorbed upon ingestion. Absorption of the pure chemical in the gut is inherently evaluated in the USEPA reference doses and oral cancer slope factors as each are based on oral animal or human toxicity studies. Therefore, bioavailability, as used in this HRA refers to the site-specific "bioaccessibility" of the chemicals from the soil or slag matrix and represents the difference in absorption between chemicals in soil and chemicals in a pure (100% bioaccessibility) form. Because the COIs are expected to be tightly bound in the slag and/or soil matrix at the South Works Site, bioaccessibility is most likely very low.

Oral Bioavailability of PAHs

Animal studies have been conducted on the bioavailability of ingested PAHs in food and water (ATSDR, 1993; Rahman *et al.*, 1986; Hecht *et al.*, 1979). Two studies have specifically addressed the bioavailability of benzo(a)pyrene [B(a)P] from ingested soil particles (Goon *et al.*, 1990; 1991). These authors reported an oral bioavailability for B(a)P of 44 to 64%, depending

on the nature of the soil matrix (*e.g.*, clay or sandy soils). These bioavailability factors were reduced even more after "aging" of the B(a)P-soil complex for over six months, to an absorption between 34 and 51% (Goon *et al.*, 1991). The South Works site has not been in operation since 1992 and, therefore, the PAH-soil complex is likely to be similar to the aged matrix used in the Goon *et al.* (1991) study. Additionally, since all of the PAHs that are COIs are considered immobile in soil based on their respective organic carbon coefficients (K_{oc}) (Lyman *et al.*, 1982; Dragun 1988), it is reasonable to assume that the bioavailability of the PAHs other than B(a)P in South Works soil are not significantly different than that for B(a)P. Therefore, based on the Goon *et al.* (1990; 1991) studies, an oral bioavailability factor of 50% for PAHs on a soil matrix was used in this risk assessment for both exposure levels (MEI and MLEI).

Site-Specific Oral Bioavailability

An oral bioavailability study was conducted to determine the site-specific bioavailability of manganese, lead, and beryllium, in South Works soil. For this experiment, the fraction of each metal that could be released from the soil matrix under simulated gastric conditions was determined. The protocol for this study was provided to IEPA on March 15, 1995, and approved for use on March 30, 1995 (Appendix B). A modification was made to the protocol in that soil samples were sieved to 500 μm or smaller to remove larger pieces of gravel from the samples. Based on professional judgment, it was determined that individuals, including children, would not ingest these larger particles. The sieved fraction (<500 μm) was then analyzed to determine the concentration of each of these metals in this size fraction.

For this study, gastric conditions were simulated by using pH 1.4 (0.04 molar) hydrochloric acid (HCl) to extract manganese, beryllium, and lead from soil samples collected from the South Works site. The volume of acid and mass of soil were based on the amount of gastric juice in the stomach of a child (50 ml; Clinical Diagnosis by Laboratory Methods, 1974) and the USEPA daily estimated soil ingestion rate (200 mg; USEPA, 1989a; 1991b). The pH was maintained at 1.4 throughout the extraction (1 hour) and the soil/simulated gastric solution was kept in a

37°C water bath. The results of the experiment are presented in Tables 4-2 and 4-3 and are discussed below.

For manganese, the percent extraction under simulated gastric conditions ranged from 15.9% to 33.3%, with an arithmetic mean extraction percentage of 23.5% which was used in this assessment to represent the amount of manganese available for gastrointestinal absorption (Table 4-2). For lead, the percent extracted ranged from 40.2% to 60.2% with an arithmetic mean of 48.8%. This mean value was used in the PBPK model for lead as discussed in Section 4.5. For beryllium, the protocol was modified such that 10 grams of soil and 50 ml of HCl were used. This was done to raise the concentration of beryllium in the extracts so that it could be measured by standard analytical protocol (See Appendix B for more details of study and analysis). The results of this study indicate that 25.6% (average of the two samples) of beryllium was extracted from the soil sample. This arithmetic mean value was used in the HRA.

The arithmetic mean percent extractions obtained from the experiment referenced above for beryllium, lead, and manganese were used in the HRA to represent the fraction of each metal that could be released from the soil matrix in the gut (oral bioavailability). For those inorganics not addressed by this study (*i.e.*, cadmium and antimony), a default value of 100% bioavailability was used.

4.3.3 Inhalation of Particulates Pathway

The inhalation of particulates was quantified for the construction worker scenario only. This exposure pathway was deemed complete for the construction scenario because construction activities (bulldozing, grading, etc) are known to generate considerable dust unless suppressants are used.

Inhalation Rate

For a construction worker, the upper-bound (95th percentile) inhalation rate of 20 m^3/8 hour day was used for both MEI and MLEI based on USEPA guidance (1991b).

Soil to Air Suspension Factor

For the calculation of RGs, it was necessary to estimate the amount of soil that could be suspended into ambient air and subsequently inhaled by site construction workers. The USEPA has developed guidance on the amount of soil that can be suspended (emission rate) under specific construction activities (bulldozing, scraping, back hoeing). However, these emission rates are very sensitive to site-specific parameters including soil particle size, moisture content, area of site being worked, and the amount of time spent at each activity. For this reason, it is generally necessary to develop a reasonably realistic construction activity scenario for each portion of the site. Because redevelopment plans are preliminary at this time, a default approach to estimating soil suspension during construction activities was used for the South Works site.

It was assumed for the MEI that during construction activities, the amount of dust in air will not exceed the permissible exposure limit (PEL) set by the Occupational Safety and Health Administration (OSHA) for respirable nuisance particulates of 5 mg/m^3 (CFR, 1992). This standard is applicable to construction sites. It is possible that some construction activities could produce dust levels in exceedence of this level. However, it was assumed that suppressants would be used during construction to prevent a violation of this OSHA limit. For the MLEI, it was assumed that dust levels would not exceed the National Ambient Air Quality Standard for respirable particulates of 50 μg/m^3 (USEPA, 1993a). Conservatively, it was assumed that all of the dust in the air is suspended soil from the site and that the concentration of suspended soil in air will be equal to these standards throughout construction activities.

Further, it was conservatively assumed that all soil particles are of a size that can be suspended in ambient air, inhaled, and retained in the lung for absorption. This is a very conservative assumption for two reasons. First, only particles of a diameter less than 1.5 mm can be

suspended to ambient air even with heavy vehicle traffic (USEPA, 1989c). Therefore, soil/slag particles larger than 1.5 mm cannot contribute to the inhalation dose. As referenced earlier, slag is the primary material used as fill on the site.

Secondly, of the total amount of airborne suspended particulate matter that may potentially be inhaled, only a small fraction is respirable. The respirable fraction is defined as particulate >0.2 μm and <10 μm (ICRP, 1968; Cowherd *et al.*, 1985). The inspirable fraction, that which can be inhaled, is defined as particulates between 10 μm and 75 μm based on an assumption that 75 μm is representative of the upper size of airborne particulates. The two particle-size fractions are based on physiological differences and their consequent toxicological implications. Inhaled particles may have diameters between 0 to 75 μm. These particles can be inhaled, but the inspirable fraction, between 10 and 75 μm, will be removed from the air by the nose or nasal pharyngeal cavity prior to reaching the deep lung. These removed particles are rapidly transferred from the respiratory tract to the gastrointestinal tract. In contrast, respirable particles, those >0.2 μm and <10 μm, will not be as easily removed by biological processes, and therefore, they can reach the deep lung and become trapped by alveoli. If trapped by alveoli, they can either be absorbed or remain in the lung. As particle size diminishes in the <0.2 μm range, the particles begin behaving more like a gas and have a tendency to be exhaled.

While particle size data are not available for the South Works surface soil, slag generally consists of more of the larger sized particles than most soil types. Therefore, the assumption that all soil/slag particle sizes can be suspended to ambient air, inhaled and retained in the alveolar region of the lungs for absorption is extremely conservative.

4.3.4 Dermal Contact Pathway

Consistent with IEPA guidance (IEPA, 1994), dermal contact with organic COIs (*i.e.*, PAHs) in soil was estimated to be equal to that of the oral administered dose. However, for the

inorganic COIs, potential exposure was quantitatively assessed using the parameters discussed below.

Total Skin Surface Area

Adult exposure to outdoor soils is assumed to be primarily from contacting soil with the hands and forearms (USEPA, 1989a). Upon consulting the USEPA's *Development of Statistical Distributions or Ranges of Standard Factors Used in Exposure Assessments* (USEPA, 1985), an estimate of 2,836 cm^2 was determined for adult skin surface area for these body parts. This value is based on skin surface areas for the forearms (one-half of the arms) and hands of adults and was used for the adult MEI and MLEI evaluations for the residential, industrial/commercial and recreational scenarios. For the construction worker scenario, a skin surface area of 4,300 cm^2, representing the head, hands and forearms of an adult male, was used (USEPA, 1985).

The same USEPA sources (USEPA, 1989d; 1985) were used to determine the exposed skin surface areas for children (1-6 years). Specifically, the area for the arms, hands and head is 2,195 cm^2 based on the average for females (2,190 cm^2) and males (2,200 cm^2). This value was used for both the MEI and MLEI evaluations for the recreational and residential scenarios.

Soil-to-Skin Adherence Factor

Several studies have evaluated the amount of soil or dust that is likely to be in contact with skin. These studies (Lepow *et al.*, 1975; Roels *et al.*, 1980; Que Hee *et al.*, 1985; Driver *et al.*, 1989; Yang *et al.*, 1989) were evaluated in USEPA's *Dermal Exposure Assessment: Principles and Applications* (USEPA, 1992b), and it was determined that a range of values from 0.2 mg/cm^2 to 1.5 mg/cm^2 appears to be plausible. The report also concluded that since these studies are based on measurements of soil adherence to hands, they may in fact overestimate soil adherence for other body parts. Consequently, the USEPA believes that the lower end of the range (0.2 mg/cm^2) may be the best value to represent an average overall soil adherence factor, and 1 mg/cm^2 may be a reasonable upper bound value. Therefore, the upper bound value of 1 mg/cm^2 is used for the MEI evaluations, and 0.2 mg/cm^2 was used for the MLEI evaluations

for children and adults under the residential, industrial/commercial and recreational scenarios. As per IEPA guidance, the maximum reported soil adherence rate (1.5 mg/cm^2), which was determined for male children playing in a dirt school yard (Roels *et al.*, 1980), was conservatively used for the construction worker scenario (Hornshaw, *pers comm.* 1995).

Dermal Bioavailability

For dermal contact, Ryan *et al.* (1987) reports that a correction factor for dermal absorption of 1% is conservative for inorganics. This value represents the differential absorption of inorganics from dermal contact as compared with the ingestion exposure pathway. This value was used for the MEI and MLEI evaluations for all exposure scenarios and is consistent with IEPA guidance (IEPA, 1992).

Site-Specific Dermal Bioavailability

Similar to oral absorption, only the fraction of inorganics that can be released from the soil matrix in sweat on the skin is available for dermal absorption. Therefore, a simulated human sweat extraction experiment was conducted using South Works soil and simulated human sweat to determine the fraction of beryllium and manganese that could be extracted in sweat on the skin. Lead was not included in this study since lead is not dermally absorbed, and therefore, is not included in either the O'Flaherty or USEPA lead biokinetic models (Section 4.5). The experimental protocol was developed according to that outlined by Horowitz and Finley (1993); the complete protocol, which was approved by IEPA (March 30, 1995) prior to implementation, is presented in Appendix B. It should be noted that a high sweat to soil ratio (20:1) is a reasonable but conservative estimate of the amount of soil and sweat on the skin under heavy work activities (Horowitz and Finley, 1993). The extraction was performed at 37°C for 12 hours to simulate sweat and soil on the skin under worst-case or maximum extraction conditions. The results of this sweat extraction study are presented in Tables 4-2 and 4-3.

For manganese, the extraction percentages ranged from 0.02% to 0.96% with an arithmetic mean of 0.49%. For beryllium, the laboratory analyses for two of the samples (SW-A1 and

SW-A2) were affected by high levels of calcium, and as a result, the limits of detection (LODs) were raised (35 ppb). Neither of these samples contained detectable levels of beryllium. Because of this interference, these samples were excluded from the extraction percentages presented in this HRA. However, for the samples SW-B1 and SW-B2, the LODs (0.7 ppb) were not affected by this interference. These samples did not contain measurable levels of beryllium. Assuming beryllium is present at one-half the LOD (USEPA, 1989a), an extraction percentage of 0.34% was obtained. The arithmetic mean extraction percentages for beryllium (0.34%) and manganese (0.49%) were used in this HRA to represent release of these metals from the soil matrix in sweat on the skin. These values were multiplied by the dermal absorption correction factor of 1% reported by Ryan *et al.* (1987) to obtain bioavailability factors of 0.0034% for beryllium and 0.0049% for manganese. For those inorganics not addressed by this study, only the dermal absorption factor of 1% was used (assuming 100% extraction). These values were used for both the MEI and MLEI evaluations for all exposure scenarios as per IEPA guidance (IEPA, 1992).

4.4 CALCULATION OF REMEDIATION GOALS (RGs)

This section of the HRA presents the algorithms that were used to calculate the RGs using the exposure parameters and pathways described in the previous section, and in the IEPA approved PRA. Specifically, health-based RGs were developed for each exposure scenario (industrial/ commercial, recreational, residential, and construction). By using this approach, the RG specific to the ultimate land use can be applied to appropriate areas at the site.

Regulatory Criteria

RGs were calculated for an acceptable hazard index of 1 for noncarcinogenic chemicals, and an acceptable increased cancer risk range of 1×10^{-5} (one in a one hundred thousand theoretical excess cancer risk) to 1×10^{-6} (one in a million) for carcinogens. A hazard index of one indicates that the level of exposure is equal to an acceptable exposure level (reference dose) determined by the USEPA. An increased cancer risk of 1×10^{-6} indicates that, on a strictly

theoretical basis, one additional person of a population containing one million people will develop cancer. For a 1 x 10^{-5} risk, one excess cancer will theoretically occur in a population of one hundred thousand people. It is noteworthy that the natural background rate of cancer in the U.S. is 250,000 of a population containing one million people. The RG for each COI was calculated based on the above referenced hazard index and target risk range according to the calculations presented below. The potential total site risks, assuming additivity of effects, and the meaning of cancer risk estimates is discussed further in the Risk Characterization Section (Section 5.0).

Determination of RGs

The determination of RGs is a three-step process. First, the target level of acceptable cancer risk or noncarcinogenic health hazard is defined. Second, exposure rate is quantified using the exposure parameters for each route of uptake, and third, RGs are calculated. The methods for determining health-based acceptable soil concentrations (RGs) are presented as follows. RGs were calculated in this HRA to be protective against both potential noncarcinogenic and carcinogenic health effects for each potential future land use scenario.

Remediation goals in soil are derived by rearranging the pathway-specific dose equation to solve for an "acceptable" concentration of an individual chemical in soil. The standard equation to calculate dose for each pathway is as follows:

$$Dose = \frac{CS * CR * EF * ED * B * MET * DAF}{BW * AT}$$

where:

CS = Concentration in soil

CR = Contact rate (*i.e.*, soil ingestion rate)

EF = Exposure frequency

ED = Exposure duration

B = Bioavailability

MET = Meteorological factor

DAF = Dilution/Attenuation factor

BW = Body weight

AT = Averaging time

Rearranging the dose equation to solve for the acceptable concentration, or RG, of the individual chemical in soil yields:

$$CS = Dose * \left(\frac{BW * AT}{DAF * CR * EF * ED * B * MET}\right)$$

In this equation, CS is the chemical-specific RG calculated for soil at the beginning of exposure (time equal to 0). The dilution/attenuation factor (DAF) was derived as follows.

The concentration in soil, CS, used to calculate the dose is actually the average concentration in soil during the exposure duration, ED. For inorganics, this concentration is constant over the entire exposure duration. However, the concentration of an organic chemical in soil will decrease over time because of various chemical and biological degradation processes as discussed in Section 2.5. Assuming that the degradation of an organic chemical in soil is a first-order process, the concentration at a time, t is:

$$CS(t) = CS_0 e^{(-kt)}$$

where:

CS(t) = Concentration in soil at time t

CS_0 = Initial concentration in soil at time equal to 0

k = First order degradation constant

t = time

The degradation constant is related to the degradation half-life, and is equal to the natural logarithm of 2 (0.693) divided by the half-life ($T_{1/2}$). The average concentration in soil during the exposure duration can be calculated by integrating CS(t) and dividing the integral by the exposure duration. The resulting expression for the time-average soil concentration during the exposure duration, ED, is:

$$CS_{avg} = \frac{CS_0}{k\,ED} * [1 - e^{(-k\,ED)}] = CS_0 * DAF$$

The DAF for each organic COI incorporates a degradation constant calculated from the highest (or longest) literature reported half-life (Section 2.5). Use of this degradation constant facilitated the calculation of an RG that accounts for environmental degradation. For the inorganic COIs, the DAF is set equal to 1 (no degradation).

The exposure parameters, presented in the previous sections, were used to estimate the exposure factor portion of the dose equation for each pathway. The resulting "exposure factor" is in units of kg soil/kg body weight-day and represents the daily uptake of chemical per body weight. The exposure factors (XF) for each route of uptake were then combined with the appropriate dose-response criteria and target risk level to calculate the RGs, or the concentration of each COI in soil that will not pose a risk to human health under each exposure scenario.

Using XF to represent the exposure parameter portion of each pathway specific equation:

$$RG = Dose * XF$$

where:

$$XF = \frac{BW * AT}{DAF * CR * EF * ED * B * MET}$$

For the calculation of RGs, dose is defined as the acceptable daily intake of the COI. The acceptable daily intake for a chemical is defined by the following relationships:

$$Dose = \frac{TR}{CSF} \qquad \textit{(for carcinogens)}$$

$$Dose = THI * RfD \qquad \textit{(for noncarcinogens)}$$

where:

TR	=	Target risk level (1×10^{-5} or 1×10^{-6})
CSF	=	Cancer slope factor $(mg/kg\text{-}day)^{-1}$
THI	=	Target hazard index (1)
RfD	=	USEPA Reference Dose (mg/kg-day)

Each exposure scenario was assessed for soil ingestion and dermal contact as discussed previously. The construction worker scenario was evaluated for these pathways and the inhalation of particulates. Therefore, the denominator of the RG equation accounts for multiple routes of exposure by incorporating each complete exposure pathway. However, in accordance with IEPA guidance (1994), the soil ingestion pathway was counted twice for the PAHs (once for soil ingestion and once for dermal exposure). Therefore, the RG equations for the PAHs differ from those for the inorganics. The RGs were calculated as follows for the inorganics with the parameters previously defined.

Carcinogenic Responses for Inorganics for Residential, Industrial/Commercial and Recreational Scenarios:

$$RGs = \frac{TR}{(XF_{soil\ ingestion} * CSF_{oral}) + (XF_{dermal} * CSF_{oral})}$$

Carcinogenic Responses for Inorganics for Construction Worker Scenario:

$$RGs = \frac{TR}{(XF_{soil\ ingestion} * CSF_{oral}) + (XF_{dermal} * CSF_{oral}) + (XF_{inhalation} * CSF_{inhalation})}$$

Noncarcinogenic Response for Inorganics for the Residential, Industrial/Commercial and Recreational Scenarios:

$$RGs = \frac{THI}{(\frac{XF_{soil\ ingestion}}{RfD_{oral}}) + (\frac{XF_{dermal}}{RfD_{oral}})}$$

Noncarcinogenic Response for Inorganics for the Construction Worker Scenario:

$$RGs = \frac{THI}{(\frac{XF_{soil\ ingestion}}{RfD_{oral}}) + (\frac{XF_{dermal}}{RfD_{oral}}) + (\frac{XF_{inhalation}}{RfD_{inhalation}})}$$

For the PAHs, the following equations were used for evaluating carcinogenic response:

For the Residential, Industrial/Commercial and Recreational Scenarios:

$$RGs = \frac{TR}{2(XF_{soil\ ingestion} * CSF_{oral})}$$

For the Construction Worker Scenario:

$$RGs = \frac{TR}{2(XF_{soil\ ingestion} * CSF_{oral}) + (XF_{inhalation} * CSF_{inhalation})}$$

Because the PAHs that are COIs are considered carcinogenic, no equations for RGs protective of a noncarcinogenic response are required.

4.5 NONCANCER ASSESSMENT FOR LEAD

The USEPA has not promulgated an RfD or SF for lead on which to base a risk assessment. However, several modeling approaches have been developed to evaluate blood lead levels associated with environmental and dietary exposures to lead. As discussed in the preliminary risk assessment, the physiologically-based pharmacokinetic (PBPK) model for lead, developed by Dr. Ellen O'Flaherty of the University of Cincinnati, was deemed the most appropriate to evaluate potential future exposures at South Works because the PBPK model is: 1) capable of evaluating both children and adults, 2) capable of evaluating both short- and long-term exposure durations, 3) validated for a variety of exposure settings, and 4) published in the peer-reviewed scientific literature. However, at the request of IEPA, two other USEPA modeling approaches were presented in this assessment for comparison with the PBPK results and to ensure that all modeling approaches were adequately investigated. RGs for lead for the South Works site were determined using the O'Flaherty PBPK model and the USEPA modified-Bowers model for adults.

Each of the modeling approaches are discussed below.

The USEPA Integrated Exposure Uptake Biokinetic IEUBK Model For Lead

In 1989, the USEPA Office of Air Quality Planning and Standards (OAQPS) developed the IEUBK model to provide a method for predicting blood lead levels in populations exposed to lead in the air, diet, drinking water, indoor dust, soil, and paint (USEPA, 1994b). The model has been continually updated, and the most recent version (0.99D) was released in February, 1994. The IEUBK Model for lead estimates the total lead uptake (μg Pb/day) in children that results from diet, inhalation and ingestion of soil, dust, and paint. The model predicts a distribution of blood lead levels (μg Pb/dL) based upon total lead uptake. The model incorporates information on environmental levels of lead, estimates uptake based on several sets of exposure parameters, and outputs distributions of blood lead levels for children of ages 0 - 7 years, the most sensitive age group.

The IEUBK model is a classic multi-compartment pharmacokinetic model (the compartments represent volumes of chemical distribution) in which the rate constants governing the transfer of lead between compartments are based in part on kinetic data from a study in baboons (Mallon, 1983). Certain non-linearities associated with the uptake and distribution of lead have been included in the model, but the rate constants and compartmental parameters are not based on the actual anatomy or physiology of humans (O'Flaherty, 1995). Therefore, the IEUBK model is not expected to reliably predict blood lead levels outside certain conditions in which the model was validated. In this regard, USEPA (1994b) has listed certain limitations of the IEUBK model. These include:

1) The IEUBK model is not appropriate for rapidly varying exposures (on the order of days or weeks). It is only appropriate for evaluating relatively stable exposure situations that can be approximated by annual average values.

2) The IEUBK model is not appropriate for multi-unit residential dwellings.

3) The IEUBK model is designed for population averages, not individual specific exposure scenarios, and thus should only be used with average soil lead concentrations for a community.

4) The IEUBK model is only adequate for predicting blood lead concentrations for children up to seven years of age.

The model starts with an initial lead body burden for the fetus which is determined by a maternal uptake/biokinetic model that is also incorporated in the code. The geometric standard deviation of blood lead levels in children is used in conjunction with the mean blood lead level predicted by the model to determine a lognormal distribution of blood lead levels in children at six month age intervals.

O'Flaherty PBPK Model for Lead

A PBPK model for lead kinetics has been developed and validated for children and adults for a wide range of exposures to lead from a variety of exposure media (*i.e.*, soil, paint, diet, air, etc.) (O'Flaherty, 1991a,b,c; 1993; 1995). Appendix D contains the O'Flaherty publications on the PBPK model for lead.

This PBPK model consists of seven compartments: blood, plasma, bone, liver, kidney, other well-perfused tissue, and other poorly perfused tissue. The model incorporates bone as an explicit compartment whose volume, composition, and metabolic activity are all age-dependent (O'Flaherty, 1991a,b,c; 1993; 1995). The relationship between plasma lead and blood lead is expressed as a capacity-limited binding associated with the erythrocyte. Bone is divided into two subcompartments or regions, a surface region and a metabolically active region. Blood flows first through the surface region of rapid exchange before entering the metabolically active region where lead may be incorporated into mineralizing bone or returned to the blood from resorbing bone (O'Flaherty, 1991a,b,c; 1993; 1995). All remaining compartments store lead to different extents following exposure. The kinetic interactions of lead between compartments are all accounted for in this model description which allows for accurate determinations of blood lead concentrations.

The O'Flaherty PBPK model has the potential to predict the likely blood lead levels for a wide range of scenarios, including that of a single person by using the physiological parameters unique to that individual. This model has been carefully validated for humans and is well documented in the peer-reviewed literature (O'Flaherty, 1991a,b,c; 1993; 1995). The O'Flaherty PBPK model has been validated for: 1) both children and adults, 2) a wide range of exposure concentrations, 3) both short- and long-term exposure durations, and 4) both individuals and community populations. In fact, one of the validation tests of the O'Flaherty PBPK model was comparing model simulated output to blood lead concentrations for single individuals exposed to known concentrations of lead under a controlled setting. It is noteworthy that some of the default exposure parameters used in the PBPK model, such as background environmental media concentrations are more conservative (*i.e.*, health protective) than those used in the USEPA IEUBK model.

USEPA modified Bowers *et al.* (1994) Model

The USEPA modified Bowers *et al.*, (1994) model is also a biokinetic model, although less complex than the IEUBK. The Bowers model, which consists of one equation, was developed as a tool for predicting the adult blood lead concentration resulting from exposure to lead in different media. The parameters of the model were either adapted from other published sources or were derived by fitting the model to experimental results. The biokinetic slope factor (the model parameter which relates blood lead concentrations to lead exposures) was obtained by fitting the model equation to results form a study which related the blood lead concentration in 941 middle aged men to the lead concentration in their drinking water (Pocock *et al.*, 1983). Therefore, the Bowers model was derived for middle-aged men exposed for extended periods of time to background levels of lead. Because the parameters of the Bowers model have no physiological relation, the Bowers model cannot be expected to be reliable outside the range in which it was developed (*i.e.*, long-term exposures, adults, near background exposure levels). For these reasons, the USEPA modified Bowers model cannot be used to evaluate the short-term construction worker scenario which is discussed further in the following section.

Exposure Scenarios and Applications of Human Lead Models

At the request of IEPA, an additional scenario, the short-term construction worker, was evaluated for lead exposures. This scenario is protective of a female construction worker of child-bearing age who works for one month (5 days per week) in an area with the maximum measured levels of lead in soil.

As discussed above, each human lead disposition model has a theoretical scenario for which it is applicable. Thus, each model was not used for all previously defined exposure scenarios in this HRA. In particular, the short-term construction worker scenario was only modeled using the PBPK model because it is the only model which is valid for short durations of exposure. The models were utilized as described in the following table:

Scenario	USEPA IEUBK Model[a]	PBPK (O'Flaherty)[b]	Bowers *et al.* (1994)
Residential (child)	Blood Level (MEI)	RG (MEI, MLEI)	---
Recreational (child)	---	RG (MEI, MLEI)	---
Industrial/Commercial (adult)	---	RG (MEI, MLEI)	RG (MEI, MLEI)
Construction (adult)	---	RG (MEI, MLEI)	RG (MEI, MLEI)
Short-Term Construction (adult)	---	RG (MEI, MLEI)	---

--- Model not used for this evaluation.

a IEUBK model predicts blood lead concentrations, not used to calculate RGs.

b Model used to derive an RG for each exposure scenario.

The IEUBK model was used only to determine if exposure to lead at the site would elevate the blood lead concentrations of the potentially exposed residential child population above the acceptable blood level of 10 μg/dL established by the Centers for Disease Control (CDC) and the USEPA (CDC, 1991; USEPA, 1994b). This model was not used to determine an RG, as

it's methodology does not allow for one. The PBPK model was used to calculate RGs for all scenarios. The USEPA modified Bowers *et al.* (1994) model was used for the industrial/commercial and long-term construction (8 month of exposure) adult exposure scenarios and not the short-term construction because it is not validated for evaluating short-term exposures. The specific approach used for each modeling exercise and the results are detailed below.

4.5.1 USEPA IEUBK Model for Lead

For the MEI evaluation, the USEPA IEUBK model, with all USEPA recommended standard default input parameters, was employed. These parameters are presented in Table 4-4. It should be noted that some default values (*i.e.*, soil ingestion and inhalation rates) are not consistent with the parameters used in this HRA to calculate the RGs for the other chemicals. The only non-default site-specific input to the model was the soil concentration term as discussed below.

The USEPA IEUBK model was evaluated for the child MEI residential scenario. Only this scenario was evaluated as the model is only valid for children, and this scenario represents the greatest potential for exposure to the most sensitive population. For the calculation of the soil concentration term, the IEUBK guidance manual specifically states that the model

> "... is designed to evaluate relatively stable exposure situations, rather than rapidly varying exposures.... We recommend using a simple average or arithmetic mean of soil lead concentrations from a respective area of the child's yard..." (USEPA, 1994b)

As an added measure of conservatism, the 95% upper confidence limit on the arithmetic mean surface soil concentration (95% UCL) of 387 mg/kg was used in the evaluation rather than the simple arithmetic mean as suggested by USEPA guidance. This conservatism was incorporated to limit the potential underestimation of long-term average exposures.

Typically, a site is considered to pose no concern if the 95th percentile of the population blood lead distribution determined by the model is at or below 10 μg/dL (CDC, 1991; USEPA, 1994b). For this site, two different approaches were used to evaluate the potential health concerns at the site as a result of lead in soil. Specifically, the model was run with and without the meteorological adjustment factor. For the evaluation including the meteorological adjustment (Method A), an adjusted 95% UCL concentration was calculated and input to the model. This was performed because the IEUBK model does not have a means to input the meteorological factor, only a soil concentration term. The 95% UCL soil concentration was multiplied by the meterological factor in the following manner to calculate the adjusted 95% UCL:

$$\textit{Adjusted } 95\% \ UCL = 95\% \ UCL * MET$$

Where:

Adjusted 95% UCL	=	Concentration input term for surface soil lead;
MET	=	Meteorological factor (62%); and

Based upon this adjustment, a surface soil lead concentration of 240 mg/kg was input to the IEUBK model for Method A to represent a time-averaged concentration term to which children may be exposed at the site.

For Method B, all USEPA model defaults, as presented in Table 4-4, were used in conjunction with the 95% UCL for lead in surface soil at the site (387 mg/kg). No adjustment for meteorological conditions was made.

IEUBK Model Lead Results

The results of Method A and B are presented in Table 4-5 and are graphically illustrated in Figures 4-1 and 4-2. The results of Method A indicate that 97.89% of the exposed population will have blood level concentrations less than the regulatory criteria of 10 μg/dL. As stated previously, a site is not considered to pose a threat to human health if 95% of the potentially exposed population is at or below this regulatory criteria. For Method B, the results of the modeling exercise indicate that the site does not pose an unacceptable health threat as 95.58%

of the population will be at or below the regulatory criteria 10 μg/dL. Therefore, the USEPA IEUBK model indicates that, for the most sensitive population at the site (MEI, residential children) under a worst-case scenario (no meteorological adjustment and all USEPA default exposure factors), there is no significant risk due to lead exposure.

4.5.2 PBPK Model

The PBPK model was used in this HRA to determine RGs for each scenario based upon an acceptable blood lead level of 10 μg/dL (USEPA, 1994b; CDC, 1991). This criteria has been established to protect young children from the potential adverse health effects of lead on the neurological system. However, this value (10 μg/dL) was also used to evaluate adults under the residential, recreational, industrial/commercial and construction worker exposure scenarios to ensure the protection of any pregnant women or women of child-bearing age.

Exposure Parameters in the PBPK Model

For this HRA, USEPA default exposure parameters that were used in the USEPA IEUBK model for lead were also used in the PBPK model (Table 4-6). However, consistent with acceptable model inputs, the exposure frequencies (EFs) used for each scenario were converted into unitless values, and the site-specific meteorological factor was incorporated. For example, the residential EF for the MEI evaluation was derived by multiplying 350 days/year by the meteorological factor of 62% and then dividing the product by 365 days/year to yield a unitless EF of 0.59. The EFs for the recreational and industrial/commercial scenarios were derived in the same manner. For the long-term construction scenario (8 months), the 160 day/year exposure frequency was divided by 365 days/year to yield a unitless EF of 0.438, and, consistent with the assumptions for the construction scenario, the meteorological factor was not applied. For the short-term construction worker scenario, the model was run for an exposure duration of one month, and the EF was set at 0.71 (5/7 day). Additionally, the mean fraction of lead that was released from the soil matrix in the simulated gastric extraction study of 48.8% (as discussed

in Section 4.3.2) was input to the model to account for bioavailability via the soil ingestion pathway.

For the long-term construction scenarios, the predicted concentrations of lead in air were calculated using the 95% UCL and mean lead soil concentrations for the MEI and MLEI, respectively, and the soil suspension factors discussed in Section 4.3.3. The air concentration terms were developed as described below.

Long-term Construction Worker

$$\textit{MEI Air Concentration}\left(1.1\ \frac{\mu g}{m^3}\right) = \left(5.0\ \frac{mg}{m^3}\right) * \left(1 \times 10^{-6}\ \frac{kg}{mg}\right) * \left(225\ \frac{mg\ Pb}{kg}\right) * \left(1{,}000\ \frac{\mu g}{mg}\right)$$

$$\textit{MLEI Air Concentration}\left(0.008\ \frac{\mu g}{m^3}\right) = \left(0.05\ \frac{mg}{m^3}\right) * \left(1 \times 10^{-6}\ \frac{kg}{mg}\right) * \left(163\ \frac{mg\ Pb}{kg}\right) * \left(1{,}000\ \frac{\mu g}{mg}\right)$$

As described below, for the MEI long-term construction scenario, the 95% UCL for both surface and subsurface soil (225 mg/kg) was used as the lead concentration term for particulates. For the MLEI, the site-wide mean for surface and subsurface soil (163 mg/kg) was used. This approach was utilized as it is reasonable to expect that suspended particulates will be derived from the entire site for 8 month construction period rather than individual sample locations. For the short-term construction scenario (30 days), it is assumed that a worker could be exposed to the maximum concentration of lead in soil throughout the exposure period. Therefore, the air concentration term in the model is dependant on the soil concentration (or RG) and is derived using the model.

The resulting RGs calculated for each scenario are presented in Table 4-7. The resulting RG for a residential child scenario is consistent with the USEPA interim soil cleanup guidance, developed in 1989 by the Office of Solid Waste and Emergency Response (directive number

9355.4-02) which states that cleanup levels of 500 to 1,000 mg/kg for residential settings should be health protective (USEPA, 1989c). This USEPA cleanup guidance was reiterated in a memorandum dated July 14, 1994 (OSWER Directive 9355.4-12).

4.5.3 USEPA Modified Bowers *et al.* Model for Lead

The results of the USEPA modified Bowers *et al.* (1994) model for evaluating adult lead exposure was used for comparison with those of the PBPK model. The USEPA modified Bowers *et al.* model is not a physiologically-based biokinetic model, and as such, does not account for the different capacity-limiting processes associated with the inter-compartmental transfer of lead. With this in mind, the Bower *et al.* model was used to calculate RGs for the adult long-term construction and industrial/commercial scenarios. The equation used is presented below:

$$RG = \frac{(PbB_{GM}\ target - PbB_o)}{BKSF\ (IR * AF * B * EF * ED * MET)}$$

$$PbB_{GM}\ Target = PbB_{GM}\ Maternal = \frac{PbB_{95th}\ Maternal}{GSD^{1.645}}$$

where:

$$Pb_{95th}\ maternal = \frac{PbB_{95th}\ fetal}{R}$$

where:

PbB_{GM}target	=	Target geometric mean blood lead concentration
PbB_o	=	Initial blood lead concentration
BKSF	=	Biokinetic Slope Factor

IR	=	Soil Ingestion Rate
AF	=	Fraction of lead in soil that is systemically absorbed
B	=	Fraction of lead in soil that is released from the soil matrix and available for absorption based on the site-specific bioavailability study
EF	=	Exposure Frequency
ED	=	Exposure Duration
MET	=	Meteorological Adjustment Factor
GSD	=	Geometric Standard Deviation
PbB_{GM}Maternal	=	Geometric mean blood lead concentration of mother
PbB_{95th}Fetal	=	95th percentile blood lead concentration of fetus
R	=	Ratio of blood lead concentration of fetus vs. mother

The USEPA modified Bowers *et al.*, exposure parameters are presented in Table 4-8. Soil ingestion bioavailability and the meteorological factor were incorporated into the model consistent with the other modeling approaches. However, as for the PBPK model, the exposure frequencies (EFs) were input to the model as unitless fractions. For the MEI and MLEI industrial/commercial evaluations, a unitless EF of 0.68 (250/365 days) was derived assuming 250 days of exposure per year. For the long-term construction worker evaluations, a unitless EF of 0.44 (160/365 days) was derived assuming 5 days of exposure per week for 8 months.

The RGs calculated using the USEPA modified Bowers *et al.*, model for the MEI and MLEI industrial/commercial worker scenarios are 6,580 mg/kg and 40,900 mg/kg, respectively. These concentrations are generally consistent with the RGs calculated using the PBPK model of 6,150 mg/kg and 72,800 mg/kg for the MEI and MLEI, respectively. The RGs calculated for the long-term construction worker MEI and MLEI scenarios were 1,660 mg/kg and 6,640 mg/kg,

respectively. The corresponding RGs calculated using O'Flaherty were approximately two-fold higher (3,750 mg/kg for the MEI and 15,600 mg/kg for the MLEI).

TABLE 4-1

EXPOSURE PARAMETER SUMMARY FOR THE
SOUTH WORKS RISK ASSESSMENT

EXPOSURE PARAMETER	Industrial Commercial Scenario		Residential Scenario				Recreational Scenario				Construction Scenario	
	Adult		Adult		Child		Adult		Child		Adult	
	MEI	MLEI	MEI	MLEI	MEI	MLEI	MEI	MLEI	MEI	MLEI	MEI	MLEI
Exposure Duration (year):	25	4.5	24	3.3	6	6	24	3.3	6	6	1	1
Exposure Frequency (days/year):	250	250	350	350	350	350	104	104	104	104	160	160
Body Weight (kg):	70	70	70	70	15	15	70	70	15	15	70	70
Bioavailability												
oral (antimony, cadmium):	100%	100%	100%	100%	100%	100%	100%	100%	100%	100%	100%	100%
oral (beryllium)[a]:	6.9%	6.9%	6.9%	6.9%	6.9%	6.9%	6.9%	6.9%	6.9%	6.9%	6.9%	6.9%
oral (manganese)[a]:	23.5%	23.5%	23.5%	23.5%	23.5%	23.5%	23.5%	23.5%	23.5%	23.5%	23.5%	23.5%
oral (PAHs):	50%	50%	50%	50%	50%	50%	50%	50%	50%	50%	50%	50%
dermal (antimony, cadmium):	1%	1%	1%	1%	1%	1%	1%	1%	1%	1%	1%	1%
dermal (beryllium)[a]:	0.0034%	0.0034%	0.0034	0.0034%	0.0034%	0.0034%	0.0034%	0.0034%	0.0034%	0.0034%	0.0034%	0.0034%
dermal (manganese)[a]:	0.0049%	0.0049%	0.0049%	0.0049%	0.0049%	0.0049%	0.0049%	0.0049%	0.0049%	0.0049%	0.0049%	0.0049%
Averaging Time (days)												
Potential Carcinogens:	25,550	25,550	25,550	25,550	25,550	25,550	25,550	25,550	25,550	25,550	25,550	25,550
Noncarcinogens:	9,125	1,643	8,760	1,205	2,190	2,190	8,760	1,205	2,190	2,190	365	365
Soil Ingestion Rate (mg/day):	50	10	50	10	200	50	50	10	200	50	200	50
Exposed Skin Surface Area (cm^2):	2,836	2,836	2,836	2,836	2,195	2,195	2,836	2,836	2,195	2,195	4,300	4,300
Adherence Factor (mg/cm^2):	1.0	0.2	1.0	0.2	1.0	0.2	1.0	0.2	1.0	0.2	1.5	1.5
Meteorological Factor (unitless):	0.62	0.52	0.62	0.52	0.62	0.52	0.62	0.52	0.62	0.52	NA	NA
Inhalation Rate (m^3/8 hrs a day):	NA	NA	NA	NA	NA	NA	NA	NA	NA	NA	20	20
Particulate Concentration (mg/m^3):	NA	NA	NA	NA	NA	NA	NA	NA	NA	NA	5	0.05

NA Not applicable.
a Based on the site-specific extraction studies (Section 4.3).

TABLE 4-2
SWEAT AND GASTRIC STUDY ALIQUOT DATA

Sample Identification	Aliquot Volume Recovered (mL)	Recovered Aliquot Concentration		
		Manganese (mg/L)	Beryllium (mg/L)	Lead (mg/L)
SIMULATED HUMAN SWEAT STUDY				
SW-A1	185	0.32	NE	NA
SW-A2	174	0.26	NE	NA
SW-B1	184	2.7	0.00035	NA
SW-B2	188	2.7	0.00035	NA
Sweat Solution Blank	NA	0.027	<0.005	NA
SIMULATED GASTRIC CONDITIONS STUDY				
GA-A1	244	NA	NA	1.8
GA-A2	244	NA	NA	1.6
GA-B1	245	16	---	NA
GA-B2	244	16	---	NA
GA-C1	243	7.2	---	1.3
GA-C2	244	6.1	---	1.1
GA-Y	96.[illegible]	NA	0.039	NA
GA-Z	97	NA	0.035	NA
Gastric Acid Blank	NA	<0.010	<0.005	0.003

NE Not evaluated due to matrix interference.
NA Not analyzed for this aspect of the study.
< Chemical not detected at the limit of detection indicated.
--- Chemical not evaluated for this sample due to insufficient reporting limit.

TABLE 4-3
RESULT OF THE SWEAT AND GASTRIC STUDIES

Sample ID	Soil Sample Weight (grams)	Manganese			Beryllium			Lead		
		Mass in Soil (mg)	Mass in Aliquot (mg)	Percent Extracted	Mass in Soil (mg)	Mass in Aliquot (mg)	Percent Extracted	Mass in Soil (mg)	Mass in Aliquot (mg)	Percent Extracted
SIMULATED HUMAN SWEAT STUDY SAMPLES										
SW-A1	10.01	240.2	0.0592	0.02%	0.01602	NE	NA	1.4014	NA	NA
SW-A2	9.17	220.1	0.04524	0.02%	0.01467	NE	NA	1.2838	NA	NA
SW-B1	10.00	52.0	0.4968	0.96%	0.0190	0.000064	0.34%	5.200	NA	NA
SW-B2	10.01	52.1	0.5076	0.98%	0.0190	0.000066	0.35%	5.2052	NA	NA
		Mean Extraction Percentage:		**0.49%**	**Mean Extraction Percentage:**		**0.34%**	**Mean Extraction Percentage:**		**NA**
SIMULATED GASTRIC CONDITIONS STUDY SAMPLES										
GA-A1	1.04	11.44	NA	NA	0.00125	NA	NA	1.0192	0.4392	43.1%
GA-A2	0.99	10.89	NA	NA	0.00119	NA	NA	0.9702	0.3904	40.2%
GA-B1	1.03	24.72	3.92	15.9%	0.00165	---	NA	0.1442	NA	NA
GA-B2	1.01	24.24	3.904	16.1	0.00162	---	NA	0.1414	NA	NA
GA-C1	1.01	5.252	1.7496	33.3%	0.00192	---	NA	0.5252	0.3159	60.2%
GA-C2	1.00	5.200	1.4884	28.6%	0.00190	---	NA	0.5200	0.2684	51.6%
GA-Y	NA	NA	NA	NA	0.014	0.003764	26.88	NA	NA	NA
GA-Z	NA	NA	NA	NA	0.014	0.003395	24.25	NA	NA	NA
		Mean Extraction Percentage:		**23.5%**	**Mean Extraction Percentage:**		**25.6%**	**Mean Extraction Percentage**		**48.8%**

NA Not analyzed.
NE Not evaluated for this sample.
--- Chemical not evaluated for this sample due to insufficient reporting limit.

TABLE 4-4

PARAMETERS USED IN USEPA IEUBK MODEL FOR LEAD

Parameter		MEI Evaluation	
		Method A	Method B
Estimated Outdoor Air Concentration ($\mu g/m^3$) [a]		0.1	0.1
Estimated Indoor Air Concentration (% of outdoor) [a]		30	30
Ventilation Rate (m^3/day) [a]			
	Age 0-1	2	2
	1-2	3	3
	2-3	5	5
	3-4	5	5
	4-5	5	5
	5-6	7	7
	6-7	7	7
Dietary Intake (μg/day) [a]			
	Age 0-1	5.53	5.53
	1-2	5.78	5.78
	2-3	6.49	6.49
	3-4	6.24	6.24
	4-5	6.01	6.01
	5-6	6.34	6.34
	6-7	7.00	7.00
Concentration in Drinking Water (μg/L) [a]		4	4
Drinking Water Consumption (L/day) [a]	Age 0-1	0.2	0.2
	1-2	0.5	0.5
	2-3	0.52	0.52
	3-4	0.53	0.53
	4-5	0.55	0.55
	5-6	0.58	0.58
	6-7	0.59	0.59
Concentration in Soil (mg/kg)		240[c]	387[b]
Concentration in Dust (mg/kg) [a]		200	200

TABLE 4-4 (Cont.)

PARAMETERS USED IN USEPA IEUBK MODEL FOR LEAD

Parameter		MEI Evaluation	
		Method A	Method B
Soil/Dust Ingestion Rate (mg/day) [b]			
	Age 0-1	85	85
	1-2	135	135
	2-3	135	135
	3-4	135	135
	4-5	100	100
	5-6	90	90
	6-7	85	85
Bioavailability (%) [b]			
	Soil/Dust	30	30
	Water	50	50
	Food	50	50
Lung Absorption (%) [b]		32	32

a Default values (USEPA, 1994d).
b 95% UCL of site surface soil.
c Adjusted 95% UCL of site surface soil incorporating the site-specific meteorological factor (62%).

TABLE 4-5

IEUBK MODEL RESULTS

Methodology	MEI Evaultion[c] Resulting Percentile Below 10 μg/dL
Method A[a]	97.89
Method B[b]	95.58

a Method relied upon USEPA model defaults and the site-specific meteorological factor.

b Method relied upon USEPA model defaults (1994).

c USEPA/CDC criteria stipulate that at least 95 % of the population must be below 10 μg/dL.

TABLE 4-6

PARAMETERS USED IN PBPK MODEL FOR LEAD

Parameter	MEI Evaluation	MLEI Evaluation
Exposure Frequency - Soil Ingestion[a]		
Construction Scenario:	0.438	0.438
Industrial/Commercial Scenario:	0.423	0.356
Residential Scenario	0.594	0.499
Recreational Scenario:	0.177	0.148
Exposure Frequency - Particulate Inhalation[a]		
Construction Scenario:	0.438	0.438
Estimated Outdoor Air Concentration ($\mu g/m^3$)		
Construction Scenario[b]:	1.1	0.008
All Other Scenarios[c]:	0.15	0.15
Inhalation Rate (m^3/day)[c]		
Child:	14.2	14.2
Adult:	9.7	9.7
Dietary Intake (μg/day)[c]		
Child:	6.2	6.2
Adult:	30.0	30.0
Concentration in Drinking Water (μg/L)	4	4
Drinking Water Consumption (L/day)[c]		
Child:	0.5	0.5
Adult:	2.0	2.0
Soil Ingestion Rate (mg/day)[d]		
Child (age specific): 0 - 1:	85	85
1 - 4:	135	135
4 - 5:	100	100
5 - 6:	90	90
6 - 7:	85	85
Adult (Construction Scenario):	200	50
Adult (All Other Scenarios)	50	10
Gastrointestinal Absorption (%)[e]		
Child:	26	26
Adult:	8	8
Bioavailability (%)[e]	48.8	48.8

a Based upon the exposure frequencies discussed in Section 4.3.
b Based upon the particulate air concentrations discussed in Section 4.3.
c Model default parameters (O'Flaherty, 1991a,b,c; 1993; 1995)
d USEPA default parameters (USEPA, 1994a).
e Site-specific bioavailability (Section 4.3.2).

TABLE 4-7

PBPK MODEL RESULTS

Scenario	RGs for Soil (mg/kg)	
	MEI Evaluation	MLEI Evaluation
Residential Scenario	932	932
Recreational Scenario	3,790	3,790
Industrial/Commercial Scenario	6,150	72,800
Long-term Construction Scenario	3,750	15,600
Short-term Construction Scenario	2,080	18,650

TABLE 4-8

PARAMETERS USED IN THE BOWERS *et al.* MODEL FOR LEAD INDUSTRIAL/COMMERCIAL SCENARIO

MODEL PARAMETER	VALUE
R (Mean ratio of fetal to maternal PbB)	0.85[a]
Individual geometric standard deviation (GSD)	1.8[a]
Baseline blood lead value (PbB_0) (μg/dL)	2.2[a]
Biokinetic slope factor (BKSF) (μg/dL per μg/day)	0.4[a]
Soil ingestion rate (IR) (mg/day)	
Industrial Commercial MEI:	50[b]
MLEI:	10[b]
Construction MEI:	200
MLEI:	50
Exposure frequency (days/week) (%) Industrial/Commercial:	0.68[c]
Construciton:	0.44[d]
Meterological factor (%)	
Industrial/ Commercial MEI:	0.62
MLEI:	0.52
Construction:	1.0
Oral absorption fraction for lead in soil or dust (%)	0.08[a]
Bioavailability Matrix Release Fraction (%)	48.8[e]

a IEPA suggested value.
b See Section 4.3.2.
c Based upon 250 days/365 days (USEPA, 1991).
d Based on 160/365 days.
e Based on site-specific bioavailability study (Section 4.3.2.).

FIGURE 4-1

INTEGRATED EXPOSURE UPTAKE BIOKINETIC MODEL RESULTS METHOD A

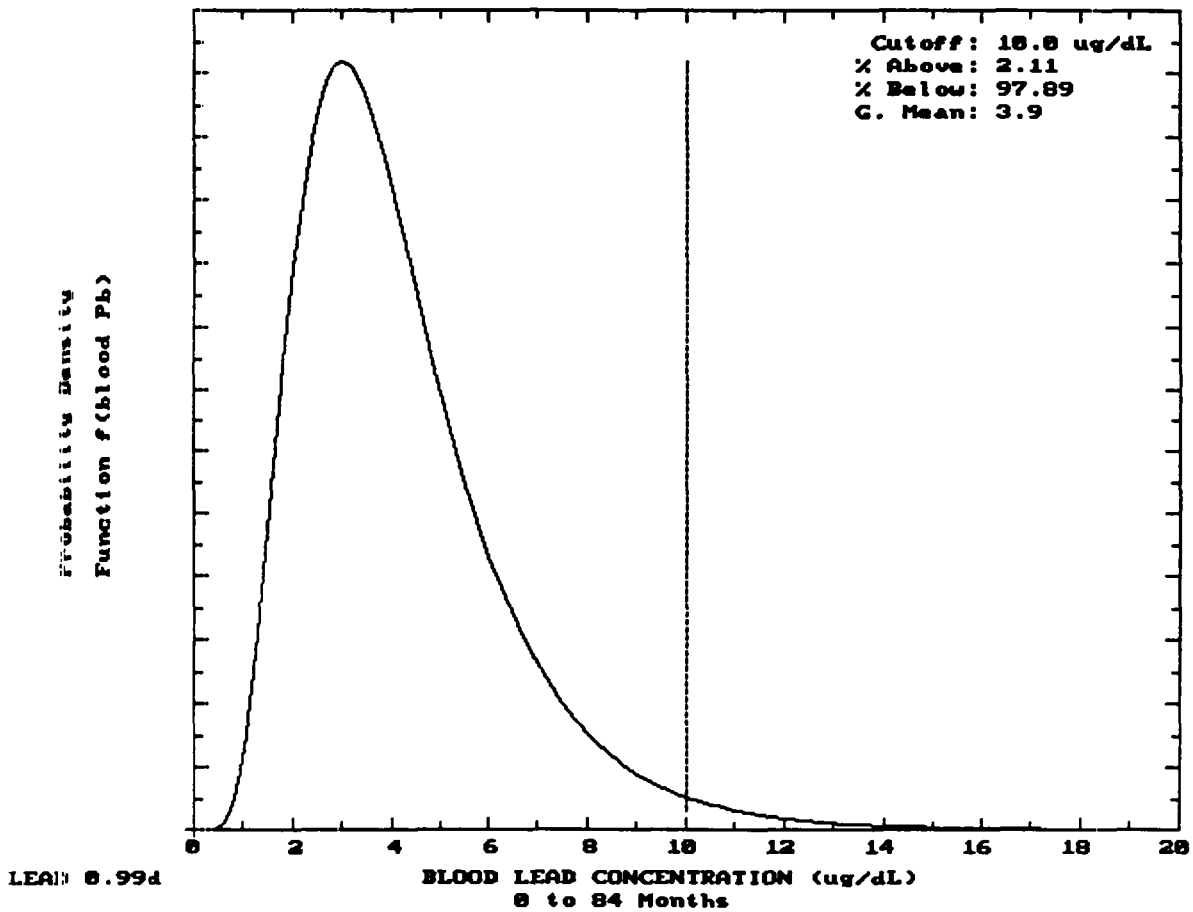

Results obtained using 387 mg/kg surface soil concentration and site-specific meteorological factor.

FIGURE 4-2

INTEGRATED EXPOSURE UPTAKE BIOKINETIC MODEL RESULTS METHOD B

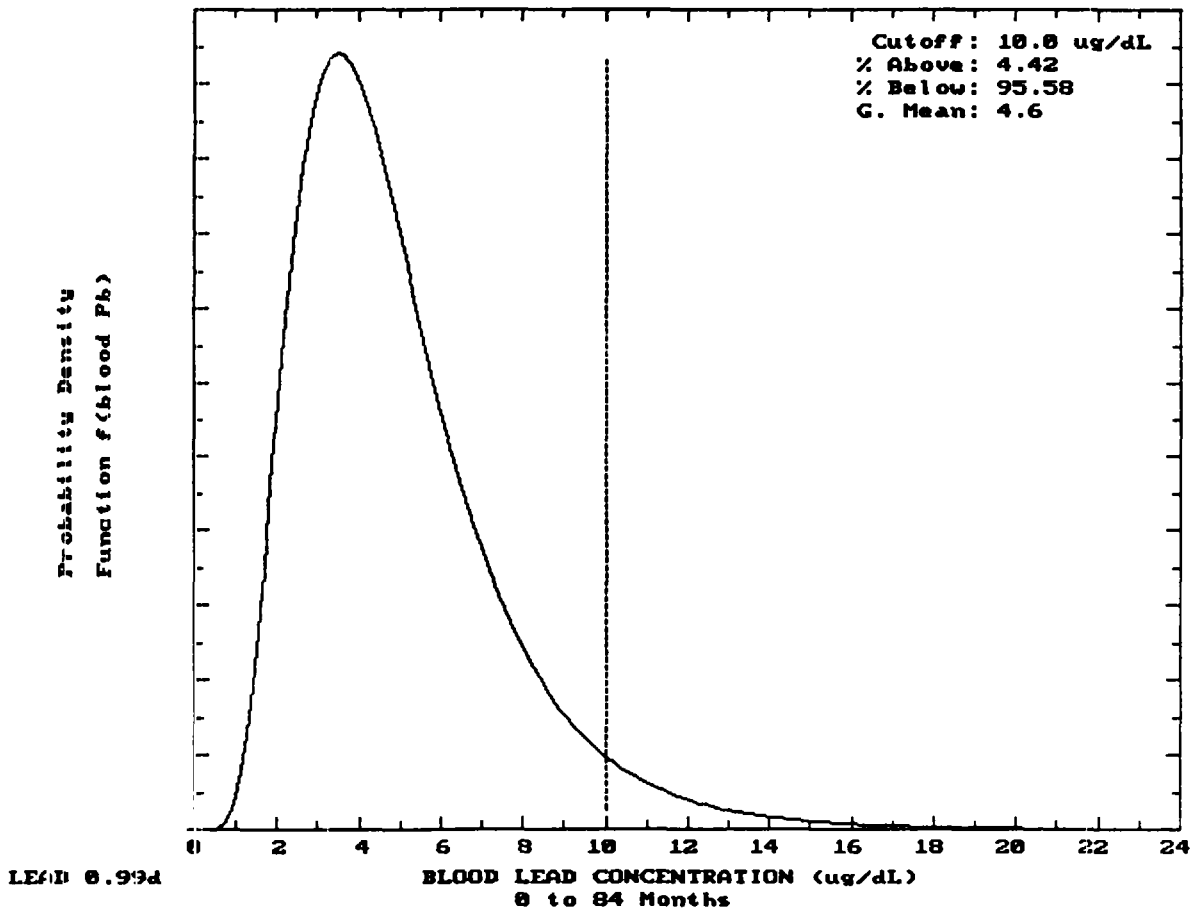

Results obtained using 387 mg/kg surface soil concentration and USEPA default parameters.

5.0 RISK CHARACTERIZATION

This section of the risk assessment compares the RGs to each individual soil sample collected in the Phase III Site Investigation and the RGs for lead to sampling data from all three phases (WTI, 1993a,b; 1994). The RGs protective of carcinogenic responses are based on a theoretical excess cancer risk range of 1×10^{-5} to 1×10^{-6} for each chemical individually, and the RG for each noncarcinogenic COI is based on a hazard index of one as previously agreed upon by USX and the IEPA (ChemRisk®, 1995).

Should two or more carcinogens occur in the same area at or just below their respective RGs at a 10^{-5} risk, the total additive risk will exceed the 1×10^{-5} risk level. However, even if all of the carcinogens occur together at any one location at their RG levels at the South Works site, the total cancer risk will not exceed the USEPA acceptable risk range of 10^{-4} to 10^{-6} (USEPA, 1989a), as there are less than 10 potential carcinogens identified in soil at the South Works site ($10^{-5} * 10 = 10^{-4}$). The same relationship holds true for noncarcinogens affecting the same target organ. Additivity of cancer risk and noncancer hazards due to multiple chemical exposures at South Works are discussed further in the Section 5.1.

5.1 REMEDIATION GOALS (RGs)

As discussed in Section 4.0, RGs were calculated for the following future land use scenarios: residential (child and adult), recreational (child and adult), industrial/commercial (adult only), and construction scenarios (adult only). For the carcinogenic COIs, child and adult exposures were combined to calculate the lifetime average exposure per USEPA guidance (USEPA, 1989a). Each scenario evaluated potential exposure via incidental soil ingestion and dermal

1991), and 10 mg per day for adults (Paustenbach, 1987; Calabrese *et al.*, 1991) as discussed in Section 4.3.2], the resulting RG would be 10 mg/kg. Therefore, even the maximum concentration of beryllium in site soil (9.8 mg/kg) would fall below the RG for the residential MEI scenario for the 10^{-6} risk level. These rates of soil ingestion, as taken from the recent scientific literature, are more realistic and have been used for evaluating the MEI scenario in another IEPA-approved risk assessment (ChemRisk®, 1989).

Uncertainties associated with the evaluation of beryllium as a carcinogen and the USEPA cancer slope factor for beryllium are discussed in Section 5.2.2.

Comparison of Site Data with RGs Protective of a 10^{-5} Cancer Risk

The concentrations of all chemicals in South Work's soil were below the RGs protective of a 10^{-5} theoretical increased cancer risk. As discussed in Section 5.3, the use of a 10^{-5} acceptable risk level is consistent with past regulatory decision making.

Comparison of Site Data with RGs Protective of a Noncancer Hazard

The RGs for all noncarcinogenic chemicals, except lead, for all exposure scenarios (MEI and MLEI) are higher than the concentrations of the noncarcinogenic chemicals in site soils. Three samples contained lead at levels that exceed the residential RG calculated for the MEI scenario (932 mg/kg) using the O'Flaherty PBPK model. Specifically, samples SS-9-01, SS-27-01, and SS-28-01 contain lead concentrations of 3,200, 1,200, and 1,500 mg/kg, respectively. In addition, the lead RG for the MEI short-term construction worker scenario (2,080 mg/kg) exceeded the concentration of lead at one sampling location (SS-9-01) which contained the maximum lead concentration (3,200 mg/kg). This location also exceeded the RG for the long-term construction MEI scenario calculated using the USEPA modified Bowers *et al.* (1994) modeling approach, as well as the residential MEI, and should be addressed prior to site redevelopment. Site soil concentrations did not exceed the lead RGs for any other scenario.

The locations of samples where lead concentrations exceed the RGs are provided on Figure 5-2. Analytical data from confirmatory sampling in areas currently undergoing demolition,

remediation (sewers) or sediment removal will be compared to the RGs calculated in this HRA to ensure protection of public health.

Additivity of Risk

With the exception of beryllium, the RGs for all of the carcinogenic COIs at a 10^{-5} risk are more than an order of magnitude higher than the maximum measured concentrations. Therefore, the total additive risk associated with multiple chemical exposures, for all scenarios, at South Works does not exceed the 10^{-5} acceptable risk level. Likewise, for the noncarcinogenic chemicals, multiple chemical exposures would not result in a total hazard index greater than one, except where the concentrations of lead alone exceed the RG for the MEI residential scenario. This is because, as discussed in the Dose Response Section (3.0), only lead and manganese have the same critical effect (the central nervous system disorders) by the oral and/or dermal routes of exposure (the only exposure pathways of interest for the residential, recreational and industrial/commercial scenarios), and the RGs for manganese are more than twice the maximum levels of manganese measured in surface and subsurface soils.

If beryllium was excluded from consideration, the total additive risk would exceed the 10^{-6} risk level at only one sample location, SB-37-1, where, for the residential MEI, both benzo(a)pyrene and dibenz(a,h)anthracene were detected at their maximum concentrations. This conclusion was drawn by comparing the measured concentrations of each PAH to their residential RGs at a 10^{-6} risk level. For both PAHs at SB-37-1, the measured concentration was less than half of the RG (Table 5-2), and therefore, when considered together, the total risk would exceed the 10^{-6} risk level. For all other scenarios and sample locations, the total additive risk would not exceed 10^{-6}.

5.2 UNCERTAINTY ANALYSIS

There are multiple sources of uncertainty that may be identified for any risk characterization. These include, among others, uncertainty associated with the toxicity criteria used to derive dose-response factors, uncertainties associated with exposure parameters used in the exposure

assessment and uncertainties associated with combining exposure parameters and toxicity criteria in the risk characterization.

Some level of uncertainty is introduced into a risk assessment each time an assumption is relied upon to describe a dynamic parameter. Some assumptions have a significant scientific basis, while others do not which results in the selection and use of conservative, default exposure parameters in the exposure assessment. The selection of multiple conservative assumptions in the exposure assessment generally results in an overestimation of potential health risks associated with exposure to specific chemical constituents. The primary areas of uncertainty for this risk assessment are qualitatively discussed below.

5.2.1 Uncertainties Associated with Site Sampling

Three major soil sampling efforts have been completed by Waste Technology, Inc. (WTI) to characterize the environmental condition of the South Works site. Samples obtained during both the Phase I and Phase II investigations were deliberately biased in an attempt to locate the greatest level of potential contamination at the site. Sample biasing was accomplished based on visual observations such as color, texture and moisture. Odor was also considered in sample location selection. For example, if 1,000 square feet of TPH staining was observed, the individual conducting the sampling obtained the sample from that spot within the 1,000 square feet having the darkest color and most odor. Similarly, if suspected electric furnace dust was observed covering an area, the sample was obtained only of the dust, at the exclusion of slag, soil or other soil components.

A soil sampling grid was established for the Phase III investigation of the South Works site. Soil samples were obtained at pre-determined locations and depths throughout the entire site. Unlike sampling in previous phases, all materials (*e.g.*, soil, slag, etc.) found within the pre-established sampling locations were included in the sample sent to the laboratory for analyses. Because the sampling methodology employed in the Phase III investigation was not biased, but evenly and uniformly covered the site, the Phase III data are the most appropriate for use in the

risk assessment. Uncertainties associated with these data do not bias the assessment in either direction (*i.e.*, neither overestimate or underestimate risk).

It should be noted that analytical data from confirmatory sampling in areas currently undergoing demolition, remediation (sewers) or sediment removal will be compared to the RGs calculated in this HRA. Additional areas of remediation may be identified in the future and are not shown in this report.

5.2.2 Uncertainties Associated With the Dose-Response Assessment

A large source of uncertainty in risk assessment is derived from the quantitative indices of toxicity [reference doses (RfDs) and slope factors (SFs)]. To compensate for uncertainties, RfDs and SFs are based on concepts and assumptions that bias an evaluation in the direction of overestimation of health risk. The degree of uncertainty associated with RfDs and SFs is dependent on the amount and type of information available, as well as the overall confidence in the data set used to derive these factors.

As discussed in Section 3.0, an RfD is an estimate of the daily exposure to the population that is likely to be without an appreciable risk of deleterious effects during a lifetime. An uncertainty factor is used in calculating the RfD and reflects scientific judgement regarding the various types of data used to estimate RfD values. An uncertainty factor of 10 is generally used to account for variations in human sensitivity when extrapolating from valid human studies involving long term exposure of average healthy subjects or worker populations. An additional factor, ranging in value from 1 to 10, is generally used to account for the uncertainty in each of the following extrapolations: from long-term animal studies to humans, from a LOAEL (lowest observed adverse effect level) to a NOAEL (no observed adverse effect level) and from subchronic exposures to lifetime exposures, as appropriate. An additional modifying factor ranging from 1 to 10 may be applied based on professional judgement in the quality of the toxicity data base. The default value for this modifying factor is 1 (USEPA, 1993a).

The uncertainty factor associated with the RfD for manganese is 1, indicating a low level of uncertainty although the overall level of confidence in the toxicity data is low. In this case, the RfD is based on an epidemiological study of a sensitive human population, exposed over their lifetime, to manganese in drinking water (Kondakis *et al.*, 1989). Greater uncertainty is present in the RfD for antimony with an uncertainty factor of 1,000. Because uncertainty factors are always incorporated into RfDs, it is unlikely that any RfD underestimates risk.

Additionally, USEPA cancer SFs are developed using variations of the Linear Multistage Model (LMS) for carcinogenicity. The LMS is highly conservative as it assumes strict linearity between dose and effect to zero dose assuming no threshold for carcinogenicity. However, the human body has mechanisms to detoxify most chemicals particularly at low doses, and therefore many scientists believe that most, if not all carcinogens, only cause cancer above a "threshold dose."

Beryllium

Beryllium has never been shown to cause cancer in animals or humans by the oral route of exposure. Even though occupational exposure to beryllium has been studied extensively, no studies have demonstrated a statistically significant increased risk of cancer in humans exposed to beryllium. However, based on an evaluation of all toxicity data combined, USEPA associates an increased lung cancer rate with inhalation exposure to beryllium, ranking it as a probable human carcinogen (B2). Beryllium has been shown to induce lung cancer in rats and monkeys upon inhalation and osteosarcomas (bone cancer) in rabbits upon intravenous and intramedullary injection. The Agency for Toxic Substances and Disease Registry (ATSDR) conducted a literature search to review the published research regarding the carcinogenic potential of beryllium, when administered orally, and concluded that "beryllium has not been found to cause cancer in animals after oral exposure." The animal carcinogenicity data that do exist are described briefly below.

Morgareidge *et al.* (1975) found a carcinogenic response (osteosarcomas) in male rats upon exposure to 0.3 and 2.8 mg beryllium/kg-day in the diet for two years. However, no increased

incidence was observed among the highest dose group (31 mg beryllium/kg-day) in either male or female rats. Schroeder and Mitchener (1975a,b) did not observe an increased incidence of tumors in rats or mice exposed chronically to 0.7-0.95 mg beryllium/kg-day, respectively, as beryllium sulfate in drinking water. The incidence of total tumors in treated male rats (9 of 33) was slightly increased (but not statistically significantly elevated) as compared to controls (4 of 26). ATSDR concludes that none of the available literature provide conclusive evidence that beryllium is carcinogenic via oral exposure.

Despite this lack of evidence, the USEPA has derived an oral slope factor (SF) for beryllium. The *Integrated Risk Information System* (IRIS) (USEPA, 1995b) provides the basis of the USEPA derived SF. Specifically, osteogenic sarcomas were observed in a total of 16 separate studies evaluating rabbits by intravenous and intramedullary injection (USEPA, 1991c). Tumors were induced by beryllium oxide, zinc beryllium silicate, beryllium phosphate, beryllium silicate, and beryllium metal. No bone tumors were reportedly induced by intravenous injection of beryllium oxide or zinc beryllium silicate in rats or guinea pigs (Gardner and Heslington, 1946). The Agency's discussion of confidence for the oral SF provides very little as to the rationale for classifying beryllium as an oral carcinogen. In fact, the IRIS states that

> "...the estimate [slope factor] is derived from a study which did not show a significant increase in tumorigenic response. While this study is limited by use of only one non-zero dose group, the occurrence of high mortality and unspecified type and site of tumors, it was used as the basis of the quantitative estimate because exposure occurred via the most relevant route [oral]."

The SF for beryllium is particularly conservative (*i.e.*, health protective) in that it is based on a single (non-zero) data point from a rat bioassay which represents a nonstatistically significant increased rate of cancer found in the Schroeder and Mitchener (1975a) study (USEPA, 1995b). In addition, the SF was calculated using the "ultra risk" version of the Linearized Multi-Stage Model which assumes that the slope of the line between the single data point and zero dose is linear. Therefore, the evaluation of beryllium as a carcinogen, as well as the method for quantifying the theoretical increased risk of cancer, should be considered extremely conservative.

5.2.3 Uncertainties Associated with Exposure Parameters

A variety of uncertainties are associated with the exposure assessment portion of the risk assessment. Several conservative, default exposure parameters were incorporated into the exposure assessment to define general population behavior. These default exposure parameters are USEPA recommended values that are intended to be conservative and representative of an individual who consistently and frequently contacts site soil. Additionally, "soil" at South Works consists mostly of molten slag and the bioavailability of COIs from this matrix is expected to be very low, much lower than from soil. Therefore, the potential for systemic absorption upon direct contact with the soil/slag at South Works is reduced and potential future exposures are likely to be overestimated.

It is also important to note that the RGs that were developed in this risk assessment are based upon the assumption that an individual will be continuously exposed to the RG concentration calculated for each exposure scenario (*i.e.*, children ingest all of their daily soil from the site and none from other sources). This will not likely be the case because individuals will contact soil at non-site locations (*i.e.*, a school yard) and most of the concentrations of each COI detected in soil across the site are significantly below their calculated RGs. Therefore, the actual risk to human health will be much less than the 1×10^{-5} or 1×10^{-6} theoretical increased cancer risk level and the hazard index of 1.

In order to understand the effect of using an upper-bound estimate for daily soil ingestion on the results of this HRA, the RG for the residential MEI was recalculated using more reasonable soil ingestion rates from the recent peer-reviewed scientific literature. Specifically, as discussed in detail in Section 4.3.2, more reasonable rates of soil ingestion for children and adults are approximately 25 mg/day and 10 mg/day, respectively (Calabrese *et al.*, 1989; Calabrese and Stanek, 1991; Paustenbach, 1987; Calabrese *et al.*, 1991). When these soil ingestion rates are used in the RG equation, the resulting MEI residential RG for beryllium, at a 10^{-6} risk level, is 10 mg/kg. While this RG is less than an order of magnitude greater than the RG calculated in this HRA for the MEI residential scenario at a 10^{-6} risk level (1.3 mg/kg), the results of the

assessment would be substantially different in that the measured levels of beryllium in site soil are all less than 10 mg/kg (maximum concentration=9.8 mg/kg). These more realistic rates of soil ingestion have been used for the MEI evaluation of another IEPA-approved risk assessment (ChemRisk, 1989).

5.2.4 Uncertainties Associated with Risk Characterization

Uncertainties in the risk characterization portion of the risk assessment for the site are a combination of the uncertainties associated with both the dose-response assessment and the exposure assessment. As discussed above, the assumptions and parameters used for both the dose response and exposure assessments are extremely conservative. In addition, since the toxicity criteria and exposure parameters are combined in the risk characterization, the conservatism is compounded. The RGs calculated in this HRA ensure the protection of even the most highly exposed sensitive subpopulations (*i.e.*, a pregnant female construction worker and young child) and will overestimate the degree of necessary remediation to protect the general population. Therefore, the results of this HRA must be carefully interpreted considering the uncertainty and conservatism associated with the analysis, especially where management decisions are made.

5.3 Cancer Risk Criteria And Regulatory Policy

Recent reviews of USEPA decisions (Travis *et al.*, 1987a;b) indicate that the theoretical cancer risks associated with currently enforced environmental regulations are in the vicinity of 1 in 100,000 (1×10^{-5}), versus 1 in 1,000,000 (1×10^{-6}). In a retrospective review of the use of cancer risk estimates in 132 federal decisions, Travis *et al.* (1987a) examined the level of cancer risk that triggered regulatory action. The authors considered three measures of risk: individual risk (an upper-limit estimate of the probability that the most highly exposed individual in a population will develop cancer as a result of a lifetime exposure), size of the population exposed, and population risk (an upper-limit estimate of the number of additional cases of cancer in the exposed population).

Travis *et al.* (1987a) found that for exposures resulting in a small-population risk, the level of risk above which agencies almost always acted to reduce risk was approximately 4×10^{-3}. For small-population risks, agencies typically acted on risks of about 3×10^{-4}. For effects on small populations, regulatory action was never taken for individual risk levels below 1×10^{-4}. For large-population effects (*e.g.*, potential nationwide exposure), the *de minimis* risk level dropped to 1×10^{-6}. Consequently, the level of acceptable individual risk is usually dictated by the size of the exposed population. While the size of the South Works site is large (approximately 567 acres), the analysis conducted in this HRA evaluates each individual sampling location separately by comparing RGs to the measured levels of COIs in each sample. The size of a population that could be exposed to the area represented by a single sampling location is expected to be quite small under any land use scenario. Therefore, the potentially exposed future populations at the South Works site may be thought of as small populations exposed to relatively small areas.

Rodricks *et al.* (1987) also evaluated regulatory decisions and reached similar conclusions. In decisions relating to promulgation of National Emission Standards for Hazardous Air Pollutants (NESHAPs), the USEPA has found the maximum individual risks and total population risks from a number of radionuclide and benzene sources too low to be judged significant. Maximum individual risks were in the range of 3.6×10^{-5} to 1.0×10^{-3}. In view of the risks deemed insignificant by USEPA, Rodricks *et al.* (1987) noted that 1×10^{-5} (1 in 100,000) appears to be in the range of what the USEPA might consider an insignificant average lifetime risk, at least where aggregate population risk is no greater than a fraction of a cancer yearly.

The National Contingency Plan (USEPA, 1990) has set the acceptable risk range between 10^{-4} and 10^{-6} at hazardous waste sites regulated under CERCLA. In the recently promulgated Hazardous Waste Management System Toxicity Characteristics Revisions (55 FR 11798-11863), the USEPA has stated that:

> "For drinking water contaminants, EPA sets a reference risk range for carcinogens at 10^{-4} to 10^{-6} excess individual cancer risk from lifetime exposure. Most regulatory actions in a variety of EPA programs have generally targeted this range using conservative models which are not likely to underestimate the risk."

The USEPA has selected and promulgated a single risk level of 1 in 100,000 (1×10^{-5}) in the Hazardous Waste Management System Toxicity Characteristics (TC) Revisions (55 FR 11798-11863). In their justification, the USEPA cited the following rationale:

> "The chosen risk level of 10^{-5} is at the midpoint of the reference risk range for carcinogens (10^{-4} to 10^{-6}) targeted in setting MCLs. This risk level also lies within the reference risk range (10^{-4} to 10^{-6}) generally used to evaluate CERCLA actions. Furthermore, by setting the risk level at 10^{-5} for TC carcinogens, EPA believes that this is the highest risk level that is likely to be experienced, and most if not all risks will be below this level due to the generally conservative nature of the exposure scenario and the underlying health criteria. For these reasons, the Agency regards a 10^{-5} risk level for Group A, B, and C carcinogens as adequate to delineate, under the Toxicity Characteristics, wastes that clearly pose a hazard when mismanaged."

When considering these limits, it is interesting to note that many common human activities involve annual risks greatly in excess of one in one million. These have been discussed by Grover Wrenn (1986), former director of Federal compliance and State Programs at OSHA, as follows:

> "Examination of the risks of common human activities demonstrates ... a lifetime risk of 1 in 100,000 or more is within the realm of, or orders of magnitude below, everyday risks that generally do not cause undue concern. These are risks that people, while they are aware of them and may have some concern or fear over them, do not in general alter their behavior to avoid. The risks from many activities greatly exceed the level of one in 100,000. In comparison to these background risks of "everyday activities," a lifetime risk of 1 in 100,000 is relatively small. Accordingly, regulatory action will not generally be justifiable unless risks are substantially higher than this 1 in 100,000 benchmark."

Ultimately, the selection of an acceptable and *de minimis* risk level is a policy decision in which both costs and benefits of anticipated courses of action should be thoroughly evaluated. It is noteworthy that actuarial data and risk estimates of common human activities, regulatory precedents, and the relationship between the magnitude and variance of background and incremental risk estimates all provide compelling support for the adoption of the *de minimis* risk level of 1×10^{-5}, or greater, for regulatory purposes.

Summary

In this assessment, the RGs for the carcinogenic COIs were calculated based upon a cancer risk range of 10^{-5} to 10^{-6}. Determining the level of risk that is acceptable for a particular site is a risk management decision for state and federal regulators. However, this target risk range is within the range considered acceptable by the USEPA for Superfund Sites (10^{-6} to 10^{-4}) (USEPA, 1990).

Further, it is noteworthy that only the RGs protective of a 1 x 10^{-6} increased risk level for beryllium are exceeded by site concentrations, and as discussed throughout this HRA, the beryllium RGs for a 10^{-6} risk level should not be used to guide remedial efforts because: 1) they are within the range of naturally occurring background levels of beryllium in soil, 2) beryllium has never been shown to cause cancer in animals or humans following oral exposure, 3) the bioavailability of metals in slag material on the site is very low, and 4) the RGs were calculated using very conservative assumptions regarding the level, frequency and duration of exposure. For these reasons, the RGs for beryllium protective of a 1 x 10^{-5} increased cancer risk level, which were not exceeded by concentrations of beryllium in site soil, are protective of human health.

TABLE 5-1
REMEDIATION GOALS BASED ON A 1 x 10^{-5} CANCER RISK AND HAZARD INDEX OF ONE FOR THE RESIDENTIAL, RECREATIONAL, AND INDUSTRIAL/COMMERCIAL SCENARIOS
(mg/kg)

Chemical	Maximum Surface Soil Concentration (mg/kg)	Residential Scenario				Recreational Scenario				Industrial/Commercial Scenario	
		MEI		MLEI		MEI		MLEI			
		Adult	Child	Adult	Child	Adult	Child	Adult	Child	MEI	MLEI
Antimony	7.6	601	46	1,960	158	2,020	153	12,100	745	841	5,020
Beryllium	9.3	11[a]		62[a]		37[a]		210[a]		83.3[b]	2,760[b]
Cadmium	89.1	1,500	114	4,890	394	5,060	383	30,200	1,860	2,100	12,500
Lead	3,200	NC[c]	932	NC[c]	932	NC[c]	3,790	NC[c]	3,790	6,150	72,800
Manganese	29,900	$> 10^6$	75,000	$> 10^6$	355,000	$> 10^6$	253,000	$> 10^6$	$> 10^6$	$> 10^6$	$> 10^6$
Benzo(a)anthracene	1.3	185[a]		1,050[a]		624[a]		3,530[a]		1,180[b]	39,000[b]
Benzo(a)pyrene	1.7	23.8[a]		135[a]		80[a]		453[a]		151[b]	5,000[b]
Benzo(b)fluoranthene	1.6	207[a]		1,170[a]		695[a]		3,930[a]		1,310[b]	43,400[b]
Dibenz(a,h)anthracene	0.57	134[a]		75.9[a]		45.1[a]		255[a]		85.2[b]	2,820[b]
Indeno(1,2,3-cd)pyrene	1.3	173[a]		977[a]		581[a]		3,290[a]		1,100[b]	36,300[b]

a Value is for adult and child exposure combined based on carcinogenic effects.
b Based on carcinogenic effects for adults only.
c RG for child exposure is also protective for adult exposures.
NC Not Calculated

TABLE 5 - 2
REMEDIATION GOALS BASED ON A 1 x 10^{-5} CANCER RISK
AND A HAZARD INDEX OF ONE
FOR THE CONSTRUCTION SCENARIO
(mg/kg)

Chemical	Maximum Soil Concentration[b] (mg/kg)	Construction Scenario		Short-Term Construction Scenario	
		MEI	MLEI	MEI	MLEI
Antimony	64.7	241	558	NC	NC
Beryllium	9.8	224[a]	1,900[a]	NC	NC
Cadmium	89.1	534	1,390	NC	NC
Lead	3,200	3,750	15,600	2,080	18,650
Manganese	35,900	443,000	$>10^6$	NC	NC
Benzo(a)anthracene	1.7	805[a]	3,650[a]	NC	NC
Benzo(a)pyrene	1.7	84.6[a]	383[a]	NC	NC
Benzo(b)fluoranthene	1.6	821[a]	3,720[a]	NC	NC
Dibenz(a,h)anthracene	0.57	76.7[a]	347[a]	NC	NC
Indeno(1,2,3-cd)pyrene	1.3	796[a]	3,600[a]	NC	NC

a Based on carcinogenic effects for adults only.
b Soil concentrations for both surface and subsurface soils.
NC Not Calculated

TABLE 5-3
REMEDIATION GOALS BASED ON A 1 x 10^{-6} CANCER RISK AND HAZARD INDEX OF ONE FOR THE RESIDENTIAL, RECREATIONAL, AND INDUSTRIAL/COMMERCIAL SCENARIOS
(mg/kg)

Chemical	Maximum Surface Soil Concentration (mg/kg)	Residential Scenario				Recreational Scenario				Industrial/Commercial Scenario	
		MEI		MLEI		MEI		MLEI			
		Adult	Child	Adult	Child	Adult	Child	Adult	Child	MEI	MLEI
Antimony	7.6	601	46	1,960	158	2,020	153	12,100	745	841	5,020
Beryllium	9.3	1.1[a]		6.2[a]		3.7[a]		21[a]		8.3[b]	276[b]
Cadmium	89.1	1,500	114	4,890	394	5,060	383	30,200	1,860	2,100	12,500
Lead	3,200	NC[c]	932	NC[c]	932	NC[c]	3,790	NC[c]	3,790	6,150	72,800
Manganese	29,900	$> 10^6$	75,000	$> 10^6$	355,000	$> 10^6$	253,000	$> 10^6$	$> 10^6$	$> 10^6$	$> 10^6$
Benzo(a)anthracene	1.3	18.5[a]		105[a]		62.4[a]		353[a]		118[b]	3900[b]
Benzo(a)pyrene	1.7	2.38[a]		13.5[a]		8.0[a]		45.3[a]		15.1[b]	500[b]
Benzo(b)fluoranthene	1.6	20.7[a]		117[a]		69.5[a]		393[a]		131[b]	4340[b]
Dibenz(a,h)anthracene	0.57	13.4[a]		7.59[a]		4.51[a]		25.5[a]		8.5[b]	282[b]
Indeno(1,2,3-cd)pyrene	1.3	17.3[a]		97.7[a]		58.1[a]		329[a]		110[b]	3630[b]

a Value is for adult and child exposure combined based on carcinogenic effects.
b Based on carcinogenic effects for adults only.
c RG for child exposure is also protective for adult exposures.
NC Not Calculated

I:\USS\SWORKS\RA\TABLES\TBL5-3

TABLE 5 - 4
REMEDIATION GOALS BASED ON A 1 x 10^{-6} CANCER RISK
AND A HAZARD INDEX OF ONE
FOR THE CONSTRUCTION SCENARIO
(mg/kg)

Chemical	Maximum Soil Concentration[b] (mg/kg)	Construction Scenario		Short-Term Construction Scenario	
		MEI	MLEI	MEI	MLEI
Antimony	64.7	241	558	NC	NC
Beryllium	9.8	22.4[a]	190[a]	NC	NC
Cadmium	89.1	53.4	1,390	NC	NC
Lead	3,200	3,750	15,600	2,080	18,650
Manganese	35,900	443,000	$> 10^6$	NC	NC
Benzo(a)anthracene	1.7	80.5[a]	365[a]	NC	NC
Benzo(a)pyrene	1.7	8.46[a]	38.3[a]	NC	NC
Benzo(b)fluoranthene	1.6	82.1[a]	372[a]	NC	NC
Dibenz(a,h)anthracene	0.57	7.7[a]	34.7[a]	NC	NC
Indeno(1,2,3-cd)pyrene	1.3	80[a]	360[a]	NC	NC

a Based on carcinogenic effects for adults only.
b Soil concentrations for both surface and subsurface soils.
NC Not Calculated

TABLE 5-5

SITE SAMPLES WHICH EXCEED THE CALCULATED RGs FOR THE SITE BASED ON A RISK OF 1 x 10^{-6}

Maximally Exposed Individual (MEI)		Most Likely Exposed Individual (MLEI)	
RESIDENTIAL SCENARIO[a]			
Beryllium:		**Beryllium:**	
SB-7D-1	SB-14D-1	SB-28-1	SB-29-1
SB-27-1	SB-28-1		
SB-29-1	SB-30-1		
SB-31-1	SB-32-1		
SB-33-1	SB-34-1		
SB-35-1	SB-36-1		
SB-37-1	SB-38-1		
SB-39-1	SB-40-1		
SB-41-1	SB-43-1		
SB-43-1	SB-44-1		
SB-9D-1	SB-46-1		
SB-45-1			
RECREATIONAL SCENARIO[a]			
Beryllium:		-None-	
SB-28-1	SB-29-1		
SB-34-1	SB-35-1		
SB-36-1	SB-46-1		
SB-7D-1	SB-31-1		
INDUSTRIAL/COMMERCIAL SCENARIO[a]			
-None-		-None-	
CONSTRUCTION SCENARIO[b]			
Cadmium:		-None-	
SB-39-2			

a RGs compared to surface soil sampling data only.
b RGs compared to both surface and subsurface soil sampling data.

TABLE 5-6

SITE SAMPLES WHICH EXCEED THE CALCULATED RGs FOR LEAD AT THE SITE

Maximally Exposed Individual (MEI)	Most Likely Exposed Individual (MLEI)
RESIDENTIAL SCENARIO[a] PBPK MODEL	
SS-9-1[d] SS-27-1[d] SS-28-1[d]	SS-9-1[d] SS-27-1[d] SS-28-1[d]
RECREATIONAL SCENARIO[a] PBPK MODEL	
-none	-none-
INDUSTRIAL/COMMERCIAL SCENARIO[a] PBPK MODEL	
-none-	-none-
LONG-TERM CONSTRUCTION SCENARIO[b] PBPK MODEL	
SS-9-1[c]	-none-
SHORT-TERM CONSTRUCTION SCENARIO[b] PBPK MODEL	
SS-9-1	-none-

a RGs compared to surface soil sampling data only.
b RGs compared to both surface and subsurface soil sampling data.
c Only exceeded for USEPA modified Bowers *et al.* (1994) modeling approach.
d Only exceeded for O'Flaherty modeling approach.

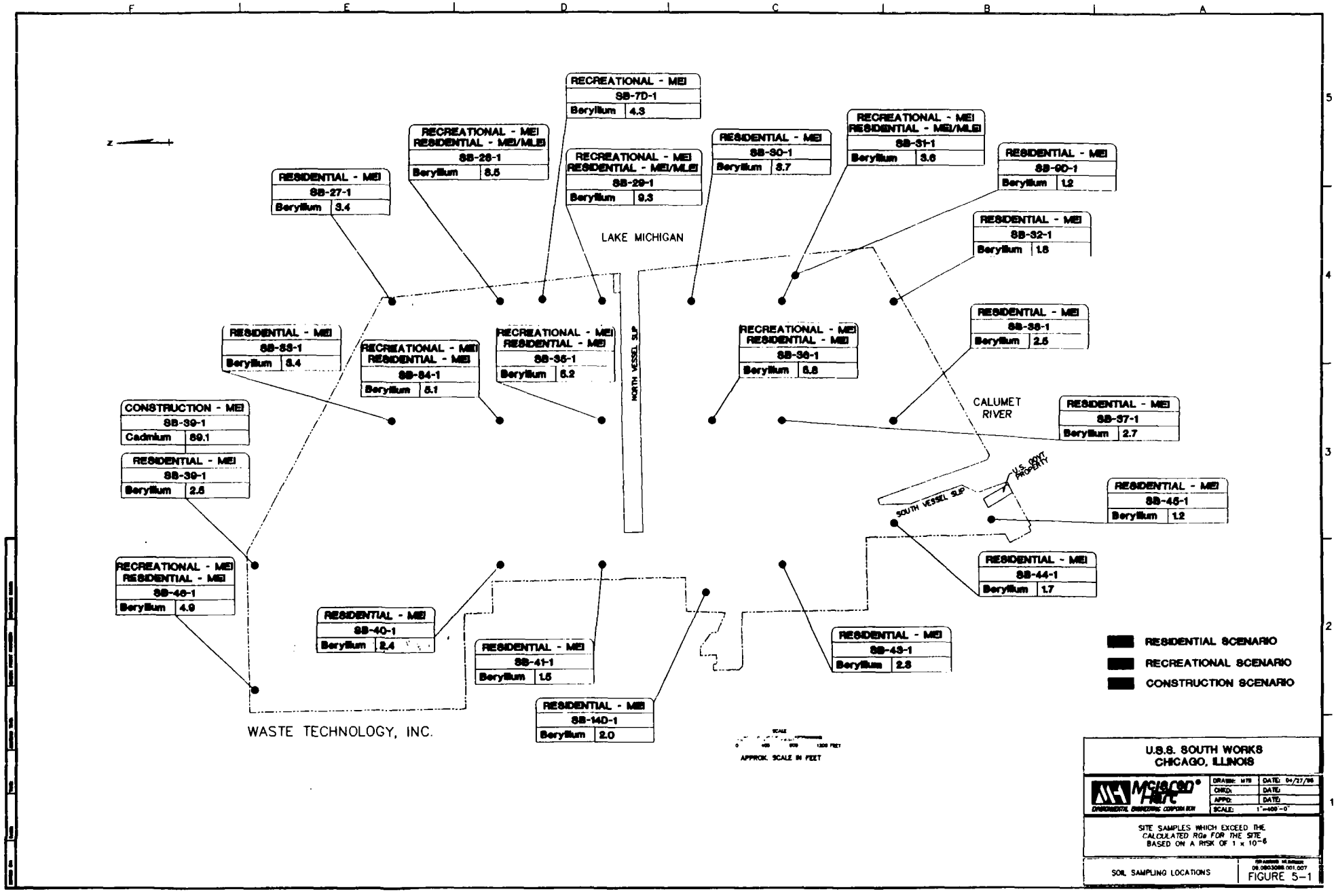

RECREATIONAL - MEI
SB-7D-1
Beryllium 4.3
RECREATIONAL - MEI
RESIDENTIAL - MEI/MLEI
SB-28-1
Beryllium 8.5
RECREATIONAL - MEI
RESIDENTIAL - MEI/MLEI
SB-29-1
Beryllium 9.3
RESIDENTIAL - MEI
SB-30-1
Beryllium 3.7
RECREATIONAL - MEI
RESIDENTIAL - MEI/MLEI
SB-31-1
Beryllium 3.6
RESIDENTIAL - MEI
SB-9D-1
Beryllium 1.2
RESIDENTIAL - MEI
SB-27-1
Beryllium 3.4
RESIDENTIAL - MEI
SB-32-1
Beryllium 1.8
LAKE MICHIGAN
RESIDENTIAL - MEI
SB-33-1
Beryllium 3.4
RECREATIONAL - MEI
RESIDENTIAL - MEI
SB-34-1
Beryllium 5.1
RECREATIONAL - MEI
RESIDENTIAL - MEI
SB-35-1
Beryllium 5.2
NORTH VESSEL SLIP
RECREATIONAL - MEI
RESIDENTIAL - MEI
SB-36-1
Beryllium 5.8
RESIDENTIAL - MEI
SB-38-1
Beryllium 2.5
CALUMET RIVER
RESIDENTIAL - MEI
SB-37-1
Beryllium 2.7
CONSTRUCTION - MEI
SB-39-1
Cadmium 89.1
RESIDENTIAL - MEI
SB-39-1
Beryllium 2.5
U.S. GOVT PROPERTY
SOUTH VESSEL SLIP
RESIDENTIAL - MEI
SB-45-1
Beryllium 1.2
RECREATIONAL - MEI
RESIDENTIAL - MEI
SB-46-1
Beryllium 4.9
RESIDENTIAL - MEI
SB-44-1
Beryllium 1.7
RESIDENTIAL - MEI
SB-40-1
Beryllium 2.4
RESIDENTIAL - MEI
SB-41-1
Beryllium 1.5
RESIDENTIAL - MEI
SB-43-1
Beryllium 2.8
RESIDENTIAL - MEI
SB-14D-1
Beryllium 2.0
WASTE TECHNOLOGY, INC.
APPROX. SCALE IN FEET
RESIDENTIAL SCENARIO
RECREATIONAL SCENARIO
CONSTRUCTION SCENARIO
U.S.S. SOUTH WORKS
CHICAGO, ILLINOIS
McLaren Hart
ENVIRONMENTAL ENGINEERING CORPORATION
DRAWN: MTB
DATE: 04/27/96
CHKD:
DATE:
APPD:
DATE:
SCALE: 1"=400'-0"
SITE SAMPLES WHICH EXCEED THE CALCULATED RGs FOR THE SITE BASED ON A RISK OF 1 x 10^-6
SOIL SAMPLING LOCATIONS
FIGURE 5-1

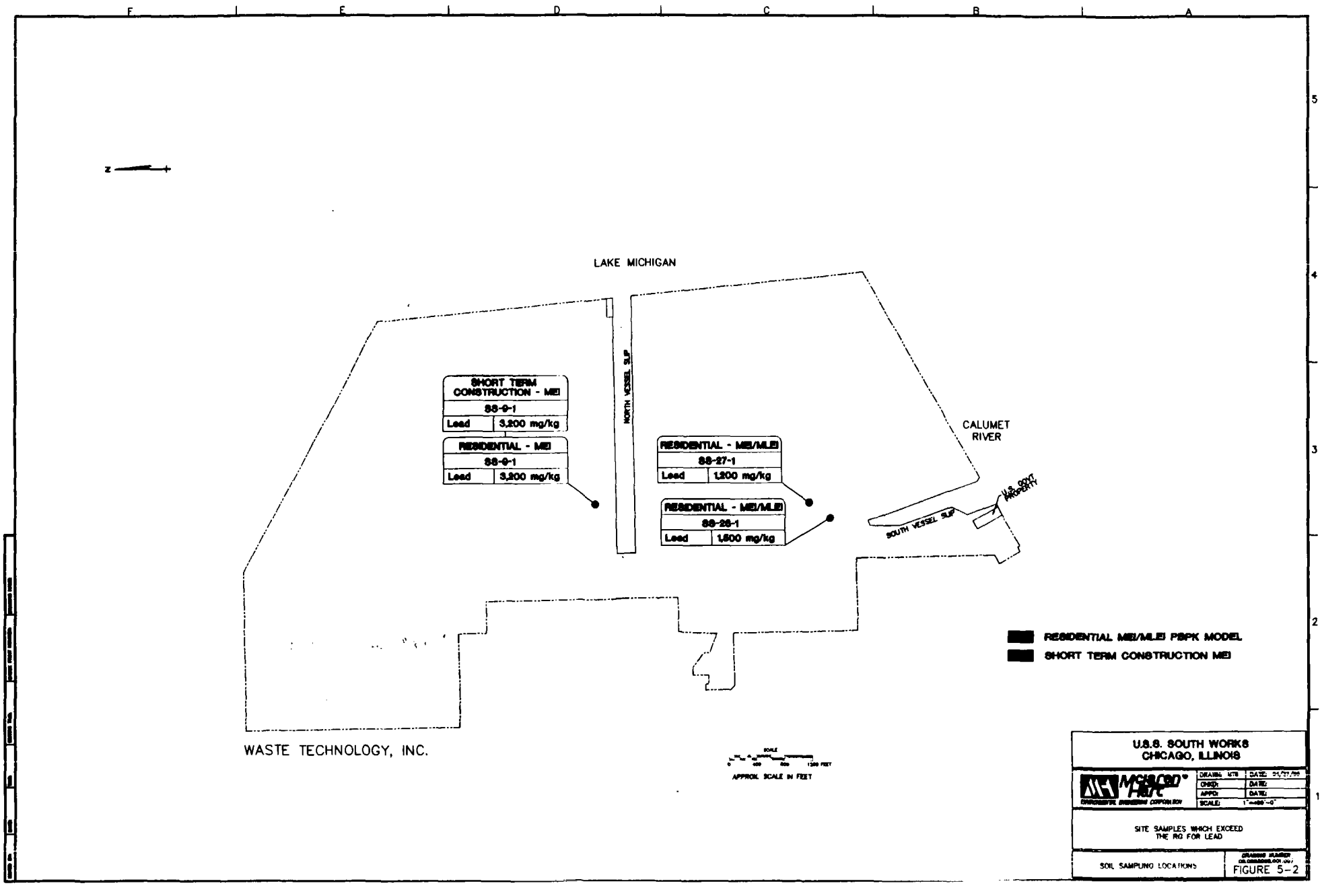
LAKE MICHIGAN
NORTH VESSEL SLIP
SHORT TERM CONSTRUCTION - MEI
SS-9-1
Lead 3,200 mg/kg
RESIDENTIAL - MEI
SS-9-1
Lead 3,200 mg/kg
RESIDENTIAL - MEI/MLEI
SS-27-1
Lead 1,200 mg/kg
RESIDENTIAL - MEI/MLEI
SS-26-1
Lead 1,500 mg/kg
CALUMET RIVER
U.S. GOVT PROPERTY
SOUTH VESSEL SLIP
RESIDENTIAL MEI/MLEI PBPK MODEL
SHORT TERM CONSTRUCTION MEI
WASTE TECHNOLOGY, INC.
SCALE
APPROX. SCALE IN FEET
U.S.S. SOUTH WORKS
CHICAGO, ILLINOIS
McLaren Hart
ENVIRONMENTAL ENGINEERING CORPORATION
DRAWN: MTB
DATE:
CHKD:
DATE:
APPD:
DATE:
SCALE:
SITE SAMPLES WHICH EXCEED THE RG FOR LEAD
SOIL SAMPLING LOCATIONS
FIGURE 5-2

6.0 CONCLUSIONS

This HRA presents site-specific remedial goals (RGs) for chemicals of interests (COIs) measured in soil at the South Works Site. The purpose of developing RGs was to direct remedial efforts such that there would not be a significant health risk to future site users after the site is redeveloped. RGs were developed for residential, recreational, industrial/commercial and construction land use scenarios, and two levels of exposure, a Maximum Exposed Individual (MEI) and a Most Likely Exposed Individual (MLEI) were evaluated. RGs were calculated for an acceptable cancer risk range of 10^{-6} to 10^{-5} and an acceptable hazard index of one. A comparison of RGs to each sampling location yields the following conclusions:

- The RGs calculated for the industrial/commercial land use scenario at both the 10^{-5} and 10^{-6} risk levels and/or a hazard index of one were all higher than the measured levels of COIs in site soil. Therefore, remediation of soils for future industrial/commercial land use is not deemed necessary.

- The RG calculated for cadmium at the 10^{-6} risk level for the MEI construction scenario (53 mg/kg) was exceeded at one sampling location (SB-39-2, 89.1 mg/kg). All other construction scenario RGs were higher than their measured levels in site soils. This single exceedence of the cadmium RG is driven by the inhalation of particles during future construction activities. Because the total mass of soil particulates in the air would be from a large part of the site during construction activities, rather than a single location, remediation of this single sampling location is not deemed necessary.

- As shown in the above table, at a 10^{-6} risk level, 23 of 24 surface soil samples had concentrations of beryllium above the residential MEI RG of 1.1 mg/kg, and 2 had concentrations of beryllium above the residential MLEI RG of 6.2 mg/kg. The 10^{-6} RG calculated for beryllium for the MEI recreational scenario of 3.7 mg/kg was exceeded by concentrations of beryllium at 8 sampling locations.

- The RG for beryllium for the residential MEI and MLEI and recreational MEI scenarios at the 10^{-6} risk level are within the range of naturally occurring background concentrations. Therefore, these RGs are not meaningful because remediation below naturally occurring background concentrations is neither feasible nor reasonable. Further, because no animal or human study in the scientific literature has ever demonstrated an increased incidence of cancer following oral exposure to beryllium, the evaluation of beryllium as an oral carcinogen is highly questionable.

- Concentrations of the COIs, including beryllium, did not exceed the RGs for any scenario at the 10^{-5} risk level.

- The residential MEI RG for lead of 932 mg/kg (child scenario), calculated using O'Flaherty PBPK model, was exceeded by the concentrations of lead at three sampling locations. This RG is consistent with the USEPA recommended range of cleanup levels for lead at Superfund sites of 500 to 1,000 mg/kg. Because future residential children could be exposed to these areas, these lead levels should be addressed prior to residential development.

- The MEI short- and long-term construction worker RGs were exceeded by the maximum concentration of lead (3,200 mg/kg) measured at one sampling location (SS-9-01). This area also exceeds the MEI residential RG and should be addressed prior to site redevelopment.

- The total additive theoretical cancer risk associated with multiple chemical exposures does not exceed the USEPA acceptable risk range of 10^{-4} to 10^{-6} for Superfund sites (USEPA, 1990). Additionally, the acceptable hazard index associated with multiple chemical exposures does not exceed one except in the three locations where lead exceeds 932 mg/kg. With the exception of beryllium, the total cancer risk marginally exceeds the 10^{-6} risk level at one location (SB-37-1) where benzo(a)pyrene and dibenz(a,h)anthracene both occur at their maximum concentrations. At this location, the total cancer risk does not exceed the 10^{-5} risk level.

Based on the blood-lead modeling analysis, it may be necessary to remediate lead in three areas identified in this HRA, should these areas be developed for residential use in the future. One area, with the maximum concentration of lead in soil, should be addressed prior to site redevelopment to protect future construction workers. In addition, it should be noted that analytical data from confirmatory sampling in areas currently undergoing demolition, remediation (sewers) and/or sediment removal will be compared to the RGs calcuated in this HRA.

At a 10^{-5} risk level, it should not be necessary to remediate soils at the South Works site for beryillium (or any other COI) in the areas evaluated in this HRA. At all but one sampling location, the 10^{-6} RG for beryllium for the residential MEI scenario (*i.e.*, the "maximally exposed individual") was exceeded. This is due to a combination of the highly conservative nature of the residential MEI scenario evaluated in this HRA and the highly conservative USEPA oral cancer slope factor for beryllium. For example, for the MEI scenario, this assessment used the USEPA default soil ingestion rates of 200 mg/day for a child and 50 mg/day for an adult. If, for example, more realistic soil ingestion rates presented in recent scientific literature of 25 mg/day and 10 mg/day were used for children and adults, respectively, an RG for the MEI residential scenario would be 10 mg/kg at a 10^{-6} risk level. The concentrations of beryllium in site soil (maximum concentration = 9.8 mg/kg) do not exceed this RG. These soil ingestion rates have been used to describe the MEI scenario in another IEPA-approved HRA (ChemRisk, 1989).

Finally, it is noteworthy that only the RGs protective of a 1 x 10^{-6} increased risk level for beryllium are exceeded by site concentrations. These beryllium RGs for a 10^{-6} risk level should not be used to guide remedial efforts because: 1) they are within the range of naturally occurring background levels of beryllium in soil, 2) beryllium has never been shown to cause cancer in animals or humans following oral exposure, 3) the bioavailability of metals in slag material on the site is very low, and 4) the RGs were calculated using very conservative assumptions regarding the level, frequency and duration of exposure. For these reasons, the RGs for beryllium protective of a 1 x 10^{-5} increased cancer risk level, which were not exceeded by concentrations of beryllium in site soil, should be protective of human health.

7.0 REFERENCES

Abramowitz, M, Stegun I.A. (1972). *Handbook of Mathematical Functions With Formulas, Graphs, and Mathematical Tables.* National Bureau of Standards. Applied Mathematics Series 55.

Agency for Toxic Substances and Disease Registry. (ATSDR). (1993a). *Toxicological Profile for Polycyclic Aromatic Hydrocarbons (PAHs).* U.S. Department of Health & Human Services. Prepared by Clement International Corporation Under Contract No. 205-88-0608.

Agency for Toxic Substances and Disease Registry. (ATSDR). (1993b). *Toxicological Profile for Beryllium.* U.S. Department of Health & Human Services. Prepared by Clement International Corporation Under Contract No. 205-88-0608.

American Conference of Governmental and Industrial Hygienists [ACGIH]. (1986). *Documentation of Threshold Limit Values and Biological Exposure Indices for 1989-1990.* Cincinnati, OH.

American Conference of Governmental and Industrial Hygienists [ACGIH]. (1991). *Documentation of Threshold Limit Values and Biological Exposure Indices.* ACGIH, Cincinnati, OH.

American Conference of Governmental and Industrial Hygienists [ACGIH]. (1994). *Threshold Limit Values for Chemical Substances and Physical Agents.* ACGIH, Cincinnati, OH.

American Petroleum Institute. (API). (1990). *Sediment Toxicity Evaluation.* Health and Environmental Sciences API Publication Number 4501.

Ames, B.N., Magaw, R. and Gold, L.S. (1987). Ranking possible carcinogenic hazards. *Science* 236:271-273.

Berggreen, R.G., Grumman, Jr., D.L., Blindauer, P.R. (1991). Polynuclear Aromatic Hydrocarbon Contamination in Downtown Chicago Fill Soils. Proceedings, 34th Annual Meeting Association of Engineering Geologists. September 29 - October 4, Chicago, Illinois.

Bonnell, J.A. (1955). Emphysema and Proteinuria in Men Casting Copper-Cadmium Alloys. *Brit. J. Ind. Med* 12:181-197.

Bowers, T.S., Beck, B.D., Karam, H.S. (1994). Assessing the Relationship Between Environmental Lead Concentrations and Adult Blood Lead Levels. *Risk Anal.* 14(2):183-189.

Bureau of Labor Statistics. (1990). *Statistical Summary: Tenure with Current Employer as of January 1987* (as cited in USEPA, 1991).

Calabrese, E.J., Barnes, R., Stanek, E.J., Pastides, H., Gilbert, C.E., Veneman, P., Wang, X., Lasztity, A. and Kostecki, P.T. (1989). How much soil do young children ingest: An epidemiologic study. *Reg. Toxicol. Pharm.* 10:123-137.

Calabrese, E.J., E.J. Stanek, C.E. Gilbert. (1991). A Preliminary Decision Framework for Deriving Soil Ingestion Rates. In: (Kostecki, Calabrese, and Bell, eds.) *Hydrocarbon Contaminated Soils and Groundwater: Analysis, Fate, Environmental and Public Health Effects, Remediation*

Calabrese, E.J. Stanek, E.J., III. (1991). A guide to interpreting soil ingestion studies. *Reg. Toxicol. Pharm.* 13:278-292.

Calabrese, E.J., Stanek, E.J., Gilbert, C.E. Barnes, R.M. (1990). Preliminary adult soil ingestion estimates: Results of a pilot study. *Reg. Tox. Pharm.* 12:88-95.

Cerniglia, C.E. (1981). Aromatic Hydrocarbons: Metabolism by Bacteria, Fungi, and Algae. *Rev. Biochem. Toxicol.* 3:321-361.

ChemRisk® a Division of McLaren/Hart. (1989). *Risk Assessment for Atlanta, Illinois.* April.

ChemRisk® a Division of McLaren/Hart. (1995). Preliminary Human Health and Ecological Risk Assessment for the South Works Site. Chicago, Illinois. March, 1995, Pittsburgh, PA.

Centers for Disease Control [CDC]. (1991). *Preventing Lead Poisoning in Young Children.* A statement by the Centers for Disease Control. U.S Department of Health and Human Services.

Code of Federal Regulation (CFR). (1992). 29CFR1910.1000.

Cowherd, D., Muleske, G.E., Englehart, P.J. and Gillette, D.A. (1985). *Rapid Assessment of Exposure to Particulate Emissions from Surface Contamination Sites.* U.S. Environmental Protection Agency, Office of Health and Environmental Assessment. EPA/600-8-85/002.

Davis, S., Waller, P., Buschbom, R., Ballou J. White, P. (1990). Quantitative estimates of soil ingestion in normal children between the ages of 2 and 7 years: Population-based estimates using aluminum, silicon, and titanium as soil tracer elements. *Arch. of Environ. Health.* 45(2):112-122.

Dagley, S. (1971). Catabolism of Aromatic Compounds by Microorganisms. *Adv. Microbiol. Physiol.* 6(1):1-46.

Dragun, J. (1988). The Fate of Hazardous Materials in Soil (What Every Geologist and Hydrologist Should Know): Part 2. *Hazardous Materials Control* 1(3):41-65.

Dragun, J., Chiasson, A. (1991). *Elements in North American Soils.* Greenbelt MD: Hazardous Materials control Resources Institutes.

Driver, T.N., Konz, J.J., Whitmyre, G.K. (1989). Soil adherence to human skin. *Bull. Environ. Contam. Toxicol. 43*:814-820.

Finn, R.H., Noal, P.A., Reinhart, W.H., et al. (1940). Chronic Manganese Poisoning in an Ore-Crushing Mill. U.S. Public Health Services No: 247. USPHS, Washington, D.C.

Friberg, L., Picastor, M., Nordberg G.F., Kjellstrom, T. (1974). *Cadmium in the Environment*, 2nd Edition. CRC Press, Boca Raton, Florida.

Friberg, L., Noeverg, G., Piscator, M> (1977). Cadmium. In: *Toxicology of Metals - Volume II.* pp. 124-163.

Gardner, L.U., Heslington, H.F. (1946). Osteo-Sarcoma from Intravenous Beryllium Compounds in Rabbits. *Fed. Proc.* 5:221.

Gibson, D.T. (1977). Biodegradation of Aromatic Petroleum Hydrocarbons. In: *Fate and Effect of Petroleum Hydrocarbons in Marine Ecosystems and Organisms.* D.A. Wolfe, Ed., Pergamon Press, N.Y.

Goon, D., Hatoum, N.S., Jernigan, J.D., Schmitt, S.L., and Garvin, P.J. (1990). Pharmacokinetics and oral bioavailability of soil-adsorbed benozo[a]pyrene (BaP) in rats. *Toxicologist* 10:218.

Goon, D., Hatoum, N.S., Jernigan, J.D., Klan, M.J., and Farmer, R.G. (1991). Oral bioavailability of "aged" soil-adsorbed benzo[a]pyrene in rats. *Toxicologist* 11:345.

Guttman, I., Wilks, S.S., and Hunter, J.S. (1965). *Introductory Engineering Statistics.* John Wiley & Sons, Inc. 2nd Edition.

Hawley, J.K. (1985). Assessment of health risk from exposure to contaminated soil. *Risk Anal.* 5(4):289-302.

Hect, S.S., Grabowski, W., Groth, K. (1979). Analysis of Feces for B[a]P after Consumption of Charcoal-Broiled Beef by Rats and Humans. *Food Cosmet. Toxicol.* 17:223-227.

Hornshaw, T. (1995). Personal Communications with D. Proctor, ChemRisk; and M. Zak, USX.

Horowitz, S.B., and Finley, B.L. (1993). Using Human Sweat to Extract Chromium from Chromite Ore Processing Residue: Applications to Setting Health-Based Cleanup Levels. *Journal of Toxicology and Environmental Health* 40:585-599.

Howard, P.H., Boethling, R.S., Jarvis, W.F., Meylan, W.M., Michalenko, E.M. (1991). *Handbook of Environmental Degradation Rates.* Lewis Publishers, Chelsea, MI.

Illinois Environmental Protection Agency. (IEPA). (1992). *Guidance for Developing a Site-Specific Soil Cleanup Level Proposal for RCRA Clean Closures.* Springfield, Illinois.

Illinois Environmental Protection Agency. (IEPA). (1994). *Interim Default Values for the Estimation of the Dermal Absorption of Chemicals from Soil.* Memorandum from T. Hornshaw.

International Commission on Radiological Protection [ICRP]. (1968). *Report of Committee IV on Evaluation of Radiation Dose to Body Tissues from Internal Contamination Due to Occupational Exposure.* ICRP Publication 10. New York: Pergamon Press.
International Commission on Radiological Protection [ICRP]. (1974). Report of the Task Group on Reference Man.

Klaassen C.D, Amdur M.O, and Doull, J. eds. (1986). *Cassarett and Doull's Toxicology: The Basic Science of Poisons.* 3rd Ed. New York: MacMillan Publishing Co.

Kondakis, X.G., Makris, N., Leotsinidis, M. *et al.* (1989). Possible Health Effects of High Manganese Concentration in Drinking Water. *Arch. Environ. Health* 44:175-178.

Kubala, A.O. and Pilja, G. (1994). *Minutes for IEPA and U.S. Steel Meeting (Former South Works).* June 8.

Lepow, M.L., Bruckman, L., Gillette, M., Markowitz, S., Fubino, R. and Kapish, J. (1975). Investigations into Sources of Lead in the Environment of Urban Children. *Environ. Res.* 10:415-426.

Lilliefors, H. (1967). On the Kolmogorov-Smirnov test for normality with mean and variance unknown. *J. Am. Stat. Assoc.* 62(318):399-402.

Lloyd-Davies, T.A. and Harding, H.E. (1946). *British Journal of Industrial Medicine.* 3:111.

Lyman, W.J., Reehl, W.F. and Rosenblatt, D.H. (1982). *Handbook of Chemical Property Estimation Methods. Environmental Behavior of Organic Compounds.* New York: McGraw-Hill.

Mallon, R.P. (1993). A Metabolic Model of Lead Kinetics Based upon Measured Organ Burdens during Chronic Exposure Experiments with Infant and Juvenile Baboons. Ph.D. dissertation, New York University, University Microfilms International, Ann Arbor, Michigan.

Matthews, J.E., Hastings, L. (1987). Evaluation of Toxicity Test Procedure for Screening Treatability Potential of Waste in Soil. *Tox. Assess.* 2:265-281.

Morgareidge, K. Cox, G.E., Bailey, D.E. (1975) Chronic Feeding Studies with Beryllium Sulfate in Rats: Evaluation of Carcinogenic Potential. Pittsburgh, PA: Food and Drug Research Laboratories, Inc. Final Report to the Aluminum Company of America.

National Academy of Sciences [NAS]. (1983). *Risk Assessment in the Federal Government: Managing the Process.* Washington, D.C.: National Academy Press.

National Oil and Hazardous Substances Pollution Contingency Plan [NCP]. (1990). 40 CFR Part 300. Environmental Protection Agency.

National Institute for Occupational Safety and Health. [NIOSH]. (1976). *Criteria for a Recommended Standard.* HEW Publication No. NIOSH-76-192.

O'Flaherty, E.J. (1991a). Physiologically Based Models for Bone-Seeking Elements, I. Rat Skeletal and Bone Growth. *Toxicol. App. Pharm.* 111:299-312.

O'Flaherty, E.J. (1991b). Physiologically Based Models for Bone-Seeking Elements, II. Kinetics of Lead Disposition in Rats. *Toxicol. App. Pharm.* 111:313-331.

O'Flaherty, E.J. (1991c). Physiologically Based Models for Bone-Seeking Elements, III. Human Skeletal and Bone Growth. *Toxicol. App. Pharm.* 111:332-341.

O'Flaherty, E.J. (1993). Physiologically Based Models for Bone-Seeking Elements, IV. Kinetics of Lead Disposition in Humans. *Toxicol. App. Pharm.* 118:16-29.

O'Flaherty, E.J. (1995). Physiologically Based Models for Bone-Seeking Elements, V. Lead Absorption and Disposition in Childhood. *Toxicol. App. Pharm.* 131:297-308.

Park, K.S., Sims, R.C., Dupont, R.R. (1990). Transformation of PAHs in Soil Systems. *J. Environ. Eng.* 116(3):632-640.

Paustenbach, D.J. (1987). Assessing the Potential Environmental and Human Health Risks of Contaminated Soil. *Comments Toxicol.* 1(3-4):185-226.

Paustenbach, D.J. (1989a). A survey of health risk assessment. In: D.J. Paustenbach, ed. *The Risk Assessment of Environmental and Human Health Hazards: A Textbook of Case Studies.* New York: Wiley.

Paustenbach, D.J. (1989b). Important recent advances in the practice of health risk assessment: Implications of the 1990s. *Regul. Toxicol. Pharmacol.* 10:204-243.

Paustenbach, D.J., Jernigan, J.D., Finley, B.L., Ripple, S.R., Keenan, R.E. (1990). The Current Practice of Health Risk Assessment: Potential Impact on Standards for Toxic Air Contaminants. *J. Air Waste & Manag. Assoc.* 40(12):1620-1630.

Pocock, S.J., Shaper, A.G., Walker, M., Wale, C.J., Clayton, B., Delves, T., Lacey, R.F., Packham, R.F., Powell, P. (1983). Effects of Tap Water Lead, Water Hardness, Alcohol, and Cigarettes on Blood Lead Concentrations. *J. Epidem. Comm. Health.* 37:1-7.

Que Hee, S.S., Peace, B., Scott, C.S, Boyle, J.R., Bornschein, R.L. and Hammond, P.B. (1985). Evolution of efficient methods to sample lead sources, such as house dust and hand dust, in the homes of children. *Environ. Res.* 38:77-95. (cited in SCAQMD, 1988).

Rahman, A., Barrowman, J.A., and Rahimtula, A. (1986). The influence of bile on the bioavailability of polynuclear aromatic hydrocarbons from rat intestine. *Can. J. Physiol. Pharm.* 64:1214-1218.

Rodricks, J.V., Brett, S.M. and Wrenn G.C. (1987). Significant risk decisions in federal regulatory agencies. *Regul. Toxicol. Pharmacol.* 7:307-320.

Roels, H.A., Buchett, J., Lauwerys, R.R., Bruaux, P., Claeys-Thoreau, F., Lafontaine, A. and Verduyn, G. (1980). Exposure to Lead by the Oral and the Pulmonary Routes of Children Living in the Vicinity of a Primary Lead Smelter. *Environ. Res.* 22:81-94.

Ryan *et al.* (1987). As cited in Ohio Environmental Protection Agency (OEPA) 1991 *Closure Plan Review Guidance*. Division of Solid and Hazardous Waste Management.

Schroeder, H.A., Mitchener, M. (1975a). Life-Term Studies in Rats: Effects of Aluminum, Barium, Beryllium, and Tungsten. *J. Nutr.* 105:421-427.

Schroeder, H.A., Mitchener, M. (1975b). Life-Term Effects of Mercury, Methyl Mercury, and Nine Other Trace Metals on Mice. *J. Nutr.* 105:452-458.

Seiler, H.G., Sigel, H. Sigel, A. (1988) *Handbook on Toxicity of Inorganic Compounds.* Marcel Dekker, Inc., New York.

Sheehan, P.J., Meyer, D.M., Sauer, M.M., and Paustenbach, D.J. (1991). Assessment of the human health risks posed by exposure to chromium-contaminated soils. *J. Toxicol. Environ. Health* 32:161-201.

Sheehan, P.J., Finley, B.L., Meyer, D.M., Lau, V., and Paustenbach, D.J. (1992). Critical factors for assessing human uptake of chromium from contaminated soil.

Sims, R. C. and Overcash, M. R. (1983). Fate of polynuclear aromatic compounds (PNAs) in soil-plant systems. *Res. Rev.* 88:1-68.

Stokinger, H.E. (1981). Chapter 29. The Metals. In: *Patty's Industrial Hygiene and Toxicology*, 3rd Edition, Volume 2A. G.D. Clayton and F.E. Clayton (eds.). Wiley and Sons, New York. pp. 1493-2060.

Suter, G. W. (1993). *Ecological Risk Assessment.* Lewis Publishers, Chelsea, Michigan.

Tanaka, S., and Lieben, J. (1969). Manganese Poisoning and Exposure in Pennsylvania. *Arch. Environmental Health.* 19:674-684.

Thomas, W. (1986). Accumulation of Airborne Trace Pollutants by Arctic Plants and Soil. *Water Sci. Technol.* 18:47-57.

Travis, C.C., Richter, S.A., Crouch, E.A., Wilson, R. and Wilson, E. (1987a). Cancer risk management. A review of 132 federal regulatory decisions. *Environ. Sci. Technol.* 21(5):415-420.

Travis, C.C. and Hattemer-Frey, H.A. (1987b). Human exposure to 2,3,7,8-TCDD. *Chemosphere.* 16(10-12):2331-2342.

U.S. Army Corps of Engineers. (1978, 1980, 1981). Sediment Sample Analytical Data from Small Burns Harbor, Burns Waterway Harbor, and Big and Small Burns Harbor.

U.S. Army Corps of Engineers. (1984). Water Quality Monitoring Chicago Area Confined Disposal Facility. Contract No: DACW 23-84-0-0012. Final Report.

U.S. Environmental Protection Agency [USEPA]. (1985). *Development of Statistical Distributions or Ranges of Standard Factors Used in Exposure Assessments.* Office of Health and Environmental Assessment, Washington, D.C. EPA 600/8-85-010.

U.S. Environmental Protection Agency [USEPA]. (1986). *Superfund Public Health Evaluation Manual.* Office of Emergency and Remedial Response. Washington, D.C. EPA/540/1-86/060. OSWER Directive 9285.4-1. October.

U.S. Environmental Protection Agency [USEPA]. (1989b). *Soil Sampling Quality Assurance User's Guide 2nd Edition.* Cooperative Agreement No. CR 814701. EPA/600/8-89/046.

U.S. Environmental Protection Agency. (USEPA). (1989c). *Interim Guidance on Establishing Soil Lead Cleanup Levels at Superfund Sites.* Memorandum from Henry L. Longest II, Director. Office of Emergency and Remedial Response.

U.S. Environmental Protection Agency [USEPA]. (1989a). *Risk Assessment Guidance for Superfund, Volume 1. Human Health Evaluation Manual (Part A)*, interim final. Office of Emergency and Remedial Response, Washington, D.C. EPA/540/1-89/002.

U.S. Environmental Protection Agency [USEPA]. (1989c). *Hazardous Waste Treatment/Storage and Disposal Facilities - Air Emission Model.* Office of Air and Radiation, Research Triangle Park, NC. EPA/450/3-87/026.

U.S. Environmental Protection Agency [USEPA]. (1989d). *Exposure Factor Handbook.* Office of Health and Environmental Assessment, Washington, D.C. May.

U.S. Environmental Protection Agency [USEPA]. (1991a). *Risk Assessment Guidance for Superfund, Volume 1. Human Health Evaluation Manual (Part B, Development of Risk-Based Preliminary Remediation Goals)*, interim. Office of Emergency and Remedial Response, Washington, D.C. PB92-963333.

U.S. Environmental Protection Agency [USEPA]. (1991b). *Supplemental Guidance Standard Default Exposure Factors.* Interim Final. Office of Emergency and Remedial Response, Toxics Integration Branch, Washington, D.C.

U.S. Environmental Protection Agency [USEPA]. (1991c). *Criteria Document for Beryllium.* Prepared by the Office of Health and Environmental Assessment. Environmental Criteria and Assessment Office, Cincinnati, OH for the Office of Drinking Water, Washington, DC.

U.S. Environmental Protection Agency [USEPA]. (1992a). *EPA Region 5 Interim Sediment Inventory (version 1; 7/31/92).* H. Zar USEPA Region 5, Water Division.

U.S. Environmental Protection Agency [USEPA]. (1992b). *Guidance for Exposure Assessment.* Federal Register 59(104)22888-22936. March 29, 1992.

U.S. Environmental Protection Agency [USEPA]. (1992b). *Dermal Exposure Assessment: Principles and Applications.* USEPA Office of Research and Development. Washington, D.C. EPA/600/8-91/011B.

U.S. Environmental Protection Agency [USEPA]. (1993). *Provisional Guidance for Quantitative Risk Assessment for Polycyclic Aromatic Hydrocarbons.* Office of Research and Development. Washington, DC. EPA/600/R-93/089

U.S. Environmental Protection Agency [USEPA]. (1993c). *Drinking Water Regulations and Health Advisories.* Office of Water. Washington DC. December.

U.S. Environmental Protection Agency [USEPA]. (1993a). *Health Effects Assessments Summary Tables and Users Guide.* USEPA Office of Emergency and Remedial Response, Washington, D.C.

U.S. Environmental Protection Agency [USEPA]. (1994b). *Guidance Manual for the Integrated Exposure Uptake Biokinetic Model for Lead in Children (Version 0.99D)*. Office of Emergency and Remedial Response. Washington, DC. EPA 540-R-93-081

U.S. Environmental Protection Agency [USEPA]. (1994a). *Revised Interim Soil Lead Guidance for CERCLA Sites and RCRA Corrective Actions Facilities*. Office of Solid Waste and Emergency Response. OSWER Directive 9355.4-12.

U.S. Environmental Protection Agency [USEPA]. (1995a). *Risk-Based Concentration Table, First Quarter 1995*. Memorandum from Roy L. Smith, Senior Toxicologist, Region III.

U.S. Environmental Protection Agency [USEPA]. (1995b). *Integrated Risk Information Service [IRIS]*. Cincinnati, OH.

U.S. Environmental Protection Agency [USEPA]. (1995c). *NOAA Meteorological Data for Years 1970 through 1979*. Center for Exposure Assessment. Athens, GA.

Waste Technology, Inc. (WTI). (1993a). *Environmental Assessment of the Former South Works Plant Chicago, Illinois*. Naperville, Illinois.

Waste Technology, Inc. (WTI). (1993b). *Phase II Environmental Assessment of the Former South Works Plant Chicago, Illinois*. Naperville, Illinois.

Waste Technology, Inc. (WTI). (1994). *Phase III Environmental Assessment of the Former South Works Plant Chicago, Illinois*. Naperville, Illinois.

Wrenn, G. (1986). U.S. Environmental Protection Agency Asbestos Ban and Phase-out Proposal: Testimony of Grover Wrenn. June 29.

Van Wijnen, J.H., Clausing, P. and Brunekreef, B. (1990). Estimated soil ingestion by children. *Environ. Res.* 51:147-162.

Velazquez, S. (1995). Personal communication with K. Fehling regarding manganese RfC. March 1995.

Yang, J.J., Roy, T.A., Krueger, A.J., and Mickerer, C.R. (1989). *In vitro* and *in vivo* percutaneous absorption of benzo(a)pyrene from petroleum-crude-fortified soil in the rat. *Bull. Environ. Contam. Toxicol.* 43:207-214.

Zak, M. A. (1994). Letter dated September 27, 1994, to Vickie Moy, Illinois Environmental Protection Agency.

APPENDIX A

Calculation Spreadsheets

Date:	7/6/95	Scenario:	Residential - MEI				
	Child Soil Ingestion	Adult Soil Ingestion	Child Dermal Contact	Adult Dermal Contact	Child Inhalation	Adult Inhalation	
Body Weight:	15	70	15	70	15	70	kg
Averaging Time (non):	2190	8760	2190	8760	2190	8760	days
Averaging Time (car):	25550	25550	25550	25550	25550	25550	days
Exposure Duration:	6	24	6	24	6	24	years
Exposure Frequency:	350	350	350	350	350	350	days/yr
Conversion Factor:	1.00E-06	1.00E-06	1.00E-06	1.00E-06	1.00E-06	1.00E-06	kg/mg
Soil Ingestion Rate:	200	50	200	50	200	50	mg/day
Skin Surface Area:	2195	2836	2195	2836	2195	2836	cm2
Adherence Factor:	1	1	1	1	1	1	mg/cm2
Meteorological Factor:	0.62	0.62	0.62	0.62	0.62	0.62	unitless
Inhalation Rate:	14.2	20	14.2	20	14.2	20	m3/day

Chemical-specific parameters

Chemical	Target Hazard Index	Target Risk	Soil Half-Life (years)	Dilution/ Attenuation Factor	Oral Bioavailability	Dermal ABS	Oral RfD mg/kg-day	Inhalation RfD mg/kg-day	Oral SF (mg/kg-day)-1	Inhalation SF (mg/kg-day)-1	VF (m3/kg)
Antimony	1	1.00E-06		1.00E+00	100.00%	1.0000%	4.00E-04	4.00E-04			
Beryllium	1	1.00E-06		1.00E+00	25.57%	0.0034%	5.00E-03	5.00E-03	4.30E+00	0.00E+00	
Cadmium	1	1.00E-06		1.00E+00	100.00%	1.0000%	1.00E-03	1.00E-03			
Manganese	1	1.00E-06		1.00E+00	23.47%	0.0049%	1.40E-01	1.43E-05			
Benzo(a)anthracene	1	1.00E-06	1.863	8.96E-02	50.00%	10.0000%			7.30E-01	0.00E+00	
Benzo(a)pyrene	1	1.00E-06	1.452	6.98E-02	50.00%	10.0000%			7.30E+00	0.00E+00	
Benzo(b)fluoranthene	1	1.00E-06	1.671	8.04E-02	50.00%	10.0000%			7.30E-01	0.00E+00	
Dibenzo(ah)anthracene	1	1.00E-06	2.575	1.24E-01	50.00%	10.0000%			7.30E+00	0.00E+00	
Indeno(123cd)pyrene	1	1.00E-06	2.000	9.62E-02	50.00%	10.0000%			7.30E-01	0.00E+00	
Benzene	1	1.00E-06	2.000	9.62E-02	100.00%	3.0000%	0.00171	0.00171	2.90E-02	2.90E-02	3.60E+05
Ethylbenzene	1	1.00E-06	0.625	3.01E-02	100.00%	3.0000%	0.1	0.286			3.79E+05
Toluene	1	1.00E-06	0.575	2.77E-02	100.00%	3.0000%	0.2	0.114			3.70E+05
Xylene	1	1.00E-06	1.000	4.81E-02	100.00%	3.0000%	2	2			3.86E+05

PRGs Noncarcinogenic Effects - Child

Chemical	Soil Ingestion XF kg/kg-day	Dermal Contact XF kg/kg-day	Vapor Inhalation XF kg/kg-day	Soil HBCL mg/kg
Antimony	7.92694E-06	8.69982E-07	#DIV/0!	4.55E+01
Beryllium	2.02692E-06	2.95794E-09	#DIV/0!	2.46E+03
Cadmium	7.92694E-06	8.69982E-07	#DIV/0!	1.14E+02
Manganese	1.86045E-06	4.26291E-09	#DIV/0!	7.51E+04
Benzo(a)anthracene	3.96347E-06	3.96347E-06	#DIV/0!	#DIV/0!
Benzo(a)pyrene	3.96347E-06	3.96347E-06	#DIV/0!	#DIV/0!
Benzo(b)fluoranthene	3.96347E-06	3.96347E-06	#DIV/0!	#DIV/0!
Dibenzo(ah)anthracene	3.96347E-06	3.96347E-06	#DIV/0!	#DIV/0!
Indeno(123cd)pyrene	3.96347E-06	3.96347E-06	#DIV/0!	#DIV/0!
Benzene	0	0	2.52E-06	7.05E+03
Ethylbenzene	0	0	2.40E-06	3.97E+06
Toluene	0	0	2.45E-06	1.68E+06
Xylene	0	0	2.35E-06	1.77E+07

PRGs for Noncarcinogenic Effects - Adult

Chemical	Soil Ingestion XF kg/kg-day	Dermal Contact XF kg/kg-day	Vapor Inhalation XF kg/kg-day	Soil HBCL mg/kg
Antimony	4.24658E-07	2.40866E-07	#DIV/0!	6.01E+02
Beryllium	1.08583E-07	8.18944E-10	#DIV/0!	4.57E+04
Cadmium	4.24658E-07	2.40866E-07	#DIV/0!	1.50E+03
Manganese	9.96671E-08	1.18024E-09	#DIV/0!	1.39E+06
Benzo(a)anthracene	2.12329E-07	2.12329E-07	#DIV/0!	#DIV/0!
Benzo(a)pyrene	2.12329E-07	2.12329E-07	#DIV/0!	#DIV/0!
Benzo(b)fluoranthene	2.12329E-07	2.12329E-07	#DIV/0!	#DIV/0!
Dibenzo(ah)anthracene	2.12329E-07	2.12329E-07	#DIV/0!	#DIV/0!
Indeno(123cd)pyrene	2.12329E-07	2.12329E-07	#DIV/0!	#DIV/0!
Benzene	0	0	7.61E-07	2.34E+04
Ethylbenzene	0	0	7.23E-07	1.32E+07
Toluene	0	0	7.40E-07	5.57E+06
Xylene	0	0	7.10E-07	5.86E+07

PRGs for Carcinogenic Effects

Chemical	Soil Ingestion XF kg/kg-day	Dermal Contact XF kg/kg-day	Vapor Inhalation XF kg/kg-day	Soil HBCL mg/kg
Antimony	8.25049E-07	1.57152E-07	#DIV/0!	#DIV/0!
Beryllium	2.10965E-07	5.34318E-10	#DIV/0!	1.10E+00
Cadmium	8.25049E-07	1.57152E-07	#DIV/0!	#DIV/0!
Manganese	1.93639E-07	7.70047E-10	#DIV/0!	#DIV/0!
Benzo(a)anthracene	4.12524E-07	4.12524E-07	#DIV/0!	1.85E+01
Benzo(a)pyrene	4.12524E-07	4.12524E-07	#DIV/0!	2.38E+00
Benzo(b)fluoranthene	4.12524E-07	4.12524E-07	#DIV/0!	2.07E+01
Dibenzo(ah)anthracene	4.12524E-07	4.12524E-07	#DIV/0!	1.34E+00
Indeno(123cd)pyrene	4.12524E-07	4.12524E-07	#DIV/0!	1.73E+01
Benzene	0	0	4.77E-07	7.52E+02
Ethylbenzene	0	0	4.53E-07	#DIV/0!
Toluene	0	0	4.64E-07	#DIV/0!
Xylene	0	0	4.45E-07	#DIV/0!

PRG Calculation for US Steel - South Works

Date:	7/6/95	Scenario:	Residential - MLEI				
	Child Soil Ingestion	Adult Soil Ingestion	Child Dermal Contact	Adult Dermal Contact	Child Inhalation	Adult Inhalation	
Body Weight:	15	70	15	70	15	70	kg
Averaging Time (non):	2190	1205	2190	1205	2190	8760	days
Averaging Time (car):	25550	25550	25550	25550	25550	25550	days
Exposure Duration:	6	3.3	6	3.3	6	3.3	years
Exposure Frequency:	350	350	350	350	350	350	days/yr
Conversion Factor:	1.00E-06	1.00E-06	1.00E-06	1.00E-06	1.00E-06	1.00E-06	kg/mg
Soil Ingestion Rate:	50	10	50	10	200	50	mg/day
Skin Surface Area:	2195	2836	2195	2836	2195	2836	cm2
Adherence Factor:	0.2	0.2	0.2	0.2	1	1	mg/cm2
Meteorological Factor:	0.52	0.52	0.52	0.52	0.52	0.52	unitless
Inhalation Rate:	14.2	20	14.2	20	14.2	20	m3/day

Chemical-specific parameters

Chemical	Target Hazard Index	Target Risk	Soil Half-Life (years)	Surface Dilution/ Attenuation Factor	Oral Bioavailability	Dermal ABS	Oral RfD mg/kg-day	Inhalation RfD mg/kg-day	Oral SF (mg/kg-day)-1	Inhalation SF (mg/kg-day)-1	VF (m3/kg)
Antimony	1	1.00E-06		1.00E+00	100.00%	1.0000%	4.00E-04	4.00E-04			
Beryllium	1	1.00E-06		1.00E+00	25.57%	0.0034%	5.00E-03	5.00E-03	4.30E+00	8.40E+00	
Cadmium	1	1.00E-06		1.00E+00	100.00%	1.0000%	1.00E-03	1.00E-03			
Manganese	1	1.00E-06		1.00E+00	23.47%	0.0049%	1.40E-01	1.43E-05			
Benzo(a)anthracene	1	1.00E-06	1.863	8.96E-02	50.00%	10.0000%			7.30E-01	6.10E-01	
Benzo(a)pyrene	1	1.00E-06	1.452	6.98E-02	50.00%	10.0000%			7.30E+00	6.10E+00	
Benzo(b)fluoranthene	1	1.00E-06	1.671	8.04E-02	50.00%	10.0000%			7.30E-01	6.10E-01	
Dibenzo(ah)anthracene	1	1.00E-06	2.575	1.24E-01	50.00%	10.0000%			7.30E+00	6.10E+00	
Indeno(123cd)pyrene	1	1.00E-06	2.000	9.62E-02	50.00%	10.0000%			7.30E-01	6.10E-01	
Benzene	1	1.00E-06	2.000	9.62E-02	100.00%	3.0000%	0.00171	0.00171	2.90E-02	2.90E-02	3.60E+05
Ethylbenzene	1	1.00E-06	0.625	3.01E-02	100.00%	3.0000%	0.1	0.286			3.79E+05
Toluene	1	1.00E-06	0.575	2.77E-02	100.00%	3.0000%	0.2	0.114			3.70E+05
Xylene	1	1.00E-06	1.000	4.81E-02	100.00%	3.0000%	2	2			3.86E+05

PRGs Noncarcinogenic Effects - Child

Chemical	Soil Ingestion XF kg/kg-day	Dermal Contact XF kg/kg-day	Vapor Inhalation XF kg/kg-day	Soil HBCL mg/kg
Antimony	1.6621E-06	8.75595E-07	#DIV/0!	1.58E+02
Beryllium	4.24999E-07	2.97702E-09	#DIV/0!	1.17E+04
Cadmium	1.6621E-06	8.75595E-07	#DIV/0!	3.94E+02
Manganese	3.90095E-07	4.29041E-09	#DIV/0!	3.55E+05
Benzo(a)anthracene	8.3105E-07	8.3105E-07	#DIV/0!	#DIV/0!
Benzo(a)pyrene	8.3105E-07	8.3105E-07	#DIV/0!	#DIV/0!
Benzo(b)fluoranthene	8.3105E-07	8.3105E-07	#DIV/0!	#DIV/0!
Dibenzo(ah)anthracene	8.3105E-07	8.3105E-07	#DIV/0!	#DIV/0!
Indeno(123cd)pyrene	8.3105E-07	8.3105E-07	#DIV/0!	#DIV/0!
Benzene	0	0	2.52E-06	7.05E+03

Ethylbenzene	0	0	2.40E-06	3.97E+06
Toluene	0	0	2.45E-06	1.68E+06
Xylene	0	0	2.35E-06	1.77E+07

PRGs for Noncarcinogenic Effects - Adult

Chemical	Soil Ingestion XF	Dermal Contact XF	Vapor Inhalation XF	Soil HBCL
	kg/kg-day	kg/kg-day	kg/kg-day	mg/kg
Antimony	7.12033E-08	1.33276E-07	#DIV/0!	1.96E+03
Beryllium	1.82067E-08	4.53137E-10	#DIV/0!	2.68E+05
Cadmium	7.12033E-08	1.33276E-07	#DIV/0!	4.89E+03
Manganese	1.67114E-08	6.5305E-10	#DIV/0!	8.06E+06
Benzo(a)anthracene	3.56017E-08	1.33276E-06	#DIV/0!	#DIV/0!
Benzo(a)pyrene	3.56017E-08	1.33276E-06	#DIV/0!	#DIV/0!
Benzo(b)fluoranthene	3.56017E-08	1.33276E-06	#DIV/0!	#DIV/0!
Dibenzo(ah)anthracene	3.56017E-08	1.33276E-06	#DIV/0!	#DIV/0!
Indeno(123cd)pyrene	3.56017E-08	1.33276E-06	#DIV/0!	#DIV/0!
Benzene	0	0	1.05E-07	1.70E+05
Ethylbenzene	0	0	9.94E-08	9.57E+07
Toluene	0	0	1.02E-07	4.05E+07
Xylene	0	0	9.76E-08	4.26E+08

PRGs for Carcinogenic Effects

Chemical	Soil Ingestion XF	Dermal Contact XF	Vapor Inhalation XF	Soil HBCL
	kg/kg-day	kg/kg-day	kg/kg-day	mg/kg
Antimony	1.45824E-07	1.44132E-08	#DIV/0!	#DIV/0!
Beryllium	3.72872E-08	4.90049E-11	#DIV/0!	6.23E+00
Cadmium	1.45824E-07	1.44132E-08	#DIV/0!	#DIV/0!
Manganese	3.42249E-08	7.06248E-11	#DIV/0!	#DIV/0!
Benzo(a)anthracene	7.29119E-08	7.29119E-08	#DIV/0!	1.05E+02
Benzo(a)pyrene	7.29119E-08	7.29119E-08	#DIV/0!	1.35E+01
Benzo(b)fluoranthene	7.29119E-08	7.29119E-08	#DIV/0!	1.17E+02
Dibenzo(ah)anthracene	7.29119E-08	7.29119E-08	#DIV/0!	7.59E+00
Indeno(123cd)pyrene	7.29119E-08	7.29119E-08	#DIV/0!	9.77E+01
Benzene	0	0	2.52E-07	1.42E+03
Ethylbenzene	0	0	2.39E-07	#DIV/0!
Toluene	0	0	2.45E-07	#DIV/0!
Xylene	0	0	2.35E-07	#DIV/0!

PRG Calculation for US Steel - South Works

Date: 7/6/95 Scenario: Recreational - MEI

	Child Soil Ingestion	Adult Soil Ingestion	Child Dermal Contact	Adult Dermal Contact	Child Inhalation	Adult Inhalation	
Body Weight:	15	70	15	70	15	70	kg
Averaging Time (non):	2190	8760	2190	8760	2190	8760	days
Averaging Time (car):	25550	25550	25550	25550	25550	25550	days
Exposure Duration:	6	24	6	24	6	24	years
Exposure Frequency:	104	104	104	104	104	104	days/yr
Conversion Factor:	1.00E-06	1.00E-06	1.00E-06	1.00E-06	1.00E-06	1.00E-06	kg/mg
Soil Ingestion Rate:	200	50	200	50	200	50	mg/day
Skin Surface Area:	2195	2836	2195	2836	2195	2836	cm2
Adherence Factor:	1	1	1	1	1	1	mg/cm2
Meteorological Factor:	0.62	0.62	0.62	0.62	0.62	0.62	unitless
Inhalation Rate:	14.2	20	14.2	20	14.2	20	m3/day

Chemical-specific parameters

Chemical	Target Hazard Index	Target Risk	Soil Half-Life (years)	Dilution/ Attenuation Factor	Oral Bioavailability	Dermal ABS	Oral RfD mg/kg-day	Inhalation RfD mg/kg-day	Oral SF (mg/kg-day)-1	Inhalation SF (mg/kg-day)-1	VF (m3/kg)
Antimony	1	1.00E-06		1.00E+00	100.00%	1.0000%	4.00E-04	4.00E-04			
Beryllium	1	1.00E-06		1.00E+00	25.57%	0.0034%	5.00E-03	5.00E-03	4.30E+00	8.40E+00	
Cadmium	1	1.00E-06		1.00E+00	100.00%	1.0000%	1.00E-03	1.00E-03			
Manganese	1	1.00E-06		1.00E+00	23.47%	0.0049%	1.40E-01	1.43E-05			
Benzo(a)anthracene	1	1.00E-06	1.863	8.96E-02	50.00%	10.0000%			7.30E-01	6.10E-01	
Benzo(a)pyrene	1	1.00E-06	1.452	6.98E-02	50.00%	10.0000%			7.30E+00	6.10E+00	
Benzo(b)fluoranthene	1	1.00E-06	1.671	8.04E-02	50.00%	10.0000%			7.30E-01	6.10E-01	
Dibenzo(ah)anthracene	1	1.00E-06	2.575	1.24E-01	50.00%	10.0000%			7.30E+00	6.10E+00	
Indeno(123cd)pyrene	1	1.00E-06	2.000	9.62E-02	50.00%	10.0000%			7.30E-01	6.10E-01	
Benzene	1	1.00E-06	2.000	9.62E-02	100.00%	3.0000%	0.00171	0.00171	2.90E-02	2.90E-02	3.60E+05
Ethylbenzene	1	1.00E-06	0.625	3.01E-02	100.00%	3.0000%	0.1	0.286			3.79E+05
Toluene	1	1.00E-06	0.575	2.77E-02	100.00%	3.0000%	0.2	0.114			3.70E+05
Xylene	1	1.00E-06	1.000	4.81E-02	100.00%	3.0000%	2	2			3.86E+05

PRGs Noncarcinogenic Effects - Child

Chemical	Soil Ingestion XF kg/kg-day	Dermal Contact XF kg/kg-day	Vapor Inhalation XF kg/kg-day	Soil HBCL mg/kg
Antimony	2.35543E-06	2.58509E-07	#DIV/0!	1.53E+02
Beryllium	6.02284E-07	8.7893E-10	#DIV/0!	8.29E+03
Cadmium	2.35543E-06	2.58509E-07	#DIV/0!	3.83E+02
Manganese	5.5282E-07	1.26659E-09	#DIV/0!	2.53E+05
Benzo(a)anthracene	1.17772E-06	1.17772E-06	#DIV/0!	#DIV/0!
Benzo(a)pyrene	1.17772E-06	1.17772E-06	#DIV/0!	#DIV/0!
Benzo(b)fluoranthene	1.17772E-06	1.17772E-06	#DIV/0!	#DIV/0!
Dibenzo(ah)anthracene	1.17772E-06	1.17772E-06	#DIV/0!	#DIV/0!

Indeno(123cd)pyrene	1.17772E-06	1.17772E-06	#DIV/0!	#DIV/0!
Benzene	0	0	7.49E-07	2.37E+04
Ethylbenzene	0	0	7.12E-07	1.34E+07
Toluene	0	0	7.29E-07	5.66E+06
Xylene	0	0	6.99E-07	5.95E+07

PRGs for Noncarcinogenic Effects - Adult

Chemical	Soil Ingestion XF kg/kg-day	Dermal Contact XF kg/kg-day	Vapor Inhalation XF kg/kg-day	Soil HBCL mg/kg
Antimony	1.26184E-07	7.15715E-08	#DIV/0!	2.02E+03
Beryllium	3.22652E-08	2.43343E-10	#DIV/0!	1.54E+05
Cadmium	1.26184E-07	7.15715E-08	#DIV/0!	5.06E+03
Manganese	2.96154E-08	3.50701E-10	#DIV/0!	4.67E+06
Benzo(a)anthracene	6.3092E-08	6.3092E-08	#DIV/0!	#DIV/0!
Benzo(a)pyrene	6.3092E-08	6.3092E-08	#DIV/0!	#DIV/0!
Benzo(b)fluoranthene	6.3092E-08	6.3092E-08	#DIV/0!	#DIV/0!
Dibenzo(ah)anthracene	6.3092E-08	6.3092E-08	#DIV/0!	#DIV/0!
Indeno(123cd)pyrene	6.3092E-08	6.3092E-08	#DIV/0!	#DIV/0!
Benzene	0	0	2.26E-07	7.86E+04
Ethylbenzene	0	0	2.15E-07	4.43E+07
Toluene	0	0	2.20E-07	1.87E+07
Xylene	0	0	2.11E-07	1.97E+08

PRGs for Carcinogenic Effects

Chemical	Soil Ingestion XF kg/kg-day	Dermal Contact XF kg/kg-day	Vapor Inhalation XF kg/kg-day	Soil HBCL mg/kg
Antimony	2.45157E-07	4.66967E-08	#DIV/0!	#DIV/0!
Beryllium	6.26867E-08	1.58769E-10	#DIV/0!	3.70E+00
Cadmium	2.45157E-07	4.66967E-08	#DIV/0!	#DIV/0!
Manganese	5.75384E-08	2.28814E-10	#DIV/0!	#DIV/0!
Benzo(a)anthracene	1.22579E-07	1.22579E-07	#DIV/0!	6.24E+01
Benzo(a)pyrene	1.22579E-07	1.22579E-07	#DIV/0!	8.00E+00
Benzo(b)fluoranthene	1.22579E-07	1.22579E-07	#DIV/0!	6.95E+01
Dibenzo(ah)anthracene	1.22579E-07	1.22579E-07	#DIV/0!	4.51E+00
Indeno(123cd)pyrene	1.22579E-07	1.22579E-07	#DIV/0!	5.81E+01
Benzene	0	0	1.42E-07	2.53E+03
Ethylbenzene	0	0	1.35E-07	#DIV/0!
Toluene	0	0	1.38E-07	#DIV/0!
Xylene	0	0	1.32E-07	#DIV/0!

PRG Calculation for US Steel - South Works

Date: 7/6/95 Scenario: Recreational - MLEI

	Child Soil Ingestion	Adult Soil Ingestion	Child Dermal Contact	Adult Dermal Contact	Child Inhalation	Adult Inhalation	
Body Weight:	15	70	15	70	15	70	kg
Averaging Time (non):	2190	1205	2190	1205	2190	8760	days
Averaging Time (car):	25550	25550	25550	25550	25550	25550	days
Exposure Duration:	6	3.3	6	3.3	6	3.3	years
Exposure Frequency:	104	104	104	104	104	104	days/yr
Conversion Factor:	1.00E-06	1.00E-06	1.00E-06	1.00E-06	1.00E-06	1.00E-06	kg/mg
Soil Ingestion Rate:	50	10	50	10	200	50	mg/day
Skin Surface Area:	2195	2836	2195	2836	2195	2836	cm2
Adherence Factor:	0.2	0.2	0.2	0.2	1	1	mg/cm2
Meteorological Factor:	0.52	0.52	0.52	0.52	0.52	0.52	unitless
Inhalation Rate:	14.2	20	14.2	20	14.2	20	m3/day

Chemical-specific parameters

Chemical	Target Hazard Index	Target Risk	Soil Half-Life (years)	Dilution/ Attenuation Factor	Oral Bioavailability	Dermal ABS	Oral RfD mg/kg-day	Inhalation RfD mg/kg-day	Oral SF (mg/kg-day)-1	Inhalation SF (mg/kg-day)-1	VF (m3/kg)
Antimony	1	1.00E-06		1.00E+00	100.00%	1.0000%	4.00E-04	4.00E-04			
Beryllium	1	1.00E-06		1.00E+00	25.57%	0.0034%	5.00E-03	5.00E-03	4.30E+00	8.40E+00	
Cadmium	1	1.00E-06		1.00E+00	100.00%	1.0000%	1.00E-03	1.00E-03			
Manganese	1	1.00E-06		1.00E+00	23.47%	0.0049%	1.40E-01	1.43E-05			
Benzo(a)anthracene	1	1.00E-06	1.863	8.96E-02	50.00%	10.0000%			7.30E-01	6.10E-01	
Benzo(a)pyrene	1	1.00E-06	1.452	6.98E-02	50.00%	10.0000%			7.30E+00	6.10E+00	
Benzo(b)fluoranthene	1	1.00E-06	1.671	8.04E-02	50.00%	10.0000%			7.30E-01	6.10E-01	
Dibenzo(ah)anthracene	1	1.00E-06	2.575	1.24E-01	50.00%	10.0000%			7.30E+00	6.10E+00	
Indeno(123cd)pyrene	1	1.00E-06	2.000	9.62E-02	50.00%	10.0000%			7.30E-01	6.10E-01	
Benzene	1	1.00E-06	2.000	9.62E-02	100.00%	3.0000%	0.00171	0.00171	2.90E-02	2.90E-02	3.60E+05
Ethylbenzene	1	1.00E-06	0.625	3.01E-02	100.00%	3.0000%	0.1	0.286			3.79E+05
Toluene	1	1.00E-06	0.575	2.77E-02	100.00%	3.0000%	0.2	0.114			3.70E+05
Xylene	1	1.00E-06	1.000	4.81E-02	100.00%	3.0000%	2	2			3.86E+05

PRGs Noncarcinogenic Effects - Child

Chemical	Soil Ingestion XF kg/kg-day	Dermal Contact XF kg/kg-day	Vapor Inhalation XF kg/kg-day	Soil HBCL mg/kg
Antimony	4.93881E-07	4.33628E-08	#DIV/0!	7.45E+02
Beryllium	1.26285E-07	1.47433E-10	#DIV/0!	3.95E+04
Cadmium	4.93881E-07	4.33628E-08	#DIV/0!	1.86E+03
Manganese	1.15914E-07	2.12478E-10	#DIV/0!	1.21E+06
Benzo(a)anthracene	2.46941E-07	2.46941E-07	#DIV/0!	#DIV/0!
Benzo(a)pyrene	2.46941E-07	2.46941E-07	#DIV/0!	#DIV/0!
Benzo(b)fluoranthene	2.46941E-07	2.46941E-07	#DIV/0!	#DIV/0!
Dibenzo(ah)anthracene	2.46941E-07	2.46941E-07	#DIV/0!	#DIV/0!

Indeno(123cd)pyrene	2.46941E-07	2.46941E-07	#DIV/0!	#DIV/0!
Benzene	0	0	7.49E-07	2.37E+04
Ethylbenzene	0	0	7.12E-07	1.34E+07
Toluene	0	0	7.29E-07	5.66E+06
Xylene	0	0	6.99E-07	5.95E+07

PRGs for Noncarcinogenic Effects - Adult

Chemical	Soil Ingestion XF	Dermal Contact XF	Vapor Inhalation XF	Soil HBCL
	kg/kg-day	kg/kg-day	kg/kg-day	mg/kg
Antimony	2.11576E-08	1.20006E-08	#DIV/0!	1.21E+04
Beryllium	5.40999E-09	4.08019E-11	#DIV/0!	9.17E+05
Cadmium	2.11576E-08	1.20006E-08	#DIV/0!	3.02E+04
Manganese	4.96568E-09	5.88028E-11	#DIV/0!	2.79E+07
Benzo(a)anthracene	1.05788E-08	1.05788E-08	#DIV/0!	#DIV/0!
Benzo(a)pyrene	1.05788E-08	1.05788E-08	#DIV/0!	#DIV/0!
Benzo(b)fluoranthene	1.05788E-08	1.05788E-08	#DIV/0!	#DIV/0!
Dibenzo(ah)anthracene	1.05788E-08	1.05788E-08	#DIV/0!	#DIV/0!
Indeno(123cd)pyrene	1.05788E-08	1.05788E-08	#DIV/0!	#DIV/0!
Benzene	0	0	3.11E-08	5.72E+05
Ethylbenzene	0	0	2.95E-08	3.22E+08
Toluene	0	0	3.03E-08	1.36E+08
Xylene	0	0	2.90E-08	1.43E+09

PRGs for Carcinogenic Effects

Chemical	Soil Ingestion XF	Dermal Contact XF	Vapor Inhalation XF	Soil HBCL
	kg/kg-day	kg/kg-day	kg/kg-day	mg/kg
Antimony	4.33305E-08	4.28279E-09	#DIV/0!	#DIV/0!
Beryllium	1.10796E-08	1.45615E-11	#DIV/0!	2.10E+01
Cadmium	4.33305E-08	4.28279E-09	#DIV/0!	#DIV/0!
Manganese	1.01697E-08	2.09856E-11	#DIV/0!	#DIV/0!
Benzo(a)anthracene	2.16653E-08	2.16653E-08	#DIV/0!	3.53E+02
Benzo(a)pyrene	2.16653E-08	2.16653E-08	#DIV/0!	4.53E+01
Benzo(b)fluoranthene	2.16653E-08	2.16653E-08	#DIV/0!	3.93E+02
Dibenzo(ah)anthracene	2.16653E-08	2.16653E-08	#DIV/0!	2.55E+01
Indeno(123cd)pyrene	2.16653E-08	2.16653E-08	#DIV/0!	3.29E+02
Benzene	0	0	7.49E-08	4.79E+03
Ethylbenzene	0	0	7.11E-08	#DIV/0!
Toluene	0	0	7.29E-08	#DIV/0!
Xylene	0	0	6.98E-08	#DIV/0!

PRG Calculation for US Steel - South Works

Date: 7/6/95 | Scenario: [illegible]/Commercial [illegible]

	Adult Soil Ingestion	Adult Dermal Contact	Adult Inhalation	
Body Weight:	70	70	70	kg
Averaging Time (non):	9125	9125	9125	days
Averaging Time (carc.):	25550	25550	25550	days
Exposure Duration:	25	25	25	years
Exposure Duration:	25	25	25	years
Exposure Frequency:	250	250	250	days/year
Conversion Factor:	1.00E-06	1.00E-06	1.00E-06	kg/mg
Soil Ingestion Rate:	50			mg/day
Meteorological Factor:	0.62	0.62	0.62	
Skin Surface Area:		2836		cm2
Adherence Factor:		1		mg/cm2
PM10 Conc for Site:				mg/m3
Exposure Time:			8	hours
Inhalation Rate:			0.83	m3/hr

Chemical-specific parameters

Chemical	Target Hazard Index	Target Risk	Soil Half-Life (years)	Dilution/ Attenuation Factor	Oral Bioavailability	Dermal ABS	Oral RfD mg/kg-day	Inhalation RfD mg/kg-day	Oral SF (mg/kg-day)-1	Inhalation SF (mg/kg-day)-1	VF (m3/kg)
Antimony	1	1.00E-06		1.00E+00	100.00%	1.0000%	4.00E-04	4.00E-04			
Beryllium	1	1.00E-06		1.00E+00	25.57%	0.0034%	5.00E-03	5.00E-03	4.30E+00	8.40E+00	
Cadmium	1	1.00E-06		1.00E+00	100.00%	1.0000%	1.00E-03	1.00E-03			
Manganese	1	1.00E-06		1.00E+00	23.47%	0.0049%	1.40E-01	1.43E-05			
Benzo(a)anthracene	1	1.00E-06	1.863	1.08E-01	50.00%	10.0000%			7.30E-01	6.10E-01	
Benzo(a)pyrene	1	1.00E-06	1.452	8.38E-02	50.00%	10.0000%			7.30E+00	6.10E+00	
Benzo(b)fluoranthene	1	1.00E-06	1.671	9.64E-02	50.00%	10.0000%			7.30E-01	6.10E-01	
Dibenzo(ah)anthracene	1	1.00E-06	2.575	1.48E-01	50.00%	10.0000%			7.30E+00	6.10E+00	
Indeno(123cd)pyrene	1	1.00E-06	2.000	1.15E-01	50.00%	10.0000%			7.30E-01	6.10E-01	
Benzene	1	1.00E-06	2.000	1.15E-01	100.00%	3.0000%	0.00171	0.00171	2.90E-02	2.90E-02	3.02E+05
Ethylbenzene	1	1.00E-06	0.625	3.61E-02	100.00%	3.0000%	0.1	0.286			3.20E+05
Toluene	1	1.00E-06	0.575	3.32E-02	100.00%	3.0000%	0.2	0.114			3.11E+05
Xylene	1	1.00E-06	1.000	5.77E-02	100.00%	3.0000%	2	2			3.27E+05

HBCLs for Carcinogenic Effects

Chemical	Soil Ingestion XF kg/kg-day	Dermal Contact XF kg/kg-day	Particulate Inhalation XF kg/kg-day	Vapor Inhalation XF kg/kg-day	Soil HBCL mg/kg
Antimony	1.08E-07	6.14E-08	0.00E+00	#DIV/0!	#DIV/0!
Beryllium	2.77E-08	2.09E-10	0.00E+00	#DIV/0!	8.33E+00
Cadmium	1.08E-07	6.14E-08	0.00E+00	#DIV/0!	#DIV/0!
Manganese	2.54E-08	3.01E-10	0.00E+00	#DIV/0!	#DIV/0!
Benzo(a)anthracene	5.42E-08	5.42E-08	0.00E+00	#DIV/0!	1.18E+02
Benzo(a)pyrene	5.42E-08	5.42E-08	0.00E+00	#DIV/0!	1.51E+01
Benzo(b)fluoranthene	5.42E-08	5.42E-08	0.00E+00	#DIV/0!	1.31E+02
Dibenzo(ah)anthracene	5.42E-08	5.42E-08	0.00E+00	#DIV/0!	8.52E+00

Indeno(123cd)pyrene	5.42E-08	5.42E-08	0.00E+00	#DIV/0!	1.10E+02
Benzene	0.00E+00	0.00E+00	0.00E+00	7.68E-08	3.89E+03
Ethylbenzene	0.00E+00	0.00E+00	0.00E+00	7.25E-08	#DIV/0!
Toluene	0.00E+00	0.00E+00	0.00E+00	7.46E-08	#DIV/0!
Xylene	0.00E+00	0.00E+00	0.00E+00	7.10E-08	#DIV/0!

HBCLs for Noncarcinogenic Effects

Chemical	Soil Ingestion XF kg/kg-day	Dermal Contact XF kg/kg-day	Particulate Inhalation XF kg/kg-day	Vapor Inhalation XF kg/kg-day	Soil HBCL mg/kg
Antimony	3.03E-07	1.72E-07	0.00E+00	#DIV/0!	8.41E+02
Beryllium	7.76E-08	5.85E-10	0.00E+00	#DIV/0!	6.40E+04
Cadmium	3.03E-07	1.72E-07	0.00E+00	#DIV/0!	2.10E+03
Manganese	7.12E-08	8.43E-10	0.00E+00	#DIV/0!	1.94E+06
Benzo(a)anthracene	1.52E-07	1.52E-07	0.00E+00	#DIV/0!	#DIV/0!
Benzo(a)pyrene	1.52E-07	1.52E-07	0.00E+00	#DIV/0!	#DIV/0!
Benzo(b)fluoranthene	1.52E-07	1.52E-07	0.00E+00	#DIV/0!	#DIV/0!
Dibenzo(ah)anthracene	1.52E-07	1.52E-07	0.00E+00	#DIV/0!	#DIV/0!
Indeno(123cd)pyrene	1.52E-07	1.52E-07	0.00E+00	#DIV/0!	#DIV/0!
Benzene	0.00E+00	0.00E+00	0.00E+00	2.15E-07	6.89E+04
Ethylbenzene	0.00E+00	0.00E+00	0.00E+00	2.03E-07	3.91E+07
Toluene	0.00E+00	0.00E+00	0.00E+00	2.09E-07	1.64E+07
Xylene	0.00E+00	0.00E+00	0.00E+00	1.99E-07	1.74E+08

PRG Calculation for US Steel South Works

Date	7/6/95	Scenario:	Industrial/Commercial - MLEI	
	Adult Soil Ingestion	Adult Dermal Contact	Adult Inhalation	
Body Weight:	70	70	70	kg
Averaging Time (non):	1642.5	1642.5	1642.5	days
Averaging Time (carc.):	25550	25550	25550	days
Exposure Duration	4.5	4.5	4.5	years
Exposure Duration:	4.5	4.5	4.5	years
Exposure Frequency	250	250	250	days/year
Conversion Factor:	1.00E-06	1.00E-06	1.00E-06	kg/mg
Soil Ingestion Rate:	10			mg/day
Meteorological Factor	0.52	0.52	0.52	
Skin Surface Area:		2836		cm2
Adherence Factor:		0.2		mg/cm2
PM10 Conc for Site:				mg/m3
Exposure Time:			8	hours
Inhalation Rate:			0.83	m3/hr

Chemical-specific parameters

Chemical	Target Hazard Index	Target Risk	Soil Half-Life (years)	Surface Dilution/ Attenuation Factor	Oral Bioavailability	Dermal ABS	Oral RfD mg/kg-day	Inhalation RfD mg/kg-day	Oral SF (mg/kg-day)-1	Inhalation SF (mg/kg-day)-1	VF (m3/kg)
Antimony	1	1.00E-06		1.00E+00	100.00%	1.0000%	4.00E-04	4.00E-04			
Beryllium	1	1.00E-06		1.00E+00	25.57%	0.0034%	5.00E-03	5.00E-03	4.30E+00	8.40E+00	
Cadmium	1	1.00E-06		1.00E+00	100.00%	1.0000%	1.00E-03	1.00E-03			
Manganese	1	1.00E-06		1.00E+00	23.47%	0.0049%	1.40E-01	1.43E-05			
Benzo(a)anthracene	1	1.00E-06	1.863	1.08E-01	50.00%	10.0000%			7.30E-01	6.10E-01	
Benzo(a)pyrene	1	1.00E-06	1.452	8.38E-02	50.00%	10.0000%			7.30E+00	6.10E+00	
Benzo(b)fluoranthene	1	1.00E-06	1.671	9.64E-02	50.00%	10.0000%			7.30E-01	6.10E-01	
Dibenzo(ah)anthracene	1	1.00E-06	2.575	1.48E-01	50.00%	10.0000%			7.30E+00	6.10E+00	
Indeno(123cd)pyrene	1	1.00E-06	2.000	1.15E-01	50.00%	10.0000%			7.30E-01	6.10E-01	
Benzene	1	1.00E-06	2.000	1.15E-01	100.00%	3.0000%	0.00171	0.00171	2.90E-02	2.90E-02	3.02E+05
Ethylbenzene	1	1.00E-06	0.625	3.61E-02	100.00%	3.0000%	0.1	0.286			3.20E+05
Toluene	1	1.00E-06	0.575	3.32E-02	100.00%	3.0000%	0.2	0.114			3.11E+05
Xylene	1	1.00E-06	1.000	5.77E-02	100.00%	3.0000%	2	2			3.27E+05

HBCLs for Carcinogenic Effects

Chemical	Soil Ingestion XF kg/kg-day	Dermal Contact XF kg/kg-day	Particulate Inhalation XF kg/kg-day	Vapor Inhalation XF kg/kg-day	Soil HBCL mg/kg
Antimony	3.27E-09	1.86E-09	0.00E+00	#DIV/0!	#DIV/0!
Beryllium	8.36E-10	6.31E-12	0.00E+00	#DIV/0!	2.76E+02
Cadmium	3.27E-09	1.86E-09	0.00E+00	#DIV/0!	#DIV/0!
Manganese	7.68E-10	9.09E-12	0.00E+00	#DIV/0!	#DIV/0!
Benzo(a)anthracene	1.64E-09	1.64E-09	0.00E+00	#DIV/0!	3.90E+03
Benzo(a)pyrene	1.64E-09	1.64E-09	0.00E+00	#DIV/0!	5.00E+02
Benzo(b)fluoranthene	1.64E-09	1.64E-09	0.00E+00	#DIV/0!	4.34E+03
Dibenzo(ah)anthracene	1.64E-09	1.64E-09	0.00E+00	#DIV/0!	2.82E+02
Indeno(123cd)pyrene	1.64E-09	1.64E-09	0.00E+00	#DIV/0!	3.63E+03
Benzene	0.00E+00	0.00E+00	0.00E+00	1.38E-08	2.16E+04
Ethylbenzene	0.00E+00	0.00E+00	0.00E+00	1.31E-08	#DIV/0!

Toluene	0.00E+00	0.00E+00	0.00E+00	1.34E-08	#DIV/0!						
Xylene	0.00E+00	0.00E+00	0.00E+00	1.28E-08	#DIV/0!						
HBCLs for Noncarcinogenic Effects											
	Soil	Dermal	Particulate	Vapor							
Chemical	Ingestion XF	Contact XF	Inhalation XF	Inhalation XF	Soil HBCL						
	kg/kg-day	kg/kg-day	kg/kg-day	kg/kg-day	mg/kg						
Antimony	5.09E-08	2.89E-08	0.00E+00	#DIV/0!	5.02E+03						
Beryllium	1.30E-08	9.81E-11	0.00E+00	#DIV/0!	3.81E+05						
Cadmium	5.09E-08	2.89E-08	0.00E+00	#DIV/0!	1.25E+04						
Manganese	1.19E-08	1.41E-10	0.00E+00	#DIV/0!	1.16E+07						
Benzo(a)anthracene	2.54E-08	2.54E-08	0.00E+00	#DIV/0!	#DIV/0!						
Benzo(a)pyrene	2.54E-08	2.54E-08	0.00E+00	#DIV/0!	#DIV/0!						
Benzo(b)fluoranthene	2.54E-08	2.54E-08	0.00E+00	#DIV/0!	#DIV/0!						
Dibenzo(ah)anthracene	2.54E-08	2.54E-08	0.00E+00	#DIV/0!	#DIV/0!						
Indeno(123cd)pyrene	2.54E-08	2.54E-08	0.00E+00	#DIV/0!	#DIV/0!						
Benzene	0.00E+00	0.00E+00	0.00E+00	2.15E-07	6.89E+04						
Ethylbenzene	0.00E+00	0.00E+00	0.00E+00	2.03E-07	3.91E+07						
Toluene	0.00E+00	0.00E+00	0.00E+00	2.09E-07	1.64E+07						
Xylene	0.00E+00	0.00E+00	0.00E+00	1.99E-07	1.74E+08						

PRG Calculation for US Steel - South Works

Date:	7/5/95	Scenario:	Construction - MEI								
	Adult Soil Ingestion	Adult Dermal Contact	Adult Inhalation								
Body Weight	70	70	70	kg							
Averaging Time (non):	365	365	365	days							
Averaging Time (carc.):	25550	25550	25550	days							
Exposure Duration:	1	1	1	years							
Exposure Duration:	1	1	1	years							
Exposure Frequency:	160	160	160	days/year							
Conversion Factor:	1.00E-06	1.00E-06	1.00E-06	kg/mg							
Soil Ingestion Rate:	200			mg/day							
Fraction Ingested:	1	1	1								
Skin Surface Area:		4300		cm2							
Adherence Factor:		1.5		mg/cm2				PELs	RfD - Inh		
PM10 Conc for Site:			5	mg/m3				0.5	1.43E-01		
Exposure Time:			8	hours	1.14E-04			0.002	5.71E-04		
Inhalation Rate:			0.83	m3/hr				0.005	1.43E-03		
								5	1.43E+00		

Chemical-specific parameters

Chemical	Target Hazard Index	Target Risk	Soil Half-Life (years)	Dilution/ Attenuation Factor	Oral Bioavailability	Dermal ABS	Oral RfD mg/kg-day	Inhalation RfD mg/kg-day	Oral SF (mg/kg-day)-1	Inhalation SF (mg/kg-day)-1	VF (m3/kg)
Antimony	1	1.00E-06		1.00E+00	100.00%	1.0000%	4.00E-04	1.43E-01			
Beryllium	1	1.00E-06		1.00E+00	25.57%	0.0034%	5.00E-03	5.71E-04	4.30E+00	8.40E+00	
Cadmium	1	1.00E-06		1.00E+00	100.00%	1.0000%	1.00E-03	1.43E-03		6.30E+00	
Manganese	1	1.00E-06		1.00E+00	23.47%	0.0049%	1.40E-01	1.43E+00			
Benzo(a)anthracene	1	1.00E-06	1.863	8.35E-01	50.00%	10.0000%			7.30E-01	6.10E-01	
Benzo(a)pyrene	1	1.00E-06	1.452	7.95E-01	50.00%	10.0000%			7.30E+00	6.10E+00	
Benzo(b)fluoranthene	1	1.00E-06	1.671	8.19E-01	50.00%	10.0000%			7.30E-01	6.10E-01	
Dibenzo(ah)anthracene	1	1.00E-06	2.575	8.77E-01	50.00%	10.0000%			7.30E+00	6.10E+00	
Indeno(123cd)pyrene	1	1.00E-06	2.000	8.45E-01	50.00%	10.0000%			7.30E-01	6.10E-01	
Anthracene	1	1.00E-06	5.860	9.43E-01	50.00%	10.0000%	3.00E-01	3.00E-01			1.42E+06
Acenaphthene	1	1.00E-06	0.279	3.69E-01	50.00%	10.0000%	6.00E-02	6.00E-02			6.01E+05
Acenaphthylene	1	1.00E-06	0.164	2.34E-01	50.00%	10.0000%	6.00E-02	6.00E-02			2.19E+04
Benzo(ghi)perylene	1	1.00E-06	1.781	8.28E-01	50.00%	10.0000%	6.00E-02	6.00E-02			
Benzo(k)fluoranthene	1	1.00E-06	5.860	9.43E-01	50.00%	10.0000%			7.30E-02	6.10E-02	
Chrysene	1	1.00E-06	2.720	8.83E-01	50.00%	10.0000%			7.30E-03	6.10E-03	
Fluoranthene	1	1.00E-06	1.205	7.61E-01	50.00%	10.0000%	4.00E-02	4.00E-02			
Fluorene	1	1.00E-06	0.164	2.34E-01	50.00%	10.0000%	4.00E-02	4.00E-02			9.01E+05
Pyrene	1	1.00E-06	5.200	9.36E-01	50.00%	10.0000%	3.00E-02	3.00E-02			3.76E+06
Phenanthrene	1	1.00E-06	0.548	5.67E-01	50.00%	10.0000%	6.00E-02	6.00E-02			9.04E+05
Benzene	1	1.00E-06	2.000	8.45E-01	100.00%	3.0000%	1.71E-03	1.71E-03	2.90E-02	2.90E-02	1.81E+04
Ethylbenzene	1	1.00E-06	0.625	6.04E-01	100.00%	3.0000%	1.00E-01	2.86E-01			2.51E+04
Toluene	1	1.00E-06	0.575	5.81E-01	100.00%	3.0000%	2.00E-01	1.14E-01			2.17E+04
Xylenes	1	1.00E-06	1.000	7.21E-01	100.00%	3.0000%	2.00E+00	2.00E+00			2.99E+04

HBCLs for Carcinogenic Effects

Chemical	Soil Ingestion XF kg/kg-day	Dermal Contact XF kg/kg-day	Particulate Inhalation XF kg/kg-day	Vapor Inhalation XF kg/kg-day	Soil HBCL mg/kg
Antimony	1.79E-08	5.77E-09	2.97E-09	#DIV/0!	#DIV/0!

Beryllium	4.58E-09	1.96E-11	2.97E-09	#DIV/0!	2.24E+01
Cadmium	1.79E-08	5.77E-09	2.97E-09	#DIV/0!	5.34E+01
Manganese	4.20E-09	7.88E-11	2.97E-09	#DIV/0!	#DIV/0!
Benzo(a)anthracene	8.95E-09	8.95E-09	2.97E-09	#DIV/0!	8.05E+01
Benzo(a)pyrene	8.95E-09	8.95E-09	2.97E-09	#DIV/0!	8.46E+00
Benzo(b)fluoranthene	8.95E-09	8.95E-09	2.97E-09	#DIV/0!	8.21E+01
Dibenzo(ah)anthracene	8.95E-09	8.95E-09	2.97E-09	#DIV/0!	7.67E+00
Indeno(123cd)pyrene	8.95E-09	8.95E-09	2.97E-09	#DIV/0!	7.96E+01
Anthracene	8.95E-09	8.95E-09	2.97E-09	4.18E-10	#DIV/0!
Acenaphthene	8.95E-09	8.95E-09	2.97E-09	9.88E-10	#DIV/0!
Acenaphthylene	8.95E-09	8.95E-09	2.97E-09	2.71E-08	#DIV/0!
Benzo(ghi)perylene	8.95E-09	8.95E-09	2.97E-09	#DIV/0!	#DIV/0!
Benzo(k)fluoranthene	8.95E-09	8.95E-09	2.97E-09	#DIV/0!	7.13E+02
Chrysene	8.95E-09	8.95E-09	2.97E-09	#DIV/0!	7.62E+03
Fluoranthene	8.95E-09	8.95E-09	2.97E-09	#DIV/0!	#DIV/0!
Fluorene	8.95E-09	8.95E-09	2.97E-09	6.59E-10	#DIV/0!
Pyrene	8.95E-09	8.95E-09	2.97E-09	1.58E-10	#DIV/0!
Phenanthrene	8.95E-09	8.95E-09	2.97E-09	6.57E-10	#DIV/0!
Benzene	1.79E-08	1.73E-08	2.97E-09	3.28E-08	5.75E+02
Ethylbenzene	1.79E-08	1.73E-08	2.97E-09	2.37E-08	#DIV/0!
Toluene	1.79E-08	1.73E-08	2.97E-09	2.74E-08	#DIV/0!
Xylenes	1.79E-08	1.73E-08	2.97E-09	1.99E-08	#DIV/0!

HBCLs for Noncarcinogenic Effects

Chemical	Soil Ingestion XF kg/kg-day	Dermal Contact XF kg/kg-day	Particulate Inhalation XF kg/kg-day	Vapor Inhalation XF kg/kg-day	Soil HBCL mg/kg
Antimony	1.25E-06	4.04E-07	2.08E-07	#DIV/0!	2.41E+02
Beryllium	3.20E-07	1.37E-09	2.08E-07	#DIV/0!	2.34E+03
Cadmium	1.25E-06	4.04E-07	2.08E-07	#DIV/0!	5.55E+02
Manganese	2.94E-07	1.98E-09	2.08E-07	#DIV/0!	4.43E+05
Benzo(a)anthracene	6.26E-07	6.26E-07	2.08E-07	#DIV/0!	#DIV/0!
Benzo(a)pyrene	6.26E-07	6.26E-07	2.08E-07	#DIV/0!	#DIV/0!
Benzo(b)fluoranthene	6.26E-07	6.26E-07	2.08E-07	#DIV/0!	#DIV/0!
Dibenzo(ah)anthracene	6.26E-07	6.26E-07	2.08E-07	#DIV/0!	#DIV/0!
Indeno(123cd)pyrene	6.26E-07	6.26E-07	2.08E-07	#DIV/0!	#DIV/0!
Anthracene	6.26E-07	6.26E-07	2.08E-07	2.93E-08	2.54E+05
Acenaphthene	6.26E-07	6.26E-07	2.08E-07	6.92E-08	1.30E+05
Acenaphthylene	6.26E-07	6.26E-07	2.08E-07	1.90E-06	2.05E+05
Benzo(ghi)perylene	6.26E-07	6.26E-07	2.08E-07	#DIV/0!	4.96E+04
Benzo(k)fluoranthene	6.26E-07	6.26E-07	2.08E-07	#DIV/0!	#DIV/0!
Chrysene	6.26E-07	6.26E-07	2.08E-07	#DIV/0!	#DIV/0!
Fluoranthene	6.26E-07	6.26E-07	2.08E-07	#DIV/0!	3.60E+04
Fluorene	6.26E-07	6.26E-07	2.08E-07	4.62E-08	1.37E+05
Pyrene	6.26E-07	6.26E-07	2.08E-07	1.11E-08	2.56E+04
Phenanthrene	6.26E-07	6.26E-07	2.08E-07	4.60E-08	8.44E+04
Benzene	1.25E-06	1.21E-06	2.08E-07	2.30E-06	4.07E+02
Ethylbenzene	1.25E-06	1.21E-06	2.08E-07	1.66E-06	5.31E+04
Toluene	1.25E-06	1.21E-06	2.08E-07	1.92E-06	5.56E+04
Xylenes	1.25E-06	1.21E-06	2.08E-07	1.39E-06	6.82E+05

PRG Calculation for US Steel - South Works

Date:	7/6/95	Scenario:	Construction -MLEI	

	Adult Soil Ingestion	Adult Dermal Contact	Adult Inhalation								
Body Weight:	70	70	70	kg							
Averaging Time (non):	365	365	365	days							
Averaging Time (carc.):	25550	25550	25550	days							
Exposure Duration:	1	1	1	years							
Exposure Duration:	1	1	1	years							
Exposure Frequency:	160	160	160	days/year							
Conversion Factor:	1.00E-06	1.00E-06	1.00E-06	kg/mg							
Soil Ingestion Rate:	50			mg/day							
Fraction Ingested:	1	1	1								
Skin Surface Area:		4300		cm2							
Adherence Factor:		1.5		mg/cm2				PELs	RfD - Inh		
PM10 Conc for Site:			0.05	mg/m3				0.5	1.43E-01		
Exposure Time:			8	hours	1.14E-04			0.002	5.71E-04		
Inhalation Rate:			0.83	m3/hr				0.005	1.43E-03		
								5	1.43E+00		

Chemical-specific parameters

Chemical	Target Hazard Index	Target Risk	Soil Half-Life (years)	Dilution/ Attenuation Factor	Oral Bioavailability	Dermal ABS	Oral RfD mg/kg-day	Inhalation RfD mg/kg-day	Oral SF (mg/kg-day)-1	Inhalation SF (mg/kg-day)-1	VF (m3/kg)
Antimony	1	1.00E-06		1.00E+00	100.00%	1.0000%	4.00E-04	1.43E-01			
Beryllium	1	1.00E-06		1.00E+00	25.57%	0.0034%	5.00E-03	5.71E-04	4.30E+00	8.40E+00	
Cadmium	1	1.00E-06		1.00E+00	100.00%	1.0000%	1.00E-03	1.43E-03		6.30E+00	
Manganese	1	1.00E-06		1.00E+00	23.47%	0.0049%	1.40E-01	1.43E+00			
Benzo(a)anthracene	1	1.00E-06	1.863	8.35E-01	50.00%	10.0000%			7.30E-01	6.10E-01	
Benzo(a)pyrene	1	1.00E-06	1.452	7.95E-01	50.00%	10.0000%			7.30E+00	6.10E+00	
Benzo(b)fluoranthene	1	1.00E-06	1.671	8.19E-01	50.00%	10.0000%			7.30E-01	6.10E-01	
Dibenzo(ah)anthracene	1	1.00E-06	2.575	8.77E-01	50.00%	10.0000%			7.30E+00	6.10E+00	
Indeno(123cd)pyrene	1	1.00E-06	2.000	8.45E-01	50.00%	10.0000%			7.30E-01	6.10E-01	
Anthracene	1	1.00E-06	5.860	9.43E-01	50.00%	10.0000%	3.00E-01	3.00E-01			1.42E+06
Acenaphthene	1	1.00E-06	0.279	3.69E-01	50.00%	10.0000%	6.00E-02	6.00E-02			6.01E+05
Acenaphthylene	1	1.00E-06	0.164	2.34E-01	50.00%	10.0000%	6.00E-02	6.00E-02			2.19E+04
Benzo(ghi)perylene	1	1.00E-06	1.781	8.28E-01	50.00%	10.0000%	6.00E-02	6.00E-02			
Benzo(k)fluoranthene	1	1.00E-06	5.860	9.43E-01	50.00%	10.0000%			7.30E-02	6.10E-02	
Chrysene	1	1.00E-06	2.720	8.83E-01	50.00%	10.0000%			7.30E-03	6.10E-03	
Fluoranthene	1	1.00E-06	1.205	7.61E-01	50.00%	10.0000%	4.00E-02	4.00E-02			
Fluorene	1	1.00E-06	0.164	2.34E-01	50.00%	10.0000%	4.00E-02	4.00E-02			9.01E+05
Pyrene	1	1.00E-06	5.200	9.36E-01	50.00%	10.0000%	3.00E-02	3.00E-02			3.76E+06
Phenanthrene	1	1.00E-06	0.548	5.67E-01	50.00%	10.0000%	6.00E-02	6.00E-02			9.04E+05
Benzene	1	1.00E-06	2.000	8.45E-01	100.00%	3.0000%	1.71E-03	1.71E-03	2.90E-02	2.90E-02	1.81E+04
Ethylbenzene	1	1.00E-06	0.375	5.81E-01	100.00%	3.0000%	1.00E-01	2.86E-01			2.51E+04
Toluene	1	1.00E-06	0.625	6.04E-01	100.00%	3.0000%	2.00E-01	1.14E-01			2.17E+04
Xylenes	1	1.00E-06	1.000	7.21E-01	100.00%	3.0000%	2.00E+00	2.00E+00			2.99E+04

HBCLs for Carcinogenic Effects Chemical	Soil Ingestion XF kg/kg-day	Dermal Contact XF kg/kg-day	Particulate Inhalation XF kg/kg-day	Vapor Inhalation XF kg/kg-day	Soil HBCL mg/kg
Antimony	4.47E-09	5.77E-09	2.97E-11	#DIV/0!	#DIV/0!
Beryllium	1.14E-09	1.96E-11	2.97E-11	#DIV/0!	1.90E+02
Cadmium	4.47E-09	5.77E-09	2.97E-11	#DIV/0!	5.34E+03
Manganese	1.05E-09	2.83E-11	2.97E-11	#DIV/0!	#DIV/0!
Benzo(a)anthracene	2.24E-09	2.24E-09	2.97E-11	#DIV/0!	3.65E+02
Benzo(a)pyrene	2.24E-09	2.24E-09	2.97E-11	#DIV/0!	3.83E+01
Benzo(b)fluoranthene	2.24E-09	2.24E-09	2.97E-11	#DIV/0!	3.72E+02
Dibenzo(ah)anthracene	2.24E-09	2.24E-09	2.97E-11	#DIV/0!	3.47E+01
Indeno(123cd)pyrene	2.24E-09	2.24E-09	2.97E-11	#DIV/0!	3.60E+02
Anthracene	2.24E-09	2.24E-09	2.97E-11	4.18E-10	#DIV/0!
Acenaphthene	2.24E-09	2.24E-09	2.97E-11	9.88E-10	#DIV/0!
Acenaphthylene	2.24E-09	2.24E-09	2.97E-11	2.71E-08	#DIV/0!
Benzo(ghi)perylene	2.24E-09	2.24E-09	2.97E-11	#DIV/0!	#DIV/0!
Benzo(k)fluoranthene	2.24E-09	2.24E-09	2.97E-11	#DIV/0!	3.23E+03
Chrysene	2.24E-09	2.24E-09	2.97E-11	#DIV/0!	3.45E+04
Fluoranthene	2.24E-09	2.24E-09	2.97E-11	#DIV/0!	#DIV/0!
Fluorene	2.24E-09	2.24E-09	2.97E-11	6.59E-10	#DIV/0!
Pyrene	2.24E-09	2.24E-09	2.97E-11	1.58E-10	#DIV/0!
Phenanthrene	2.24E-09	2.24E-09	2.97E-11	6.57E-10	#DIV/0!
Benzene	4.47E-09	1.73E-08	2.97E-11	3.28E-08	7.47E+02
Ethylbenzene	4.47E-09	1.73E-08	2.97E-11	2.37E-08	#DIV/0!
Toluene	4.47E-09	1.73E-08	2.97E-11	2.74E-08	#DIV/0!
Xylenes	4.47E-09	1.73E-08	2.97E-11	1.99E-08	#DIV/0!

HBCLs for Noncarcinogenic Effects

Chemical	Soil Ingestion XF kg/kg-day	Dermal Contact XF kg/kg-day	Particulate Inhalation XF kg/kg-day	Vapor Inhalation XF kg/kg-day	Soil HBCL mg/kg
Antimony	3.13E-07	4.04E-07	2.08E-09	#DIV/0!	5.58E+02
Beryllium	8.01E-08	1.37E-09	2.08E-09	#DIV/0!	5.02E+04
Cadmium	3.13E-07	4.04E-07	2.08E-09	#DIV/0!	1.39E+03
Manganese	7.35E-08	1.98E-09	2.08E-09	#DIV/0!	1.85E+06
Benzo(a)anthracene	1.57E-07	1.57E-07	2.08E-09	#DIV/0!	#DIV/0!
Benzo(a)pyrene	1.57E-07	1.57E-07	2.08E-09	#DIV/0!	#DIV/0!
Benzo(b)fluoranthene	1.57E-07	1.57E-07	2.08E-09	#DIV/0!	#DIV/0!
Dibenzo(ah)anthracene	1.57E-07	1.57E-07	2.08E-09	#DIV/0!	#DIV/0!
Indeno(123cd)pyrene	1.57E-07	1.57E-07	2.08E-09	#DIV/0!	#DIV/0!
Anthracene	1.57E-07	1.57E-07	2.08E-09	2.93E-08	9.23E+05
Acenaphthene	1.57E-07	1.57E-07	2.08E-09	6.92E-08	4.23E+05
Acenaphthylene	1.57E-07	1.57E-07	2.08E-09	1.90E-06	1.16E+05
Benzo(ghi)perylene	1.57E-07	1.57E-07	2.08E-09	#DIV/0!	2.30E+05
Benzo(k)fluoranthene	1.57E-07	1.57E-07	2.08E-09	#DIV/0!	#DIV/0!
Chrysene	1.57E-07	1.57E-07	2.08E-09	#DIV/0!	#DIV/0!
Fluoranthene	1.57E-07	1.57E-07	2.08E-09	#DIV/0!	1.67E+05
Fluorene	1.57E-07	1.57E-07	2.08E-09	4.62E-08	4.74E+05
Pyrene	1.57E-07	1.57E-07	2.08E-09	1.11E-08	9.82E+04
Phenanthrene	1.57E-07	1.57E-07	2.08E-09	4.60E-08	2.93E+05
Benzene	3.13E-07	1.21E-06	2.08E-09	2.30E-06	5.29E+02
Ethylbenzene	3.13E-07	1.21E-06	2.08E-09	1.66E-06	8.18E+04
Toluene	3.13E-07	1.21E-06	2.08E-09	1.92E-06	6.77E+04
Xylenes	3.13E-07	1.21E-06	2.08E-09	1.39E-06	9.50E+05

APPENDIX B

Extraction Protocols

EXTRACTION STUDIES TO DETERMINE THE LEACHING OF BERYLLIUM AND MANGANESE IN SIMULATED GASTRIC CONDITIONS IN SIMULATED SWEAT

March 15, 1995

SCOPE OF WORK

ChemRisk will perform extraction studies to determine the amount of Beryllium (Be), Manganese (Mn), and lead (Pb) that can be extracted from South Works site soil under simulated gastric conditions and the amount of Be and Mn that can be extracted by sweat on the skin. The percent of each metal released from the soil matrix in these experiments will be used to develop site-specific bioavailability factors for the South Works health risk assessment (HRA) versus the use of standard default bioavailability factors.

Extraction in Simulated Gastrointestinal Conditions

Only the fraction of Be, Mn, and Pb that can be released from the soil matrix (into solution) in the acid conditions of the stomach will be absorbed systemically. Some absorption may occur within the intestinal tract, however, the alkaline conditions are expected to significantly reduce the solubility of metals and, hence, limit the systemic absorption. To estimate the absorbed dose of each metal for the soil ingestion pathway, it is important to determine the fraction of these metals that could potentially be solubilized from South Works soils in the acid conditions of the stomach.

ChemRisk will perform a simple extraction experiment to evaluate the amount of Be, Mn, and Pb that can be extracted from South Works soil for simulated gastric conditions. The protocol will include an initial analysis of the soil (in duplicate) to determine the amount of Be, Mn, and Pb in the soil before the extraction is performed. For this study, a small amount of soil will be added to a flask containing strong acid (pH 1.4 HCl) to simulate soil ingestion. The volume of acid and mass of soil are based on the amount of gastric juice in the stomach of a child and the amount of soil ingested under an upper bound exposure condition (200 mg). The pH of the solution will be monitored during the experiment to ensure that the high pH soil does not act as a buffer to the acid. Similar to the stomach conditions, the pH of the acid solution will be kept at approximately 1.4 throughout the extraction study, and the temperature will be kept at 37°C (normal body temperature). The extraction experiment will be conducted for one hour, similar to the residence time for consumed contents in the stomach. The amount of Be, Mn, and Pb released from the soil matrix and in solution at the end of the experiment will be measured and the percent release will be calculated for each metal.

Soil materials for this study will be obtained from WTI. Soil sampling locations were selected based on previous analyses, to collect soils with high and average concentrations for each metal. Soil samples will be collected from the same areas as samples SB-29-1, SS-9-01, and SB-30-1 which were collected during the previous site assessments and which represent samples with high Be and Mn (SB-29-1) and high Pb (SS-9-01). Sample SB-30-1 contained levels of Be, Mn, and Pb that are similar to the average concentrations on the site. The samples are to be collected by WTI and split with ChemRisk®. WTI will have each sample analyzed for Be, Mn, and Pb. New samples shall be named as follows: S-29 (SB-29-1 location), S-9 (SS-9-01 location), and S-30 (SB-30-1 location).

The aqueous solution used as the extractant will be 0.04 M HCl. This molarity concentration represents a fluid with a pH of approximately 1.4, which is within the normal range of gastric fluid pH (normal = <2.0; Clinical Diagnosis by Laboratory Methods, 1974). A ratio of 200 mg soil to 50 mL acid solution will be used in this study. This amount of soil is the USEPA default value for incidental daily soil ingestion by children (USEPA, 1989) and 50 mL is a volume within the range of normal gastric fluid volumes (under basal conditions) for children (20 - 100 mL; Clinical Diagnosis by Laboratory Methods, 1974). However, to facilitate a more precise measurement of soil and to provide the laboratory with an adequate aliquot sample, 1.00 gram portions of soil and 400 mL of HCL are to be used. Soils will be extracted with the acidic solution for 1 hour at 37°C with gentle agitation. The complete gastric extraction protocol is provided as Attachment I. One extraction sample from each soil sample plus one duplicate will be used in the gastric extraction study for a total of six samples. In addition, one laboratory and one HCl spike will be analyzed for quality control.

Procedures and results of this experiment will be discussed in detail in the final HRA.

Extraction in Simulated Sweat on the Skin

Similar to oral absorption, only the fraction of Be and Mn that can be released from the soil matrix in sweat on the skin will be available for dermal/systemic absorption. Hence, it is important to determine the fraction of Be and Mn which could be released from South Works soils in sweat on the skin. Lead will not be evaluated in this study since it is not absorbed dermally to any appreciable degree (USEPA, 1991; ATSDR, 1991) and is not evaluated for dermal contact in either the USEPA IEUBK blood-lead model or the PBPK model developed by Dr. Ellen O'Flaherty (USEPA, 1994; O'Flaherty, 1993).

ChemRisk will perform an extraction experiment to evaluate the amount of Be and Mn that can be extracted from South Works soil in conditions that simulate sweat on the skin. This study will be based on the protocol for sweat extraction discussed in Horowitz and Finley (1993). For this study, a small amount of soil will be added to a flask containing simulated sweat (obtained commercially) at a ratio of 20:1 (sweat to soil), and the temperature will be kept at 37°C

(normal body temperature). This ratio is representative of soil on the skin during work activities and was calculated using the USEPA soil adherence rate as described in Horowitz and Finley (1993) (attached). The extraction experiment will be conducted for 12 hours, similar to the amount of time soil could be in contact with the skin. The amount of Be and Mn released from the soil matrix and in the sweat solution at the end of the experiment will measured and percent release will be calculated for each metal. A total of four extraction samples will be analyzed; one from each soil sample and one duplicate from each soil sample. To ensure proper quality control and assurance, laboratory spike and blank samples will also be analyzed including a spike of the simulated sweat aliquot. The complete sweat extraction protocol is provided as Attachment II. Procedures and results of this experiment will be discussed in detail in the final HRA.

ATTACHMENT I

SIMULATED GASTRIC CONDITION
EXTRACTION PROTOCOL FOR BERYLLIUM, MANGANESE, AND LEAD STUDY

NOTE: *The following protocol is for samples S-29, S-9, and S-30. The samples are to be collected by WTI and split with ChemRisk®. WTI will have each sample analyzed for beryllium, manganese, and lead. Complete the protocol for each sample.*

Step 1: Dry and homogenize all soil contained in each sample.

Step 2: Weigh out 12 soil portions of 1.00 gram each (four from each sample).

Step 3: Initial analysis: Analyze two 1.00 gram portions from S-29 for manganese and beryllium (Method 6010), two 1.00 gram portions from S-9 for lead (Method 6010), and two 1.00 gram portions from S-30 for manganese, beryllium, and lead (Method 6010).

Step 4: Analyze each of the remaining 1.00 gram sample portions as shown below.

Step 5: Prepare a 0.04 molar solution of reagent grade HCl.

Step 6: Mix each two 1.00 gram soil portions (two from each sample) with 250 mL 0.04M HCl in a pre-cleaned 400 mL jar.

Step 7: Gently agitate jar with sample portion for 1 hour and maintain temperature at 37°C.

Step 8: Every ten minutes measure pH and adjust with 10 mL of 0.04M HCL if pH is not equal to 1.4. Repeat as necessary.

Step 9: After 1 hour, decant solution through filter paper to obtain the aqueous solution containing beryllium, manganese, and lead (filtrate). Rinse filter with 5 - 20 mL of 0.04 M HCl as appropriate. Record volume of filtrate recovered.

Step 10a: Analyze a 150 mL aliquot of filtrate from each sample using Method 6010 for beryllium, manganese, and lead.

Step 10b: Spike an additional 50 mL aliquot of the filtrate and analyze using Method 6010 for manganese, beryllium, and lead (matrix spike level to be determined from results of Step 10a).

Step 11: Archive the remaining filtrate.

Step 12: Archive the extracted soil portions.

Step 13: Archive remaining homogenized soil sample for future analyses.

Step 14: Calculate the percent extracted by dividing the total amount of beryllium, manganese, lead in the filtrate by the amount measured in soil.

ATTACHMENT II

SWEAT EXTRACTION STUDY PROTOCOL FOR BERYLLIUM AND MANGANESE

NOTE: *The following protocol is for samples S-29 and S-30. The samples are to be collected by WTI and split with ChemRisk®. WTI will have each sample analyzed for beryllium, manganese, and lead. Complete the protocol for each sample.*

Step 1: Dry and homogenize all soil contained in each sample.

Step 2: Sieve the soil in each sample using a sieve with a diameter of $\leq$ 500 μm (#35 mesh).

Step 3: Weigh out four soil portions of 10.00 grams each (two from each sample) and two portions of 1.00 gram each (one from each sample).

Step 4: Analyze the 1.00 gram portion from S-29 for manganese and beryllium (Method 6010) and the 1.00 gram portion from S-30 for manganese and beryllium (Method 6010).

Step 5: Add the simulated sweat to one of each soil sample in the sweat-to-soil ratio of 20:1. Two hundred milliliters of sweat and 10 grams of soil should be used for 20:1.

Step 6: Cover the bottles tightly, let them sit partially immersed in a 37°C water bath for 12 hours, and gently swirl samples one time per hour (5 revolutions) for the last three hours of extraction. At the end of the extraction period, separate the sweat from the soil by vacuum filtration using a 1.0 μm filter.

Step 7: Measure the volume of sweat in milliliters to determine sweat loss during the experiment.

Step 8: Analyze the filtered sweat (100 mL aliquot) from each group for Beryllium and Manganese using EPA Method 6010.

Step 9: Spike a 50 mL aliquot of each filtrate using Method 6010.

Step 10: Archive the remaining filtrate.

Step 11: Calculate the percent extracted by dividing the total amount of beryllium or manganese in the sweat by the amount measured in soil.

APPENDIX C

Toxicity Profiles

TOXICITY PROFILES FOR THE COIS

Brief descriptions of the toxicity of each of the COIs are provided below.

Antimony

Antimony is a naturally occurring element found mainly in the environment as sulfides and oxides. It is included in alloys in the metals industry, and is used for producing fireproofing chemicals, ceramics, glassware, and pigments. High level acute toxicity in rats is marked by weight loss, loss of hair, dry and scaly skin, vomiting, and diarrhea (Klaassen *et al.*, 1986; ACGIH, 1986). Occupational exposure to antimony may result in irritation of the upper respiratory tract (including laryngitis, bronchitis and pneumonitis), abdominal pain and ulcers, high blood pressure and chronic heart disease (Klaassen *et al.*, 1986; ACGIH, 1986, Seiler *et al.*, 1988). Antimony is also a contact allergen (Seiler *et al.*, 1988).

Beryllium

Beryllium is a hard, brittle metallic element that is used in ceramics, electron tubes, and high temperature reaction systems. The primary noncarcinogenic effects of beryllium, upon inhalation, are to the lungs. In workers occupationally exposed to beryllium, chronic pulmonary beryllium disease (berylliosis) has been observed; it is characterized by shortness of breath, pulmonary inflammation and chemical pneumonitis (Klaassen *et al.*, 1986; ACGIH, 1986, Seiler *et al.*, 1988). Beryllium is also a contact allergen (Seiler *et al.*, 1988).

Beryllium has not been shown to cause cancer in humans, even among populations with increased rates of berylliosis (USEPA, 1995). It has been suggested that humans may be susceptible to beryllium diseases but resistant to the development of lung cancer (Seiler *et al.*, 1988). However, beryllium has been shown to cause lung cancer in rats and monkeys via inhalation and to induce osteosarcomas in rabbits via intravenous and intramedullary injections (USEPA, 1995). Beryllium has not been shown to cause a statistically significant increased rate of cancer in either animals or humans upon oral exposure (USEPA, 1995).

Cadmium

Cadmium is a naturally occurring element most often encountered in the environment as an oxide, chloride or sulfide. Ingestion of high doses of cadmium causes irritation of the stomach, vomiting and diarrhea. Acute inhalation toxicity is characterized by dyspnea, cough and tightness in the chest which could further develop into pulmonary edema and possibly bronchopneumonia (Friberg *et al.*, 1974).

In the cases of low-level chronic exposure, the kidney is the most sensitive organ. Cadmium affects the proximal tubule's reabsorption capabilities which leads to abnormalities in metabolism of uric acid, calcium, and phosphorous. Abnormal metabolism leads to kidney stones and osteomalacia (Friberg *et al.*, 1977; NIOSH, 1976; Stokinger, 1981). Additionally, pulmonary fibrosis and emphysema have been observed in factory workers exposed to high levels of cadmium in air (Bonnell, 1955). Epidemiological studies of humans exposed to cadmium provide limited evidence that inhaled cadmium is a lung carcinogen; however, chronic inhalation exposure to cadmium chloride is associated with increased frequency of lung tumors in animal studies.

Lead

Lead is a naturally occurring metal found in all environmental media, primarily in the inorganic form. Acute lead poisoning in humans results in symptoms of fatigue, disturbance of sleep and constipation, followed by colic, anemia and neuritis (Stokinger, 1981). Low-level chronic exposure to lead has resulted in neurobehavioral effects, and young children, because of their premature neurological systems, are the most sensitive. The USEPA and Centers for Disease Control have identified a blood lead concentration threshold for neurological effects in children of 10 μg/dL (CDC, 1991).

Rats exposed to very high levels of lead in their diets showed a statistically increased rate of kidney tumors. The mean blood lead concentration for these rats was 78 g/dL. Therefore, it is concluded that the renal carcinogenic effects of lead are observed at dosages significantly higher than the doses that result in neurological effects.

Manganese

Manganese is a naturally occurring metal found at relatively high concentrations in the earth's crust. It is also an essential element with an average consumption rate of 10 mg/day (WHO, 1973). Among workers occupationally exposed to high levels of manganese dust and fumes via inhalation, the reported effects are primarily in the pulmonary and central nervous systems. Effects on the nervous system have included psychiatric disturbances (*i.e.*, excessive weeping, laughing, sleep disturbances, irritability) at the onset of exposure, followed by neurological symptoms (dysarthria, clumsiness, muscle cramps and tremors). Final stages of manganese intoxication may include irreversible dystonia and hyperflexion of muscles (Cotzias *et al.*, 1968). Chronic effects of manganese on the pulmonary system include manganese fume poisoning, lung damage and pneumonia (ACGHI, 1991).

Toxicity from ingested manganese is rarely observed (USEPA, 1995). However, an epidemiological study of manganese in drinking water performed by Kondakis *et al.* (1989) reported dose-dependant neurological effects among a population in Greece. It should be noted that the methodology and results of this study have recently been questioned by the USEPA (Velazquez, pers. comm., 1995).

Carcinogenic PAHs

PAHs are a group of chemicals that are formed during the incomplete burning of coal, oil, wood, garbage, or other organic substances such as tobacco and charbroiled meat. PAHs can either be man-made or occur naturally, and most of these chemicals have no known use except in research (ATSDR, 1993). The primary effect of the PAHs that are COIs in this HRA is cancer via the oral, dermal and inhalation routes of exposure. Although there is only limited evidence that PAHs cause cancer in humans, the carcinogenic PAHs have been shown to cause a significant increased rate of cancer in animals (USEPA, 1995). All of the PAHs that are COIs have been shown to cause skin tumors in animals following dermal exposures (ATSDR, 1993). Of the PAHs that are COIs, benzo(a)anthracene, benzo(a)pyrene and dibenz(a,h)anthracene have been shown to cause cancer via the oral route of exposure in laboratory animals (ATSDR, 1993). Of the PAHs that are COIs, only benzo(a)pyrene has been shown to cause cancer in laboratory animals (ATSDR, 1993). Via the oral and inhalation routes of exposure, increased tumor rates of the liver and lung are most frequently reported.

REFERENCES

Agency for Toxic Substances and Disease Registry. (ATSDR). (1993). *Toxicological Profile for Polycyclic Aromatic Hydrocarbons (PAHs).* U.S. Department of Health & Human Services. Prepared by Clement International Corporation Under Contract No. 205-88-0608.

American Conference of Governmental and Industrial Hygienists [ACGIH]. (1986). *Documentation of Threshold Limit Values and Biological Exposure Indices for 1989-1990.* Cincinnati, OH.

American Conference of Governmental and Industrial Hygienists [ACGIH]. (1991). *Documentation of Threshold Limit Values and Biological Exposure Indices.* ACGIH, Cincinnati, OH.

Bonnell, J.A. (1955). Emphysema and Proteinuria in Men Casting Copper-Cadmium Alloys. *Brit. J. Ind. Med* 12:181-197.

Centers for Disease Control [CDC]. (1991). *Preventing Lead Poisoning in Young Children.* A statement by the Centers for Disease Control. U.S Department of Health and Human Services.

Cotrias, G.C., K. Horiuchi, S. Fuenzalida, and I. Mena. (1968). Chronic Manganese Poisoning: Clearance of Tissue Manganese Concentrations with Persistence of the Neurological Picture. *Neurology.* 18:376-382.

Friberg, L., Picastor, M., Nordberg G.F., Kjellstrom, T. (1974). *Cadmium in the Environment*, 2nd Edition. CRC Press, Boca Raton, Florida.

Friberg, L., Noeverg, G., Piscator, M> (1977). Cadmium. In: *Toxicology of Metals - Volume II.* pp. 124-163.

Klaassen C.D, Amdur M.O, and Doull, J. eds. (1986). *Cassarett and Doull's Toxicology: The Basic Science of Poisons.* 3rd Ed. New York: MacMillan Publishing Co.

Kondakis. X.G., Makris, N., Leotsinidis, M. *et al.* (1989). Possible Health Effects of High Manganese Concentration in Drinking Water. *Arch. Environ. Health* 44:175-178.

National Institute for Occupational Safety and Health. [NIOSH]. (1976). *Criteria for a Recommended Standard.* HEW Publication No. NIOSH-76-192.

Seiler, H.G., Sigel, H. Sigel, A. (1988) *Handbook on Toxicity of Inorganic Compounds.* Marcel Dekker, Inc., New York.

Stokinger, H.E. (1981). Chapter 29. The Metals. In: *Patty's Industrial Hygiene and Toxicology*, 3rd Edition, Volume 2A. G.D. Clayton and F.E. Clayton (eds.). Wiley and Sons, New York. pp. 1493-2060.

U.S. Environmental Protection Agency [USEPA]. (1995). *Integrated Risk Information Service [IRIS]*. Cincinnati, OH.

Velazquez, S. (1995). Personal communication with K. Fehling regarding manganese RfC. March 1995.

World Health Organization (WHO). (1973). *Trace Elements in Human Nutrition: Manganese*. Report of a WHO Expert Committee. Technical Report Service, 532, WHO, Geneva, Switzerland.

APPENDIX D

O'Flaherty PBPK Model for Lead

TOXICOLOGY AND APPLIED PHARMACOLOGY 111, 299–312 (1991)

Physiologically Based Models for Bone-Seeking Elements

I. Rat Skeletal and Bone Growth[1]

ELLEN J. O'FLAHERTY

Department of Environmental Health, University of Cincinnati College of Medicine, 3223 Eden Avenue, Cincinnati, Ohio 45267-0056

Received October 25, 1990; accepted July 18, 1991

Physiologically-Based Models for Bone-Seeking Elements. I. Rat Skeletal and Bone Growth. O'FLAHERTY, E. J. (1991). *Toxicol. Appl. Pharmacol.* 111, 299–312. A review of features of bone structure and bone growth critical to the development of a physiologically based model of the whole-body kinetics of bone-seeking elements is presented. Allometric equations describing the volume and weight of the bone, bone marrow, and skeleton during growth of the rat from birth to maturity are derived. Weights of body calcium and bone ash are also expressed allometrically as functions of body weight during growth. The simplicity of these functions will allow them to form the basis of a flexible model of the movement of bone-seeking elements in and out of bone. Blood flow rates to bone and bone marrow are incorporated into the model of the mature skeleton. The predictions of the skeletal growth model are in good agreement with measured quantities of bone, skeletal ash, and calcium in growing rats. © 1991 Academic Press, Inc.

Physiologically based kinetic (PBK) models are enjoying broad acceptance in toxicology and risk assessment practice. Because these models are based on actual organ and tissue volume, blood flows, and alveolar ventilation rates, and where possible incorporate experimentally derived metabolic parameters as well, they are especially well adapted to applications requiring conversion of effective dose across species or from one route of exposure to another (Andersen *et al.*, 1987).

To date, PBK models have been developed for a variety of chemicals with relatively short residence times in the body. Over short time periods, the physiological and biochemical parameters that define the model are constant. For toxicants that persist in the body for extended periods, inclusion in the PBK model of growth and maturation dependence of physiological and biochemical functions will be required.

One class of agents with extended residence times in the body is the bone-seeking elements, for which whole-body kinetic behavior is determined largely by the balance among excretion, bone uptake, and release from bone. This group includes lead, radium, strontium, uranium, barium, and aluminum, among others. While these elements may enter the bone by different mechanisms, once incorporated into the crystalline bone matrix they can be retained for extended periods, and in some cases act to alter bone tissue or growth rate (Talwar *et al.*, 1986; Shukla *et al.*, 1989). If present in the bone as radionuclides, they can provide a continuous local source of radioactivity. De-

[1] This work was supported by U.S. Public Health Service Grant ES04125. Portions of it were presented at the Seventeenth Conference on Toxicology cosponsored by the U.S. Air Force Armstrong Aerospace Medical Research Laboratory and the U.S. Naval Medical Research Institute, November 1987 (O'Flaherty, 1988).

0041-008X/91 $3.00
Copyright © 1991 by Academic Press, Inc.
All rights of reproduction in any form reserved.

pendence of the kinetics of bone-seeking elements on the characteristics of bone and bone growth requires a better understanding of the relationship of skeletal composition and metabolism to age and body size.

The purposes of this paper are to review those features of bone structure and bone growth that are crucial to development of a PBK model for bone-seeking elements. Expressions are devised that describe bone growth and blood flow rate to bone within a framework that is adaptable to simulation of the kinetics of bone-seeking elements, and an explicit model of skeletal and bone growth is developed for the rat.

During the search of the literature for the experimental observations on which this model is based, no attempt was made to be exhaustive. Rather, data were selected from representative, well-designed and carefully performed studies whose conclusions are internally consistent and also consistent with the results of comparable studies performed by other investigators. Quality, thoroughness, and appropriateness of the studies from which the data are drawn have been the criteria for selection. Isolated observations have been given less weight than series of observations showing, for example, age or weight dependence; and observations made incidental to other purposes have been given less weight than data from studies whose specific purposes were to define the skeleton, its tissue components, or its blood flows. A degree of subjectivity is inevitable. It is hoped that it has been minimized by imposition of the demand made of all models: that they unify a broad range of observations and illuminate systematic interrelationships.

METHODS AND RESULTS

The skeleton can be defined in terms of two compartments: marrow- and cartilage-free bone, and marrow–vascular tissue. Marrow- and cartilage-free bone consists of four chemical fractions: water, volatile inorganic material, organic material, and ash. Dry marrow- and cartilage-free bone will be considered to be made up of the organic and ash fractions. "Skeletal tissue" will always include marrow, as will "whole bone," which may refer to a subunit of the skeleton, as in "cortical and trabecular whole bone."

Cortical and Trabecular Bone

Bone is a heterogeneous tissue. This heterogeneity complicates efforts to model the skeleton as a limited number of discrete compartments. Some simplifications are possible, however. Four distinct bone surfaces, which respond differently to physiologic and endocrinologic modulation, are recognized. These are the trabecular, cortical, endosteal, and periosteal surfaces, of which trabecular and cortical surfaces together account for virtually all of the bone surface.

Division of the skeleton into cortical and trabecular whole bone fractions is based on porosity. Cortical bone is compact and dense, with only 5–30% of its volume occupied by marrow and vascular space. It is found in the shafts of the long bones and at the outer surfaces of many bones, such as ribs and vertebrae, whose interior consists of trabecular bone. The areas where blood or a superfusate of blood comes into direct contact with cortical bone are the endosteal (inner) and periosteal (outer) surfaces of the shafts of the long bones; the surfaces of the haversian canals that channel blood vessels through bone; the surfaces of the lacunae that house the bone cells, or osteocytes; and the surfaces of the canalicules that originate from lacunar and other surfaces to penetrate and perfuse bulk bone tissue. In general, surface-to-volume ratios in human cortical bone are: for the endosteal or periosteal surface, 5–7 cm^2/cm^3; for the total haversian canal surface, 20–30 cm^2/cm^3 (Beddoe, 1977); for the total osteocyte lacunar surface, 240 cm^2/cm^3; and for the total canalicular surface, 2250 cm^2/cm^3 (Frost, 1962). In mature rats, the surface-to-volume ratio for end-

osteal and periosteal surfaces taken together is [illegible]0 cm^2/cm^3 (Sontag, 1986 a,b).

Trabecular whole bone consists of an intricate network of leaves and struts of marrow-free bone surrounding small communicating pockets of marrow-vascular space. It has a porosity of from 30% to greater than 90% (Carter and Hayes, 1977). Few haversian canals are found in trabecular bone, presumably because the leaves and plates of bone tissue are sufficiently thin that their metabolic demands can be met by contact with blood vessels at the trabecular bone surfaces. Surface-to-volume ratios in trabecular bone are very variable, depending as they do on local bone structure. Values from 100–300 cm^2/cm^3 have been recorded (see, for example, Beddoe *et al.*, 1976).

Although examples of the two principal categories of skeletal tissue may be structurally distinct, there is not a sharp distinction between the physicochemical characteristics of marrow-free trabecular bone and those of marrow-free cortical bone. In fact, mineralized bone tissue without marrow spaces or other porosities is strikingly consistent both in different types of bone and across species.

Having marrow-free bone consists of water, volatile inorganic material, and organic materials—principally collagen, but including a variety of complex, functionally specialized chemicals—in addition to the nonvolatile inorganic material or ash. In general, bone density and the amount of ash per unit volume of bone are slightly higher in cortical marrow-free bone than in trabecular marrow-free bone. The difference, however, is not sufficiently large to require consideration in modeling the skeleton. The volume of organic material per unit volume of bone is nearly the same in marrow-free cortical and trabecular bone. Most of the small difference in ash content is matched by a difference in water content. Table 1, taken from Gong *et al.* (1964b), illustrates these points. Mean ash contents in the four species examined are 0.373 cm^3/cm^3 of cortical marrow-free bone and 0.332 cm^3/cm^3 of trabecular marrow-free bone. This difference is fully compensated by the mean difference in water contents: 0.238 cm^3/cm^3 of cortical marrow-free bone and 0.278 cm^3/cm^3 of trabecular marrow-free bone. The corresponding mean organic fractions, 0.344 cm^3/cm^3 and 0.349 cm^3/cm^3, are essentially the same.

Based on the data in Table 1, both mature cortical and mature trabecular marrow-free bone may be considered to be made up of 70% dry bone, 25.5% water, and 4.5% volatile inorganic fractions by volume, with densities of 2.28 g/cm^3 for dry bone and 1.92 g/cm^3 for hydrated marrow-free bone (Table 2). The amount of ash in this bone model is 68.1% by weight of marrow-free dry bone or 56.4% by weight of hydrated marrow-free bone.

The rule of thumb that the skeleton consists of 80% cortical bone and 20% trabecular bone is based on two studies, one in a single dog (Gong *et al.*, 1964a) and one in humans (Johnson, 1964). In the absence of observations to the contrary, this fractional assignment of bone structure in the skeleton is here taken to apply to the rat as well as to the species in which it has been studied directly.

The Mature Skeleton

Direct measurements of both marrow-free bone mass and marrow mass have been carried out, for single bones and for the entire skeleton, in several small animal species. Only limited data are available for the rat. MacPherson and Tothill (1978) reported a fat-free wet bone weight in 20 male rats of 4.77 ± 0.17% of body weight. Caster *et al.* (1956), in a series of dissections with manual cleaning of the bones of 22 adult rats, recorded a mean skeletal weight of 5.8% of body weight and a fat-free dry bone weight of 3.4% of body weight. Fairman and Corner (1934) used a marrow replacement technique to obtain a mean fat-free dry bone weight of 3.0 ± 0.4% of body weight and mean marrow weight of 3.0 ± .2% of body weight in 4 adult rats. Studies in other small animal species (Hudson, 1958, 1960a,b; Nye, 1931;

TABLE I

VOLUMES, WEIGHTS, AND DENSITIES OF MARROW-FREE BONE AND ITS FRACTIONS

	Water	Organic	Volatile inorganic	Ash	Ash + organic[a]	Marrow-free bone
			Volume, cm^3/cm^3 marrow-free bone			
Trabecular bone						
Steer	0.281	0.342	0.042	0.335	0.677	1.00
Dog	0.288	0.345	0.042	0.326	0.671	1.00
Monkey	0.271	0.361	0.040	0.329	0.690	1.00
Human	0.270	0.349	0.042	0.339	0.688	1.00
Cortical Bone						
Steer	0.252	0.336	0.046	0.366	0.702	1.00
Dog	0.223	0.363	0.046	0.368	0.731	1.00
Monkey	0.237	0.337	0.047	0.382	0.719	1.00
Human	0.239	0.338	0.046	0.377	0.715	1.00
			Weight, g/cm^3 marrow-free bone			
Trabecular bone						
Steer	0.281	0.514	0.072	1.067	1.581	1.934
Dog	0.292	0.507	0.070	1.049	1.556	1.918
Monkey	0.271	0.514	0.068	1.011	1.525	1.864
Human	0.270	0.497	0.071	1.076	1.573	1.914
Cortical bone						
Steer	0.252	0.486	0.078	1.178	1.664	1.994
Dog	0.223	0.519	0.078	1.175	1.694	1.995
Monkey	0.239	0.487	0.081	1.228	1.715	2.035
Human	0.237	0.476	0.078	1.182	1.658	1.973
			Density, g/cm^3			
Trabecular bone						
Steer	1.00	1.503	1.71	3.185	2.335	1.934
Dog	1.00	1.470	1.67	3.218	2.319	1.918
Monkey	1.00	1.424	1.70	3.073	2.210	1.864
Human	1.00	1.424	1.69	3.174	2.286	1.914
Cortical bone						
Steer	1.00	1.446	1.70	3.218	2.370	1.994
Dog	1.00	1.430	1.70	3.193	2.317	1.995
Monkey	1.00	1.445	1.72	3.215	2.385	2.035
Human	1.00	1.408	1.70	3.135	2.319	1.973

Note. From Gong *et al.* (1964b).
[a] Marrow-free dry bone.

Dietz, 1944) suggest that marrow mass averages about 2.3% and marrow-free dry bone mass about 3.5% of adult body weight. The model of the mature small animal skeleton in Table 3 consists of a marrow-free bone weight of 5.0% of body weight (marrow-free dry bone weight of 4.1% of body weight), which is consistent with measurements of total skeletal ash; see discussion of the growing skeleton, below. This model of the mature small animal skeleton is 53.1% marrow-free bone and 46.9% marrow–vascular space by volume. Mean skeletal density is 1.47 g/cm^3.

TABLE 2

WEIGHTS, VOLUMES, AND DENSITIES OF MATURE BONE AND ITS FRACTIONS

	Bone					
	Water	Organic	Volatile inorganic	Ash	Ash + organic	Marrow-free bone
ısıty, g/cm³	1.00[a]	1.45[a]	1.7[a]	3.1[a]	2.28	1.92
ume fraction, cm³/cm³						
ıarrow-free bone[1]	0.255	0.35	0.045	0.35	0.70	1.0
ıght fraction, g/g						
ıarrow-free bone	0.132	0.264	0.040	0.564	0.828	1.0
ıght fraction, g/g						
ıarrow-free dry bone	—	0.319	—	0.681	1.0	

[1] See Table 1 for values.

Marrow may be either red (hematopoietic) yellow (fatty). Essentially all the bone mar-ıw of mammalian newborns is red. With age, d marrow in the distal skeleton is replaced some extent by yellow marrow, although ellow marrow may become hematopoieti-ally active again in response to demand for nhanced hemoglobin synthesis. Small ani-nals in general have relatively more red mar-ow than do humans. Gross inspection of the ones indicates that yellow marrow in adult at, and guinea pigs is confined to the tail ınd to distal portions of the limbs (Nye, 1931; Hudson, 1958 1960b), and many estimates of the relative amounts of red and yellow mar-row in small animals are based on the as-sumption that this distribution holds across species. Hudson (1958, 1960b) estimated that red marrow was 88–89% of total marrow in guinea pigs, or about 2% of body weight.

The Growing Skeleton

The skeleton of the fetus and newborn is incompletely mineralized, large parts consisting of cartilage having a density considerably less than that of fully mineralized bone. Mineralization begins during gestation and continues after birth. The amount of calcium in the body rises rapidly after birth and steadily throughout the period of continuing body growth, tending to stabilize around the time of sexual maturity. At this time, chemical development and growth of bones are almost complete, although male rats may continue to show increasing total body calcium concentrations as they continue to grow (Sherman and MacLeod, 1925; Widdowson and Dickerson, 1964). Mineralization is reflected in an increase in skeletal density and in shifts among the volume and weight fractions of the skele-

TABLE 3

THE MATURE SMALL ANIMAL SKELETON, DEFINED AS MARROW-FREE BONE PLUS MARROW

	Marrow-free bone	Marrow	Skeleton (without cartilage)
Weight, g/100 g body wt	5.00	2.30	7.30
Volume, cm³/100 g body wt	2.60	2.30	4.90
Density, g/cm³	1.92	1.00	1.47
Weight, g/g skeleton	0.685	0.315	—
Volume, cm³/cm³ skeleton	0.531	0.469	—

ton assignable to skeletal components such as volatile and nonvolatile inorganic constituents, water, cartilage and other organic constituents of bone, and bone marrow.

The model of the growing skeleton of the rat is constructed from an allometric equation giving whole-body (equivalent to skeletal) ash as a function of body weight, together with direct measurements of the weight of the organic plus volatile inorganic fraction of the growing rat humerus. Allometric relationships are based on the principle that anatomic and physiologic characteristics tend to change in a regular fashion as body size changes. Specifically, the allometric equation has the general form

$$y = ax^b,$$

where y is the dependent variable (in this case, skeletal ash), x is the independent variable (body weight), and a and b are constants. When plotted in a logarithmic coordinate system, the allometric equation is a straight line with slope b. It has been found to describe the behavior of many growth-related biological variables.

Skeletal ash has been measured directly in some studies, but here it is estimated from combined measurements of whole-body calcium content and the amount of calcium present in skeletal ash. The whole-body calcium of the rat is dependent on the amount of calcium in the diet, and the amount of calcium in the body follows body weight more closely than it does age. Sherman and MacLeod (1925) found that total body calcium increased as the 1.23 power of body weight in male rats from birth to 340 g and as the 1.28 power of body weight in female rats followed to 230 g. Body calcium was 1.05 g Ca/100 g body wt in adult male rats and as much as 1.2 g Ca/100 g body wt in adult female rats that had not reared young. Widdowson and Dickerson (1964), in a tabulation of data from a number of species, concluded that the calcium content of the adult rat was about 1.2 g Ca/100 g body wt.

TABLE 4

THE DEPENDENCE OF THE GROWING RAT SKELETON AND ITS FRACTIONS ON BODY WEIGHT

Skeletal weight, g = 0.0801 (body wt, $g^{0.983}$)
Marrow weight, g = 0.0469 (body wt, $g^{0.866}$)
Marrow-free bone weight, g = 0.0373 (body wt, $g^{1.06}$)
Marrow-free dry bone weight, g = 0.0257 (body wt, $g^{1.10}$)
Ash weight, g = 0.0114 (body wt, $g^{1.17}$)
Marrow-free bone volume, cm^3 = 0.0252 (body wt, $g^{1.02}$)
Skeletal calcium, g = 0.002 (body wt, $g^{1.30}$

The allometric equation (Table 4) for whole-body calcium as a function of body weight in the rat represents an increase as the 1.30 power of body weight during growth to a value of about 1.05 g Ca/100 g body wt in young adulthood. According to this equation, the body of the 5-g newborn rat would contain 0.15 g calcium, or 0.3 g Ca/100 g body wt. Sherman and MacLeod (1925) reported 0.23 g Ca/100 g newborn body wt; Widdowson and Dickerson (1964), 0.3 g Ca/100 g; and recent data from this laboratory (Hamilton, J.D. and O'Flaherty, E.J., unpublished) give a mean of 0.236 g Ca/100 g body wt in 15 Day-21 fetuses each from a different litter, maintained on a diet adequately but not excessively provided with essential nutrients.

Over 99% of total body calcium in the adult is in the bone. Consistent with the constancy of chemical composition of mature bone across species, the calcium content of mature bone is essentially the same across species (Morgulis, 1931). Careful studies of rat and human bone suggest that the calcium content of mature bone ash is close to 0.39 g Ca/100 g ash (Hammett, 1925; Mitchell *et al.*, 1945; Forbes *et al.*, 1953, 1956). Skeletal ash of the newborn rat contains less calcium. The degree of calcification of newborn rat bone is dependent on the quality of maternal nutrition. It probably is also dependent on other factors affecting the growth of the fetus, such as litter size. Pickering *et al.* (1956) found 0.2 (range

99–0.213) g Ca/g skeletal ash in 20 new-
m male Wistar rats. In the unpublished
dy from this laboratory, 0.159 (SD 0.008)
C skeletal ash was measured in 15 rat
ps on Day 21 of gestation.

These values for whole-body calcium and
e amount of calcium present in skeletal ash
ggest that skeletal ash is about 1.5 g/100 g
dy wt in the newborn rat and 2.7 g/100 g
dy wt in the young adult rat. The allometric
uation for ash (Table 4) is based on these
timates. It gives 1.5 g skeletal ash/100 g body
at birth and 2.9 g ash/100 g body wt at a
dy weight of 250 g. These estimates can be
mpared to a limited number of direct mea-
rements of rat skeletal ash weights. Pickering
al. (1956) determined the ash content of the
inned and eviscerated rat body from age 1
age 75 days. Hammett (1925) determined
e ash content of the femur and humerus
om age 23 days to age 150 days. While ab-
olute ash contents of the bones of the young
ts in these older studies are low, inspection
f the data sets suggests that by age 20 days,
eletal ash had reached a point halfway be-
veen the value at birth and the ash content
f the mature skeleton, which was estimated
be 2.83 g/100 g body wt by fitting a hyper-
ol the data. The allometric equation in
able 4 also gives a skeletal ash value at age
0 days that is midway between the values at
irth and at maturity. Pickering *et al.* (1956),
n their series of 20 newborn rats, found an
sh weight of about 1 g ash/100 g skinned and
viscerated carcass. In the unpublished study
rom this laboratory, the mean ash content of
he 15 rat fetuses was found to be 1.7 g ash/
00 g body wt. Like the calcium content of
keletal ash, body ash content reflects the nu-
ritional status of the rat. El-Maraghi *et al.*
1965) showed that even the calcium content
of the diet affects total bone ash in growing
ats.

Hammett (1925) determined the fractional
weight of the organic plus volatile inorganic
fraction of the humerus of the rat from 23–
150 days of age. Hammett's data show that as
mineralization proceeds, mineral replaces water while the relative amount of organic plus volatile inorganic material is very nearly constant. This constancy of the organic fraction of bone is a feature of bone growth in all species. It has been remarked by a number of authors (see, for example, Mueller *et al.*, 1966). Thus, the growing rat skeleton can be constructed by working back from the model of the mature skeleton (Table 3), using the allometric equation for ash weight (Table 4) and assuming that mineralization has proceeded through displacement of water by an equal volume of mineral having three times the weight of the displaced water (Robinson, 1975; Table 2).

The constructed growing skeleton and its fractions are described by a set of allometric equations relating weights or volumes to body weight. These equations are given in Table 4. In Fig. 1, the simulated weights of bone, marrow, and skeleton are plotted as functions of body weight.

Growth and maturation are reflected in a change not only in the relative amount but also in the nature of the bone marrow. As discussed above, essentially all marrow in the newborn is hematopoietic, or red. In small animals, 90% by weight of total bone marrow in the adult is red marrow. The difference between the relative amount of red marrow in the newborn and the adult is so slight that a

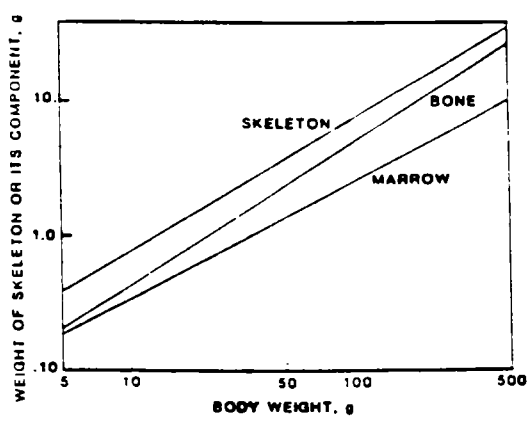

FIG. 1. Simulated skeletal, marrow-free bone, and bone marrow weights in rats as functions of body weight.

linear decline from 100% red marrow by weight in the newborn to 90% red marrow by weight in the adult should adequately describe compartmentalization of total bone marrow in the rat.

Blood Flow to Bone

Circulation of blood to bone has been measured by a variety of techniques including direct cannulation, plethysmography, and either fractional distribution or clearance of various bone-seeking markers. The fractional distribution and clearance techniques give estimates that are less than actual bone perfusion rates if extraction of tracer is assumed to be complete when it is not. It has been shown that extraction of many commonly used tracers by rat bone is not only incomplete but is dependent on bone blood flow within the physiological flow range (Schoutens *et al.*, 1979; Tothill and Hooper, 1984). Because bone blood flow is regionally variable, fractional extraction is regionally variable as well (Tothill *et al.*, 1985). Consequently, a radiolabeled microsphere method has largely supplanted other techniques for measurement of bone blood flow (Gross *et al.*, 1981).

When certain experimental restrictions are met (Buckberg *et al.*, 1971), the microsphere method is accurate. It allows measurement of blood flow to individual bone regions in unanesthetized animals. Measurements of bone blood flow with the microsphere technique have established that the magnitude of bone blood flow is much larger than it was previously believed to be and that it is variable from bone to bone and from region to region within a single bone. In general, blood flow rate is lowest to cortical bone and highest to trabecular bone and hematopoietic marrow. Table 5 gives bone blood flow rates to different regions of rat bone as measured with the radiolabeled microsphere technique. These studies were generally directed at defining the range of regional variability of bone blood flow, and did not consider total bone blood flow. One group of studies (Tothill and McCormick, 1976; MacPherson and Tothill, 1978), in which total skeletal blood flow was measured in rats by estimating the radioactivity of the whole skeleton, gave an estimate of 3% of cardiac output.

Measurements of blood flow to bone marrow in rats were not found. Measurements of blood flow to bone marrow in dogs, using the radiolabeled microsphere technique, suggest that flow rate to hematopoietic marrow is around 35 ml/min/100 g tissue, while to yellow marrow it is only about 10 ml/min/100 g tissue (Gross *et al.*, 1979; Light *et al.*, 1984; Tothill *et al.*, 1985). Based on the flow rates in Table 5, a reasonable estimate of blood flow rate to trabecular bone is 35 ml/min/100 g and to cortical bone, 5 ml/min/100 g. From these estimates, compartmentalization of the skeleton as in Table 3, further compartmentalization of bone as 80% by weight cortical and 20% trabecular, and further compartmentalization of marrow as 90% by weight red and 10% yellow, the skeleton of the mature rat can be modeled together with its blood flows (Table 6).

Several kinds of observations suggest that bone blood flow rate is proportional to the rate of deposition of new bone. Bone blood flow is correlated with remodeling activity in adult dogs (Sim and Kelly, 1970) and regional bone blood flow with osteoblast activity in the rabbit tibia (Whiteside *et al.*, 1977). Blood flow to immature, growing bone is greater than blood flow to mature bone (Whiteside *et al.*, 1977; Niv and Hungerford, 1979).

Schnitzer *et al.* (1982) conducted a detailed study of blood flow to different regions of the tibia and femur of neonatal (4–5 days old), immature (4 months old), and mature (more than 2 years old) dogs of different breeds and both sexes. Lee *et al.* (1965) studied regional bone formation rates in a 3–4 month-old puppy and a mature dog. It is useful to compare their bone formation rate and regional blood flow rate data. Figure 2 is a plot of blood flow rate vs bone formation rate for whole tibias and for proximal, medial, and distal shafts

TABLE 5

BLOOD FLOW RATES, OBTAINED USING RADIOLABELED MICROSPHERES, TO MARROW-FREE BONES AND BONE REGIONS

ecies	N	Tissue	Flow rate, ml/min/100 g tissue	Reference
'at[a]	22	Femur	13 ± 5	Schoutens *et al.*, 1979
		Total tibia	11 ± 4	
		Tibial epiphyses	15 ± 8	
'at[b]	7	Femoral shaft	12 ± 6	
		Femoral epiphyses	9 ± 2	
		Tibia and fibula	5 ± 2	
		Fore and hind paws	4 ± 2	
		Humeri	14 ± 6	
		Radii and ulnae	21 ± 11	
		Ribs	6 ± 2	
		Scapulae	20 ± 17	
		Pelvis	9 ± 3	Tothill and McCormick, 1976
		Skull	15 ± 11	
		Jaw	4 ± 4	
		Cervical spine	41 ± 12	
		Thoracic spine	17 ± 9	
		Lumbar spine	23 ± 7	
		Sacrum	28 ± 12	
		Tail	5 ± 3	

[a] Cardiac output is calculated for a 450-g rat as

$$\left(\frac{450\ g^{0.75}}{1000\ g}\right)(230\ ml/min),$$

here 230 ml/min is the reference flow rate in a 1-kg animal. The plasma flow rates given by Schoutens *et al.* were djusted to blood flow assuming a hematocrit of 25% in whole bone and 20% in tibial epiphyses (Tondevold and liasen, 1982).

[b] A mean test animal body weight of 450 g was assumed. The experimental range was given as 400–500 g.

of the femurs. Ranges are shown for blood flow ate where a single value was not given or could not be estimated. The accretion rates given by Lee *et al.* for proximal and distal femur ends are not included, since flow rates are so tremendously variable within these regions. With

TABLE 6

THE MATURE SKELETON OF THE 350-g MALE RAT, INCORPORATING BLOOD FLOW

Tissue	Weight, % of body weight	Weight, g	Perfusion rate, ml/min/g of fraction weight	Perfusion rate, ml/min
Red marrow	2.1	6.30	0.35	2.21
Trabecular bone	1.0	3.00	0.35	1.05
Cortical bone	4.0	12.0	0.05	0.60
Yellow marrow	0.2	0.60	0.10	0.06
Total	7.3	21.9		3.92

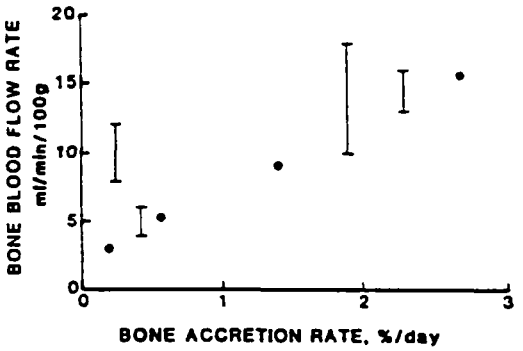

FIG. 2. Correlation of bone accretion rate and bone blood flow rate in matched regions of bone from dogs of different ages. Accretion rates from Lee *et al.* (1965). Blood flow rates from Schnitzer *et al.* (1982).

the exception of the proximal shaft of the mature femur (the 8–12 ml/min/100 g blood flow rate range), accretion rate and blood flow rate are closely correlated.

DISCUSSION

This skeletal growth model can be compared to actual growth measurements of several different kinds. A detailed examination of the ash weights of bones of 225 Rochester (Wistar-derived) rats, 15–170 days old (Weikel *et al.*, 1955), gave a log–log plot of bone ash weight vs body weight with a slope of 1.2–1.3 for most bones, the precise value being dependent on the type of bone. These results duplicated and extended an earlier observation of Zucker and Zucker (1946) on femoral growth rate in over 1000 rats, 2–750 days old. Figure 1 illustrates the model relationship for skeletal ash weight and body weight. The slope of the line is 1.17 (Table 4).

Hudson (1958), in a detailed and thorough series of measurements of guinea pig marrow volumes and marrow-free bone weights, found that marrow volume increased approximately as the 0.5 power of body weight, while marrow-free bone weight was proportional to the 1.045 power of body weight. These two measures—marrow volume and marrow-free bone weight as they are predicted by the model—are also plotted in Fig. 1. Predicted marrow volume is proportional to body weight to the 0.87 power, and predicted marrow-free bone weight to body weight to the 1.06 power. These exponents are similar to the values obtained by Hudson despite the species difference.

A comparison of model calcium concentrations in the growing rat with data from a number of investigators is given in Table 7. The diets used in these studies ranged from controlled, semipurified diets to mixtures of natural foodstuffs, but all were judged to be supportive of normal growth in rats. The variability in body calcium content across studies is readily apparent. The predictions of the model tend to lie below observed values for the dense long bones, but compare well with whole-body and whole-skeletal measurements.

A common generalization is that dry marrow-free bone contains 0.25 g calcium/g. Dickerson (1962) found 0.254 g calcium/g dry marrow-free femoral cortex from 33-day-old rats, and Burnell *et al.* (1983) found 0.254 g calcium/g dry marrow-free tibia/fibula midshaft in 154-day-old rats. According to the mature bone model of Table 2, 0.25 g calcium/g dry marrow-free bone would be equivalent to 0.21 g calcium/g hydrated marrow-free bone, or 0.40 g calcium/cm^3 of marrow-free bone having a density of 1.92 g/cm^3. Rowland *et al.* (1959) used a microradiographic technique to determine calcium densities in microscopic volumes of bone, containing no cavities larger than canalicules, from a single rat. They recorded a low of 0.56–0.57 g/cm^3 and a high of 0.68 g/cm^3. They also examined bones from several other species, noting that rat bones had the highest mineral density: other values, also in single representatives of each species except humans, ranged from 0.36–0.62 g/cm^3. The values they reported suggest that the calcium content of marrow-free rat bone could actually be as high as 0.29–0.35 g calcium/g in dense bone regions with virtually no non-bone volume and that there may be slight species differences in bone density. The model of mature rat bone presented

TABLE 7

COMPARISON OF PREDICTED AND OBSERVED CALCIUM CONTENTS OF RATS OF DIFFERENT AGES AND WEIGHTS

(days)	Weight (g)	Calcium content: Observed	Calcium content: Predicted	Reference
		Bone ash, g/g		
23	27.3 ± 0.6	0.359	0.269	Hammett (1925) (Humerus)
30	41.3 ± 0.8	0.368	0.284	
50	74.5 ± 1.8	0.368	0.307	
65	120.8 ± 2.1	0.373	0.327	
75	133.2 ± 3.2	0.372	0.331	
100	162.3 ± 4.6	0.374	0.340	
150	244.3 ± 6.9	0.375	0.358	
		Whole body, g		
29	46	0.311	0.290	Sherman and MacLeod (1925)
61	138	1.023	1.210	
90	222	2.013	2.245	
118	253	2.517	2.730	
188	304	3.132	3.379	
28	40.3	0.385	0.244	Lanford and Sherman (1938)
60	116.6	1.128	0.972	
90	172.5	1.765	1.618	
180	282.2	3.137	3.067	
365	320.6	3.839	3.621	
1	5.8	0.012	0.020	Pickering *et al.* (1956)
21	25	0.14	0.13	
2[illegible]	27	0.20	0.14	
3[illegible]	60	0.44	0.41	
45	85	0.71	0.64	
75	190	1.71	1.83	
		Bone ash, g/g		
1	5.8	0.21	0.22	Pickering *et al.* (1956) (Total skeleton)
21	25	0.27	0.27	
25	27	0.29	0.27	
32	60	—	0.30	
45	85	0.32	0.31	
75	190	0.33	0.35	
		Fat-free bone, g/g		
—	450–500	0.272	0.232–0.238	McClendon *et al.* (1962) (Femur)
28	85	0.201	0.156	Burnell *et al.* (1980) (Tibia/fibula midshaft)
56	206	0.226	0.192	
98	394	0.248	0.225	
154	521	0.254	0.241	

here contains 0.255 g calcium/g of dry marrow-free bone.

The mean density of the mature skeletal model of Table 3 is 1.47 g/cm^3. Jankovich (1971) recorded densities of about 1.5 g/cm^3 for whole tibias from 280–day-old rats. The densities of femurs from the same rats were lower, clustering around 1.35 g/cm^3.

Total blood flow in the mature rat skeletal model (Table 6) is 17.9 ml/min/100 g skeletal tissue including bone marrow, or 2.8% of the total cardiac output of 139 ml/min in a rat of this size. This estimate compares well with those of Tothill and McCormick (1976) (3.1%) and MacPherson and Tothill (1978) (3%) for the rat.

According to the model in Table 6, about 58% of the total blood flow to the skeleton reaches bone marrow before it has the opportunity to perfuse bone. The remaining 42% of bone blood flow goes directly to mineralized bone tissues. These estimates are reasonably consistent with data of Wootton (1974) for rabbit tibia and femur. When marrow was separated from a femur that had been perfused with radiolabeled microparticles, about 40% of the trapped particles were removed with the marrow (30% in the tibia). Since the tissues were separated manually, some inaccessible trabecular marrow probably remained with the bone. Further, the femur and tibia presumably contain relatively more yellow marrow than does the skeleton as a whole, so that blood flows to femoral and tibial marrow would be expected to be less than the average marrow perfusion rates in Table 6. Shim *et al.* (1968) concluded that the nutrient artery, which goes principally to the marrow with some branching to cortical bone, is normally responsible for about 50% of the blood supply to the rabbit femur. Metaphyseal arteries, which are responsible for a portion of the total blood supply to metaphyseal trabecular bone and marrow, traverse relatively more bone before they reach marrow spaces.

Once maturity is reached and the skeleton has stabilized, it appears likely that skeletal blood flow stabilizes also, although it continues to be capable of responding to local or regional demands for increased flow. Blood flow to specific bones may diminish with age. Hruza and Wachtlova (1969) observed that aging in both male and female rats was associated with diminution of blood flow to tibia and parietal bone, and MacPherson and Tothill (1978) also found that blood flow to certain bones diminished with age in male rats weighing 200–615 g. Nonetheless, MacPherson and Tothill (1978) observed no age-related change in the fraction of cardiac output going to the skeleton: total skeletal blood flow remained constant at 3.03 ± 0.21% of cardiac output.

Blood flow rates have been incorporated only into the model of the mature skeleton. In order to model blood flow rates to the growing skeleton, advantage will be taken of the observation that bone blood flow rate is closely correlated with bone formation rate. Bone formation rates are examined in the second paper in this series (O'Flaherty, 1991a).

The model of rat skeletal growth presented here should not be extrapolated to humans using conventional allometric scaling procedures. In contrast to bone itself, which is essentially the same in different species, the fraction of the body occupied by the skeleton and the relative amounts of bone and bone marrow can vary widely across species. In particular, the skeleton occupies a larger fraction of the bodies of large animals than of small animals. In addition, the small animal skeleton appears to contain a larger fraction of bone than the human skeleton. These points are considered, and a model of the growing human skeleton is developed, in the third paper in this series (O'Flaherty, 1991b).

The model of the growing rat skeleton also is not intended to describe skeletal growth beyond maturity (body weight about 300 g in male rats, 250 g in female rats). Predictions of the model in a range of larger body sizes would be inaccurate. One of the reasons is the sexual dimorphism of adult rats. Until early adulthood, bone and skeletal growth of male and female rats are not markedly different. In maturity, however, the male rat continues to form

.ew bone while the bone volume of the female at not change substantially. In addition, ne bone of the rat, like that of the human, displays osteoporotic changes during aging. The aging skeleton will be considered in a separate paper. The model presented here satisfactorily reproduces measurements of skeletal and bone weights, bone ash, and bone calcium made during the growth of rats from birth to maturity.

REFERENCES

ANDERSEN, M. E., CLEWELL, H. J., GARGAS, M. L., SMITH, F. A., AND REITZ, R. H. (1987). Physiologically based pharmacokinetics and the risk assessment process for methylene chloride. *Toxicol. Appl. Pharmacol.* 87, 185–205.

BEDDOE, A. H. (1977). Measurements of the microscopic structure of cortical bone. *Phys. Med. Biol.* 22, 298–308.

BEDDOE, A. H., DARLEY, P. J., AND SPIERS, F. W. (1976). Measurements of trabecular bone structure in man. *Phys. Med. Biol.* 21, 589–607.

BRANEMARK, P. I. (1959). Vital microscopy of bone marrow in rabbit. *Scand. J. Clin. Lab. Invest.* 11(Suppl. 38), 5–82.

BURG, G. D., LUCK, J. C., PAYNE, D. B., HOFFMAN, A. [illegible], ARCHIE, J. P., AND FIXLER, D. E. (1971). Some sources of error in measuring regional blood flow with radioactive microspheres. *J. Appl. Physiol.* 31, 598–604.

BURNELL, J. M., TEUBNER, E. J., AND MILLER, A. G. (1980). Normal maturational changes in bone matrix, mineral, and crystal size in the rat. *Calcif. Tiss. Int.* 31, 13–19.

CARTER, D. R., AND HAYES, W. C. (1977). The compressive behavior of bone as a two-phase porous structure. *J. Bone Jt. Surg.* 59A, 954–962.

CASTER, W. O., PONCELET, J., SIMON, A. B., AND ARMSTRONG, W. D. (1956). Tissue weights of the rat. I. Normal values determined by dissection and chemical methods. *Proc. Soc. Exp. Biol. Med.* 91, 122–126.

DICKERSON, J. W. T. (1962). Changes in the composition of the human femur during growth. *Biochem. J.* 82, 56–61.

DIETZ, A. (1944). Distribution of bone marrow, bone, and bone-ash in rabbits. *Proc. Soc. Exp. Biol. Med.* 57, 60–62.

EL-MARAGHI, N. R. H., PLATT, B. S., AND STEWART, R. J. C. (1965). The effect of the interaction of dietary protein and calcium on the growth and maintenance of the bones of young, adult and aged rats. *Br. J. Nutr.* 19, 491–509.

FAIRMAN, E., AND CORNER, G. W. (1934). The bone-marrow volume of the albino rat. *Anat. Rec.* 60, 1–4.

FORBES, R. M., COOPER, A. R., AND MITCHELL, H. H. (1953). The composition of the adult human body as determined by chemical analysis. *J. Biol. Chem.* 203, 359–366.

FORBES, R. M., MITCHELL, H. H., AND COOPER, A. R. (1956). Further studies on the gross composition and mineral elements of the adult human body. *J. Biol. Chem.* 223, 969–975.

FROST, H. M. (1962). Specific surface and specific volume of normal human lamellar bone. *Henry Ford Hosp. Med. Bull.* 10, 35–41.

GONG, J. K., ARNOLD, J. S., AND COHN, S. H. (1964a). The density of organic and volatile and non-volatile inorganic components of bone. *Anat. Rec.* 149, 319–324.

GONG, J. K., ARNOLD, J. S., AND COHN, S. H. (1964b). Composition of trabecular and cortical bone. *Anat. Rec.* 149, 325–331.

GROSS, P. M., MARCUS, M. L., AND HEISTAD, D. D. (1981). Current concepts review: Measurement of blood flow to bone and marrow in experimental animals by means of the microsphere technique. *J. Bone. Jt. Surg.* 63A, 1028–1031.

GROSS, P. M., HEISTAD, D. D., AND MARCUS, M. L. (1979). Neurohumoral regulation of blood flow to bones and marrow. *Am. J. Physiol.* 237, H440–H448.

HAMMETT, F. S. (1925). A biochemical study of bone growth. I. Changes in the ash, organic matter, and water during growth (mus Norvegicus albinus). *J. Biol. Chem.* 64, 409–428.

HRUZA, Z., AND WACHTLOVA, M. (1969). Diminution of bone blood flow and capillary network in rats during aging. *J. Gerontol.* 24, 315–320.

HUDSON, G. (1958). Bone marrow volume in guinea-pigs. *J. Anat.* 92, 150–161.

HUDSON, G. (1960a). Bone-marrow volume in cats. *J. Anat.* 94, 274–278.

HUDSON, G. (1960b). Volume and cellular constitution of bone marrow in guinea pigs hypoxic from birth. *Blood* 16, 1199–1204.

JANKOVICH, J. P. (1971). Structural development of bone in the rat under earth gravity, simulated weightlessness, hypergravity and mechanical vibration. NASA Contractor Report, Wenner-Gren Aeronautical Research Laboratory, University of Kentucky, NASA CR-1823.

JOHNSON, L. C. (1964). In *Bone Biodynamics*. (H. M. Frost, Ed.), Chap. 129, pp. 543–654. Little, Brown, Boston.

LANFORD, C. S., AND SHERMAN, H. C. (1938). Further studies of the calcium content of the body as influenced by that of the food. *J. Biol. Chem.* 126, 381–387.

LEE, W. R., MARSHALL, J. H., AND SISSONS, H. A. (1965). Calcium accretion and bone formation in dogs. An experimental comparison between the results of Ca^{45} kinetic analysis and tetracycline labelling. *J. Bone Jt. Surg.* 47B, 157–180.

TOXICOLOGY AND APPLIED PHARMACOLOGY 111, 313–331 (1991)

M. Gargas

Physiologically Based Models for Bone-Seeking Elements

II. Kinetics of Lead Disposition in Rats[1]

ELLEN J. O'FLAHERTY

Department of Environmental Health, University of Cincinnati College of Medicine, 3223 Eden Avenue, Cincinnati, Ohio 45267-0056

Revised October 25, 1990; accepted July 27, 1991

Physiologically Based Models for Bone-Seeking Elements. II. Kinetics of Lead Disposition in Rats. O'FLAHERTY, E. J. (1991). *Toxicol. Appl. Pharmacol.* 111, 313–331. For toxicants with long residence times in the body, body burden is determined largely by exposure history rather than by current exposure. There is a need for physiologically based toxicokinetic models capable of integrating exposure over time by incorporating growth, development, and aging. Such a model is presented for lead kinetics in the growing rat from birth to adulthood. The model incorporates age dependence of the physiologic and metabolic processes that control lead distribution to bone and soft tissues, as well as age dependence of lead absorption from the gastrointestinal tract and age dependence of elimination of lead. The essential features of bone structure and metabolism are integrated into a framework that determines bone lead kinetics. Parameter values used in the model are taken from the literature or are estimated from the best visual fit of the model to data from chronic and short-term studies of lead exposure in rats. The model accommodates any pattern of lead exposure. The uptake of lead by bone varies with the age at which exposure occurs. The predictions of the model are compared with data from a chronic study in rats in which lead exposure was discontinued after exposure periods varying from 3 to 12 months. © 1991 Academic Press, Inc.

Lead and its potential toxicities have become the focus of increasing attention in recent years. While the occupational hazards of lead exposure are fairly well understood, lead is also widely disseminated in the general environment due to its historical use in gasoline and in paints, from which it has entered soils through fallout and through flaking and disintegration of old paint. The persistence of lead-based paint in older homes also represents a hazard to young children as a result of consumption of paint flakes or as a result simply of ordinary hand-to-mouth activity. Environmental lead exposure extends throughout childhood and adult life.

Ninety-five percent or more of the adult's body burden of lead is in the bone (Barry, 1975). Because large amounts of lead can be sequestered in the bone, there is potential for return of lead from bone at biologically significant rates either as the result of normal bone metabolic activity or as a result of conditions such as osteoporosis that are characterized by net bone resorption with a decrease in bone mineral mass. Even in childhood, bone is not a sink for lead, because active modeling of growing bone involves resorption of existing bone, some of which may contain

[1] Portions of this work were supported by U.S. Public Health Service Grants ES01872 and ES04125. The concepts and data have been presented in part at annual meetings of the Society of Toxicology in 1988 and 1989.

0041-008X/91 $3.00
Copyright © 1991 by Academic Press, Inc.
All rights of reproduction in any form reserved.

localized high concentrations of lead reflecting active bone formation during earlier lead exposure.

Bone is a complex, metabolically active tissue subject to endocrinologic and physiologic control. Lead is incorporated into bone by substituting for calcium in the bone mineral matrix (MacDonald *et al.*, 1951). Movement of calcium in and out of bone is mediated by several distinct processes in which it may be presumed that lead also participates. The nature of these processes is such that the residence time of an atom of lead or other bone-seeking element in bone can be a substantial fraction of a lifetime. The lead content of bone at any time is the integrated outcome of processes that may have begun well before birth. The concentration of lead in plasma at any time is determined almost entirely by the balance among absorption, elimination, and transfers to and from bone. In order to clarify the complex relationships among magnitude, pattern, and timing of lead exposure and blood lead levels, as well as to support rational predictions related to potential lead toxicity, a model that describes lead kinetics over an entire lifetime is required.

In this paper, such a model is proposed. The model is developed for the growing rat from birth to adulthood. It applies equally to male and female rats. It does not take into account exposure during gestation and suckling, stresses of pregnancy and lactation on bone, or net bone loss that may occur in aging or disease. The model is anatomically and physiologically based. It includes reasonable descriptions of the age dependence of tissue volumes, blood flow rates, and clearances. The heart of the model is integration of the essential features of bone architecture, growth, and metabolism into a framework determining bone lead kinetics.

METHODS

Experimental

Chronic study with continuous lead exposure. Male Long-Evans rats were maintained from age 50 days on drinking water containing 0, 100, 300, 500, or 1000 ppm added lead. Lead was added as lead acetate to the drinking water, which was slightly acidified to minimize precipitation of lead carbonate and was changed two to three times each week. The rats were housed 3 to a cage and were fed Purina 5001 chow; food and drinking water were provided *ad libitum*. A 12-hr light/12-hr dark cycle was maintained. Initially, there were 36 rats per exposure group. Two and four weeks and 2, 4, 8, and 18 months after the start of the study, 6 rats from each group were killed. Blood was taken by cardiac puncture. After the remaining blood had been cleared from the tissues by perfusion through the left ventricle of the heart with physiologic saline, samples of liver and the diaphyseal region of the femur, as well as the whole kidney, were weighed and frozen at −4°C until analyzed for their content of lead. Lead analyses were carried out by flame atomic absorption spectrophotometry after wet digestion of tissues with nitric and hydrochloric acids. The kidney lead concentration data have been previously published (O'Flaherty *et al.*, 1986).

Short-term study. Two groups of six weanling (24-day-old) male Sprague–Dawley rats were given drinking water containing 1000 ppm added lead, acidified slightly as described above, for either 31 or 60 days. Housing and feeding were the same as in the chronic study with continuous exposure. Blood lead concentrations were monitored by tail bleeding just before removal of lead from the drinking water (designated Day 0) and on Days 1, 2, 3, 5, 8, 11, and 15, and weekly gradually lengthening to monthly thereafter until age 394 days. In order to minimize contamination of samples by lead, tails were thoroughly cleaned by scrubbing with a dilute solution of EDTA prior to sample collection. Blood lead concentrations were determined by Zeeman atomic absorption spectrophotometry.

Chronic study with lead exposure of varying duration. Eight groups of 10 male Sprague–Dawley rats were given drinking water containing either 1000 ppm (four groups) or 2000 ppm (four groups) added lead, acidified slightly as described above. Housing and feeding were the same as in the chronic study with continuous exposure. At each of the two exposure levels, one group of rats was started on lead-containing drinking water at age 22 days, one at age 114 days (3 months), one at age 215 days (6 months), and one at age 296 days (9 months). All controlled lead exposures were terminated when the rats were 440 days old. Blood lead concentrations were monitored by tail bleeding just before removal of lead from the drinking water (designated Day 0) and on Days 1, 2, 3, 5, 7, 10, 14, 17, and 21, and weekly lengthening to monthly thereafter for 225 days following removal of lead from the drinking water. Precautions were taken to avoid contamination as above. Blood lead analyses were carried out by Zeeman atomic absorption spectrophotometry.

Theoretical

General. A qualitative description of the structure and principal features of the model is given here. A quantitative

outline of the model, with key equations, will be found in the Appendix.

Kidney, liver, other well-perfused tissues, bone, and other poorly perfused tissues compose the model. Kidney and liver are considered individually because they are organs of lead absorption and/or elimination. Ingested lead is modeled as direct input into the liver. Fractional absorption of ingested lead declines with age from its maximum value at and before weaning. A small dose dependence of fractional absorption is incorporated into the model. Elimination of lead is considered to be 91% in the bile and 9% in the urine (Aungst *et al.*, 1981; Gregus and Klaassen, 1986). As modeled, fractional excretion is age-dependent but not dependent on body burden of lead.

The model is scaled both to age and to body weight at sexual maturity by means of a flexible expression for body weight. The body weight expression is adaptable to generic or specific growth curves, and to growth of male or female rats. Its form allows shifts in anatomic and physiological parameters during growth to be incorporated into the model. Cardiac output (O'Flaherty *et al.*, 1990), clearances, and organ and tissue volumes (Trieb *et al.*, 1976) are linked both to body weight and to degree of maturity.

Of the total cardiac output, 0.25 goes to the liver and associated tissues, 0.17 to the kidney, 0.44 to other well-perfused tissues, 0.03 to bone, and 0.11 to other poorly perfused tissues. These fractions are invariant with body weight.

The fractional composition of the total body weight of the adult rat is: liver, 0.04; kidneys, 0.01; all well-perfused tissues including liver and kidneys, 0.10; and all poorly perfused tissues including bone, 0.90. These fractions are independent on body weight during growth. Bone volume is also modeled as a power of body weight during growth from birth to maturity (O'Flaherty, 1991).

All transfers of lead out of the blood are related to plasma lead, which is a concentration-dependent fraction of blood lead. The relationship between plasma and total blood lead is expressed as a capacity-limited binding associated with the erythrocytes. Transfers of lead between plasma and tissues other than bone are modeled as conventional flow-limited exchanges. Based on the relative importance of mechanisms of calcium uptake into and release from bone, transfers of lead between plasma and bone are considered to be mediated by four qualitatively distinct mechanisms: rapid or surface exchange, slow or diffuse exchange, deposition of lead with accretion of new bone, and removal of lead with resorption of bone. Rapid exchange is a flow-limited process, while slow exchange is modeled as radial diffusion outward from the canalicules that channel nutrients into bulk bone.

Passage of blood through bone, with exchange of lead between plasma and bone, is modeled as a series of linked and partially interactive events. As blood traverses the bone, it passes first through the volume of rapid surface exchange. Lead in this bone region is considered to be in equilibrium with lead in blood plasma leaving the region and entering the metabolically active region. The metabolically active region of bone consists of actively growing, modeling, or remodeling haversian canal, endosteal, periosteal, and trabecular surfaces. In the metabolically active region, lead is removed from blood during the formation of new bone and returned to blood with resorption of existing bone. Resorbing bone contains the moving average bone lead concentration, all processes taken together.

The diffusion region of bone is the total bone volume with the exception of the rapidly exchanging surface region. It includes the metabolically active region. Radial diffusion of lead outward from canalicules is approximated as exchanges between concentric cylindrical shells whose total volume is the volume of the diffusion region. Any number of concentric cylindrical shells could in principle be incorporated into the model. Approximation to a true diffusion process improves as the number of shells increases and their thickness diminishes. The model as presently written is composed of eight shells of equal thickness. Lead is homogeneously distributed within each shell. Transfers between shells, and between the innermost shell and fluid passing through the canalicule, are diffusion-limited.

Parameter estimation. Physiological parameters required by the model define body growth; bone formation rate, net bone volume, volume of the rapidly exchanging fraction of bone mineral, and blood flow rate to bone; and bone structure (canalicule diameter and spacing), in addition to specifying the fractional tissue volumes and blood flow rates that make up more conventional physiologically based models. Values of the growth- and bone-related parameters are given here and in Table 1.

The parameters WADULT, HALF, and CONST in the expression relating body weight to age (Table 1) can be selected to reproduce an experimental growth curve or can be chosen arbitrarily to generate an average growth curve. In the applications given here, model body growth was matched to growth curves for the particular rats in each of the studies. Net bone volume as a function of body weight has been defined previously (O'Flaherty, 1991). The fractional volume of the rapidly exchanging surface region of bone was arbitrarily set at 0.002 (see Discussion). Blood flow rate to bone was set at 3% of cardiac output, independent of age (O'Flaherty, 1991). Values for canalicule diameter and spacing (Table 1) were taken from quantitative electron microscopic measurements of mouse bone by Baud (1962). None of these parameter values was adjusted; they were used as originally selected.

An expression for bone formation rate was devised based primarily on the data of Sontag (1986a,b). Sontag (1985) suggested that decline in bone formation rate with age in rats more than 60 days old could be approximated by a negative exponential term. An apparent half-life of about 40 days for the decline in bulk bone formation rate in rats in the 60–130 day age range studied by Sontag (1985, 1986a,b) (Table 3) is supported by the linear appositional growth rate data of Raman (1969) (see Discussion). The second exponential term in the expression for fractional

TABLE 1

PHYSIOLOGICAL PARAMETERS

Body weight	
WADULT	Variable: 0.350–0.500 kg
HALF	Variable: 1.5–2.0 months
CONST	0.0088 (male rats only)
Bone growth[a]	
MINFORM	0.003
ALPHAO	0.321
ALPHA	0.2
BETAO	Variable: dependent on HALF, WADULT
BETA	Variable: dependent on HALF, WADULT
Bone structure[b]	
Canalicule spacing	1.7 μm
S, specific canalicule surface	4.712×10^{-5} cm²/cm length
L, specific total canalicule length	4.511×10^{10} cm/liter bone

[a] When WADULT = 0.375 kg and HALF = 1.6 months, BETAO = 0.081 and BETA = 0.021.
[b] Baud (1962).

bone formation rate in the model presented here defines formation rate in this age range. The half-life is about 35 days. However, this term cannot account for the rapid increase in bone volume that takes place between birth and age 60 days. Another exponential term, with a half-life of about 3.5 days, has been incorporated into the expression for bone formation rate in order to describe this early, very rapid bone growth. The values of the five parameters in the expression for bone formation rate as a function of age (Table 1) were adjusted slightly so as to bring model predictions into better agreement with actual concentration measurements from the short-term study, but no attempt was made to optimize them.

Lead-related parameters for which values must be entered into the model are fractional absorption from the gastrointestinal tract; partition coefficients for lead in non-bone tissues and in the surface region of bone; maximum capacity and half-saturation concentration for capacity-limited binding in the erythrocyte; elimination clearance; fractional clearance of lead from plasma into forming bone; and the restricted permeability coefficients for lead diffusion within bone, from plasma into bone, and from bone into plasma. Values of lead-related parameters are given here and in Table 2.

Fractional lead absorption from the gastrointestinal tract was modeled as a first-order decline with a half-life of 3.5 days from about 0.15 at and before weaning to 0.007–0.01, depending on dose, during adulthood (Kostial *et al.*, 1978). For concentrations of lead greater than 1000 ppm in the drinking water, fractional absorption in adult rats was adjusted in order to eliminate residual nonlinearity (after adjustment for capacity-limited binding) in the exposure/blood lead concentration relationship.

Aungst *et al.* (1981) reported total elimination clearances of 0.4–1.0 liter of blood/day/kg body wt in rats weighing 0.3 kg. If only plasma is actually being cleared, this range translates to roughly 16–40 liters of plasma/day/kg body wt. Elimination was modeled as clearance from blood

TABLE 2

PARAMETERS RELATED TO LEAD

Partitioning in blood[a]	
BIND	10 mg/liter
KBIND	0.067 mg/liter
Partitioning between blood plasma and tissues[b]	
PL (liver)	75
PK (kidney)	Variable with dose rate
PW (other well-perfused tissues)	75
PB (bone)	6000
PP (other poorly perfused tissues)	20
Metabolically active region of bone[c]	
LEAD, fractional clearance of lead into forming bone	15,000
Diffusion region of bone	
DO, restricted permeability coefficient for within-bone movement[d]	8×10^{-7} cm/day/unit distance
RO, restricted permeability coefficient for bone-to-plasma transfer[d]	8×10^{-7} cm/day/unit distance
PO, restricted permeability coefficient for plasma-to-bone transfer[e]	0.1 cm/day/unit distance
Elimination clearance[f]	
QEC	14 liter/day/kg

[a] Based on Klaassen and Shoeman (1974).
[b] Experimental values from chronic study with continuous exposure.
[c] Empirical value giving best visual fit of model to data.
[d] Marshall and Onkelinx (1968).
[e] Based on Tothill and Hooper (1984); adjusted to obtain best visual fit of model to data.
[f] Based on Aungst *et al.* (1981).

plasma, having a value of 14 liters of plasma/day/kg body wt.

Values of partition coefficients for non-bone tissues and surface region of bone (Table 2) were determined experimentally as the mean ratios of tissue concentrations at steady state in the chronic study with continuous lead exposure. No allowance was made for possible changes in partition coefficients with age or length of exposure, nor was there indication that changes occurred in any tissue except the kidney (see Discussion).

The value of the restricted diffusion coefficient for slow exchange of lead within bone and from bone to plasma (Table 2) was that given by Marshall and Onkelinx (1968) for slow exchange of ^{45}Ca, ^{90}Sr, and ^{226}Ra in dog bone.

Initial values for maximum binding capacity BIND and half-saturation concentration KBIND (Table 2) were based on the work of Klaassen and Shoeman (1974). The initial value of the parameter LEAD, the fractional clearance of lead into newly formed bone (Table 2), was a best-guess estimate based on the rate at which lead entered the rat femur during the chronic study with continuous lead exposure. The initial value of PO, the restricted permeability coefficient for transfer of lead into bone (Table 2), was calculated from Tothill and Hooper's (1984) data for extraction of ^{85}Sr by the total skeleton of the rat as a function of blood flow rate through bone. From their data, the maximum clearance possible at infinitely large blood flow can be estimated to be about 46 ml/min/100 g skeletal bone. Thus, for diffusion of ^{85}Sr into bone from canalicules having a total surface area of 2.126×10^5 cm^2/100 cm^3 bone, as in the present model, P would be about 0.3 cm/day/skeletal density, or 0.2 cm/day when skeletal density is 1.5 g/cm^3.

The values of BIND, KBIND, LEAD, and PO were optimized by reconciling blood lead concentrations

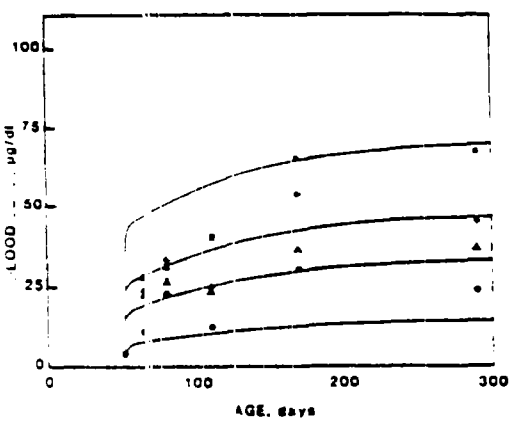

FIG. 1. Blood lead concentration during continuous exposure of rats to lead in the drinking water. Points are the means of measurements in groups of 4–6 rats at (●) 100, (▲) 300, (◆) 500, and (■) 1000 ppm lead added to the drinking water. Lines are model simulations.

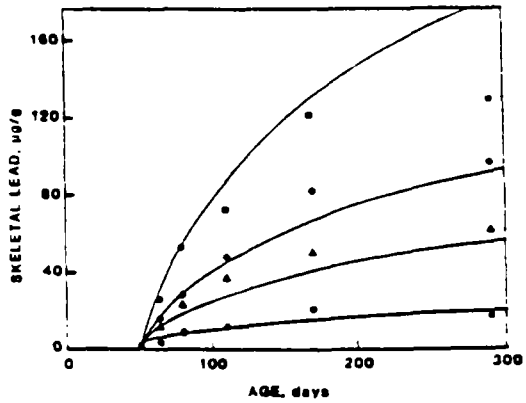

FIG. 2. Skeletal lead concentration during continuous exposure of rats to lead in the drinking water. Points are the means of measurements of lead in femoral diaphysis in groups of four to six rats at (●) 100, (▲) 300, (◆) 500, and (■) 1000 ppm lead added to the drinking water. Lines are model simulations for total skeleton.

predicted by the model with the concentration profiles from the chronic study with continuous exposure and from the short-term study.

RESULTS

The same parameter values (Table 2) were used for all the simulations illustrated. Figures 1 and 2 give the simulations and experimental data for blood lead and skeletal lead from the chronic study with continuous lead exposure. Liver and kidney lead and simulations from this data set are not shown. Because the data from this study are unfortunately somewhat erratic, the accuracy of the simulations is difficult to judge. However, they show clearly the continuing steady accumulation of lead in bone during continuing exposure, despite the rapid attainment of a pseudoequilibrium concentration of lead in blood. These data sets were used principally to fix values of the partition coefficients and of BIND and KBIND. In contrast to the values of the plasma/erythrocyte partitioning parameters, the values of the partition coefficients do not greatly influence the whole-body predictions of the model.

Figures 3 and 4 display the simulations and data from the two short-term experiments in

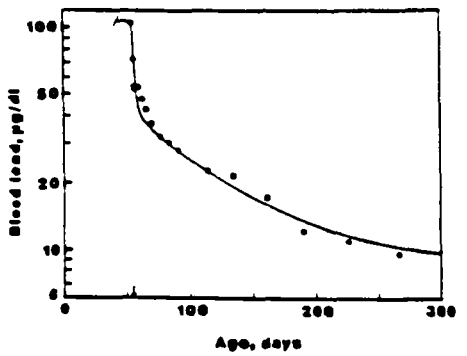

FIG. 3. Blood lead concentration after 31 days of exposure of 24-day-old rats to 1000 ppm lead in the drinking water. Points are the means of repeat measurements in a group of six rats. The line is the model simulation. Standard deviations are not shown. Coefficients of variation ranged from 6.9 to 39%.

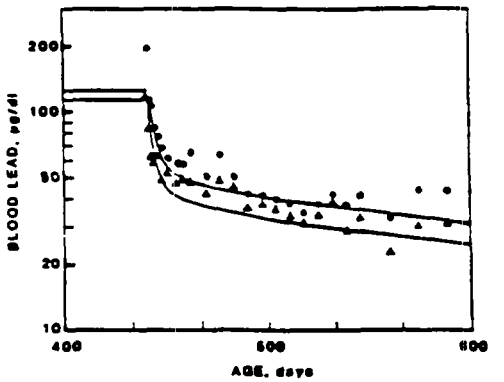

FIG. 5. Blood lead concentration from age 400 to 600 days during and after 418 days of exposure of 22-day-old rats to lead in the drinking water. Controlled lead exposure was terminated at age 440 days. Points are the means of repeat measurements in a group of four to six rats given (▲) 1000 or (●) 2000 ppm lead added to the drinking water. Lines are model simulations. Standard deviations are not shown in Figs. 5–8 for the sake of clarity. Coefficients of variation were roughly 20% at mean blood lead levels less than about 100 µg/dl, and as much as 60% at higher mean blood lead levels.

which young rats were given lead for either 31 or 60 days. A feature of these data sets is a transient stabilization of the blood lead concentration that occurs at some time between about 3 and about 11 days after removal of lead from the drinking water. Although this kinetic behavior was not observed in all animals, it was seen fairly consistently and is reflected in the shapes of the data sets in Fig. 3 and particularly in Fig. 4, after the longer exposure. These data sets were used to refine the form of the expression for bone formation rate and to fix the values of the parameters PO and LEAD. They cover a sensitive age range in which the bone formation rate is diminishing rapidly.

Figures 5–8 illustrate blood lead simulations and measured concentrations from the chronic

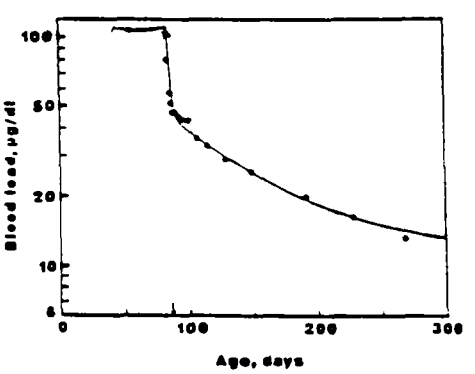

FIG. 4. Blood lead concentration after 60 days of exposure of 24-day-old rats to 1000 ppm lead in the drinking water. Points are the means of repeat measurements in a group of six rats. The line is the model simulation. Standard deviations are not shown. Coefficients of variation ranged from 8.9 to 36%.

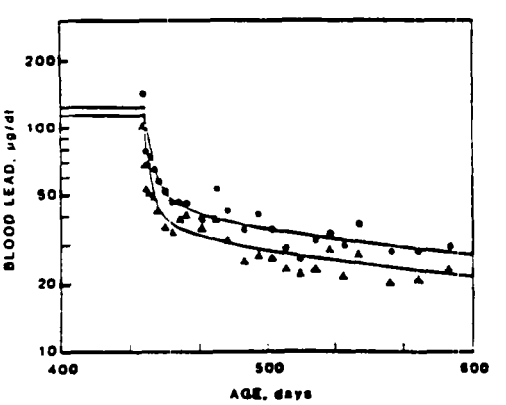

FIG. 6. Blood lead concentration from age 400 to 600 days during and after 326 days of exposure of 114-day-old rats to lead in the drinking water. See legend to Fig. 5.

the same as lead kinetics in male rats up to about 250 g body wt, and to differ subsequently primarily because of the difference in growth rate, with earlier onset of net bone loss in females than in males.

Fractional absorption of lead from the gastrointestinal tract is strongly dependent on age in the immature rat. A large fractional absorption in suckling rats falls rapidly to adult levels during a period of days to at most a few weeks after weaning (Kostial *et al.*, 1978). There is little experimental basis for selection of the particular range of fractional absorption values incorporated into the present model, although they are representative of observed values. The uncertainty is partly due to the influence of experimental conditions. Fractional absorption of lead from the gastrointestinal tract is dependent on diet and nutritional status (Conrad and Barton, 1978; Kostial and Kello, 1979) as well as on the chemical species of the lead (Barltrop and Meek, 1975). The adult chow-fed rat has been reported to absorb between about 0.4% (Kostial and Kello, 1979) and 1.0% (Barltrop and Meek, 1975) of total dietary lead. The value of 1.0% used in the present model was based on data from chow-fed rats, and was required in order to bring predicted and measured blood lead concentrations into congruence.

Gastrointestinal lead absorption has also been shown to be dose-dependent. Aungst *et al.* (1981) observed disproportionalities in tissue lead concentrations at drinking water concentrations as low as 50 ppm, but the data on which the present model is based do not require adjustment for a reduction in fractional absorption unless drinking water lead concentrations exceed 1000 ppm.

Renal clearance of lead by rats is about 9% of total clearance and is independent of blood lead concentration up to at least 100 μg/dl (Aungst *et al.*, 1981). Excluding from consideration minor routes of excretion such as nails and hair, it follows that biliary excretion accounts for 91% of lead excretion in rats regardless of dose. Most of the detailed studies of renal excretion of lead have been conducted in dogs. Lead reabsorption in the dog kidney is extensive but shows no evidence of capacity limitation (Vander *et al.*, 1977). Whether reabsorption of filtered lead takes place in the rat kidney cannot be established unless the fraction of plasma lead that is filtered at the glomerulus is known. However, in order to model lead kinetics, the relative contributions of nonfilterability of plasma lead and tubular reabsorption of filtered lead to renal lead excretion need not be known provided that both of these processes are first-order.

Occurrence of exponents less than unity in the expression for liver and kidney volumes as functions of body weight in the model (see Appendix) means that these organs occupy a slightly greater fraction of model body weight in the young than in the mature rat. The values of these exponents are taken from a detailed study of allometry of growth in the rat (Trieb *et al.*, 1976). The value (0.67) of the exponent in the expression for cardiac output as a function of body weight is the value predicted by isometric theory for growth within a species (McMahon and Bonner, 1983). Its application to cardiac output is supported by fitting an allometric relationship to published values for cardiac output in rats of different body weight (O'Flaherty *et al.*, 1990). Distribution of cardiac output among different organs and tissue groups of the adult rat for the purpose of physiologic modeling is fairly well standardized (Ramsey and Andersen, 1984). In the absence of data suggesting otherwise, the fraction of the total cardiac output going to organs and tissues making up the present model is considered to be independent of age. A modification of the model that allowed organ blood flow rates to vary as fractional organ weight did not improve its predictive accuracy.

Bone. Bone, although it occupies a very slightly larger volume fraction of the adult rat body than of the immature rat body, grows at a rate similar to that of the whole body. While total bone volume is defined as a function of body weight, it is the opposing processes of formation and resorption that control net changes in bone volume. The expression for

one formation rate is derived from published studies of two distinct kinds.

In the first kind of study, the magnitudes of accretion and rapid exchange of skeletal calcium have been estimated with the aid of radiotracers. A basic approach has been developed that allows calculation of accretion rates and rapid exchange pools from measurements of the time course of specific activity in plasma following a single injection of a calcium tracer, together with the amount of tracer excreted in urine and feces and the total amount of calcium excreted in urine (Bronner, 1964; Marshall, 1969). Estimates of bone accretion rate and exchangeable bone calcium that are based on these tracer methodologies are dependent on the time during which the measurements were carried out, because they give a value for accretion rate that includes transfer into bone by exchange processes not yet at equilibrium with plasma tracer at the time of sampling. The rate of accretion of new bone can also be measured directly by fluorescent labeling techniques, in which a fluorescing dye is used to label actively growing bone surfaces. In combination with quantitative micrography, fluorescing markers can be used as the basis for estimation of bone formation rate. Selected values of bone formation rates from surface labeling studies and accretion rates from radiotracer studies are reproduced in Table 3. These values are the basis for the expression devised to describe dependence of bone formation rate on body weight in the present model. Fractional bone formation rate defined by this expression drops from about 40%/day in the newborn rat to about 6%/day at weaning, and approaches a minimum of 0.3%/day in mature rats. This magnitude of bone formation, and the rate at which it declines with age, is in accord with the observations of Raman (1969) and of Sontag (1986b) for male rats up to 6 months old. Sontag measured bone formation rate in the midshaft of the femur. He observed a continuing decline in bone formation rate with age after 6 months that may not reflect bone formation in the whole skeleton. Other observations (Table 3) suggest that fractional bone formation rate for the whole skeleton in older rats remains at about 0.3%/day.

In the present model, bone resorption rate is defined as the difference between bone formation rate and the rate of change of net bone volume. It declines from about 3.5%/day in the newborn rat to about 1%/day at weaning, and approaches 0.25%/day in mature rats. Few estimates of actual bone resorption rates in rats of different ages are available. Sontag (1986a,b) measured bone formation and resorption in femoral midshaft of male and female rats aged 60–850 days. He found that the ratio of bone formation rate to bone resorption rate did not exceed 3 at any age, and was about 1.8 in male rats at age 60 days. In the present model, this ratio is 3 in male rats at age 60 days, which appears to be a reasonable value for the whole skeleton compared to the midshaft of the femur.

It has previously been shown (O'Flaherty, 1990) that bone blood flow rate is approximately proportional to the rate of new bone formation. Figure 10 shows that when bone blood flow rate is a constant percentage of cardiac output, as it is in the model, it is proportional to bone formation rate as defined in the model. Thus, it is not necessary to devise a more complex expression to define bone blood flow. The simplest possible relationship of bone blood flow rate to cardiac output is consistent with observed behavior.

The model suggests that as fractional bone formation rate approaches its minimum value, specific bone blood flow rate approaches a value around 20 liters/day/100 g bone wt, or about 2.9 ml/min in a 400-g rat. This value can be scaled allometrically in accordance with the 0.75 power of body weight to give a crude prediction of minimum bone blood flow rate in the dog, for which bone blood flow measurements have been published. Scaling from the 400-g rat to the 10-kg dog gives an estimate of minimum flow of about 32 ml/min. If bone weight scales as the 1.1 power of body weight (Schmidt-Nielsen, 1972, 1984), minimum specific bone blood flow rate in the adult (10-

TABLE 3

"BONE ACCRETION RATE" FROM TRACER STUDIES WITH Ca^{45} OR Sr^{90}, AND "BONE FORMATION RATE" AND "APPOSITION RATE" FROM TETRACYCLINE LABELING STUDIES

n	Sex	Age (months)	Weight (g)	Bone accretion rate (mg/day)	Bone accretion rate (%/day)	Bone formation rate (%/day)	Apposition rate, (μm/day)	Tissue	Reference
5	F	—	166	0.49	0.57			Femur, ends	Bauer (1954)
				0.19	0.24			Femur, shaft	
				0.41	0.69			Tibia, ends	
				0.17	0.22			Tibia, shaft	
32	M & F	2	120	65	6.5			Whole body	Bauer *et al.* (1955)
				4.3	12.3			Tibia, ends	
				0.91	3.4			Tibia, shaft	
	M & F	2	120	58	5.8			Whole body	Bauer *et al.* (1956)
				3.4	9.6			Tibia, ends	
				0.82	3.0			Tibia, shaft	
2		3	126	60, 53	6.0, 5.3			Whole body	Aubert and Milhaud (1960)
1				4.1	6.2			Tibia, whole	Bauer *et al.* (1961)
3				3.3	9.1			Tibia, ends	
3				0.69	2.4			Tibia, shaft	
120	F	Weanling	58	18.6	4.6			Whole body	Weikel and Neuman (1961)
?	F	Adult	180	6.5	0.39			Whole body	
23	F	3		6.2				Whole body	Lemaire and Bronner, cited in Bronner (1964)
8	F	12		9.6				Whole body	
23	M	2	230	77				Whole body	Bronner and Aubert (1965)
14	F	4	174	61.4	2.3			Whole body	Bronner and Lemaire (1969)
8	F	10	302	14.6	0.28			Whole body	
10	M	1					10.5	Femur	Raman (1969)
10	M	1.5					7.6		
10	M	2					6.0		
10	M	2.5					4.6		
10	M	3					3.6		
10	M	3.5					2.7		
10	M	4					2.4		
10	M	1					8.3	Tibia	Raman (1969)
10	M	1.5					6.3		
10	M	2					4.8		
10	M	2.5					4.0		
10	M	3					2.9		
10	M	3.5					2.2		
10	M	4					1.9		
20	M	1.25	126			3.7	10.3 (periosteum) 4.6 (endosteum)	Tibia, prox. diaphysis	Baylink *et al.* (1970)
6	M	1.25	113			3.2	11.1	Femur, periosteum	Baylink and Wergedal (1971)
1	M	2–3					3.4	Femur, midshaft	Sontag (1980)
		2–3					1.6	Femur, dist. cortex	
1	M	3–5					0.65	Femur, dist. metaphysis	
		3.5					0.50	Femur, whole	
2	M	2				2.9		Femur, dist. metaphysis	Sontag (1985)

TABLE 3—*Continued*

	Sex	Age (months)	Weight (g)	Bone accretion rate (mg/day)	Bone accretion rate (%/day)	Bone formation rate (%/day)	Apposition rate, (μm/day)	Tissue	Reference
	F					2.0		Femur, dist. metaphysis	
	M & F					0.55		Femur, dist. epiphysis	
2	M	3.3				1.6		Femur, dist. metaphysis	
	F					0.68		Femur, dist. metaphysis	
	M					0.41		Femur, dist. epiphysis	
	F					0.20		Femur, dist. epiphysis	
0	F	2				2.7	8.2	Femur midshaft	Sontag (1986a)
0	F	3.4				1.0	3.5		
6	F	9				0.10	0.30		
32	F	13.2				0.04	0.21		
6	F	22				0.03	0.16		
34	M	2				2.7	1.5	Femur midshaft	Sontag (1986b)
2	M	3.4				1.2	7.9		
8	M	7				0.26	1.6		
8	M	10.6				0.12	0.66		
6	M	15.7				0.06	0.35		
4	M	18.2				0.04	0.23		

kg) dog would be predicted to be 4.4 ml/min/100 g bone wt. Comparison of measured regional bone formation rates in the dog from Lee *et al.* (1965) with regional bone blood flow rates from Schmitzer *et al.* (1982) suggests an actual minimum specific bone blood flow rate in the 10-kg dog of about 2 ml/min/100 g bone wt (O'Flaherty, 1990; Fig. 2), close to the allometrically based estimate.

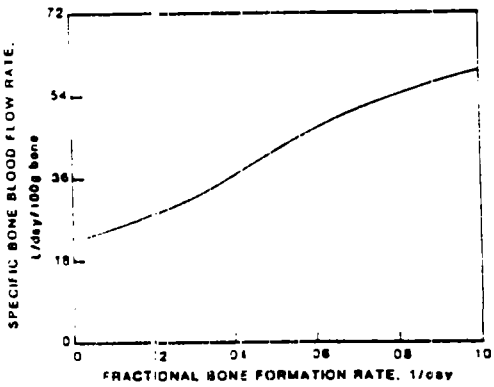

FIG. 10. The correlation of specific bone blood flow rate with fractional bone formation rate, as simulated by the model.

Lead kinetics. A fundamental premise of this model is that lead behaves like calcium in its movements into, within, and out of bone. Therefore, modeling of lead kinetics must be consistent with what is known about the kinetics of calcium disposition, including its dependence on age. Calcium is added to bone through accretion of new bone. Accretion has been defined as the net transfer of calcium atoms into a single microscopic volume of bone (Marshall *et al.* 1959). Since the microscopic volume is not necessarily fully occupied by bone mineral, accretion can represent either apposition, the increase of mineral volume, or secondary mineralization, the increase of mineral density. In addition, calcium (and lead) may enter and leave bone by exchange processes, defined as equal and opposite

transfers of atoms to and from a microscopic volume of bone. Two kinds of exchange are recognized: a rapid exchange and a slow or diffuse exchange. Return of mineral from bone can also take place by resorption. Resorption involves removal of both bone mineral and the supporting collagen matrix, so that it is the reverse of apposition.

Accretion of new bone, which is integral to bone modeling and remodeling processes, is the dominant feature of skeletal metabolism in the neonatal and young animal (Jowsey *et al.*, 1965a,b; Lee *et al.*, 1965). Bone formation rate decreases steadily throughout the period of growth and stabilizes, in rats, at a relatively low level during adulthood (Jowsey *et al.*, 1965a,b; Barer and Jowsey, 1967; Sontag, 1986a,b). New bone is not fully mineralized and will take up calcium tracers at a slightly greater rate than fully mineralized bone. However, the contribution of these locally higher specific activities to the overall specific activity of the bone is probably not large (Rowland, 1963).

Studies with calcium tracers have demonstrated that tracer uptake by bone is far too rapid to represent only accretion of new bone. A rapid (minutes to hours, depending on species) exchange between blood and bone calcium takes place at all bone surfaces in intimate contact with blood (Rowland, 1966). Surface calcium is lost as rapidly as it is gained. It is in sufficiently rapid equilibrium with plasma calcium that they can be considered part of the same kinetic compartment (Rowland, 1966; Groer and Marshall, 1973). Surface calcium is believed to be the reservoir drawn on for maintenance of plasma calcium homeostasis.

In contrast to the rapidly exchanging surface calcium compartment, the diffuse distribution of a calcium tracer throughout the bone does not reach equilibrium with plasma after a single administration (Rowland, 1966). The magnitude of this diffuse labeling increases with length of exposure to tracer, and is related to the total body burden (Rowland and Marshall, 1959). Because diffuse labeling develops without any change in the microscopic density of bone even during chronic administration of calcium tracers, it is concluded that it represents a slow exchange of blood and bone calcium rather than net accretion of calcium (Marshall *et al.* 1959; Rowland, 1960).

Four observations suggest that rate of loss of calcium tracers from the skeletons of adult animals is determined principally by slow exchange. First, diffuse labeling remains consistently uniform throughout the bone even long after a single administration of tracer (Rowland, 1960). Second, exchange has been shown to be capable of accounting fully for total autoradiographically measured loss of calcium radiotracer from bone and for loss as predicted by the power function (Rowland, 1961, 1963). Third, it has been repeatedly observed that the rate of diminution of diffuse activity and of average activity in bone are parallel (Rowland, 1960, 1961; Rowland and Marshall, 1959; Shimmins and Smith, 1966), strongly supporting the conclusion that loss of tracer from "hot spots" of new bone formation at a time of high plasma specific activity takes place at the same relative rate as loss (by exchange) from the diffuse pool. This observation is the justification for considering that loss of lead from the model rat skeleton occurs by resorption and slow diffusion from bone containing the "average" concentration of bone lead. Finally, Shimmins and Smith (1966) calculated that the rate of return of calcium radiotracer from human bone was an order of magnitude greater than their or others' estimates of bone formation rate, so that return could not have been controlled by resorption. Thus, it appears that resorption is as unable to account fully for the disappearance of diffusely distributed calcium tracer from bone of mature animals as continuing mineralization is to account for its appearance. In the growing animal whose bone is undergoing modeling, however, resorption is much more important; exchange may be insignificant relative to loss by resorption of bone (Bauer and Shtacher, 1968).

Uptake of bone-seeking elements from the fluid perfusing deeper bone regions is a dif-

sion-limited rather than a flow-limited process (Tothill *et al.*, 1985). The simplest way to present the retention of bone-seeking elements in the body after a single exposure has historically been to use the power function, in which fractional retention is a function of time to a negative power. Marshall (1969) proposed that the power function character of the kinetics of bone-seeking elements could best be pictured as a consequence of radial diffusion outward from canalicules into the bone mineral matrix, at right angles to the long axes of the canalicules. A random walk through this locally inhomogeneous volume would be expressible at a higher level of organization as diffusion through a homogeneous matrix with a single effective coefficient of diffusion. When radial diffusion is approximated by transfer between concentric cylindrical shells, as it is in the model presented here, the effective coefficient of diffusion is expressed per unit radial distance or, for the rat bone model, as the restricted coefficient of diffusion 8×10^{-7} cm/day for transfer between shells. This diffusion coefficient was used directly, without adjustment, in the model and was applied both to movement within bone and to transfer from bone to canalicular fluid. That a diffusion coefficient obtained for movement of several elements through bone of one species is applicable directly to the diffusion of another element through bone of another species is evidence that the process is indeed a passive diffusion whose attributes are not markedly dependent on the character of the diffusing element.

Model Performance

The predictions of the model are very sensitive to partitioning of lead between plasma and red cells. Klaassen and Shoeman (1974) examined this partitioning in adult male Sprague–Dawley rats. They showed that plasma and whole blood lead concentrations were roughly proportional at plasma lead concentrations up to 10 μg/dl, but that at higher concentrations plasma lead increased disproportionally to blood lead. The values of KBIND in Table 2 is not greatly different, 6.7 μg/dl of plasma, equivalent to blood lead concentrations around 200 μg/dl. With the exception of the 2000 ppm drinking water concentration, all the nonlinearity in the several experimental relationships between administered dose and blood and tissue lead levels could be accounted for by nonlinearity in the relationship of plasma lead to whole blood lead. The nonlinear relationship of blood lead levels to external measures of lead exposure has received much consideration from researchers and regulatory agencies (U.S. EPA, 1986). In the current series of experiments, a single unifying principle has proven to be capable of resolving nearly all of the observed nonlinearity between applied dose and blood lead levels. If this principle is equally successful in resolving disproportionalities in exposure–blood lead level relationships under other conditions of exposure and in other species, its application will represent a significant contribution of physiologically based models to our understanding of lead kinetics.

It is reasonable to expect that strain dependence of the values of the parameters governing the plasma lead/blood lead relationship, as well as dependence on experimental conditions, may be found. In addition, some of the marked interindividual variability in lead kinetic behavior that has been noted by many investigators may be attributable to differences in partitioning of lead between plasma and red cells. In the chronic study with lead exposure of varying duration, standard deviations of group mean blood lead concentrations tended to be about 20% of the mean up to mean blood levels of about 100 μg/dl and as much as 60% of the mean at higher blood lead levels. Other factors, such as random contamination of tail blood samples despite the precautions taken to minimize such problems, could have contributed to the greater variability in measurements at higher blood lead levels. Nonetheless, the increasing variability of blood lead concentrations at high blood lead levels suggests

individual differences in partitioning of lead between plasma and erythrocytes. Since the half-saturation concentration, as modeled, is around 200 μg/dl blood in these rats, any interindividual differences in the capacity of the erythrocytes to bind lead would be expected to be manifest at blood lead concentrations approaching and exceeding this level.

It is also entirely possible that erythrocyte or other tissue binding parameters may change with prolonged exposure to lead. Kidney lead in rats during continuous lead exposure is both dose- and time-dependent (Goyer *et al.*, 1970; O'Flaherty *et al.*, 1986). The explanation for the complex pattern of kidney lead accumulation in rats is not known, but it may involve lead binding to specific proteins. High-affinity, low-molecular-weight lead-binding proteins have been identified in both kidney and brain of rats (Mistry *et al.*, 1985; DuVal and Fowler, 1989). The model presented here does not incorporate age, dose rate, or time dependence of lead accumulation by the kidney, and it does not predict kidney lead satisfactorily. Relative to whole-body lead economy, this deficiency is inconsequential. However, to model kidney lead, and especially biologically available kidney lead, will require a much fuller understanding of the age, sex, dose rate, and time dependence of specific lead binding in the kidney than we now have.

While inclusion in the model of a small, rapidly exchanging surface bone volume is required by observations of bone uptake and loss of radiolabeled bone-seeking elements, the model is relatively insensitive to the size of this rapidly exchanging pool. Data from Bronner and Aubert (1965) may be used to calculate that rapidly exchangeable calcium is about 1% of total skeletal calcium in mature rats. This estimate of the size of the exchangeable calcium pool includes soft-tissue calcium, so that it represents an upper limit on the percentage bone volume that exchanges calcium rapidly with plasma. The model is not sensitive to variations in size of the rapidly exchanging bone volume in this range.

The values of four parameters were optimized in order to increase the descriptive accuracy of the model. These were the two parameters (BIND and KBIND) governing partitioning between plasma and erythrocytes, the fractional clearance of lead from plasma into mineralizing bone (LEAD), and the restricted permeability coefficient for plasma-to-bone transfer of lead (PO) (Table 2). Of these, LEAD is the only hypothetical parameter in the model. It is not known whether incorporation of lead into mineralizing bone actually has the characteristics of a clearance. However, this is the simplest kinetically reasonable description of the process. Many physiologically reasonable refinements to this and other components of the model can be conceived, and some of these—for example, variations in the form of the age dependence of fractional bone formation rate—were considered. Accuracy of model predictions was not materially improved by any of the refinements investigated.

The model as presently constituted appears to account for the principal physiologic, metabolic, and physicochemical processes that govern disposition of bone-seeking elements in growing rats. It consists of the simplest reasonable description of the minimum number of processes required by an understanding of bone growth and metabolism and by experimental data from studies of calcium and lead disposition. The magnitudes of the processes that mediate the movement of lead to and from bone are dependent on age. The age at which exposure occurs determines the kind and amount of bone metabolic activity, which in turn determines the amount of lead taken up by the bone. The bone is both a lead storage tissue and a source of lead. Whether it serves principally as one or the other at any particular time depends largely on age and on the pattern of lead exposure. A physiologically based model, with inclusion of a realistic description of bone metabolism, is capable of providing insight into the complex balances among absorption, excretion, and transfers of lead between plasma and bone.

APPENDIX

General features of the model. The concentration of lead in blood (CB, mg/liter blood) is related to the concentration of lead in plasma (CBP, mg/liter plasma) by the expression

$$CB = 0.55\ CBP + 0.45\ CBP\left(1 + \frac{BIND}{KBIND + CBP}\right),$$

where BIND is the maximum capacity of the erythrocytes to bind lead (mg/liter) and KBIND is the half-saturation constant (mg lead/liter) (Table 2), optimized based on data from the chronic study with continuous exposure.

A three-parameter expression for body weight as a function of age and of weight at sexual maturity has been devised:

$$WBODY = 0.005 + \frac{WADULT(e^{AGE} - 1)}{(e^{HALF} + e^{AGE} - 1))} + (CONST)(AGE),$$

where WBODY is body weight (kg) at age AGE (months), 0.005 is body weight at birth, and HALF is the age in months at which half the weight WADULT of the young mature animal is reached. WADULT is usually found to be the body weight at about age 4 months. The term (CONST) (AGE) defines the persistent growth of male rats after sexual maturity. The same expression, with a smaller value of CONST or with CONST = 0, describes the growth of female rats.

Because adult body weight is a feature of the expression for body weight, organ and tissue weights can be linked to body weight *and* to degree of maturity. Thus, liver and kidney volumes (liters) are defined as

$$VL = 0.04\ (WADULT)\left(\frac{WBODY^{0.73}}{WADULT}\right)$$

and

$$VK = 0.0[illegible]\ (WADULT)\left(\frac{WBODY^{0.67}}{WADULT}\right)$$

The values of the exponents are taken from Trieb *et al.* (1976).

Total well-perfused tissue volume (liters) is

$$VWT = 0.1\ (WADULT)\left(\frac{WBODY^{0.7}}{WADULT}\right),$$

and the volume of well-perfused tissues other than liver and kidney is calculated by difference.

The volume of poorly perfused tissues other than the bone is also calculated by difference, as

$$VPT = WBODY - VWT - VBONE,$$

where VBONE is bone volume (liters),

$$VBONE = 0.0289\ (WBODY)^{1.02}.$$

Two-tenths of one percent (0.002) of VBONE is assigned to a surface compartment of volume VS whose lead content exchanges sufficiently rapidly with plasma lead that the two can be considered to be in equilibrium. This is the rapidly exchanging compartment of bone mineral.

VBONE is the outcome of continuous, age-dependent processes of bone formation and resorption. The net rate of change of bone volume, RVBONE (liters/day), is

$$RVBONE = dVBONE/dt.$$

The fractional bone formation rate FBFR (1/day) is

$$FBFR = MINFORM + (ALPHAO) \times (e^{-(ALPHA \times AGE)}) + (BETAO)(e^{-(BETA \times AGE)}),$$

and the fractional bone resorption rate FBRR is

$$FBRR = ((FBFR)(VBONE) - RVBONE)/VBONE,$$

where AGE is in days and the constants BETA and BETAO are linked to HALF and to WADULT (Table 1).

Cardiac output depends on body weight. Cardiac blood output in the adult (liters/day) is modeled as

$$QC = (QCC)(WADULT)^{0.74},$$

where QCC = 340 liters/day/kg body wt (Holt *et al.*, 1968; Ramsey and Andersen, 1984).

Cardiac output in the growing rat (liters/day) is

$$QCG = (QC)\left(\frac{WBODY}{WADULT}\right)^{0.67}.$$

Of the cardiac output, 0.25 goes to the liver, 0.17 to the kidney, 0.44 to other well-perfused tissues, 0.03 to bone, and 0.11 to other poorly perfused tissues. These fractions are invariant with body weight.

Absorption and excretion of lead. The drop in fractional absorption FRACT of lead from the gastrointestinal tract that occurs after weaning is modeled as a first-order decline to the adult value,

$$FRACT = (0.01)(1. + (1100)(e^{-(0.2)(AGE)}),$$

where AGE is in days and fractional absorption from the diet in the adult rat is 0.01.

Elimination of lead is considered to be 91% via the liver and 9% via the kidney (Aungst *et al.*, 1981; Gregus and Klaasen, 1986). Elimination is modeled as a function of maturity, depending on body weight in the way that cardiac output does;

$$QE = (QEC)(WADULT)^{0.74},$$

where QE is total elimination clearance from plasma (liters/day) in the adult rat, and QEC is 14 liters/day/kg body wt. Total elimination clearance from the blood of the growing rat (liters/day) is

$$QEG = (QE)\left(\frac{WBODY}{WADULT}\right)^{0.67}.$$

No dose rate dependence of excretion is built into the model.

Exchange of lead with tissues other than bone. Lead in plasma leaving soft tissues is assumed to be in equilibrium with lead in the tissue. Thus, for tissue i, the rate of change (mg/day) of the amount of lead in the tissue is

$$RAi = (Qi)(CB - CBi),$$

where CBi is the concentration of lead (mg/liter) in venous blood leaving the tissue and Qi is the blood flow rate through the tissue. The expressions for liver and kidney include additional terms representing absorption and excretion of lead. The amount Ai of lead (mg) in the tissue is given by the integral of RAi, and the concentration of lead in the tissue is Ai/Vi, where Vi is tissue volume (liters). The equation is anchored by the requirement that CBPi, the concentration of lead in plasma leaving the tissue, is in equilibrium with lead in the tissue,

$$CBPi = Ai/((Vi)(Pi)),$$

where Pi is the ratio of tissue lead concentration to plasma lead concentration at equilibrium (Table 2), optimized based on data from the chronic study with continuous exposure.

Exchange of lead with bone. Blood entering the bone first traverses the volume VS of rapid surface exchange. Lead in this region is in equilibrium with lead in plasma leaving the region, so that CBPS, the concentration of lead in blood plasma leaving the surface exchange region of bone, is:

$$CBPS = (CS)(VBONE/((WSKEL)(PB))),$$

where CS is the concentration (mg/liter) of lead in surface volume VS and the partition coefficient PB has been determined experimentally for skeletal tissue rather than for bone (Table 2). The concentration (mg/liter) of lead in blood leaving the surface exchange region, CBS, is obtained from CBPS by the equation relating blood lead to plasma lead.

Lead enters the metabolically active region at a rate RABS (mg/day),

$$RABS = (CBS)(QB),$$

where QB is the flow rate (liters/day) of blood through bone.

In the metabolically active region, lead is removed from the blood at a rate RDBone (mg/day),

RDBone

$$= (LEAD)(FBFR)(VBONE)(CBPS),$$

where the value of the proportionality constant LEAD (Table 2) was established empirically by obtaining the best visual fit of predicted to observed blood and bone lead concentrations from the chronic study with continuous lead exposure. Lead is also added to the blood in the metabolically active region, at a rate RRBone (mg/day),

$$RRBone = (FBRR)(VBONE)(CBoneAv),$$

where CBoneAv is the average concentration (mg/liter) of lead in bone, excluding surface region bone. Thus, the concentration (mg/liter) of lead in blood leaving the metabolically active region of bone is

$$CBM = CBS + (RRBone - RDBone)/QB,$$

and the rate (mg/day) at which lead leaves the metabolically active region and enters the diffusion region is

$$RABM = (CBM)(QB).$$

The diffusion region of bone is the total bone volume with the exception of the rapidly exchanging surface region. It is considered to be composed of units of concentric cylindrical shells. Within each shell, lead is homogeneously distributed; but it diffuses between shells and between canalicular fluid and the innermost shell, shell 1. The net rate (mg/day) of change by diffusion of the amount of lead in fluid perfusing the diffusion region is

$$RABD = (S)(L)(VBONE - VS)((R)(CBone1) - (P)(CBPM))/1000,$$

where CBone1 is the concentration of lead in shell 1. In this expression, the concentration of lead in fluid passing through the canalicules is taken to be the same as its concentration CBPM (mg/liter) in blood plasma leaving the metabolically active region. S is the specific canalicular surface area (cm^2/cm of canalicule length), and L is the total canalicule length per liter of bone volume (cm/liter) (Table 1). R is the permeability constant for diffusion from bone to canalicule fluid (cm/day), and P is the permeability constant for diffusion from canalicule fluid to bone (cm/day). For movement of lead by diffusion within bone, P and R are replaced by D, the diffusion constant (cm/day). D, P, and R are inversely proportional to bone density:

$$D = DO/DBONE,$$

$$P = PO/PBONE,$$

$$R = RO/DBONE.$$

The values of DO, PO, and RO are given in Table 2. The value of PO was visually optimized based on data from the short-term study.

The net rate (mg/day) of change by diffusion of the amount of lead in shell 1 is

$$RABone1(diff) = [(S)(L)(VBONE - VS)((P)(CBPM) - (R)(CBone1)) - (D)(S1)(L)(VBONE - VS)(CBone1 - CBone2)]/1000,$$

where CBonei is the concentration of lead in shell i (mg/liter) and Si is the specific outer surface area (cm^2/cm of canalicule length) of shell i.

The rate of deposition of lead during formation and secondary mineralization must be added to the rate of change by diffusion of the amount of lead in each shell, and the rate of loss of lead by resorption must be subtracted from it in order to obtain the net rate of change of total lead in each shell of non-surface-region bone. The amount of lead (mg) in each shell is given by the integral of the appropriate rate expression, and the concentration is obtained by dividing by the volume of the shell. Thus, for shell 1, for example, the net rate of change of total lead is

$$RABone1 = RABone1(diff) + (F1)(RDBone) - (F1)(FBRR)(VBONE - VS)(CBone1),$$

where F1 is the volume fraction of non-surface-region bone occupied by shell 1. CBone1

is the integral of this expression divided by the term (F1) (VBONE-VS), and

$$\text{CBoneAv} = \sum_{i=1}^{8} (\text{Fi})(\text{CBonei}).$$

The concentration (mg/liters) of lead in blood leaving the diffusion region of bone—that is, leaving the bone—is

$$\text{CBB} = \text{CBM} + \text{RABD/QB},$$

and the rate at which lead leaves the bone and returns to the systemic circulation is

$$\text{RAB} = (\text{CBB})(\text{QB}).$$

REFERENCES

AUBERT, J.-P., AND MILHAUD, G. (1960). Methode de mesure des principales voies du metabolisme calcique chez l'homme. *Biochim. Biophys. Acta* 39, 122–139.

AUNGST, B. J., DOLCE, J. A., AND FUNG, H. -L. (1981). The effect of dose on the disposition of lead in rats after intravenous and oral administration. *Toxicol. Appl. Pharmacol.* 81, 48–57.

BARER, M., AND JOWSEY, J. (1967). Bone formation and resorption in normal human rib. *Clin. Orthoped.* 52, 241–247.

BARLTROP, D., AND MEEK, F. (1975). Absorption of different lead compounds. *Postgrad. Med. J.* 51, 805–809.

BARRY, P. S. I. (1975). A comparison of concentrations of lead in human tissues. *Br. J. Industr. Med.* 32, 119–139.

BAUD, C. A. (1962). Morphologie et structure inframicroscopique des osteocytes. *Acta Anat.* 51, 209–225.

BAUER, G. C. H. (1954). Rate of bone salt formation in a healing fracture determined in rats by means of radiocalcium. *Acta. Orthoped. Scand.* 23, 169–191.

BAUER, G. C. H., CARLSSON, A., AND LINDQUIST, B. (1955). A comparative study on the metabolism of Sr^{90} and Ca^{45}. *Acta Physiol. Scand.* 35, 56–66.

BAUER, G. C. H., CARLSSON, A., AND LINDQUIST, B. (1956). A comparative study on the metabolism of ^{140}Ba and ^{45}Ca in rats. *Biochem. J.* 63, 535–542.

BAUER, G. C. H., CARLSSON, A., AND LINDQUIST, B. (1961). Metabolism and homeostatic function of bone. In *Mineral Metabolism* (C. L. Comar and F. Bronner, Eds.), Vol. 1, Part B, pp. 607–676. Academic Press, New York.

BAUER, G. C. H., AND SHTACHER, G. (1968). Incorporation and release of ^{85}Sr and ^{14}C-proline–hydroxyproline in mineral and collagen of bone and incisor teeth of growing rats. *Calcif. Tissue Res.* 2, 106–110.

BAYLINK, D., STAUFFER, M., WERGEDAL, J., AND RICH, C. (1970). Formation, mineralization, and resorption of bone in vitamin D-deficient rats. *J. Clin. Invest.* 49, 1122–1134.

BAYLINK, D. J., AND WERGEDAL, J. E. (1971). Bone formation by osteocytes. *Am. J. Physiol.* 221, 669–678.

BRONNER, F. (1964). Dynamics and Function of Calcium. In *Mineral Metabolism*. (C. L. Comar and F. Bronner, Eds.), Chap. 120, Vol. 2A, pp. 341–444. Academic Press, New York.

BRONNER, F., AND AUBERT, J.-P. (1965). Bone metabolism and regulation of the blood calcium level in rats. *Am. J. Physiol.* 209, 887–890.

BRONNER, F., AND LEMAIRE, R. (1969). Comparison of calcium kinetics in man and the rat. *Calcif. Tissue Res.* 3, 238–248.

CONRAD, M. E., AND BARTON, J. C. (1978). Factors affecting the absorption and excretion of lead in the rat. *Gastroenterology* 74, 731–740.

DUVAL, G., AND FOWLER, B. A. (1989). Preliminary purification and characterization studies of a low molecular weight, high affinity cytosolic lead-binding protein in rat brain. *Biochem. Biophys. Res. Commun.* 159, 177–184.

GOYER, R. A., LEONARD, D. L., MOORE, J. F., RHYNE, B., AND KRIGMAN, M. R. (1970). Lead dosage and the role of the intranuclear inclusion body. *Arch. Environ. Health* 20, 705–711.

GREGUS, Z., AND KLAASSEN, C. D. (1986). Disposition of metals in rats: A comparative study of fecal, urinary, and biliary excretion and tissue distribution of eighteen metals. *Toxicol. Appl. Pharmacol.* 85, 24–38.

GROER, P. G., AND MARSHALL, J. H. (1973). Mechanism of calcium exchange at bone surfaces. *Calcif. Tissue Res.* 12, 175–192.

HOLT, J. P., RHODE, E. A., AND KINES, H. (1968). Ventricular volumes and body weight in mammals. *Am. J. Physiol.* 215, 704–715.

JOWSEY, J., LAFFERTY, W., AND RABINOWITZ, J. (1965a). Analysis of distribution of Ca^{45} in dog bone by a quantitative autoradiographic method. *J. Bone Jt. Surg.* 47A, 359–370.

JOWSEY, J., KELLY, P. J., RIGGS, B. L., BIANCO, A. J., SCHOLZ, D. A., AND GERSHON-COHEN, J. (1965b). Quantitative microradiographic studies of normal and osteoporotic bone. *J. Bone. Jt. Surg.* 47A, 785–806.

KLAASSEN, C. D., AND SHOEMAN, D. W. (1974). Biliary excretion of lead in rats, rabbits and dogs. *Toxicol. Appl. Pharmacol.* 29, 434–446.

KOSTIAL, K., KELLO, D., JUGO, S., RABAR, I., AND MALJKOVIC, T. (1978). Influence of age on metal metabolism and toxicity. *Environ. Health Perspect.* 25, 81–86.

KOSTIAL, K., AND KELLO, D. (1979). Bioavailability of lead in rats fed "human" diets. *Bull. Environ. Contam. Toxicol.* 21, 312–314.

E, W. R., MARSHALL, J. H., AND SISSONS, H. A. (1965). Calcium accretion and bone formation in dogs. An experimental comparison between the results of Ca^{45} kinetic analysis and tetracycline labelling. *J. Bone. Jt. Surg.* 47B, 157–180.

MACDONALD, N. S., EZMERLIAN, F., SPAIN, P., AND MCARTHUR, C. (1951). The ultimate site of skeletal deposition of strontium and lead. *J. Biol. Chem.* 189, 387–399.

MARSHALL, J. H., ROWLAND, R. E., AND JOWSEY, J. (1959). Microscopic metabolism of calcium in bone. V. The paradox of diffuse activity and long-term exchange. *Radiation Res.* 11, 258–270.

MARSHALL, J. H. (1969). Measurements and models of skeletal metabolism. In *Mineral Metabolism: An Advanced Treatise* C. L. Comar and F. Bronner, Eds.), Vol. 3, pp. 1–122. Academic Press, San Diego.

MARSHALL, J. H., AND ONKELINX, C. (1968). Radial diffusion and power function retention of alkaline earth radioisotopes in adult bone. *Nature* 217, 742–743.

MCMAHON, T. A., AND BONNER, J. T. (1983). *On Size and Life*, pp. 51–57. Scientific American Books, New York.

MISTRY, P., LUCIER, G. W., AND FOWLER, B. A. (1985). High-affinity lead binding proteins in rat kidney cytosol mediate cell-free nuclear translocation of lead. *J. Pharmacol. Exp. Ther.* 232, 462–469.

O'FLAHERTY, E. J., ADAMS, W. D., HAMMOND, P. B., AND TAYLOR, E. (1986). Resistance of the rat to development of lead-induced renal functional deficits. *J. Toxicol. Environ. Health* 18, 61–75.

O'FLAHERTY, E. J. (1991). Physiologically based models for bone-seeking elements. I. Rat skeletal and bone growth. *Toxicol. Appl. Pharmacol.* 111, 299–312.

O'FLAHERTY, E. J., SCOTT, W., SCHREINER, C., AND BELILES, R. P. (1990). A physiologically based model of rat and mouse gestation: Disposition of a weak acid. Submitted for publication.

RAMAN, A. (1969). Appositional growth rate in rat bones using the tetracycline labelling method. *Acta Orthop. Scand.* 40, 193–197.

RAMSEY, J. C., AND ANDERSEN, M. E. (1984). A physiologically based description of the inhalation pharmacokinetics of styrene in rats and humans. *Toxicol. Appl. Pharmacol.* 73, 159–175.

ROWLAND, R. E. (1960). The deposition and the removal of radium in bone by a long-term exchange process. *Clin. Orthop.* 17, 146–153.

ROWLAND, R. E. (1961). Microscopic metabolism of Ra^{226} in canine bone and its bearing on the radiation dosimetry of internally deposited alkaline earths. *Radiat. Res.* 15, 126–137.

ROWLAND, R. E. (1963). Some aspects of human bone metabolism deduced from studies of radium cases. *Clin. Orthop.* 28, 193–203.

ROWLAND, R. E. (1966). Exchangeable bone calcium. *Clin. Orthop.* 49, 233–248.

ROWLAND, R. E., AND MARSHALL, J. H. (1959). Radium in human bone: The dose in microscopic volumes of bone. *Radiat. Res.* 11, 299–313.

SCHMIDT-NIELSEN, K. (1972). *How Animals Work* pp. 88–89. Cambridge Univ. Press, Cambridge.

SCHMIDT-NIELSEN, K. (1984). *Scaling: Why Is Animal Size So Important?* Cambridge Univ. Press, Cambridge.

SCHNITZER, J. E., MCKINSTRY, P., LIGHT, T. R., AND OGDEN, J. A. (1982). Quantitation of regional chondrooseus circulation in canine tibia and femur. *Am. J. Physiol.* 282, H365–H375.

SHIMMINS, J., AND SMITH, D. A. (1966). Estimation of bone mineral transfer rate by the measurement of long-term retention of Sr^{85}. *Metabolism* 15, 436–443.

SONTAG, W. (1980). An automatic microspectrophotometric scanning method for the measurement of bone formation rates *in vivo*. *Calcif. Tiss. Int.* 32, 63–68.

SONTAG, W. (1985). The pattern of calcium deposition in rat bone as demonstrated by calcein labeling. In *Metals in Bone* (N. D. Priest, Ed.), Chapter 3. MTP Press for the Commission of the European Communities, Hingham, MA.

SONTAG, W. (1986a). Quantitative measurements of periosteal and cortical–endosteal bone formation and resorption in the midshaft of female rat femur. *Bone* 7, 55–62.

SONTAG, W. (1986b). Quantitative measurements of periosteal and cortical–endosteal bone formation and resorption in the midshaft of male rat femur. *Bone* 7, 63–70.

TOTHILL, P., AND HOOPER, G. (1984). Bone blood flow and extraction ratios: microspheres and bone seekers. In *Bone Circulation* (J. Arlet, R. P. Ficat, and D. S. Hungerford, Eds.), pp. 171–174. Williams and Wilkins, Baltimore.

TOTHILL, P., HOOPER, G., MCCARTHY, I. D., AND HUGHES, S. P. F. (1985). The variation with flow-rate of the extraction of bone-seeking tracers in recirculation experiments. In *Metals in Bone* (N. D. Priest, Ed.), pp. 363–372. MTP Press for the Commission of the European Communities, Hingham, MA.

TRIEB, G., PAPPRITZ, G., AND LUTZEN, L. (1976). Allometric analysis of organ weights. *I. Rats. Toxicol. Appl. Pharmacol.* 35, 531–542.

U.S. EPA (1986). *Air Quality Criteria for Lead.* EPA 600/8-83-028 F, June 1986. Environmental Criteria and Assessment Office, Research Triangle Park, NC.

VANDER, A. J., TAYLOR, D. L., KALITIS, K., MOUW, D. R., AND VICTERY, W. (1977). Renal handling of lead in dogs: Clearance studies. *Am. J. Physiol.* 233, F532–538.

WEIKEL, J. H., AND NEUMAN, W. F. (1961). Incorporation of dietary radiocalcium into skeleton of rats. *Metab. Clin. Exp.* 10, 83–90.

M. Langer

TOXICOLOGY AND APPLIED PHARMACOLOGY 111, 332–341 (1991)

Physiologically Based Models for Bone-Seeking Elements

III. Human Skeletal and Bone Growth[1]

ELLEN J. O'FLAHERTY

Department of Environmental Health, University of Cincinnati College of Medicine, 3223 Eden Avenue, Cincinnati, Ohio 45267-0056

Received October 25, 1990; accepted August 25, 1991

Physiologically Based Models for Bone-Seeking Elements. III. Human Skeletal and Bone Growth. O'FLAHERTY, E. J. (1991). *Toxicol. Appl. Pharmacol.* 111, 332–341. A model of skeletal and bone growth for the human from birth to maturity has been developed. Dry and hydrated bone, bone marrow, ash, and calcium are included in the model. Growth of the skeleton and its fractions is expressed as a set of allometric equations relating fraction volume or weight to body weight. Blood flow rates to mature bone and bone marrow are scaled from experimentally determined values in smaller animals, but bone and marrow volumes and growth patterns cannot be scaled directly from measurements or models in small animals. The growth model compares well with measured bone weights, ash weights, and bone and skeletal densities in humans. Its form is adaptable to physiologically based description of the kinetics of bone-seeking elements. © 1991 Academic Press, Inc.

Development of physiologically based models of the kinetics of agents that persist in the body for long periods of time requires an understanding of the dependence on growth, maturation, and aging of the anatomic and physiologic parameters that define the model. For bone-seeking elements, the skeleton is the chief determinant of whole-body kinetic behavior. A model of skeletal growth and metabolism in the rat has been developed (O'Flaherty, 1991a,b). However, the skeletons of small, short-lived animals differ in critical anatomic and metabolic respects from the skeletons of larger, longer-lived animals such as humans. The bones of small animals are known to be relatively more slender than the bones of large animals (Schmidt-Nielsen, 1972), so that conventional allometric techniques cannot be used to scale bone or skeletal volumes across species of widely varying body weights. In addition, structural remodeling of mature bone to relieve local stresses in response to changing demands on the skeleton, and to insure an adequate supply of nutrients throughout the bone volume, is an important feature of bone metabolism in large animals. Remodeling does not take place to any significant extent in cortical bone of small, short-lived animals. Therefore, mature bone metabolism is quantitatively different in small and large animals.

The purpose of this paper is to set forth a model of body and bone growth for the human from birth to maturity.

[1] This work was supported by U.S. Public Health Service Grant ES04125. Portions of it were presented at the Seventeenth Conference on Toxicology cosponsored by the U.S. Air Force Armstrong Aerospace Medical Research Laboratory and the U.S. Naval Medical Research Institute, November 1987 (O'Flaherty, 1988).

0041-008X/91 $3.00
Copyright © 1991 by Academic Press, Inc.
All rights of reproduction in any form reserved.

METHODS AND RESULTS

Cortical and Trabecular Bone

The skeleton is frequently visualized as made up of cortical and trabecular bone (O'Flaherty, 1991a). While cortical and trabecular bone are structurally distinct and have different physical properties, they are essentially identical chemically. In addition, bone tissue is virtually the same across species. Mature bone tissue may be considered to be composed of 70% dry bone, 25.5% water, and 4.5% volatile inorganic fractions by volume and to have a density of 1.92 g/cm^3 (O'Flaherty, 1991a, Table [illegible]).

It is convenient to compartmentalize the skeleton into cortical and trabecular bone because blood flow to the two regions is quite different: modeling total blood flow requires an assumption about the fraction of the skeleton occupied by each bone type. In addition, since blood flow rate to bone is correlated with the magnitude of bone formation (and resorption), it may be supposed that the residence time of bone-seeking elements is shorter in regions of high blood flow rate than in regions of lower blood flow rate. The premise that the skeleton is composed of 80% cortical bone and 20% trabecular bone is based on two studies. In one, Gong *et al.* (1964) dissected a single 11.5-kg male beagle, cleaned and separated the bones into trabecular and cortical tissue, and recorded the amounts of trabecular and cortical ash from each bone and from the whole skeleton. Trabecular bone accounted for 17% of the total weight of ash, cortical bone for 83%. In the second study, Johnson (1964) estimated the percentages of trabecular and cortical tissue in human bones by morphologic analysis. With the notable exceptions of vertebra and perhaps fibula, his estimates are closely comparable to the values reported by Gong *et al.*, which were calculated by weight of ash rather than by weight of whole bone. Reference Man (ICRP, 1975) is based on Johnson's estimates. His bone is 20% trabecular and 80% cortical by wet weight.

The Mature Skeleton

Direct measurements of bone and marrow mass or volume in human skeletons are few and are not representative of healthy adults (Mechanik, 1926). However, there are many published studies of porosity and density of whole human bones. From these data, skeletal density can be calculated. Taken together with the model mean bone density of 1.92 g/cm^3, skeletal density allows estimation of the fractional volumes and weights of the skeleton that are occupied by bone and by bone marrow.

Bone porosity is generally measured as apparent density/real density, where

$$\text{apparent density} = \frac{\text{weight of marrow-free bone}}{\text{volume of skeletal sample}}$$

and

$$\text{real density} = \frac{\text{weight of marrow-free bone}}{\text{volume of marrow-free bone}}.$$

Skeletal density can be calculated from porosity measurements together with the densities of marrow-free bone and bone marrow, from apparent density measurements together with the densities of marrow-free bone and bone marrow, or from bone ash weight per unit skeletal volume together with the ash weight of marrow-free bone.

Human vertebral (largely trabecular) whole bone has been reported to be about 12% bone with a mean density of 1.85 g/cm^3 (Galante *et al.*, 1970). If marrow density is 1.0 g/cm^3, the corresponding whole bone density would be 1.10 g/cm^3. Ash weights of lumbar vertebrae from mature men and women have been reported between 0.15–0.25 g/cm^3 (Weaver and Chalmers, 1966; Bartley *et al.*, 1966; Mueller *et al.*, 1966; Bell *et al.*, 1967). If the marrow fraction contributes nothing to skel-

TABLE 1

THE MATURE HUMAN SKELETON, DEFINED AS MARROW-FREE BONE PLUS MARROW

	Marrow free bone	Marrow	Skeleton (without cartilage)
Weight, g/100 g body wt	7.15	5.00	12.15
Volume, cm^3/100 g body wt	3.72	5.00	8.72
Density, g/cm^3	1.92	1.00	1.39
Weight, g/g skeleton	0.588	0.412	—
Volume, cm^3/cm^3 skeleton	0.427	0.573	—

etal ash weight (Dietz, 1944), then this range of ash weights corresponds to porosities of 14–24% and densities of 1.13–1.22 g/cm^3.

Direct determination of skeletal density of lumbar vertebrae, using a photon scattering technique, gave values between 1.10 and 1.30 g/cm^3 for 11 human subjects (Garnett *et al.*, 1973), in good agreement with the indirect estimates for trabecular bone. Measurement of lumbar vertebral density by a displacement technique, with marrow replaced by water, gave values of 1.09–1.17 g/cm^3 (Mueller *et al.*, 1966).

With the inclusion of bones other than the lumbar vertebra, this range of densities is extended upward. Trotter *et al.* (1960) determined apparent densities, as dry marrow-free bone weight/volume of skeletal sample, for a variety of bones from humans 25–100 years old. Apparent densities ranged from 0.3–0.9 g/cm^3 and approached 1.0 g/cm^3 in a few samples, being lowest for thoracic and lumbar vertebra and sacrum, intermediate for cervical vertebra, and highest for ulna, radius, tibia, femur, rib, and humerus. If the density of dry marrow-free bone is 2.28 g/cm^3 (O'Flaherty, 1991a, Table 2), this range of apparent densities corresponds to porosities of 13–42% and to skeletal densities of 1.17–1.53 g/cm^3. The lower end of this range is, of course, associated with trabecular bone and the upper end with cortical bone.

Recorded values for the fraction of the adult human body occupied by the skeleton vary widely, depending largely on what has been included in the skeleton by different investigators. For example, skeletal weight in an adult white female was reported to be 20.3% of body weight as wet skeleton with soft tissues attached, 7.6% as wet skeleton without soft tissues, and 6.5% as dry fat-free skeleton (Moore *et al.*, 1968).

Reference Man has a total skeletal weight of 10 kg, or 14.3% of body weight. This figure is based on the work of Forbes, Mitchell, and their co-workers (Mitchell *et al.*, 1945; Forbes *et al.*, 1953, 1956), among others. The mean ash content of the four adult male human skeletons examined by Forbes' group was 0.2796 ± 0.0125 g/g. If the ash content of marrow-free bone is taken to be 0.564 g/g (O'Flaherty, 1991a, Table 2), then these skeletons would be expected to contain a mean of 0.2796/0.564 = 0.496 g of marrow-free bone/g skeleton. The actual mean measured marrow-free bone weight was 0.4924 g/g skeleton.

Based on the model marrow-free bone, a skeleton consisting of 5000 g marrow-free bone would contain 2820 g ash, 1320 g organic and 200 g volatile inorganic material, and 660 g bone water, along with cartilage and bone marrow. Direct estimates of the marrow volume of the adult skeleton give values around 4–5% of body weight (Mechanik, 1926). Reference Man, with 5000 g of marrow-free bone, has 3000 g of marrow. The model of the mature human skeleton in Table 1 contains 3500 g of marrow, or 5% of a 70-kg body wt.

While essentially all the marrow of the human newborn is red or hematopoietic, red

arrow in the distal skeleton is gradually replaced by yellow or fatty marrow, starting peph y and moving toward the axial sketon. By adulthood, human limb bones conin little red marrow except at the proximal nds of the femur and humerus, while marrow om the axial skeleton is about 75% red (Ellis, 961). Total marrow has been estimated to be 0–50% red marrow in the adult human (Ellis, 961; ICRP, 1975). However, under hemaopoietic stimuli, yellow marrow may be ansformed to red marrow and become hematopoietically active again, even in adult life. iven the variety of influences—age, location ithin bone, and hematopoietic requirenents—that affect partitioning of marrow beween the red and yellow forms, it is not surrising that reported percentages of red and ellow marrow vary widely among individuals.

The Growing Skeleton

Construction of a model of the growing human skeleton is facilitated by the availability of a good data base giving measurements of otal skeletal volume, marrow volume, and nar -free dry bone weight in human fetuses and newborns, and by the finding that allonetric scaling with body weight provides a good description of the growth of skeletal components in the rat (O'Flaherty, 1991a). With a reliable starting point for the newborn and the model of the adult human skeleton, t is reasonable to scale skeletal growth allometrically during growth to maturity.

Trotter and Peterson (1968, 1969a,b) examined a large series of 124 skeletons of human fetuses of gestational age 16–43 weeks. They devised equations relating the weight of the dry, marrow-free skeleton to body weight. From these equations, it can be calculated that dry marrow-free bone weight is 100–105 g in a 3500-g newborn of either sex, or about 3% of body weight. Hudson (1965) also measured dry marrow-free bone weight in 16 human fetuses and newborns weighing 1.3–3.7 kg. For the four infants whose estimated gestational age was 40 or more weeks, the mean weight of the dry fat-free skeleton was 2.96 ± 0.17% of body weight. Marrow and total skeletal volumes were determined in the same series of human fetuses and newborns. Mean skeletal volume (in ml) in the four full-term fetuses was 3.38 ± 0.17% of body weight (in g), and mean marrow volume (in ml) was 1.25 ± 0.07% of body weight.

Estimates of density of either the whole skeleton or the marrow-free skeleton of the newborn were not found in the literature. However, marrow-free bone can be modeled with reasonable assurance by taking advantage of the reliability of measurements of calcium content of whole bone ash and calcium content of dry marrow-free bone to fix the ash content of marrow-free bone of the newborn.

The calcium content of femoral trabecular bone ash from a child less than 2 years old was 0.379 g/g; of femoral cortical bone ash from the same child, it was 0.385 g/g (Dyson and Whitehouse, 1968). In eight samples of femoral and tibial bone from six fetuses weighing 3050–4150 g, Swanson and Iob (1937) found a mean of 0.394 Ca/g ash. These values are essentially identical to the values for adults.

The calcium content of dry marrow-free newborn human bone has been determined by a number of investigators. In trabecular rib from 11 infants aged 3–22 months, it was 0.2439 ± 0.115 g/g (Baker *et al.*, 1946); in skull bone from eight fetuses of gestational age 40 or more weeks, it was 0.2455 ± 0.0026 g/g (MacDonald, 1954); in femoral cortex from six pools of neonatal bone, it was 0.2436 ± 0.0059 (Quelch *et al.*, 1983). Together with other assays, these fix the calcium content of the dry marrow-free bone at 0.24 g/g, slightly lower than the value in adults.

If calcium is 24% of dry marrow-free bone and 38% of bone ash at birth, then ash is 63% by weight of dry marrow-free bone. As in smaller animals, the organic volume fraction of bone is essentially constant with age

(Mueller *et al.*, 1966), while ash and water volumes are inversely related (Arnold, 1960). Therefore, the volume fraction of organic plus volatile inorganic material in marrow-free bone at birth can be assumed to be 0.395, as it is in adulthood (O'Flaherty, 1991a, Table 2). Based on these assumptions and the skeletal weights and volumes from Hudson (1965), the cartilage-free skeleton of the full-term human infant can be constructed. It consists of 75.2% by weight of marrow-free bone with a density of 1.79 g/cm^3 and 24.8% by weight of marrow, for a cartilage-free skeletal density of 1.50 g/cm^3.

Allometric equations for scaling skeletal fractions from the newborn to the adult are given in Table 2, and the equations for bone, marrow, and skeletal weight are illustrated in Fig. 1. These equations were arrived at simply by scaling allometrically between the components of the newborn skeleton and those of the adult skeleton. Combined with the growth curves for Reference Man, the equation describing the dependence of marrow- and cartilage-free skeletal weight on body weight reproduces Trotter and Peterson's (1978) data for weights of 150 skeletons from males and females 23 days–22 years old.

There is some indication that in humans, fatty or yellow marrow begins to replace red marrow even before birth, but quantitatively such replacement is minimal (Emery and Follett, 1964). In view of the limited number of observations on the nature and amount of human bone marrow as well as the readiness with which marrow can be transformed between red and yellow fractions, it is reasonable to model the makeup of human bone marrow during growth as a linear shift from 100% red marrow by weight in the newborn to 50% red marrow by weight in the adult (Ellis, 1961).

TABLE 2

THE DEPENDENCE OF THE GROWING HUMAN SKELETON AND ITS FRACTIONS ON BODY WEIGHT

Skeletal weight, g = 58.0 (BW, kg$^{1.21}$)[a]
Marrow weight, g = 7.02 (BW, kg$^{1.46}$)
Marrow- and cartilage-free dry bone weight, g = 22.6 (BW, kg$^{1.23}$)
Marrow- and cartilage-free bone weight, g = 29.0 (BW, kg$^{1.21}$)
Ash weight of marrow- and cartilage-free bone, g = 13.8 (BW, kg$^{1.25}$)
Marrow- and cartilage-free bone volume, cm^3 = 16.8 (BW, kg$^{1.188}$)
Bone calcium, g = 5.24 (BW, kg$^{1.25}$)

[a] BW, body weight.

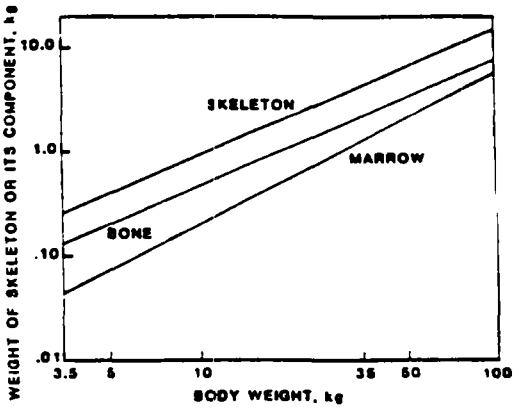

FIG. 1. Simulated skeletal, marrow-free bone, and bone marrow weights in humans as functions of body weight.

Blood Flow to Bone

The most reliable estimates of total and regional blood flows to bone are those based on distribution of radiolabeled microspheres (Gross *et al.*, 1981). Due to the use of radioisotopes, this methodology has been limited to applications in experimental animals. Because of the inadequacy of direct estimates of blood flow to human bone, regional bone blood flow rates are here scaled allometrically from the model for the rat (O'Flaherty, 1991a, Table 6) to arrive at estimates for the human. Scaling regional flows per unit tissue weight according to the −0.25 power of body weight gives blood flow estimates of 0.090 ml/min/g of red marrow and trabecular bone, 0.013 ml/

min/g of cortical bone, and 0.026 ml/min/g of yellow marrow for the 70-kg human. Based on these estimates, compartmentalization of the skeleton as in Table 1, and the assumption that 50% of total marrow in the adult human is red marrow, the skeleton of the adult human can be modeled (Table 3). Total blood flow in the human skeletal model is 4.1 ml/min/100 g skeletal tissue including bone marrow (but excluding cartilage), or 5.3% of the cardiac output of a 70-kg male, 6.5 liters/min (Mapleson, 1973)

As pointed out elsewhere (O'Flaherty, 1991a), blood flow rates are roughly proportional to bone formation rates. On the basis that bone blood flows appear to stabilize in the skeletons of adult rats, it is reasonable to infer that blood flow to bone is also approximately constant in the adult human.

DISCUSSION

A number of analyses of different kinds of human bone establish that the model of mature bone tissue (O'Flaherty, 1991a) accurately describes human bone. The model is 68.1% ash by weight of marrow-free dry bone. Mean values of ash content in a large number of human skeletons drawn equally from blacks, whites, males, and females were 0.657–0.665 g ash/g dry marrow-free bone (Trotter and Peterson, 1962).

The weight fraction of ash in the model marrow-free mature bone is 0.564. A mean ash weight of 0.558 g/g marrow-free bone from nine specimens of mature cortical bone was reported by Woodard (1962). In another series of 26 specimens, Woodard (1964) calculated means for ash as 0.579 ± 0.009 g/g or 1.11 ± 0.046 g/cm^3 marrow-free cortical bone and for water as 0.122 ± 0.009 g/g or 0.234 ± 0.016 g/cm^3 marrow-free cortical bone. Melick and Miller (1966) measured 1.186 ± .015 g ash/cm^3 of tibial cortical bone from nine human subjects under 60 years old, and Mueller *et al.* (1966) found ash contents ranging from 1.0–1.15 g/cm^3 of marrow-free human iliac and vertebral bone. The marrow-free mature bone model contains 1.085 g ash/cm^3 of bone.

The density of model marrow-free mature bone is 1.92 g/cm^3. The density of marrow-free bone has been measured in a number of studies and is generally reported to be between 1.5 and 2.0 g/cm^3. Galante *et al.* (1970) found a mean density of 1.85 g/cm^3 for human vertebral (trabecular) marrow-free bone. Mueller *et al.* (1966) observed densities of 1.86–1.96 g/cm^3 for the same bone. Robinson (1975) recorded marrow-free bone densities up to 2.0 g/cm^3 in bone specimens taken from dogs. The mean density of the nine mature human cortical bone specimens examined by Woodard (1962) was 1.87 g/cm^3.

The model of the mature human skeleton also compares well with published measure-

TABLE 3

THE MATURE SKELETON OF THE 70-kg MALE HUMAN, INCORPORATING BLOOD FLOW

Tissue	Weight, % of body wt	Weight (g)	Perfusion rate, ml/min/g of fraction weight	Perfusion rate (ml/min)
Red marrow	2.5	1750	0.090	158
Trabecular bone	1.45	1015	0.090	91
Cortical bone	5.75	4025	0.013	52
Yellow marrow	2.5	1750	0.026	46
Total	12.2	8540		347

ments and estimates. Model marrow-free bone weight is in line with what has been reported by other investigators as the fraction of body weight assignable to the marrow-free skeleton, although the degree to which the bones have been freed of their water and fat contents is usually not precisely defined. Ingalls (1931) found marrow-free skeletal weight to be about 5 kg, or about 7% of body weight, in 100 adult male skeletons. Baker and Newman (1957) took measurements on 115 skeletons, essentially without marrow, of young white and black men. They devised equations relating living weight to skeletal weight, from which it can be calculated that at 70 kg body weight, marrow-free skeletal weight would be 4310 g in white males and 5280 g in black males. One measurement is available from an adult female, although the subject had sustained weight loss prior to her death. The total marrow-free bone mass in this subject was 5.0% of a reconstructed body weight (Moore *et al.*, 1968). If this single specimen is representative, females may have a slightly smaller bone mass per unit body weight than males. Reference Man has a marrow-free bone weight of 7.1% of body weight, and Reference Woman of 5.9% of body weight (ICRP, 1975).

The amount and turnover rate of bone are the critical determinants of the kinetics of bone-seeking elements. However, it is interesting to compare the skeletal model of Table 1 with the skeleton of Reference Man, which includes cartilage as well as bone. The total skeletal weight of Reference Man is 14.3% of body weight, or 10 kg; of this, 5 kg is bone, 3 kg marrow, and 2 kg cartilage. Forty-five percent of the cartilage is periarticular and 55% skeletal. Human skeletal weights reported in the literature include variable amounts of cartilage. In the newborn, cartilage constitutes a significant fraction of total bone volume, but during the process of skeletal maturation cartilage is gradually replaced by bone although some cartilage persists in association with the skeleton.

If the model mature skeleton of Table 1 is expanded to include 1500 g of cartilage, bringing the total weight to 10 kg, the total volume of the model skeleton would be 7460 cm^3 with cartilage or 6120 cm^3 without, for a mean skeletal density of 1.34 g/cm^3 with cartilage or 1.39 g/cm^3 without. These skeletal densities correspond to a skeletal composition of 35.1% marrow-free bone, 46.9% marrow, and 18.0% cartilage by volume. A mature human skeleton consisting of 20% by weight of trabecular skeletal tissue with a mean density of 1.16 g/cm^3 and 80% by weight of cortical skeletal tissue with a mean density of 1.40 g/cm^3 would have a mean skeletal density of 1.34 g/cm^3. Ninety percent of the marrow-free bone volume is contributed by cortical bone in this model.

Swanson and Iob (1940) found that cartilage was 30.3 and 36.1% by weight of the total skeleton of two fetuses weighing 3200 and 4070 g, respectively. With the inclusion of 33% by weight cartilage, with a density of 1.1 g/cm^3 (ICRP, 1975), the density of the model skeleton of the newborn becomes 1.33 g/cm^3.

The cartilage of the newborn is not as fully mineralized as the bone, and its mineral is not as mature. Swanson and Iob (1937) determined that epiphyseal cartilage of femur and tibia of four fetuses weighing 3030–4150 g contained a mean of 10.4% ash, while the cortical bone contained 57.3% ash. The cartilage ash had only 0.032 g Ca/g, less than $\frac{1}{10}$ the concentration in bone ash. Cartilage, therefore, is not quantitatively important as a determinant of the kinetics of calcium-mimicking elements.

The ash content of the model of the newborn skeleton, including cartilage, is 0.332 g/cm^3; the ash content of the model adult skeleton, including cartilage, is 0.380 g/cm^3. The increase parallels the increase in ash content of marrow-free bone, from 0.886 g/cm^3 at birth to 1.083 g/cm^3 in adulthood. The fractional volume of the total skeleton that is accounted for by marrow-free bone is nearly constant during growth because the fractional

ss in cartilage volume of the model skeleton almost compensated by the fractional in- ... marrow volume. The increase in rel- ve marrow volume is consistent with the ative enlargement of marrow cavities and inning of the cortex of long bones that occur ring growth. Other bones may display a rel- ive decrease in marrow volume with age. rtley *et al.* (1966) determined ash in blocks trabecular skeletal tissue from the vertebrae 40 donors who had been hospitalized before ath. Ash was around 0.11 g/cm^3 in the ungest subjects, who were less than 5 years d, and about 0.165 g/cm^3 in subjects aged)–40, with several of the adult males dis- aying a much greater degree of calcification. ese increases are greater than any likely to attributable to increases in ash content of arrow-free bone, suggesting that fractional ne volume may also have increased slightly ith age in this series.

The relatively high degree of mineralization bone of the newborn human is verified by number of independent observations. In neral, skeletal ash content per unit volume creases rapidly to adult levels during early ildhood, then shows little or no further ... or may continue to increase slowly to out age 50 (Arnold, 1960; Weaver and halmers, 1966; Bartley *et al.*, 1966; Mueller *al.*, 1966; Bell *et al.*, 1967; Currey and But- r, 1975; Quelch *et al.*, 1983). The adult range ppears to be reached at least by the end of e first decade of life. Moulton (1923) tabu- ted data from the early literature suggesting at the ash content of the human body was pproaching adult levels by age 500–1000 ays.

Bone volumes, and fractional volumes of one and bone marrow, do not scale across pecies as do volumes of many other tissues. he principle of elastic similarity suggests that s the length of a long bone increases with ody size, its diameter should increase as the .5 power of its length in order for bone cross- ectional area to maintain proportionality to e accompanying increase in body weight (McMahon and Bonner, 1983). In this case, skeletal mass would be proportional to the 4/3 power of body weight. Total skeletal mass actually scales as about the 1.1 power of body weight across species, however (Schmidt-Nielsen, 1972, 1984), so that support of body weight cannot be the only factor determining skeletal volume and bone shape.

Scaling from a 250-g rat to a 70-kg human on the basis of the 1.1 power of body weight gives an expected 1.76-fold increase in skeletal weight expressed as a percentage of body weight. On this basis, if marrow plus marrow-free bone is considered to be equivalent to the skeleton, the percentage 7.30 for the rat (O'Flaherty, 1991a) would scale to 12.8% for the human. Reference Man has a marrow plus marrow-free bone weight of 11.4% of body weight, and the cartilage-free human skeletal model of Table 3 is 12.2% of body weight, which represents scaling on the basis of the 1.08 power of body weight.

If red marrow is 90% of the total marrow of the small animal skeleton (O'Flaherty, 1991a), it will make up about 2.0–2.1% of body weight. This is essentially the estimate (of 2.0%) for Reference Man, and it is interesting to note that the 2% of body weight figure for red marrow in Reference Man has been scaled linearly with body weight (Dedrick *et al.*, 1973a,b) and used successfully in several physiologically based pharmacokinetic models for anticancer drugs that act directly on the marrow (Dedrick *et al.*, 1972, 1973b; Tterlikkis *et al.*, 1977).

This model of the growing human skeleton is formulated so as to provide the anatomic and physiologic basis for a model of the kinetics of bone-seeking elements in humans from birth to maturity. It is not designed to describe bone or skeletal growth after about age 25–30, although it may be reasonably accurate to about age 40. In women after about age 50 and in men after about age 60, thinning of bone with possible net bone loss occurs. The aging skeleton will be considered in a subsequent paper. The model presented here

covers the period of rapid bone growth, during which bone-seeking elements have the highest probability of becoming incorporated into the bone mineral matrix. Accordingly, it is also the period during which environmental exposure to bone-seeking elements may be expected to have the greatest impact on the body burdens of these elements.

REFERENCES

ARNOLD, J. S. (1960). Quantitation of mineralization of bone as an organ and tissue in osteoporosis. *Clin. Orthoped.* 17, 167–175.

BAKER, S. L., BUTTERWORTH, E. C., AND LANGLEY, F. A. (1946). The calcium and nitrogen content of human bone tissue cleaned by micro-dissection. *Biochem. J.* 40, 391–396.

BAKER, P. T., AND NEWMAN, R. W. (1957). The use of bone weight for human identification. *Am. J. Physiol. Anthropol.* 15, 601–618.

BARTLEY, M. H., JR., ARNOLD, J. S., HASLAM, R. K., AND JEE, W. S. S. (1966). The relationship of bone strength and bone quantity in health, disease, and aging. *J. Gerontol.* 21, 517–521.

BELL, G. H., DUNBAR, O., AND BECK, J. S. (1967). Variations in strength of vertebrae with age and their relation to osteoporosis. *Calc. Tiss. Res.* 1, 75–86.

CURREY, J. D., AND BUTLER, G. (1975). The mechanical properties of bone tissue in children. *J. Bone Joint Surg.* 57A, 810–814.

DEDRICK, R. L., FORRESTER, D. D., AND HO, D. H. W. (1972). *In vitro–in vivo* correlation of drug metabolism—Deamination of 1-α-D-arabinofuranosylcytosine. *Biochem. Pharmacol.* 21, 1–16.

DEDRICK, R. L., FORRESTER, D. D., CANNON, J. N., EL DAREER, S. M., AND MELLETT, L. B. (1973a). Pharmacokinetics of 1-α-D-arabinofuranosylcytosine (ARA-C) deamination in several species. *Biochem. Pharmacol.* 22, 2405–2417.

DEDRICK, R. L., ZAHARKO, D. S., AND LUTZ, R. J. (1973b). Transport and binding of methotrexate *in vivo*. *J. Pharm. Sci.* 62, 882–890.

DIETZ, A. (1944). Distribution of bone marrow, bone, and bone-ash in rabbits. *Proc. Soc. Exp. Biol. Med.* 57, 60–62.

DYSON, E. D., AND WHITEHOUSE, W. J. (1968). Composition of trabecular bone in children and its relation to radiation dosimetry. *Nature* 217, 576–578.

ELLIS, R. E. (1961). The distribution of active bone marrow in the adult. *Physics Biol. Med.* 5, 255–258.

EMERY, J. L., AND FOLLETT, G. F. (1964). Regression of bone-marrow haemopoiesis from the terminal digits in the foetus and infant. *Br. J. Haematol.* 10, 485–489.

FORBES, R. M., COOPER, A. R., AND MITCHELL, H. H. (1953). The composition of the adult human body as determined by chemical analysis. *J. Biol. Chem.* 203, 359–366.

FORBES, R. M., MITCHELL, H. H., AND COOPER, A. R. (1956). Further studies on the gross composition and mineral elements of the adult human body. *J. Biol. Chem.* 223, 969–975.

GALANTE, J., ROSTOKER, W., AND RAY, R. D. (1970). Physical properties of trabecular bone. *Calc. Tiss. Res.* 5, 236–246.

GARNETT, E. S., KENNETT, T. J., KENYON, D. B., AND WEBBER, C. E. (1973). A photon scattering technique for the measurement of absolute bone density in man. *Radiology* 106, 209–212.

GONG, J. K., ARNOLD, J. S., AND COHN, S. H. (1964). Composition of trabecular and cortical bone. *Anat. Rec.* 149, 325–331.

GROSS, P. M., MARCUS, M. L., AND HEISTAD, D. D. (1981). Current concepts review: Measurement of blood flow to bone and marrow in experimental animals by means of the microsphere technique. *J. Bone Jt. Surg.* 63A, 1028–1031.

HUDSON, G. (1965). Bone-marrow volume in the human foetus and newborn. *Br. J. Haematol.* 11, 446–452.

ICRP Publication Number 23: Report of the task group on reference man. Pergamon, Oxford. 1975.

INGALLS, N. W. (1931). Observations on bone weights. *Am. J. Anat.* 48, 45–98.

JOHNSON, L. C. (1964). In *Bone Biodynamics*, (H. M. Frost, Ed.), pp. 543–654. Little, Brown & Co., Boston.

MACDONALD, I. (1954). Chemical analysis of human foetal skull bones. *Biochem. J.* 57, 437–439.

MAPLESON, W. W. (1973). Circulation–time models of the uptake of inhaled anaesthetics and data for quantifying them. *Br. J. Anaesth.* 45, 319–334.

MCMAHON, T. A., AND BONNER, J. T. (1983). *On Size and Life*, pp. 124–125. Scientific American Books, New York.

MECHANIK, N. (1926). Untersuchungen uber das Gewicht des Knochenmarkes des Menschen. *Z. Gesamte Anat. Abt. I* 79, 58–99.

MELICK, R. A., AND MILLER, D. R. (1966). Variations of tensile strength of human cortical bone with age. *Clin Sci.* 30, 243–248.

MITCHELL, H. H., HAMILTON, T. S., STEGGERDA, F. R., AND BEAN, H. W. (1945). The chemical composition of the adult human body and its bearing on the biochemistry of growth. *J. Biol. Chem.* 158, 625–637.

MOORE, F. D., LISTER, J., BOYDEN, C. M., BALL, M. R., SULLIVAN, N., AND DAGHER, F. J. (1968). The skeleton as a feature of body composition. *Human Biol.* 40, 135–188.

MOULTON, C. R. (1923). Age and chemical development in mammals. *J. Biol. Chem.* 57, 79–97.

MUELLER, K. H., TRIAS, A., AND RAY, R. D. (1966). Bone density and composition. *J. Bone Joint Surg.* 48A, 140–148.

O'FLAHERTY, E. J. (1988). A physiologically based model of skeletal growth in the rat. *Toxicol. Lett.* 43, 85–95.

O'FLAHERTY, E. J. (1991a). Physiologically based models for bone-seeking elements. I. Rat skeletal and bone growth. *Toxicol. Appl. Pharmacol.* 111, 299–312.

O'FLAHERTY, E. J. (1991b). Physiologically based models for bone-seeking elements. II. Kinetics of lead disposition in rats. *Toxicol. Appl. Pharmacol.* 111, 313–331.

ROBINSON, R. A. (1975). Physicochemical structure of bone. *Clin. Orthoped.* 112, 263–315.

QUELCH, K. J., MELICK, R. A., BINGHAM, P. J., AND MERCURI, S. M. (1983). Chemical composition of human bone. *Arch. Oral Biol.* 28, 665–674.

SCHMIDT-NIELSEN, K. (1972). *How Animals Work*, pp. 88–89. Cambridge Univ. Press, Cambridge.

SCHMIDT-NIELSEN, K. (1984). *Scaling: Why Is Animal Size So Important?* Cambridge Univ. Press, Cambridge.

SWANSON, W. W., AND IOB, L. V. (1937). Mineral composition of the bone and cartilage of the human fetus. *Am. J. Dis. Child.* 54, 1025–1029.

SWANSON, W. W., AND IOB, V. (1940). Growth and chemical composition of the human skeleton. *Am. J. Dis. Child.* 59, 107–111.

TROTTER, M., BROMAN, G. E., AND PETERSON, R. R. (1960). Densities of bones of white and Negro skeletons. *J. Bone Joint Surg.* 42(A), 50–58.

TROTTER, M., AND PETERSON, R. R. (1962). The relationship of ash weight and organic weight of human skeletons. *J. Bone Joint Surg.* 44A, 669–681.

TROTTER, M., AND PETERSON, R. R. (1968). Weight of bone in the fetus—A preliminary report. *Growth* 32, 83–90.

TROTTER, M., AND PETERSON, R. R. (1969a). Weight of bone during the fetal period. *Growth* 33, 167–184.

TROTTER, M., AND PETERSON, R. R. (1969b). Weight of bone in the fetus during the last half of pregnancy. *Clin. Orthoped. Rel. Res.* 65, 46–50.

TROTTER, M., AND PETERSON, R. R. (1978). Weight of the skeleton during postnatal development. *Am. J. Physical Anthropol.* 33, 313–323.

TTERLIKKIS, L., ORTEGA, E., SOLOMON, R., AND DAY, J. L. (1977). Pharmacokinetics of mercaptopurine. *J. Pharm. Sci.* 66, 1454–1457.

WEAVER, J. K., AND CHALMERS, J. (1966). Cancellous bone: Its strength and changes with aging and an evaluation of some methods for measuring its mineral content. *J. Bone Joint Surg.* 48A, 289–299.

WOODARD, H. Q. (1962). The elementary composition of human cortical bone. *Health Physics* 8, 513–517.

WOODARD, H. Q. (1964). The composition of human cortical bone. *Clin. Orthoped. Rel. Res.* 37, 187–193.

TOXICOLOGY AND APPLIED PHARMACOLOGY 118, 16–29 (1993)

M Gargas

Physiologically Based Models for Bone-Seeking Elements

IV. Kinetics of Lead Disposition in Humans[1]

ELLEN J. O'FLAHERTY

Department of Environmental Health, University of Cincinnati College of Medicine, 3223 Eden Avenue, Cincinnati, Ohio 45267-0056

Received December 13, 1991; accepted August 31, 1992

Physiologically Based Models for Bone-Seeking Elements. IV. Kinetics of Lead Disposition in Humans. O'FLAHERTY, E. J. (1993). *Toxicol. Appl. Pharmacol.* 118, 16–29.

A model of lead disposition in humans has been developed. In addition to liver, kidney, other well-perfused and poorly perfused tissues, the model incorporates bone as an explicit compartment whose volume, composition, and metabolic activity are all age-dependent. The rates of all transfers of lead out of the blood are related to plasma lead. The relationship between plasma lead and blood lead is expressed as a capacity-limited binding associated with the erythrocyte. Interchanges of lead between plasma and bone are modeled as partially interactive events linked in series. Blood traversing the bone passes first through a surface region of rapid exchange before entering the metabolically active region of bone, where lead is incorporated with calcium into mineralizing bone and returned to the blood with resorbing bone. After leaving the larger vessels, plasma superfusate enters the canalicules that feed bulk bone, where lead diffuses radially outward into the total bone volume. Model simulations are compared with data from epidemiologic and experimental dietary and inhalation studies in adults. © 1993 Academic Press, Inc.

The preponderance of the body burden of lead is found in the bone. Whole-body kinetic behavior of lead is determined largely by the balance between bone lead uptake and its release from bone. There are multiple mechanisms for bone uptake and release of bone volume-seeking elements, some of which result in very long residence times for these elements in bone. The quantitative importance of these slow processes leads to the need to model exposures extended in time and therefore to incorporate growth and aging.

[1] Portions of this work were supported by U.S. Public Health Service Grant ES 04125 and by U.S. EPA Assistance Agreement CR-815820. The concepts and results were presented in part at the annual meeting of the Society of Toxicology in 1991.

In the first three papers of this series (O'Flaherty, 1991a, b, c), descriptions of rat and human body, bone, and skeletal growth and a physiologically based model of lead kinetics in the rat from birth to maturity have been presented. In this paper, a physiologically based model of lead kinetics in the growing human is developed, and the fidelity with which it simulates blood lead concentrations from human epidemiologic and experimental studies is examined.

METHODS

Theoretical

General. The model is qualitatively the same in its structure and general features as the model developed for the rat. Justification for the choice of kinetic features, and for the mathematical formulation of bone metabolism and mechanisms of incorporation of lead into bone, has been given previously (O'Flaherty, 1991a, b). The model consists of kidney, liver, bone, and other well- and poorly perfused tissues. Fractional absorption of lead from the gastrointestinal tract declines from 0.5 at birth to adult values of 0.08–0.11 by age 10. Fractional absorption of lead from the lung is 0.5 for typical particle size distributions. Neither fraction is dependent on magnitude of exposure. Elimination of lead is modeled as 30% from the liver and 70% from the kidney (Chamberlain *et al.*, 1978). Clearance is independent of body burden in the model.

The model is scaled to age and to young adult body weight (age 20–25) using a five-parameter expression that accounts for both the rapid growth taking place in early childhood and the period of accelerated growth beginning at puberty. Parameter values in the growth expression are different for females and males. Cardiac output, clearances, and organ and tissue volumes are expressed as functions of both body weight and degree of maturity.

Of the total cardiac output, 0.25 goes to the liver and its associated well-perfused tissues, 0.17 to the kidneys, 0.05 to bone, 0.44 to other well-perfused tissues, and 0.09 to other poorly perfused tissues. These fractions are independent of body weight. Of the total body weight of the adult, the liver and associated tissues account for 0.04, the kidneys for 0.0085, all well-perfused tissues including the liver and kidneys for 0.10, and all poorly perfused tissues including the bone for 0.90. These fractions are dependent on body weight in children. The volume of bone is also a function of body weight.

The rates of all transfers of lead out of the blood are related to the concentration of lead in plasma. The relationship between plasma lead and blood lead is determined by a capacity-limited lead binding associated with

0041-008X/93 $5.00
Copyright © 1993 by Academic Press, Inc.
All rights of reproduction in any form reserved.

erythrocytes. Most transfers of lead between plasma and tissues are modeled as flow-limited exchanges. Those that are not are the deposition of lead with forming bone, its return to plasma as a result of bone resorption, and its slow exchange throughout bulk bone. Slow exchange of lead between plasma and bone is expressed as a diffusion-limited process.

As in the rat model, interchanges of lead between plasma and bone are modeled as virtually interactive events linked in series. Blood traversing the bone passes through a surface region of rapid, flow-limited exchange before entering the metabolically active region. The metabolically active region consists of actively growing or resorbing haversian canal, endosteal, periosteal, and trabecular surfaces of bone. Here lead is incorporated with calcium into mineralizing bone and is returned to the blood along with calcium as bone is resorbed during modeling or remodeling. The rate of return of lead to the blood with resorbing bone is modeled as proportional to the moving average concentration of lead in bone, which is determined by all transfer processes combined.

After leaving the larger vessels, plasma superfusate enters the canalicules that feed bulk bone. The exchange of lead between canalicular fluid and bone is conceptualized as a radial diffusion outward from the canalicules into the diffusion volume of bone, which is the total bone volume with the exception of the surface region. In the model, radial diffusion is approximated as successive diffusion-limited exchanges among a set of concentric cylindrical shells surrounding each canalicule. Lead is homogeneously distributed within each of the eight shells of equal thickness that compose the set.

Body weight. A three-term expression affords a good description of human body weight as a function of age.

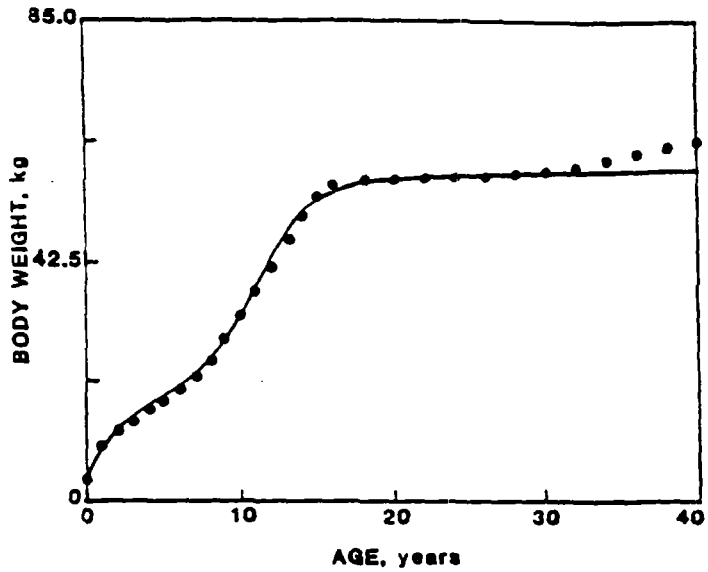

FIG. 1. Growth of human female. Points are taken from a standardized growth chart. The line is the model simulation, used to generate bone volume as a function of age. Note that the simulation does not reproduce the continuing increase in body weight after about age 30, since this weight increase is not considered to be related to further bone growth.

$$WBODY = 3.5 + (WCHILD)(AGE))/(HALF + AGE) + WADULT/(1 + (K)(EXP(-(L)(WADULT)(AGE)))).$$

where WBODY is body weight (kg) at age AGE (years) and 3.5 kg is mean body weight at birth. WCHILD is the maximum weight (kg) for the early hyperbolic section of the growth curve, and HALF is the midpoint age (years) for this hyperbolic growth segment. WCHILD and HALF define the rapid growth that takes place in early childhood. A logistic growth curve determined by empirically determined parameters WADULT (kg), K, and L, and describing growth during puberty and early adulthood is superimposed. An example of use of this expression to generate a standard growth curve for males has been published (O'Flaherty, 1991). The fit to a standard growth curve for females is shown in Fig. 1.

Parameter estimation. In addition to values of the fractional tissue volumes and blood flow rates of conventional physiologically based models, the model requires values for the following physiologic parameters: the five parameters in the expression for body weight as a function of age; the fractional powers of body weight that determine dependence of liver, kidney, and other tissue volumes on body weight; the two parameters in the expression for bone volume as a function of body weight; the fractional volume of the rapidly exchanging volume of bone mineral and the fractional blood flow rate to bone; the canalicular diameter and spacing; and the three parameters in the expression for bone formation rate as a function of body weight. The values of these growth-, bone growth-, and bone metabolism-related parameters are summarized in Table 1.

The parameters in the expression relating body weight to age are WADULT, K, L, WCHILD, and HALF. The sum of WADULT and WCHILD is 56 kg for women and 73 kg for men if reference growth curves are to be generated, but the values of these parameters may also be chosen to reproduce specific individual or group growth curves.

Liver volume and total well-perfused tissue volume are related to the 0.85 power of body weight, and kidney volume to the 0.84 power of body weight (Johnson *et al.*, 1978). For example,

$$VL = (VLA)(WBODY/(3.5 + WADULT + WCHILD))^{0.85}),$$

where VL is liver volume and VLA is liver volume in the adult.

Values of the parameters in the expression for the relationship of bone volume to body weight in humans have been developed in a separate paper (O'Flaherty, 1991c). The volume of rapidly exchanging bone mineral VS is set at 0.2% of total bone volume (see Discussion). Blood flow rate to bone is set at 5.3% of cardiac output (O'Flaherty, 1991c). Canalicular diameter and spacing in human bone are taken from studies by Frost (1962).

The expression for fractional bone formation rate is based on data from Bauer *et al.* (1957). These investigators published accretion rates, in g/day, for calcium in bone in eight individuals aged 1 month to 43 years, as calculated from the time course of calcium specific activity in plasma coupled with excretion of calcium and calcium tracer in urine and feces after a single injection of a calcium tracer. These accretion rates are reproduced by a three-parameter expression that links bone formation rate with body and bone growth.

Fractional bone formation rate by weight (1/year)

$$= MINFORM + (ALPHAO)(1 - EXP(-ALPHA) \times (RWBONE/WBONE)),$$

where WBONE is bone weight (kg), RWBONE is the rate of change of bone weight (kg/year), and MINFORM, ALPHAO, and ALPHA are constants. MINFORM is the minimum fractional bone formation rate, which applies to adults whose bone mass is stable. (MINFORM + ALPHAO) is related to fractional bone formation rate at birth, and ALPHA helps to determine the shape of the relationship of fractional bone formation rate to body weight. Fractional bone formation rate according to this expression is shown in Fig. 2 along with the data points from the Bauer *et al.* study.

The model also requires values of certain lead-related parameters: fractional absorption from the gastrointestinal tract; fractional absorption of inhaled lead; elimination clearance; maximum capacity and half-saturation concentration for capacity-limited binding in the erythrocyte; parti-

TABLE 1
Physiological Parameters

Body weight	
WCHILD	22 kg (female); 23 kg (male)
HALF	3 years
WADULT	34 kg (female); 50 kg (male) (for standardized growth curves)
K	600
L	0.017 years/kg (female); 0.0095 years/kg (male)
Tissue volume	
Allometric exponents relating growth to WBODY	
VL, liver volume, liters[a]	0.85
VK, kidney volume, liters[a]	0.84
VWT, total well-perfused tissue volume, liters[a]	0.85
VBONE, bone volume, liters[b]	1.02
WBONE, bone mass, kg[b]	1.21
VS, rapidly exchanging surface bone volume, liters	(0.002) (VBONE)
Bone growth	
MINFORM	0.1/year
ALPHAO	4.6/year
ALPHA	0.55/year
Bone structure[c]	
Canalicule spacing	8 μm
Specific canalicule surface	3.1×10^{-4} cm²/cm length
Specific total canalicule length	2.0×10^{9} cm/liter bone

[a] Johnson *et al.* (1978).
[b] O'Flaherty (1991b).
[c] Frost (1962).

tion coefficients for lead in nonbone tissues and in the surface region of bone; fractional clearance of lead from plasma into forming bone; and restricted permeability coefficients for diffusion of lead within bone, from plasma into bone, and from bone into plasma. The values of these parameters are given in Table 2.

Fractional absorption from the gastrointestinal tract is modeled as a first-order decline from 0.50 at birth to 0.25 at age 5 years to an adult value of 0.08 (see Discussion).

Fifty percent absorption of inhaled ambient air lead is assumed. This is a default value that can be more precisely tuned to reflect particle size and chemical makeup of the inhaled lead (Chamberlain *et al.*, 1978). Potential gastrointestinal uptake of inhaled and swallowed lead is not considered. There is evidence (Rabinowitz *et al.*, 1977; Gross, 1979) that gastrointestinal uptake of inhaled lead is significant only when aerosols of large particle size are respired, and even then is not measurable in all cases. Rate of entry of lead into the lung air space is calculated as respiratory rate times the concentration of lead in air. Respiratory rate is modeled as proportional to the logarithm of body weight (Johnson *et al.*, 1978).

The elimination clearance of lead is 15 liters plasma/day in a 70-kg adult (Manton and Malloy, 1983). This is 8.5% of the glomerular filtration rate, which in turn is allometrically related to body weight with two apparently different slopes during growth to adulthood (Johnson *et al.*, 1978) (Fig. 3). The elimination clearance of lead in infants and children is lower (see Discussion).

Values of the maximum binding capacity BIND for lead in human erythrocytes and of the half-saturation concentration KBIND are based on the plasma lead/blood lead data of DeSilva (1981) as published by Marcus (1985) (Fig. 4) and the plasma lead/blood lead data of Manton and Malloy (1983) and Manton and Cook (1984). These values are not adjusted for age, but dependence of hematocrit on both sex and age (Johnson *et al.*, 1978) is incorporated.

Initial values of partition coefficients for lead in nonbone tissues and in the surface region of bone, of fractional clearance of lead from plasma into forming bone, and of the three restricted permeability coefficients of diffusion were all taken directly from the rat model (O'Flaherty, 1991b). They were adjusted, in most cases only slightly, during the course of working with the human model.

SIMULATIONS

Epidemiologic Studies

The literature on human lead exposure is voluminous. It is not possible to compare model simulations with all relevant data sets relating lead exposure to blood lead. Model simulations are illustrated for the conditions of those studies that are historically the major experimental and epidemiologic studies of lead kinetics.

In simulating the results of studies in which ambient air lead is not reported, current levels in the United States are taken to be 0.5 μg/m³, whereas levels in the Glasgow studies and in the United States in the 1960s and early 1970s are assigned values up to 5 μg/m³ (Goldsmith and Hexter, 1967; Tepper and Levin, 1975). Controlled or occupational exposures to lead in air are superimposed on ambient air exposures as time-weighted averages for these simulations.

Current estimates of dietary lead in the United States range from 50 μg/day to as low as 10 μg/day. However, in the 1960s and earlier, when the Kehoe studies and others

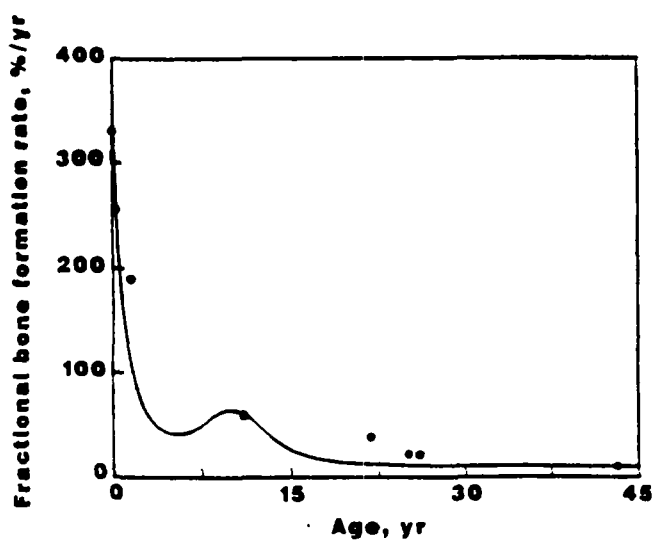

FIG. 2. Fractional bone formation rate as a function of age. Data points are taken from Bauer *et al.* (1957). The line is the model simulation.

TABLE 2
Parameters Related to Lead

Partitioning in blood	
BIND	2.7 mg/liter red cell volume
KBIND	0.0075 mg/liter red cell volume
Partitioning between blood plasma and tissues	
PL (liver)	100
PK (kidney)	100
PW (other well-perfused tissues)	100
PB (bone)	1000
PP (other poorly perfused tissues)	20
Metabolically active region of bone	
LEAD, fractional clearance of lead into forming bone	15,000 liters plasma cleared/liter new bone formed
Diffusion region of bone	
DO, restricted permeability coefficient for within-bone movement	1×10^{-7} cm/day/unit distance
RO, restricted permeability coefficient for bone-to-plasma transfer	1×10^{-7} cm/day/unit distance
PO, restricted permeability coefficient for plasma-to-bone transfer	0.08 cm/day/unit distance
Absorption	
Fractional absorption from mixed foodstuffs in GI tract	Variable with age; see text
Fractional absorption of ambient air lead in lung	0.5
Elimination	
Clearance of lead from plasma	Variable with age; see text

Note. See text for derivation of parameter values. For definition of terms, see O'Flaherty (1991b).

(see below) were carried out, dietary lead intake was 200 μg/day to as much as 300 μg/day. Therefore, in simulating the results of early studies in which dietary lead is not reported, intake of lead from food is usually set at about 200 μg/day depending on the date of the study.

Dietary lead. Several studies of the relationship of blood lead to drinking water lead have been carried out in Scotland in regions where acid (plumbosolvent) water was formerly found in conjunction with lead pipes. In the earliest of these, Moore *et al.* (1977) expressed lead concentrations in terms of the cube root of first-draw water lead in 949 blood samples.

$$\text{PbB}\ (\mu g/dl) = 11.2 + 2.37\ (\text{DWL})^{1/3},$$

where DWL is drinking water lead in μg/liter. The curve is shown in Fig. 5 with the model simulation superimposed for a 20-year-old man who has drunk water with the stipulated lead concentration throughout his life. In keeping with the authors' intercept of 11.2 μg lead/dl blood at DWL = 0, the simulation includes a constant (adult) rate of absorption from all other lead sources of 47 μg/day, which would be equivalent, for example, to 225 μg of dietary lead/day and an air lead concentration of 4 μg/m³.

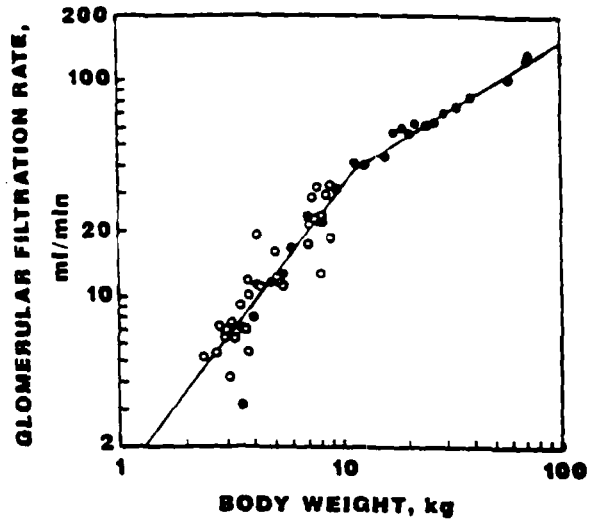

FIG. 3. Glomerular filtration rate as a function of age. Data points are from a variety of sources as tabulated in Johnson *et al.* (1978) (●) and from Rubin *et al.* (1949) (O). The line segments are linear regressions through data for body weight less than or greater than 10 kg.

In a study in Ayr, Scotland, Sherlock *et al.* (1982) also used the cube root of drinking water lead to describe the relationship of blood lead to water lead in 31 adult women:

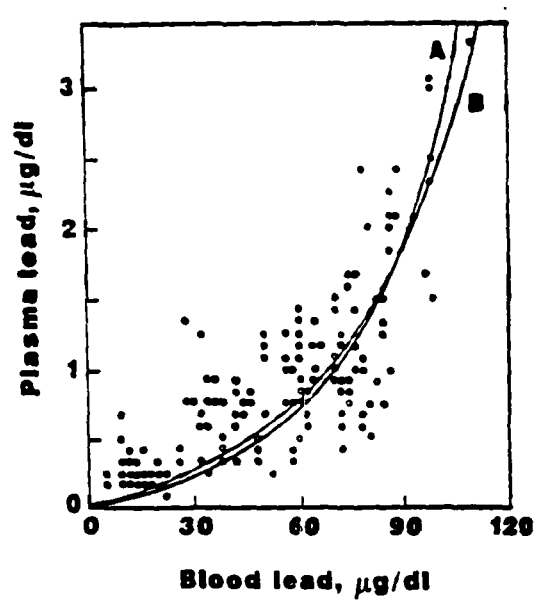

FIG. 4. The relationship between plasma lead and blood lead. Data points are from DeSilva (1981) as shown in Marcus (1985). Curve A is the model simulation. Curve B is Marcus' fit to the data, using a no-intercept model (Marcus' Model 4) consistent with the concept of a maximum erythrocyte binding capacity for lead.

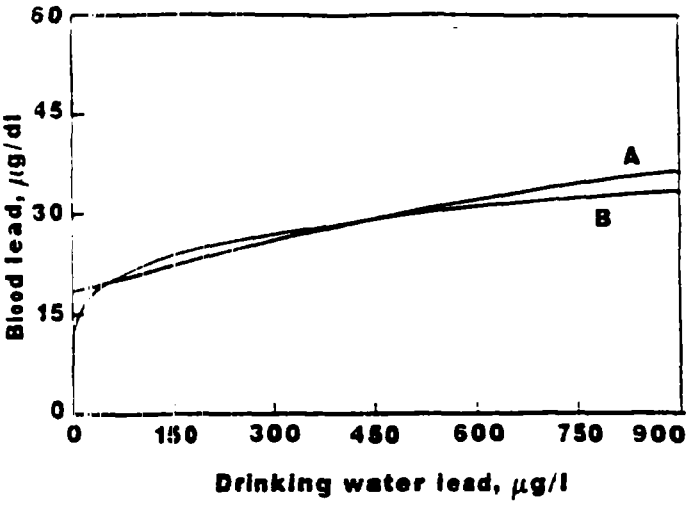

FIG. 5. Simulation for the conditions of Moore *et al.* (1977). Curve A is the model simulation for a 20-year-old man drinking water containing the stipulated lead concentration throughout his life, with (adult) absorption of 47 μg lead/day from all other sources. Curve B is a plot of the cube root equation selected by the authors to represent their data.

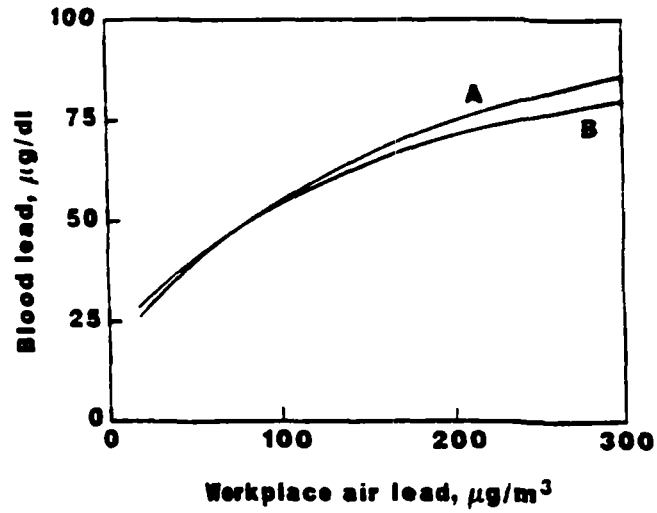

FIG. 7. Simulation for the conditions of Williams *et al.* (1969). Curve A is the model simulation for a 30-year-old man exposed from age 20 to age 30 to the range of workplace air lead concentrations shown, with other sources of lead set at 50 μg lead/liter of drinking water and 214 μg lead ingested/day from other dietary sources. Curve B is drawn through the Williams *et al.* data points.

$$\text{PbB } (\mu g/dl) = 4.7 + 2.78\ (\text{DWL})^{1/3}.$$

The authors point out that in this group of women, the contribution to blood lead from nonwater sources appears to be relatively small. Their curve is shown in Fig. 6 together with the model simulation for a 30-year-old woman who has been drinking water with the stipulated lead concentration for 10 years. For the simulation, absorption of lead from nonwater sources was set at 26 μg/day, equivalent to an air lead concentration of 2 μg/m³ and a dietary intake of 150 μg/day.

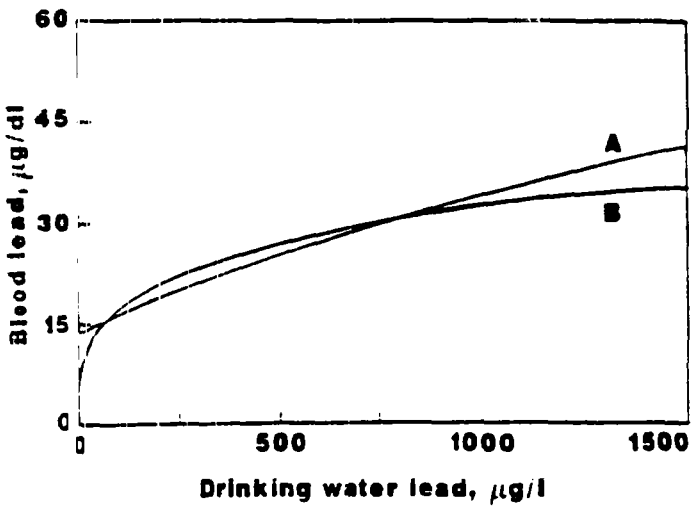

FIG. 6. Simulation for the conditions of Sherlock *et al.* (1982). Curve A is the model simulation for a 30-year-old woman drinking water containing the range of lead concentrations shown from age 20 to age 30, with (adult) absorption of 26 μg/day from all other sources. Curve B is a plot of the cube root equation selected by the authors to represent their data.

Air lead. Like the dietary lead/blood lead relationship, the air lead/blood lead relationship is curvilinear. Snee (1981) reviewed 17 studies of the relationship of blood lead to air lead. Of the studies in which personal air lead samplers were used to estimate exposure, the one by Williams *et al.* (1969) is noteworthy because some of the subjects were occupationally exposed to air lead levels as high as 300 μg/m³. Length of employment was such that the subjects can be presumed to have been at an approximate steady-state relationship of blood lead to air lead. Figure 7 shows the model simulation superimposed on a curve drawn through the Williams *et al.* data points. The simulation is for a 30-year-old man employed for 10 years in a lead-related job. Air lead concentrations entered into the simulation were time-weighed averages assuming that 40 hr per week were spent in the workplace and that the remaining time was spent in ambient air containing 3 μg lead/m³. Background exposures for the simulation were set at drinking water lead, 50 μg/liter, and other dietary lead, 214 μg/day.

Azar *et al.* (1975) also used personal air lead samplers to estimate the integrated average air lead exposure of 30 subjects from five different geographic locations and workplaces. The highest exposure was of cab drivers in Los Angeles, to an average of about 6 μg/m³. In Fig. 8 the model simulation for these average air lead concentrations is su-

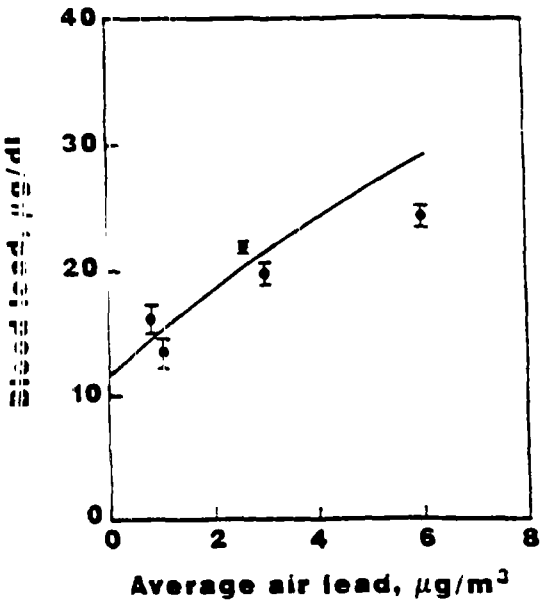

FIG. 8. Simulation for the conditions of Azar *et al.* (1975). The curve is the model simulation for a 30-year-old man exposed from birth to the range of ambient air lead concentrations shown, with other sources of lead set at 50 μg lead/liter of drinking water and 190 μg lead ingested/day from other dietary sources. The data points are arithmetic means of group blood lead concentrations as calculated by Chamberlain (1983). Standard errors are shown.

perimposed on the group average blood lead concentrations as calculated by Chamberlain (1983). The simulation is for a 30-year-old man. For the simulation, lead intake in food was set at 190 μg/day and drinking water lead at 50 μg/liter for all groups.

One interesting group of subjects for whom a general understanding of blood lead behavior has been developed (O'Flaherty, 1986) is those workers with long tenure in lead-related jobs, who were removed to low lead-exposure job locations shortly after institution of the medical removal mandate of the lead standard of the Department of Labor, Occupational Safety and Health Administration (U.S. Department of Labor, 1978). Typically, the blood lead concentrations of these men were 55–60 μg/dl or even higher at the time of medical removal: they fell to values between 40 and 50 μg/dl within 4–6 weeks and then continued to decrease so slowly that the further rate of decline was almost imperceptible during the 18-month removal period. Figure 9 illustrates simulated blood lead behavior for a man born in 1930, employed from age 20 in a setting where he was exposed to 84 μg lead/m³ of air in the workplace, and placed on medical removal, with no lead in workplace air, at age 45 after 25 years in the same job location. The simulation is of this man's blood lead concentration during the first 18 months after being removed from high workplace lead exposure. It is apparent that the model predicts the kind of blood lead behavior that was observed. It also predicts that only about 4% of total skeletal lead will have been lost within the 18-month removal period. Ten years after removal, 26% of total bone lead is predicted to have been lost. Blood lead concentration would be 34 μg/dl at this time.

Experimental Studies

Dietary lead. Studies in which lead has been ingested under controlled conditions by human subjects are few. The early, long-term studies by Kehoe (Gross, 1979) were principally inhalation exposures, but four subjects did ingest measured dietary supplements of lead daily for up to 1100 days as lead acetate in solution taken with the three main meals. Exposure data and pre- and postexposure blood lead levels are listed in Table 3 for these subjects along with simulated values for individuals of the same sex, age, and weight.

Cools *et al.* (1976) administered lead acetate for 49 days to 11 male subjects at rates calculated to sustain blood lead levels at about 40 μg/dl. Daily doses were adjusted downward at fairly regular intervals during the course of the study in order to achieve a rapid blood lead rise to 40 μg/dl followed by its maintenance at that level. Figure 10 shows the model simulation for the exposure conditions of the Cools *et al.* study along with the study results. Ages and weights of the study subjects were not given: the simulation is for a 25-year-old, 73-kg male with ambient lead exposure

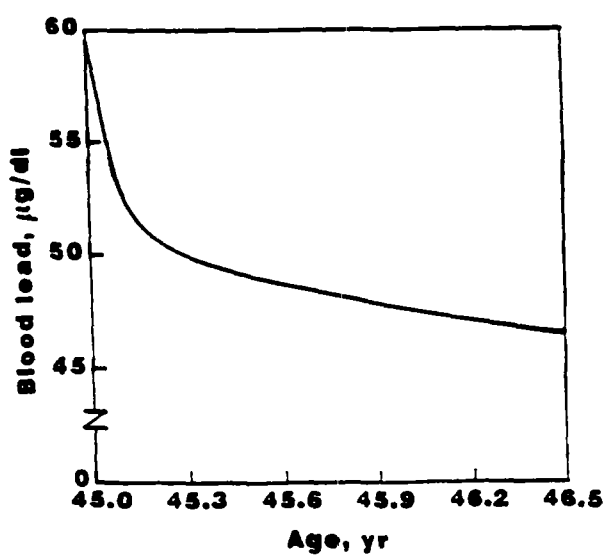

FIG. 9. Simulation of blood lead concentration during 18-month medical removal in a man employed for 25 years in a lead-related job. See text for details.

TABLE 3
The Kehoe Balance Experiments

Subject	Exposure	Simulated and (observed) blood lead, μg/dl		
		Preexposure	End of exposure	End of postexposure
EB	Oral	28 (27)	58 (60)	33 (34)
MB	Inh	24 (24)	35 (40)	26 (28)
MOB	Inh	21 (26)	40 (39)	24 (27)
PB	Inh	22 (23)	34 (33)	28 (32)
SB	Inh	18 (21)	40 (32)	22 (20)
FC	Inh	22 (22)	36 (—)	26 (20)
LD	Inh	20 (18)	45 (41)	25 (23)
IF	Oral	23 (27)	49 (46)	26 (40)
DH	Inh	17 (25)	24 (28)	19 (27)
NK	Inh	23 (20)	25 (26)	25 (25)
HR	Inh	18 (21)	22 (27)	— (—)
MR	Oral	18 (36)	44 (53)	— (—)
JOS	Inh	19 (21)	44 (46)	25 (27)
JUS	Inh	24 (21)	37 (32)	26 (19)
SS	Inh	18 (19)	27 (29)	26 (37)
SW	Oral	21 (40)	29 (39)	25 (25)

of 2 μg/m³ of air, 30 μg/liter of drinking water, and 290 μg from other dietary sources per day.

The most precise study of ingestion of lead by adults under controlled conditions was carried out by Rabinowitz *et al.* (1976). An isotopically altered lead was substituted for the usual dietary lead of the study subjects in such a way that total dietary lead intake was approximately constant. The stable isotope mix was administered for up to 124 days, and the men were followed for up to 303 days thereafter. Figures 11a–11d compare observed tracer lead concentrations with model simulations for four of the five men (the fifth received the isotope mix for only 1 day). Simulations are scaled to the subjects' ages and body weights. Exposure to the tracer is considered to be zero prior to its controlled administration.

Air lead. In the largest of the published studies of controlled air lead exposure, Kehoe (Gross, 1979) monitored blood lead concentrations in 12 subjects (11 male, 1 female) who spent 8 hr/day in a specially constructed chamber that allowed them to perform employment-related tasks while breathing air containing lead sesquioxide aerosols at concentrations up to 65 μg/m³ (time-weighted average) for up to 772 days. Follow-up periods extended to 702 days. Some subjects were studied during several sequential exposure periods, some of which involved dietary manipulation. These studies, begun in 1937 and concluded in 1971, are the earliest and still the most complete experimental human lead exposure studies. Although blood lead assays were neither as precise nor as accurate at the time of the Kehoe studies as they are now, these studies, which could not be duplicated today, contain a rich fund of information about the time dependence of blood lead concentration changes during and after prolonged lead exposure. Table 3 gives the preexposure and postexposure blood lead concentrations for the Kehoe inhalation subjects, as well as the simulated values for subjects of the same sex, age, and weight. Study periods involving dietary manipulation are not considered. Simulated background exposure was to drinking water lead of 50 μg/liter and air lead of 3.5 μg/m³. Food lead was assayed; reported values are entered into the simulations.

DISCUSSION

Model Development

The three-term expression affords a good description of human body weight as a function of age. The advantages of scaling both to age and to young adult body weight have been discussed (O'Flaherty, 1991a). It is important to point out that for the purpose of modeling skeletal growth, this expression reproduces human growth curves only to ages 20–25. Skeletal growth is considered to be complete by this age; further increase in body weight is not accompanied by an increase in model skeletal weight, as illustrated by the logistic and actual growth curves for females after age 30 (Fig. 1). After about age 50 in females or age 60 in males, the volume of bone tends to diminish slightly. Skeletal

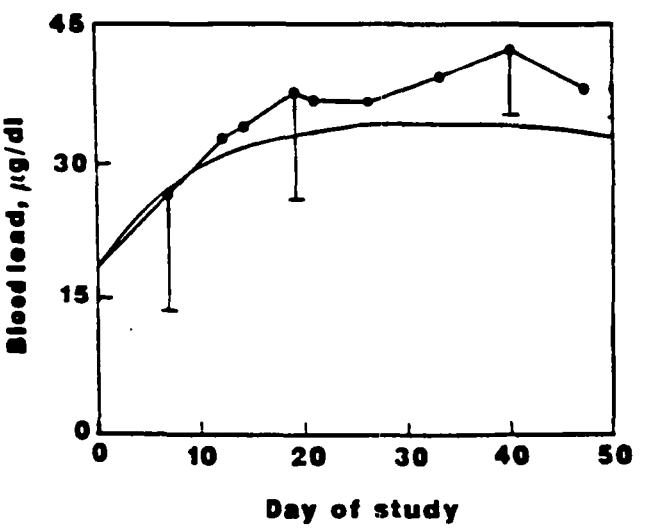

FIG. 10. Simulation for the experimental conditions of Cools *et al.* (1976). The smooth curve is the model simulation for a 25-year-old man given daily doses of lead acetate at variable rates over a 49-day period. Ambient lead exposure for the simulation is 2 μg lead/m³ of air, 30 μg lead/liter of drinking water, and 290 μg lead/day from other dietary sources. The segmented curve is drawn between mean blood lead concentrations from the Cools *et al.* study. Lead dose was adjusted after each blood lead concentration measurement. The range is shown for three of the means.

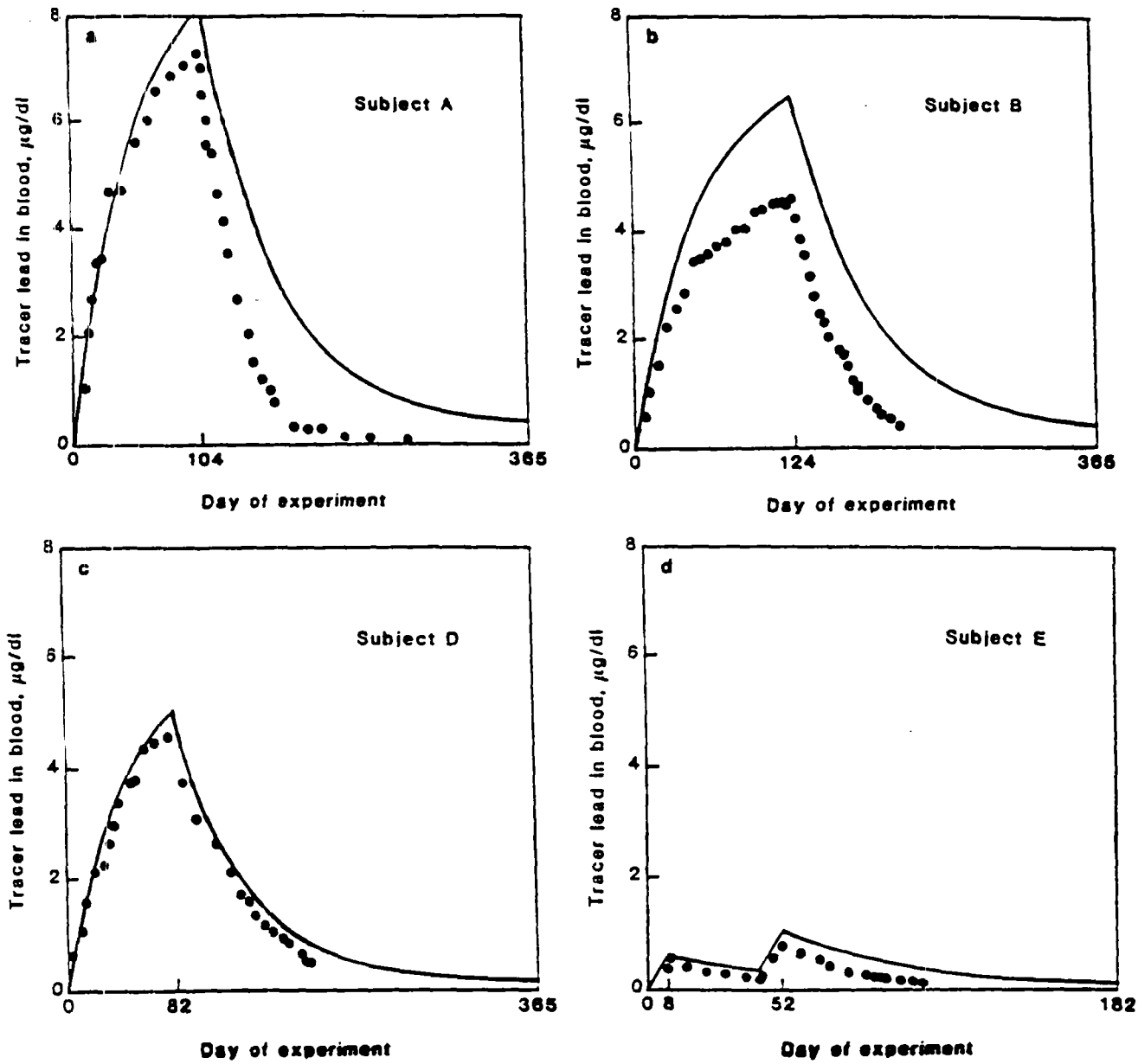

FIG. 11. Simulations for the experimental conditions of Rabinowitz *et al.* (1976). Four study subjects are shown. Data points are individual concentration measurements from the Rabinowitz *et al.* study. The curves are the model simulations for the four subjects, run for each subject's actual age, weight, and measured dietary lead, with a stable lead isotope substituted for a portion of the dietary lead during the periods shown. Drinking water lead for these simulations was set at 50 μg/liter.

changes in older adults are not incorporated into the model presented here. They will be the subject of a subsequent publication.

Gastrointestinal absorption of lead by healthy adults ingesting mixed diets is 4–11%, with a mean probably around 8–9% (Rabinowitz *et al.*, 1980; Chamberlain *et al.*, 1978; Watson *et al.*, 1986). Dietary absorption of lead by children is greater. Alexander *et al.* (1974) estimated that about 50% of the lead was absorbed from normal diets in 11 healthy children 3 months–8.5 years old. Since endogenous fecal excretion was not considered in this balance study, the value of 50% is a minimum. Adjusting the published data on the basis that 70% of excreted lead is in the urine and 30% in the bile (Chamberlain *et al.*, 1978), the percentage absorbed becomes 66%. Ziegler *et al.* (1978) performed similar balance studies in 12 normal infants and young children 14–746 days old. Their estimate of percentage absorbed, 42%, becomes 47% when the raw data are adjusted

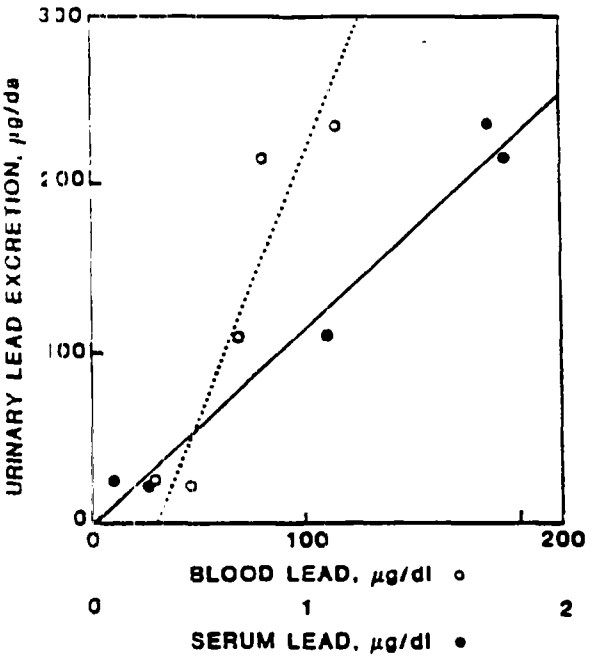

FIG. 12. Measured urinary lead excretion as a function of blood and serum lead concentration in a single adult male (Manton and Malloy, 1983). The lines are linear regressions through (—) the serum data and (- - -) the blood data and represent clearances from these media.

for endogenous excretion of lead. In the present model, fractional absorption of lead from the gastrointestinal tract is set at 0.50 at birth: it declines slowly up to about age 2 years, then more rapidly during childhood to approach the adult level of 0.08 by ages 8–10 years.

The rate of urinary excretion of lead is not directly proportional to blood lead concentration (Selander and Cramer, 1970; Manton and Malloy, 1983; Chamberlain, 1983). Review of representative studies suggests that urinary clearance of lead from the blood of adults may be as low as 0.06 liters of blood/day at low blood lead levels and approach a high of 0.25–0.30 liters of blood/day at high blood lead levels (Selander and Cramer, 1970; Griffin *et al.*, 1975; Rabinowitz *et al.*, 1976; Manton and Malloy, 1983; Chamberlain, 1983; Assennato *et al.*, 1986; Araki *et al.*, 1987; He *et al.*, 1988). While this behavior might suggest saturable reabsorption of lead from forming urine, consideration of the relationship between blood and plasma lead favors another interpretation. In Fig. 12, measured urinary lead excretion rates in a single adult male are plotted against blood and serum lead concentrations from the same subject (Manton and Malloy, 1983). The excretion/blood lead data suggest a threshold for urinary excretion of lead, but the excretion/serum lead data do not. The straight line of best fit through the excretion/serum lead data intersects the serum lead axis very near the origin. Its slope, the clearance of lead from serum in this individual, is 11.7 liters/day, independent of the concentration of lead in serum. Renal clearances of lead from plasma of 7–50 liters/day have been reported (Chamberlain *et al.*, 1978). Manton and Cook (1984) determined renal clearances of lead from serum in 13 adult human subjects, finding a range of 7.2–31.7 liters of serum/day with no dependence on serum lead concentration. It therefore appears that the apparent concentration dependence of urinary clearance of lead from blood is due in large part to the disproportionality in the plasma lead/blood lead relationship.

Urinary clearance of lead from plasma is only a fraction of the glomerular filtration rate, 180 liters of plasma/day, in the healthy adult human male, so that either plasma lead itself is not freely filterable at the glomerulus or a portion of the filtered lead is passively reabsorbed (Manton and Cook, 1984). Extensive reabsorption of filtered lead, without indication of capacity limitation, has been shown to occur in dogs (Vander *et al.*, 1977).

Clearances of lead from blood in children with blood lead concentrations up to about 20 μg/dl (Alexander *et al.*, 1974; Brockhaus *et al.*, 1988) are lower than clearances at low blood lead concentrations in adults. Clearances estimated from blood and urinary lead concentrations in these studies in children up to about age 9 are 0.045–0.06 liters of blood/day, slightly below the range of adult values for the same blood lead concentration range. Clearance of lead from blood of infants appears to be even lower. The lead intake and excretion data of Ziegler *et al.* (1978) and Ryu *et al.* (1978) for 3-month-old infants, when combined with the lead intake/blood lead relationship of Sherlock and Quinn (1986) for infants of the same age, suggest clearances of 0.015–0.04 liters of blood/day.

No information on age dependence of clearance of lead from plasma was found. Without such information, it is not possible to determine to what extent age dependence of partitioning of lead between plasma and red cells and age dependence of excretion mechanisms themselves contribute to the age dependence of clearance of lead from blood. In the model presented here, age dependence of clearance of lead from plasma is arbitrarily assigned entirely to excretion mechanisms. If, in infants and children as in adults, about 0.5% of the lead in blood at low blood lead concentrations is in the plasma, 0.015–0.04 liters of blood/day would be equivalent to 3–8 liters of plasma/day. The glomerular filtration rate in infants from birth to 3 months (5.5 kg) is about 3 to about 15 liters/day (Fig. 3). Therefore, clearance of lead from the plasma was modeled as 100% of the glomerular filtration rate at birth declining to 8% of the glomerular filtration rate in adulthood.

Values of from 1:1 to 3:1 have been reported for the ratio of urinary lead clearance to fecal lead clearance in adult humans (Chamberlain *et al.*, 1978; Campbell *et al.*, 1984). Ishihara and Matsushiro (1986) have reported that excre-

tion of lead in the bile is higher than its excretion in the urine and have suggested that enterohepatic reabsorption of lead is probably significant. In the present model, 70% of total lead clearance is assumed to be into the urine and 30% into the feces, for a ratio of 2.3:1.

The mathematical formulation of human bone metabolism is qualitatively identical to the formulation developed for the rat. It has been argued that because of the near absence of secondary remodeling of cortical bone, mature rat bone is not an acceptable surrogate for the study of metabolism of mature human bone (Frost, 1976). Remodeling of mature bone is different from the modeling of growing bone that takes place in all species. In remodeling, resorption and deposition of bone tend to be closely linked both spatially and temporally, and net bone formation rate is close to zero. In the cortical shafts of long bones, the remodeling process forms osteons, roughly cylindrical subunits of bone physically separated by cement lines which are not crossed by blood vessels. The osteons lie with their long axes approximately parallel to the long axis of the bone. Each osteon contains a haversian canal with its blood vessel; osteons are also known as haversian systems. Smaller canals and canalicules radiate from the haversian canal, carrying nutrients to osteocytes, bone cells embedded in the mineralized bone tissue.

Osteons are not formed to any significant extent in trabecular bone. Trabecular bone is structurally distinct from cortical bone, being in the form of plates and struts that are presumably sufficiently thin not to require osteons for support of osteocytes. It is found in the metaphyses and epiphyses of long bones and at the endosteal surface of the diaphyses of mature long bones, as well as in other bones such as vertebrae. Remodeling occurs at the surfaces of trabecular bone. Osteons also are not formed to any significant extent in cortical bone of small animals such as the rat. In small, short-lived animals, the need to relieve local bone stresses and to maintain a population of healthy osteocytes may be met entirely by surface remodeling processes, which do occur (Baron *et al.*, 1984).

From a kinetic point of view, this species difference in the magnitude of secondary remodeling processes is only quantitative. The potential for bone resorption and accretion of new bone is present in all species. The magnitude and age dependence of these processes are variable with species, and the critical species differences are reflected in the model in the values of the parameters in the expression for bone formation rate as a function of age. Thus, it is the quantitative balance among opposing processes, not the nature of the processes themselves, that determines the age dependence of bone metabolic activity in different species. In the same way, it is the balance among opposing processes of lead uptake into bone and lead removal from bone that determines the effect on body burden of exposure to lead at different ages and for different lengths of time.

Bone metabolic activity, as modeled, is determined by the bone formation rate expression in conjunction with the expression for total bone volume as a function of body weight. The bone formation rate expression is to be expected to reflect a combination of bone growth, bone modeling, and bone remodeling activity. Qualitatively, therefore, the dependence of bone formation rate on age should be essentially the same in all species. Quantitatively, it will be quite different in small animals and in humans. Much of the ultimate utility of this model will lie in the fidelity with which the mathematical description of bone formation rate reproduces actual whole-skeletal accretion rates. Consequently, it is not entirely satisfactory that this expression is based on very limited experimental information about whole-skeletal metabolism during infancy, childhood, and adolescence.

In addition to the observations on which the expression illustrated in Fig. 2 is based, there are estimates of bone accretion rate in human adults up to about age 60 years. These range roughly from 7%/year to 15%/year, with an average value of about 10%/year (Bauer *et al.*, 1957; Cohn *et al.*, 1965; Neer *et al.*, 1967). No dependence on age in this age range is suggested by the data. In the model, minimum fractional bone formation rate is set at 10%/year (Table 1).

In the model the assumption is made that bone removal by resorption during remodeling is a random process; that is, that it is as likely to occur in recently formed bone as in older bone. It would be reasonable to suggest that older osteons might be removed in preference to newer ones, but there is no evidence to support this premise. The assumed randomness of bone remodeling is not correct in at least one respect: circumferential lamellar bone lying just below the periosteal surface does not normally participate in secondary remodeling processes, but persists from final bone growth well into old age.

A critical determinant of lead kinetics, to which the predictions of the model are extremely sensitive, is the partitioning of lead between plasma and red cells. All nonlinearity in relationships between blood lead and exposure in the model is assigned to the capacity-limited binding of lead in erythrocytes. While the plasma lead/blood lead data sets on which the modeling of partitioning is based are reasonably complete for adults, no information on partitioning is available for infants or children. In addition, interindividual variability in this and other potential binding characteristics of lead could be an important source of the wide variability in blood lead levels characteristic of groups of subjects with comparable lead exposure. Lead is bound partly to the plasma membrane of the erythrocyte and partly to hemoglobin. An inducible low-molecular-weight erythrocyte lead-binding protein has been reported (Raghavan *et al.*, 1980;

Lolin and O'Gorman, 1988), and lead-binding proteins have been identified in kidney and brain of rats (Goering *et al.*, 1986).

Simulations

The many sources of lead exposure include air, diet, drinking water, and ingested dust and soil. The relative magnitudes of these sources shift with age and are dependent on occupation and lifestyle. In early infancy, the child's diet is essentially its sole source of lead (Ryu *et al.*, 1983). Mouthing behavior begins at about age 6 months and peaks at around 9–15 months, after which it declines gradually although it continues throughout early childhood. Mouthing results in exposure to lead in household dust and to leachable lead from the objects that are mouthed, exposures that are augmented in some children by pica, the eating of nonfood materials. The shift from a predominantly indoor lifestyle to outdoor play occurs at around ages 4–5 and is accompanied by exposure to lead in soil and ambient air. Diet is changing throughout this period and changes further once the child enters school. In addition, sources of lead exposure may be correlated with one another to some extent—for example, air and dust lead or water and food lead—so that exposures from media other than the one being sampled may not be constant over the sampling range. Clearly, it is difficult to construct an "average" lifetime exposure pattern, even for an individual without direct or indirect occupational exposure. Nonetheless, in the examples illustrated here, lifetime exposures have been simulated so that the experimental, environmental, or occupational exposure is superimposed on reasonable bone and blood lead levels for the age of the subject and date of the study. In the 1960s and early 1970s, when many studies of relationships between blood lead and lead exposure were carried out, "background" blood lead concentrations in adults were generally 15–25 μg/dl, reflecting the higher air and food lead concentrations then current. In this context, it should be noted that the low background blood lead levels, of 4.7 and 11.2 μg/dl, inferred from the empirical relationships between blood lead and drinking water lead in Moore *et al.* (1977) and Sherlock *et al.* (1982), as well as the marked curvilinearity of these relationships at low drinking water lead (Figs. 5 and 6), are artifacts of the choice of a cube root equation to describe the data. In reality, the scatter plots of data from these two studies are as well described by the model simulations shown in Figs. 5 and 6 as by the cube root equations used by the investigators.

In general, the model successfully predicts data relating average adult blood lead concentrations to lead exposure from a wide variety of sources, as illustrated in Figs. 5–11. It cannot be expected that model predictions will be accurate

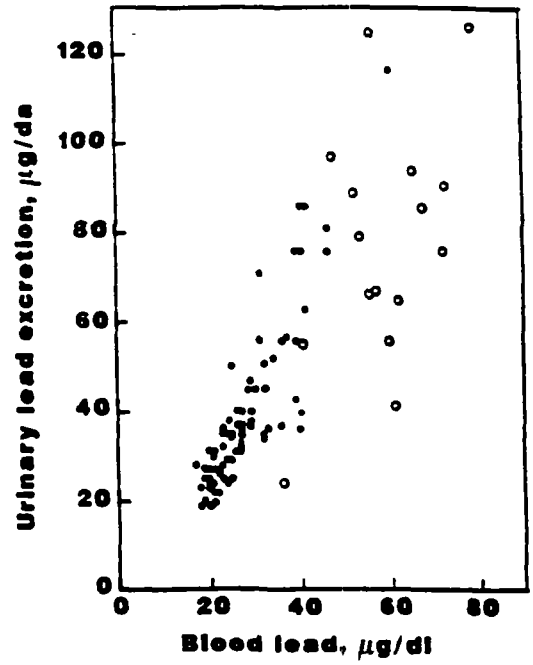

FIG. 13. Relationship of urinary lead excretion rate and blood lead concentration in the Kehoe subjects (Gross, 1979). Subject MR (O); all other subjects (●).

for individuals or for all exposure circumstances. Many of the parameter values—for example, fractional absorption from lung or gastrointestinal tract—are default values: probable values or probable values for typical conditions. It is for this reason that the experimental studies in individuals (Rabinowitz *et al.*, 1976) or small groups of subjects (Azar *et al.*, 1975; Cools *et al.*, 1976) tend to be fit less well than the epidemiologic studies (Williams *et al.*, 1969; Moore *et al.*, 1977; Sherlock *et al.*, 1982) for which the comparison is with average kinetic behavior in a large number of people.

One of the advantages offered by a physiologically based model is that parameter values can be adjusted to reflect the actual characteristics of an exposure, such as the particle size distribution of an aerosol, or the attributes of an individual, such as body size or dietary pattern. Alternatively, deviations from predicted values may help to pinpoint individuals with atypical physiologic characteristics. For example, three of the Kehoe subjects (DH, MR, and SW in Table 3) had high baseline blood lead concentrations compared to most of the other subjects, and the model underestimates both baseline and postexposure blood lead for these men. The discrepancies could be due to unrecognized sources of lead exposure, but in the case of MR they appear to have a physiological basis. Figure 13 demonstrates that the efficiency of renal lead excretion by this subject is distinctly lower than that of the other subjects. DH, whose blood lead levels were also consistently underpredicted, may have had

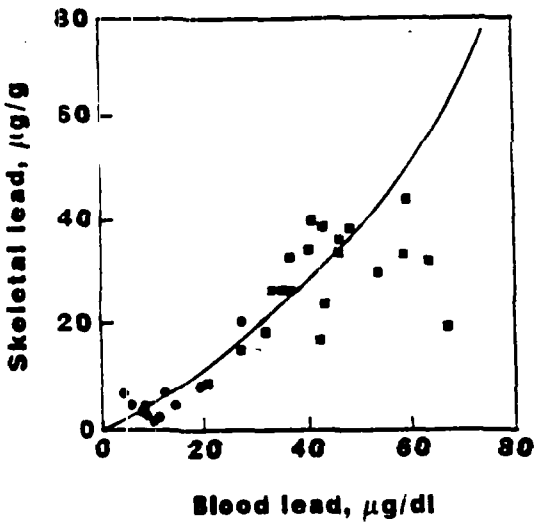

FIG. 14 The relationship of skeletal (iliac crest) lead to blood lead. Data points are redrawn from Van de Vyver *et al.* (1988) for control subjects (●) and lead workers (■). The line is the model simulation for a 50-year-old male with 30-year workplace exposure superimposed on ambient exposure.

additional exposure or may have absorbed lead more efficiently than other subjects: his excretion efficiency was unremarkable. For SW, however, it appears likely that unrecorded lead exposure early in the study resulted in an anomalous pattern of blood lead levels during the experiment. In this way, the characteristics of the discrepancies found may sometimes suggest an explanation for their occurrence.

Another advantage of a physiologically based model is that ranges of certain parameter values can be used to examine the impact of their variability on predicted blood or tissue lead. More than a sensitivity analysis, this approach allows the population distribution of blood or bone lead concentrations to be predicted.

The predictions of the model with respect to bone lead may be compared with observations of Van de Vyver *et al.* (1988), who measured total lead in ashed biopsy samples taken from the iliac crest of control and lead-exposed subjects with normal and impaired renal function. The results in 32 of the subjects are reproduced in Fig. 14. Renal functional status proved to be immaterial and is not indicated. The curve shown is made up of the endpoints of simulated 30-year exposures to various workplace air lead concentrations superimposed on a single set of ambient exposure conditions. Thirty-year exposures should produce as nearly a steady-state bone lead-to-blood lead relationship as is likely to be observed experimentally. Thus, the simulation is to be expected to lie along the upper edge of the range of experimental data points. Shorter simulated industrial exposure periods would generate points lying below the line shown.

The hypothetical worker whose blood lead behavior was simulated in Fig. 9 had been employed for 25 years in the same job. The "half-life" of bone lead in this man would have appeared to be of the order of decades. This observation would not be true for children, whose bone turns over essentially completely within a fairly short period of time, less than a year in young children growing rapidly (Fig. 2). The lability of bone in childhood implies that much of the lead incorporated during active growth will not persist into adulthood.

The model as presented simulates the integrated average behavior of bone lead. It does not take into account intraskeletal variations related to bone location or function, nor does it incorporate microregional variations in lead concentrations within individual bones, which can be quite marked (Schidlovsky *et al.*, 1990). However, because it includes slow heteroionic exchange movement of lead into bulk bone, away from potential exchange surfaces, the model does reflect what has been called the "last in, first out" phenomenon of lead transfers in bone. As a result of this kinetic diffusion mechanism and of the explicit age dependence of bone formation and resorption, the predictions of the model are responsive to the timing and duration as well as to the magnitude of lead exposure. The model has been shown to be capable of rationalizing blood lead observations from an extraordinary range of exposure patterns and magnitudes within a unifying framework grounded in understanding of bone physiology and calcium metabolism. It allows prediction not only of the effect of dietary or air lead on blood and bone lead during exposure, but also of the effect of bone lead on blood lead after cessation of exposure. Finally, because it is expressed in terms of bone physiology and metabolism, the model will be readily adaptable to states of potentially altered bone physiology such as pregnancy or aging.

REFERENCES

Alexander, F. W., Clayton, B. E., and Delves, H. T. (1974). Mineral and trace-metal balances in children receiving normal and synthetic diets. *Quart. J. Med.* **169**, 89–111.

Araki, S., Murata, K., and Aono, H. (1987). Central and peripheral nervous system dysfunction in workers exposed to lead, zinc and copper. *Int. Arch. Occup. Environ. Health* **59**, 177–187.

Arnold, J. S., Jee, W. S. S., and Johnson, K. (1956). Observations and quantitative radioautographic studies of calcium[45] deposited *in vivo* in forming Haversian systems and old bone of rabbit. *Am. J. Anat.* **99**, 291–313.

Assennato, G., Paci, C., Baser, M. E., Molinini, R., Candela, R. G., Altamura, B. M., and Giorgino, R. (1986). Sperm count suppression without endocrine dysfunction in lead-exposed men. *Arch. Environ. Health* **41**, 387–390.

Azar, A., Snee, R. D., and Habibi, K. (1975). An epidemiological approach to community air lead exposure using personal air samplers. In *Lead*

(T. B. Griffin, and J. H. Kneison, Eds.), pp. 254–290. Academic Press, London.

Baron, R., Tross, R., and Vignery, A. (1984). Evidence of sequential remodelling in rat trabecular bone: Morphology, dynamic histomorphometry, and changes during skeletal maturation. *Anat. Rec.* **208**, 137–145.

Bauer, G. C. H., Carlsson, A., and Lindquist, B. (1957). Bone salt metabolism in humans studied by means of radiocalcium. *Acta Med. Scand.* **158**, 143–151.

Brockhaus, A., Collet, W., Dolgner, R., Engelke, R., Ewers, U., Freier, I., Jermann, E., Kramer, U., Manojlovic, N., Turfeld, M., and Winneke, G. (1988). Exposure to lead and cadmium of children living in different areas of north-west Germany: Results of biological monitoring studies 1982–1986. *Int. Arch. Occup. Environ. Health* **60**, 211–222.

Bronner, F., Richelle, L. J., Saville, P. D., Nicholas, J. A., and Cobb, J. R. (1963). Quantitation of calcium metabolism in postmenopausal osteoporosis and in scoliosis. *J. Clin. Invest.* **42**, 898–908.

Campbell, B. C., Meredith, P. A., Moore, M. A., and Watson, W. S. (1984). Kinetics of lead following intravenous administration in man. *Toxicol. Lett.* **21**, 231–235.

Chamberlain, A. C., Heard, M. J., Little, P., Newton, D., Wells, A. C., and Wiffen, R. D. (1978). *Investigations into Lead from Motor Exhausts.* AERE Report R9198 HMSO, London.

Chamberlain, A. C. (1983). Effect of airborne lead on blood lead. *Atmos. Environ.* **17**, 677–692.

Cohn, S. H., Bozzio, S. R., Jesseph, J. E., Constantinides, C., Huene, D. R., and Giusmano, E. A. (1965). Formulation and testing of a compartmental model for calcium metabolism in man. *Radiat. Res.* **26**, 319–333.

Cools, A., Salle, H. J. A., Verberk, M. M., and Zielhuis, R. L. (1976). Biochemical response of male volunteers ingesting inorganic lead for 49 days. *Int. Arch. Occup. Environ. Health* **38**, 129–139.

DeSilva, P. E. (1981). Determination of lead in plasma and studies on its relationship to lead in erythrocytes. *Br. J. Ind. Med.* **38**, 209–217.

Frost, H. M. (1962). Specific surface and specific volume of normal human lamellar bone. *Henry Ford Hosp. Med. Bull.* **10**, 35–41.

Frost, H. M. (1976). Some concepts crucial to the effective study of bone turnover and bone balance in human skeletal disease and experimental models of skeletal physiology and pathophysiology. In *Bone Morphometry* (Z. F. G. Jaworski, Ed.), pp. 219–223. Ottawa Univ. Press, Ottawa.

Goering, P. L., Mistry, P., and Fowler, B. A. (1986). A low molecular weight lead-binding protein in brain attenuates lead inhibition of δ-aminolevulinic acid dehydratase: Comparison with a renal lead-binding protein. *J. Pharmacol. Exp. Ther.* **237**, 220–225.

Goldsmith, J. R., and Hexter, A. (1967). Respiratory exposure to lead. Epidemiological and experimental dose–response relationships. *Science* **158**, 132–134.

Griffin, T. B., Coulston, H. W., and Russell, J. C. (1975). Clinical studies on men continuously exposed to airborne particulate lead. In *Lead* (T. B. Griffin, and J. H. Kneison, Eds.), pp. 221–240. Academic Press, London.

Gross, S. B. (1979). *Oral and Inhalation Lead Exposures in Human Subjects (Kehoe Balance Experiments).* Lead Industries Association, New York.

He, F., Zhang, S., Li, G., Zhang, S., Huang, J., and Wu, Y. (1988). An electroneurographic assessment of subclinical lead neurotoxicity. *Int. Arch. Occup. Environ. Health* **61**, 141–146.

Ishihara, N., and Matsushiro, T. (1986). Biliary and urinary excretion of metals in humans. *Arch. Environ. Health* **41**, 324–330.

Johnson, T. R., Moore, W. M., and Jeffries, J. E. (Eds.) (1978). *Children Are Different: Developmental Physiology.* Ross Laboratories, Columbus, OH.

Lee, W. R., Marshall, J. H., and Sissons, H. A. (1965). Calcium accretion and bone formation in dogs: An experimental comparison between the results of Ca^{45} kinetic analysis and tetracycline labelling. *J. Bone Joint Surg.* **47B**, 157–180.

Lolin, Y., and O'Gorman, P. (1988). An intra-erythrocytic low molecular weight lead-binding protein in acute and chronic lead exposure and its possible protective role in lead toxicity. *Ann. Clin. Biochem.* **25**, 688–697.

Manton, W. I., and Malloy, C. R. (1983). Distribution of lead in body fluids after ingestion of soft solder. *Br. J. Ind. Med.* **40**, 51–57.

Manton, W. I., and Cook, J. D. (1984). High accuracy (stable isotope dilution) measurements of lead in serum and cerebrospinal fluid. *Br. J. Ind. Med.* **41**, 313–319.

Marcus, A. H. (1985). Multicompartment kinetic model for lead. III. Lead in blood plasma and erythrocytes. *Environ. Res.* **36**, 473–489.

Marshall, J. H., Rowland, R. E., and Jowsey, J. (1959). Microscopic metabolism of calcium in bone. V. The paradox of diffuse activity and long-term exchange. *Radiat. Res.* **10**, 258–270.

Moore, M. R., Meredith, P. A., Campbell, B. C., Goldberg, A., and Pocock, S. J. (1977). Contribution of lead in drinking water to blood-lead. *Lancet*, 661–662.

Neer, R., Berman, M., Fisher, L., and Rosenberg, L. E. (1967). Multicompartmental analysis of calcium kinetics in normal adult males. *J. Clin. Invest.* **46**, 1364–1379.

O'Flaherty, E. J. (1986). The rate of decline of blood lead in lead industry workers during medical removal: The effect of job tenure. *Fundam. Appl. Toxicol.* **6**, 372–380.

O'Flaherty, E. J. (1991). Physiologically based lead kinetics. *Trace Subst. Environ. Health* **24**, 44–54.

O'Flaherty, E. J. (1991a). Physiologically-based models for bone-seeking elements. I. Rat skeletal and bone growth. *Toxicol. Appl. Pharmacol.* **111**, 299–312.

O'Flaherty, E. J. (1991b). Physiologically-based models for bone-seeking elements. II. Kinetics of lead disposition in rats. *Toxicol. Appl. Pharmacol.* **111**, 313–331.

O'Flaherty, E. J. (1991c). Physiologically-based models for bone-seeking elements. III. Human skeletal and bone growth. *Toxicol. Appl. Pharmacol.* **111**, 332–341.

Rabinowitz, M. B., Wetherill, G. W., and Kopple, J. D. (1976). Kinetic analysis of lead metabolism in healthy humans. *J. Clin. Invest.* **58**, 260–270.

Rabinowitz, M. B., Wetherill, G. W., and Kopple, J. D. (1977). Magnitude of lead intake from respiration by normal man. *J. Lab. Clin. Med.* **90**, 238–248.

Rabinowitz, M. B., Kopple, J. D., and Wetherill, G. W. (1980). Effect of food intake and fasting on gastrointestinal lead absorption in humans. *Am. J. Clin. Nutr.* **33**, 1784–1788.

Raghavan, S. R. V., Culver, B. D., and Gonick, H. C. (1980). Erythrocyte lead-binding protein after occupational exposure. I. Relationship to lead toxicity. *Environ. Res.* **22**, 264–270.

Rowland, R. E. (1960). The deposition and the removal of radium in bone by a long-term exchange process. *Clin. Orthop.* **17**, 146–153.

Rowland, R. E. (1961). Microscopic metabolism of Ra^{226} in canine bone and its bearing on the radiation dosimetry of internally deposited alkaline earths. *Radiat. Res.* **15**, 126–137.

Ryu, J. E., Ziegler, E. E., and Fomon, S. J. (1978). Maternal lead exposure and blood lead concentration in infancy. *J. Pediatr.* **93**, 476–478.

Ryu, J. E., Ziegler, E. E., Nelson, S. E., and Fomon, S. J. (1983). Dietary

intake of lead and blood lead concentration in early infancy. *Am. J. Dis. Child.* 137 886–891.

Ilovsky, G., Jones, K. W., Burger, D. E., Milder, F. L., and Hu, H. (1990). Distribution of lead in human bone. II. Proton microprobe measurements. In *Proceedings of the International Symposium on In Vivo Body Composition Studies*, Toronto, Canada, June 1989. pp. 281–286. Plenum, New York.

Selander, S., and Cramer, K. (1970). Interrelationships between lead in blood, lead in urine, and ALA in urine during lead work. *Br. J. Ind. Med.* 27, 38–39.

Sherlock, J., Smart, G., Forbes, G. I., Moore, M. R., Patterson, W. J., Richards, W. N., and Wilson, T. S. (1982). Assessment of lead intakes and dose-response for a population in Ayr exposed to a plumbosolvent water supply. *Hum. Toxicol.* 1, 115–122.

Sherlock, J. C., and Quinn, M. J. (1986). Relationship between blood lead concentrations and dietary lead intake in infants: The Glasgow Duplicate Diet Study 1979–1980. *Food Addit. Contam.* 3, 167–176.

Snee, R. D. (1981). Models for the relationship between blood lead and air lead. *Int. Arch. Occup. Environ. Health* 50, 303–319.

Tepper, L. B., and Levin, L. S. (1975). A survey of air and population lead levels in selected American communities. In *Lead* (T. B. Griffin and J. H. Knelson, Eds.), pp. 152–196. Thieme, Stuttgart.

U.S. Department of Labor. Occupational Safety and Health Administration (1978). Occupational exposure to lead: Final standard. *Fed. Regist.* 43, 52952–53014.

Van de Vyver, F. L., D'Haese, P. C., Visser, W. J., Elseviers, M. M., Knippenberg, L. J., Lamberts, L. V., Wedeen, R. P., and DeBroe, M. E. (1988). Bone lead in dialysis patients. *Kidney Int.* 33, 601–607.

Vander, A. J., Taylor, D. L., Kalitis, K., Mouw, D. R., and Victery, W. (1977). Renal handling of lead in dogs: Clearance studies. *Am. J. Physiol.* 233, F532–F538.

Watson, W. S., Morrison, J., Baldwin, N. M., Lyon, D. T. B., Dobson, H., Moore, M. R., and Hume, R. (1986). Food iron and lead absorption in humans. *Am. J. Clin. Nutr.* 44, 248–256.

Williams, M. K., King, E., and Walford, J. (1969). An investigation of lead absorption in an electric accumulator factory with use of personal samplers. *Br. J. Ind. Med.* 26, 202–216.

Ziegler, E. E., Edwards, B. B., Jensen, R. L., Mahaffey, K. R., and Fomon, S. J. (1978). Absorption and retention of lead by infants. *Pediatr. Res.* 12, 29–34.

TOXICOLOGY AND APPLIED PHARMACOLOGY 131, 297–308 (1995)

Physiologically Based Models for Bone-Seeking Elements

V. Lead Absorption and Disposition in Childhood[1]

ELLEN J. O'FLAHERTY

Department of Environmental Health, University of Cincinnati College of Medicine, 3223 Eden Avenue, Cincinnati, Ohio 45208-0056

Received June 13, 1994; accepted December 5, 1994

Physiologically Based Models for Bone-Seeking Elements. V. Lead Absorption and Disposition in Childhood. O'FLAHERTY, E. J. (1995). *Toxicol. Appl. Pharmacol.* 131, 297–308.

A physiologically based model of lead absorption and disposition, previously developed and validated for adults, has been tested and calibrated for children. The model was modified to incorporate additional information on the age dependence of bone formation rate and to take into account increasing localization of bone modeling activity with age. A bone volume characterized by mature bone metabolic activity increases from zero at birth to the total bone volume by young adulthood. Bone formation rate is high from childhood through adolescence, with peaks at birth and around puberty. Bone resorption rate keeps pace at a rate that allows the orderly increase of bone mass. In general, the model reproduces childhood blood lead observations well, except in instances where lead is ingested at very high concentrations. Both bone and blood lead concentration are labile during early childhood because of the high rate of bone turnover. They respond rapidly to increases in lead exposure, and decrease almost as rapidly to near-preexposure concentrations when exposure returns to background levels. As the child grows, fractional bone formation and resorption rates decline and total bone lead turnover becomes more sluggish. From the time of peak bone mineralization rate in adolescence into early adulthood, the rate of bone turnover drops dramatically and the ability to reverse bone lead accumulation relatively rapidly is lost.
© 1995 Academic Press, Inc.

Children are generally acknowledged to be among the groups at greatest risk from environmental lead exposure. Many factors, including high susceptibility, elevated exposure, and special features of lead absorption, distribution, or excretion may contribute to the hazard of childhood lead exposure. Certain relevant differences between adults and children have been identified. For example, fractional absorption from the gastrointestinal tract is much greater in children than in adults (Alexander, 1974). In addition, markedly elevated lead exposure can occur in childhood, particularly as a result of ingestion of contaminated soils and dusts (Rabinowitz *et al.*, 1985) or of paint chips containing high concentrations of lead (Chisolm *et al.*, 1985).

An additional aspect of childhood lead exposure is that potentially large quantities of lead may be incorporated into rapidly forming bone. At the same time, growing bone is turning over rapidly, so that bone lead is continuously returned to the circulation. To the extent that lead incorporated into growing bone persists into adulthood, it may serve as a reservoir and source of reexposure in conditions such as pregnancy, lactation, and aging that may be associated with resorption of biologically significant amounts of bone (Nordberg *et al.*, 1991). Therefore, childhood lead exposure is of concern not only because of its immediate effects but also because of its potential delayed effects. We would like to be able to model lead kinetics in children in such a way as to predict the impact of different magnitudes and patterns of exposure both on blood lead concentrations in childhood and on the magnitude of bone lead stores persisting into adulthood.

The Integrated Exposure Uptake BioKinetic (IEUBK) model developed by the U.S. EPA (1994) is designed specifically to simulate blood and tissue lead concentrations in children up to age 7. Its accuracy as a predictor of blood lead concentrations has been verified within this age range at low environmental exposures (Choudhury *et al.*, 1992). However, its ability to simulate bone lead concentrations accurately has not been established. Furthermore, it is not linked with a model of adult lead metabolism to allow prediction of the impact of childhood lead exposure on adult lead kinetics.

The IEUBK model is a classical compartmental model of the kind routinely used for chemicals whose distribution volumes can be approximated as the sum of a limited number of well-mixed compartments. The values of the transfer rate constants are based in part on kinetic data from a study in baboons (Mallon, 1983). Certain nonlinearities, specifically capacity-limited binding in the red cell and capacity-

[1] This work was supported by a grant from the International Lead Zinc Research Organization.

0041-008X/95 $6.00
Copyright © 1995 by the Academic Press, Inc.
All rights of reproduction in any form reserved.

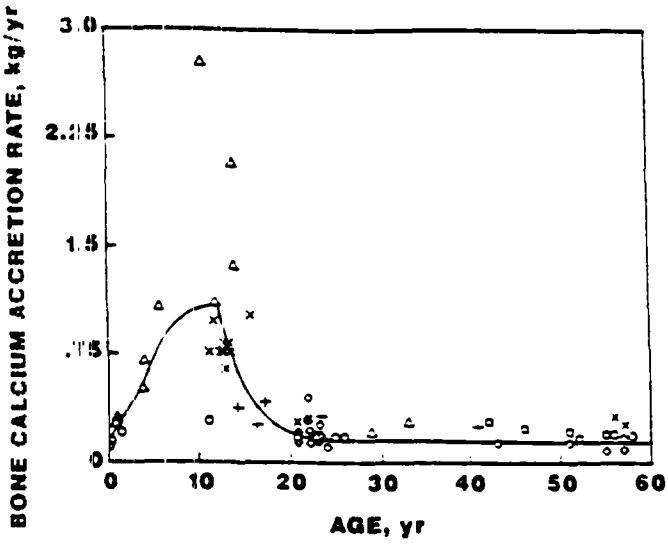

FIG. 1. Bone formation rate, as calcium accretion rate, as a function of age. ×, Bronner and Harris (1956); O, Bauer *et al.* (1957); □, Heaney and Whedon (1958); +, Bronner *et al.* (1963); ·, Neer *et al.* (1967); △, Abrams *et al.* (1992).

limited absorption from the gastrointestinal tract, are built into the model, but the parameter values are not physiologically based. Therefore, extrapolation of IEUBK model simulations outside the age and exposure ranges for which they have been calibrated is expected to be unreliable.

A physiologically based model of lead kinetics has been developed and validated for adults with a wide range of exposures from a variety of sources (O'Flaherty, 1993). While the model is designed for exposures from birth onward, it has not been rigorously tested against childhood lead data. The purpose of this paper is to examine published studies of lead exposure and blood lead in children and to determine how successfully the physiologically based model reconstructs the observed relationships.

METHODS

Model refinements

The physiologically based model of lead kinetics in humans has been previously described (O'Flaherty, 1993). The version used in these simulations has been modified in order to reflect with greater fidelity changes in bone metabolism during growth and to take into account sources of exposure, such as infant formula, that are unique to infancy and childhood.

The expression given previously for bone formation rate as a function of age has been reformulated to reflect newer and more complete published information about this process. Abrams *et al.* (1992) measured bone calcium accretion rate in healthy children and adolescents using a stable calcium isotope technique. Together with additional data from the earlier literature, the results of this study demonstrate that bone formation rate in adolescents is considerably greater than had been suggested by the limited data previously relied on in this age range (O'Flaherty, 1993). Figure 1 illustrates the revised age dependence of bone formation rate in the current version of the model. The height and shape of the curve in Fig. 1 were chosen to express a central tendency inferred from the range of observed calcium accretion rates.

The model has also been modified to acknowledge the increasing localization of active turnover that takes place during growth (see Discussion). Total bone is now divided into two fractions during childhood and adolescence. One fraction is engaged in very rapid turnover; the other has the characteristics of mature bone. The fractional volume of mature bone increases steadily from zero at birth to total bone volume by young adulthood. The fraction of total bone formation and resorption activity assigned to this bone type is related to its fractional volume. All remaining bone formation and resorption is assigned to actively modeling bone, whose volume decreases steadily from total bone at birth to zero by young adulthood. This new model structure takes into account the evolution of rapid bone turnover during growth, from involvement of the entire skeleton at birth, through increasing localization of new bone formation to regions such as the epiphyses of the long bones, to loss of intensive modeling activity by adulthood.

An important source of childhood lead exposure is the lead present in soils and dusts, particularly in and around older, deteriorated housing where lead-based paints had at one time been used. The U.S. EPA (1994) has estimated the average amounts of soil and dust ingested by children as step functions dependent on year of age from birth to age 7. Ingestion is estimated by the U.S. EPA to be 135 mg of total soil and dust/day from ages 1 to 4. In a recently completed study in which a tracer mass–balance method was used to estimate soil ingestion, the median soil ingestion rate was found to be 40 mg/day in a group of 64 children 1–3 years old (one child was 4 years old) (Calabrese, 1994). The upper 95% soil ingestion rate was 417 mg/day. Simple expressions for age-dependent soil and dust ingestion rates were devised (Fig. 2) and entered into the physiologically based model. These expressions differ from the U.S. EPA estimates in that neither dust ingestion nor soil ingestion is considered to be constant in early childhood. Dust ingestion is modeled to peak at age 2 while soil ingestion is modeled to peak at age 3. The later maximum for soil ingestion is indicated by the observation that the activity of *Toxocara canis*, a marker of exposure to the organisms present in outdoor soils, peaks at age 3 (Addiss *et al.*, 1991). It is consistent with a shift from indoor to outdoor play between ages 2 and 3. The modeled maximum total dust ingestion rate is 77 mg/day; the modeled maximum total soil ingestion rate is 60 mg/day. The shapes of the curves were designed to be consistent with the age dependence of blood lead concentrations in the Cincinnati Prospective Lead Study (see

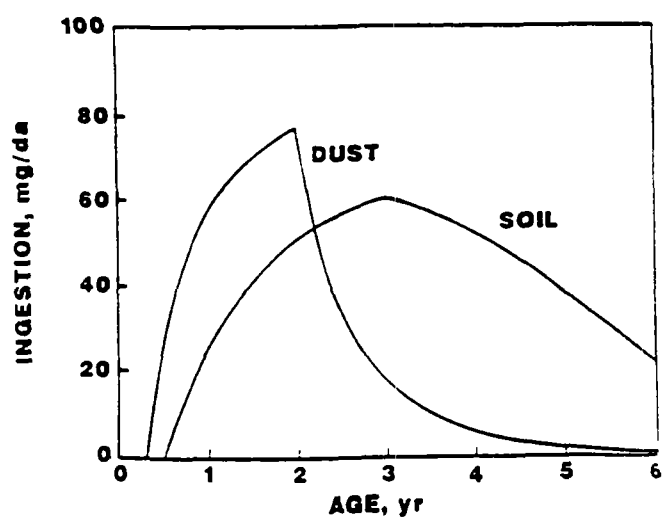

FIG. 2. Age dependence of soil and dust ingestion in childhood, as defined in the model.

below. They are plausible, if simplified, descriptions of a typical interaction of children with their environment. The dust and soil ingestion equations and their incorporation into the model are given in the Appendix.

Exposure of infants to lead in mothers' milk, infant formula, and baby foods is highly variable. These exposures are modeled as separate intakes during infancy (from birth to age 3½ months) and babyhood (from 3½ months to 1 year). The concentration in mother's milk or formula is multiplied by a formula consumption curve to obtain the rate of intake of lead from these sources up to age 3½ months. Ryu *et al.* (1983) reported the concentration of lead in infant formula as well as the actual intake of lead from formula by infants from age 8 days to 3½ months. These data were used to generate the expression for formula consumption by infants in this age range. The steady increase in calculated consumption of formula during this period is conveniently fit by a hyperbola, with lead intake on Day 5 of age being half the lead intake on Day 100 of age. Beginning at age 3½ months, this source of exposure is gradually phased out, terminating at age 1 year. Intake from mixed foods, including solid foods as well as milk and other liquids, is phased in beginning at age 3½ months. At age 1 year, a transition occurs in the model to the more general expression for lead ingestion in food and drinking water, in which consumption of both food and water is scaled to body weight to the 2/3 power. Typical values of the rate of ingestion of lead in solid and liquid foods at age 1 year would have been 30–40 μg/day around 1980, falling to 20–25 μg/day during the mid-1980s, when many of the studies simulated here were carried out, and falling further to current values around 5 μg/day or even less (Bolger *et al.*, 1991). The formula and food consumption equations are given in the Appendix.

Simulations

Infants. Ryu *et al.* (1983) studied 25 formula-fed infants from birth to age 111 days to determine the relationship between dietary lead and blood lead concentration. The babies were born in the United States (Iowa City, IA) between August 1975 and January 1976. The mean concentration of lead in formula was 20 μg/liter. These infants had low nonformula food lead exposure, determined by dietary analysis to be 1 μg/day. Seventeen of the babies were subsequently followed to age 195 days. Ten of these had a mean total lead intake rate during this second study period of 16 μg/day, and seven, who were drinking canned milk, had a mean total lead intake rate of 61 μg/day. The exposure scenario to age 111 days was modeled by setting the year of birth to 1975 and formula lead concentration to 0.020 mg/liter. Between ages 111 and 195 days, total lead intake was modeled by linearly phasing in intakes that reached 49 μg/day at age 1 year (16 μg/day at the midpoint age of 153 days) or 185 μg/day at age 1 year (61 μg/day at the midpoint age of 153 days). Both dust and soil lead were set at 100 μg/g for this simulation. Air lead concentration was set at 0.002 mg/m³.

The Glasgow Duplicate Diet Study was carried out in 1979–1980. Its primary purpose was to define the relationship of infants' blood lead concentrations to concentrations of lead in domestic water. Lacey *et al.* (1985) reported data for blood lead concentration and composite water lead in the 93 3-month-old bottle-fed and mixed-fed (that is, not exclusively breast-fed) babies in the study. The contribution of lead from the solid component of the infants' diet was shown to be negligible. These exposure scenarios were modeled by setting the year of birth to 1979 and calculating concentrations of lead in infant formula on the basis of one part concentrated formula to eight parts water, as suggested by the manufacturer's directions. Modeled water lead concentrations were from 0.04 to 0.5 mg/liter to span the observed range of domestic water lead. Air lead concentration was set at 0.002 mg/m³.

Children. The Cincinnati Prospective Lead Study (Bornschein *et al.*, 1985) is one of several similar recent prospective studies whose purpose has been to evaluate the dependence of infants' and children's blood lead levels on environmental sources of lead including air, food, water, dust, and soil, and the impact of age on these relationships. As part of this study, the 300 children in the cohort, all of whom lived in the inner city, were monitored at 3-month intervals until age 5 and thereafter at 6-month intervals in order to develop continuous blood lead concentration histories. Environmental evaluations were also carried out. These included quantitative analyses of lead in accessible painted surfaces, paint chips (when the paint was loose), interior dust and exterior soil, and street dirt. The physiologically based model was used to simulate the age dependence of blood lead concentration in children living in an urban setting in the United States in the late 1980s or early 1990s, with contemporary air lead set at 0.0003 mg/m³, water lead at 0.005 mg/liter, the concentration of lead in infant formula (or mother's milk) at 0.020 mg/liter, the oral intake of lead by children at age 1 year at 20 μg/day, the intake of lead with food by adults at 30 μg/day, and the year of birth at 1983, the first year of the study. The concentrations of lead in soil and dust required to achieve the best fits of the simulations to mean measured blood lead concentrations in four subsets of the study cohort were determined by visual optimization. The four subsets of the cohort were defined as follows: L, highest measured blood lead concentration less than 15 μg/dl (N = 70); M, highest measured blood lead concentration between 15 and 24 μg/dl (N = 120); X, highest measured blood lead concentration between 25 and 34 μg/dl (N = 60); and H, at least one measured blood lead concentration in excess of 34 μg/dl (N = 50). It should be noted that these data sets were also used to define the shapes of the dust and soil ingestion rate curves (see Methods). Simulated dust and soil lead concentrations are given in Table 1 and in the legend to Fig. 5.

The Boston Prospective Lead Study (Rabinowitz *et al.*, 1985) involved a cohort of 249 middle-class and upper-middle-class infants who did not live in the inner city. Blood lead concentrations were monitored at 1, 6, 18, and 24 months of age, and environmental sampling was carried out at the same times. Environmental assessments included quantitative analyses of house dust, drinking water, yard soil, interior paint, and respirable lead in interior air, as well as categorization of the residences as to their distance from automobile traffic and any recent occurrence of refinishing activity in the home. These suburban children had low nonpaint, nondust, and nonsoil lead exposures, as indicated by the low "control" group blood lead concentrations (see Results). Four groups were distinguished by the authors on the basis of their blood lead concentration ranges: <3.7, 3.7–6.0, 6.1–8.7, and >8.7 μg/dl. The corresponding exposures were simulated by setting air lead equal to the measured interior air lead (0.0001–0.0002 mg/m³) for each group, water lead equal to the measured water lead concentration (less than 0.005 mg/liter) for each group, soil lead concentration equal to the measured value for each group, dust lead concentration equal to 1/5 of the corresponding soil lead concentration, concentration of lead in infant formula equal to the water concentration, oral intake of lead by children at age 1 year to 3 μg/day, intake of lead with food by adults to 20 μg/day, and year of birth to 1980, the mean of the 2-year range of entry dates.

The Baltimore Lead Study (Chisholm *et al.*, 1985) presented a different experience. In this study, urban children with blood lead concentrations around 60 μg/dl, who were hospitalized when they were 2 to 3 years old for chelation treatment, were followed for a year after their return to "remediated" housing. Legal lead abatement consisted of removal, to a level 4 feet above the floor, of flaking or peeling lead-positive paint and lead-positive paint that presented a biting surface. The threshold for detection of lead in paint was 700 μg/cm² of surface area. Unsound exterior paint positive for lead was sometimes removed, but was not necessarily abated unless the child required a second round of chelation therapy. There was no requirement for cleanup of dust or debris resulting from paint removal or for repainting of the surfaces from which paint had been removed. Consequently, interior dust lead presumably remained little changed or may even have increased immediately following remediation. Housing was classified in this study according to its age and type and to the degree of lead abatement recorded. Painted interior surfaces positive for lead were identified, but other environmental measurements were not carried out. In or-

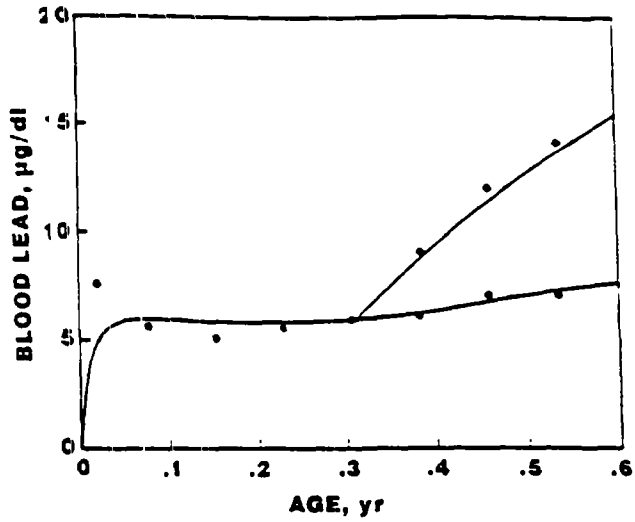

FIG. 3. Simulation for the experimental conditions of Ryu *et al.* (1983). Data points are means of measurements in from 7 to 25 infants from the Ryu *et al.* study: ●, infants receiving essentially all lead in formula to age 111 days and then dietary lead increasing to 49 µg/day at age 1 year; ♦, infants receiving dietary lead increasing after age 111 days to 185 µg/day at age 1 year. Curves are model simulations. Infant formula lead was set at 0.020 mg/liter, air lead at 0.002 mg/m^3, and dust and soil lead at 100 µg/g each. Year of birth was 1975.

der to approximate this loosely quantified exposure experience, lead concentrations in soil and dust were set to values chosen to simulate the child's prechelation exposure and blood lead concentration, and postchelation return either to old housing with continuing high lead hazard, to housing in which the lead hazard had been partially (legally) abated, or to housing in which lead exposure was substantially lower (the "lead-free public housing" category of the study). Simulated dust and soil lead concentrations are given in the legend to Fig. 6. Chelation was simulated as a 2-week period, the length of the child's hospital stay, during which the partition coefficients for soft tissues and bone surface were reduced to 30% of their usual values. Other environmental sources of lead were as follows: air lead, 0.003 mg/m^3; water lead, 0.005 mg/liter; oral intake of lead by children at age 1 year, 1 µg/day; and intake of lead with food by adults, 50 µg/day. Year of birth was set at 1977.

RESULTS

Infants. The predictions of the model are compared with blood lead data for infants from Ryu *et al.* (1983) in Fig. 3. Because the model prediction does not take into account exposure of the newborn during gestation, the simulation and measured blood lead concentration are not in agreement at the earliest time point after birth; but they rapidly become comparable. Predicted and observed blood lead concentrations are in excellent agreement throughout the 6 1-month period of the study.

Figure 4 is the model simulation for the Glasgow Infant Diet Study, superimposed on the scatter plot of individual blood lead concentration measurements for 92 bottle- and mixed-fed infants from the study (Lacey *et al.*, 1985). The empirical equation relating blood lead concentration to the cube root of the weekly rate of lead ingestion, judged by Sherlock and Quinn (1986) to be the line of best fit to these data, is also shown in Fig. 4, with lead ingestion expressed as the composite water (formula) lead concentration corresponding to the stated range of weekly lead intakes in 3-month-old infants. The model does not satisfactorily reproduce blood lead concentrations at these very high oral lead intakes.

Children. Optimized fits of the simulations to mean blood lead concentrations in groups of children representing the four blood lead ranges from the Cincinnati Prospective Lead Study (Bornschein *et al.*, 1985) are shown in Fig. 5. The optimal dust and soil lead concentrations are given in Table 1 along with selected measurements from the environmental evaluations carried out as part of the study. The soil and dust concentrations projected by the simulations are in good general agreement with spot measurements made in the actual environments of the children in the study. Again, the model does not take into account exposure during gestation. Nonetheless, the simulation suggests the relatively slight changes in blood lead concentrations during the first few months of life, followed by sharp increases that illustrate the importance of the environmental determinants of blood lead level in these children as they become more mobile.

Simulations for the exposure scenarios from the Boston Prospective Lead Study (Rabinowitz *et al.*, 1985) are given in Table 2, together with the measured blood lead concentration ranges. Background (air, food, and water) exposures required to reproduce these data are low, as illustrated by

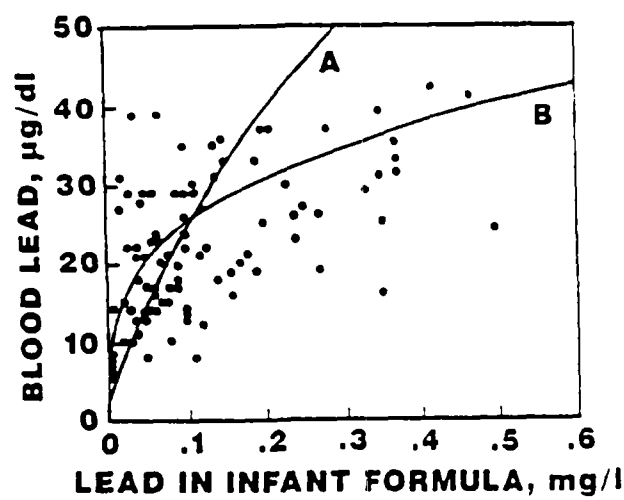

FIG. 4. Simulation for the experimental conditions of Lacey *et al.* (1985). Data points are individual measurements in 92 3-month-old infants. Curve A is the model simulation. Curve B is a plot of the cube root equation judged by Sherlock and Quinn (1986) to be the empirical line of best fit to these data. Infant formula was the only source of dietary lead for these simulations. Air lead was set at 0.002 mg/m^3, and year of birth was 1979.

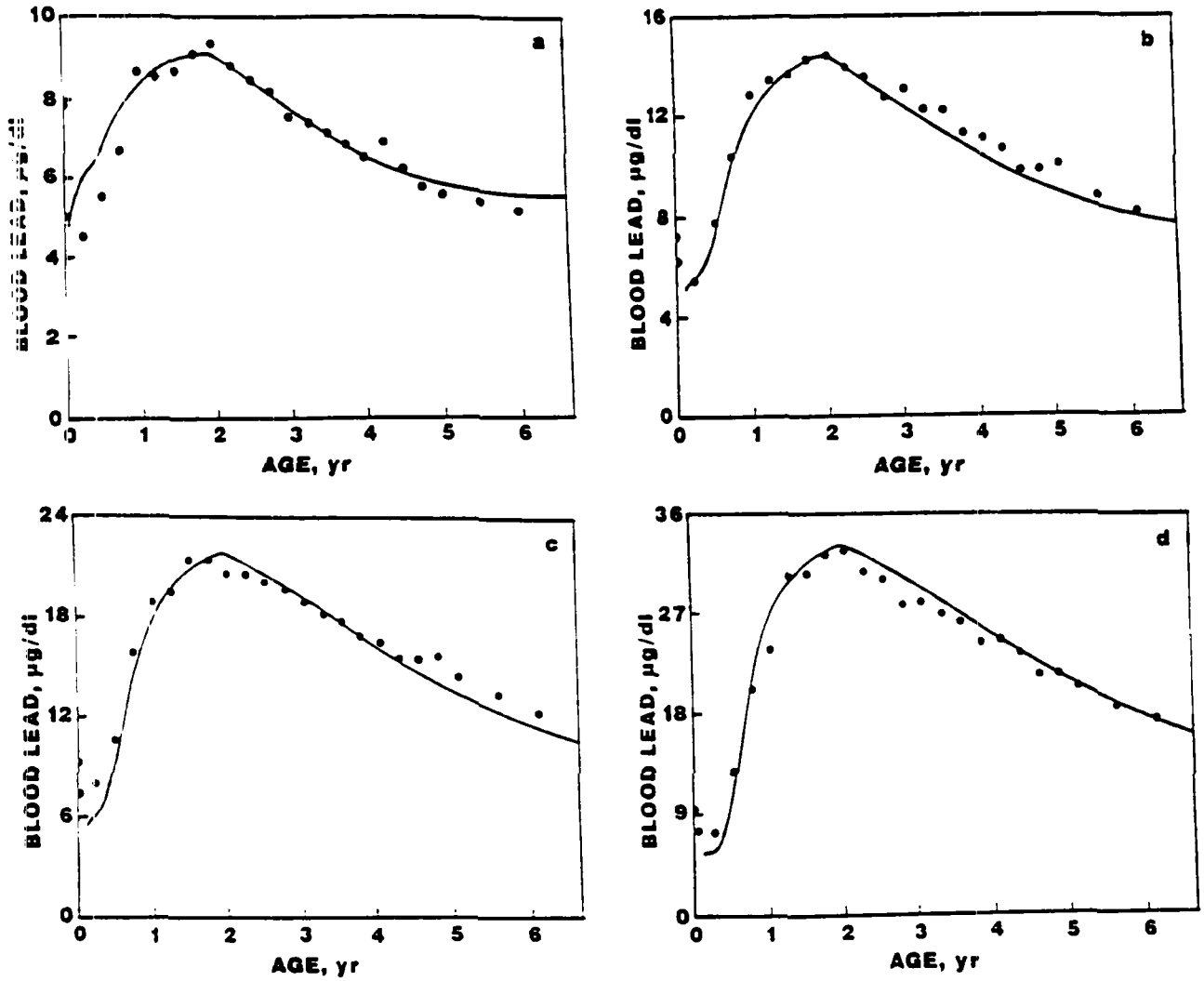

FIG. 5. Simulations for four subgroups from the Cincinnati Prospective Lead Study (Bornschein *et al.*, 1985). (a) Group L, children whose highest blood lead concentration did not exceed 15 μg/dl; (b) group M, children whose highest blood lead concentration did not exceed 24 μg/dl; (c) group X, children whose highest blood lead concentration did not exceed 34 μg/dl; (d) group H, children whose highest blood lead concentration exceeded 34 μg/dl. *Curves are model simulations, optimized to the data by setting CDUST = 200 μg/g and CSOIL = 500 μg/g* (a), CDUST = 400 μg/g and CSOIL = 1200 μg/g (b), CDUST = 600 μg/g and CSOIL = 2300 μg/g (c), and CDUST = 1200 μg/g and CSOIL = 4100 μg/g (d). Contemporary air lead was set at 0.0003 mg/m^3, water lead at 0.005 mg/liter, the concentration of lead in infant formula (or mother's milk) at 0.020 mg/liter, the oral intake of lead by children at age 1 year at 20 μg/day, the intake of lead with food by adults at 30 μg/day, and the year of birth at 1983, the first year of the study.

the predicted blood lead concentration in children of this age in the absence of any soil or dust exposure. The modeled slope of the relationship of blood lead concentration to soil lead concentration is similar to the slope observed.

Figure 6 illustrates the simulations for a group of exposure patterns designed to generate as closely as possible the blood lead concentration data from the Baltimore Lead Study (Chisholm *et al.*, 1985), along with the data themselves. These scenarios were designed as hypothetical exposures to dust and soil lead, for which no measurement data were available. Nonetheless, it is clear from the blood lead concentrations prior to chelation (some in excess of 60 μg/dl) that exposures were very high, and the dust and soil lead concentrations that generate these blood lead concentrations are in the expected range for very high inner-city environmental levels. The simulated blood lead concentrations in Fig. 6 tend to fall gradually during the 1-year follow-up, in contrast to the measured concentrations, which remained stable after reaching their postchelation levels.

DISCUSSION

Ingestion of lead by infants and young children. In modeling ingestion of lead in solid foods, formula, and milk during infancy and early childhood, the goal was to be as flexible as was reasonable to simulate magnitude of exposure

TABLE 1

Comparison of Dust and Soil Lead Concentrations Required to Fit the Cincinnati Prospective Lead Study Data with Measured Dust and Soil Concentrations

	Concentration in dust, μg/g	Concentration in soil, μg/g
Model groups		
L (Fig. 5a)	200	500
M (Fig. 5b)	400	1200
X (Fig. 5c)	600	2300
H (Fig. 5d)	1200	4100
Experimental housing groups[a]		
Post-World War II	332	327
Private, satisfactory condition	(151–733)	(118–905)
Public	490	233
	(242–996)	(87–622)
Subsidized rehab	622	1800
	(289–1340)	(611–5280)
19th century	1680	5000
Private, satisfactory condition	(586–4800)	(1430–17500)
19th century	2360	4550
Deteriorated/dilapidated	(957–5840)	(1180–17600)

[a] Measured soil concentrations are for surface scrapings; measured dust concentrations are for interior surface dust. Means and ranges are given. Data from Clark *et al.* (1991).

without requiring excessive exposure characterization. The decision was made to allow two inputs: the average concentration of lead in mother's milk or formula, which is coupled with a fixed expression for the age dependence of formula intake that phases out by age 1 year, and the average rate of ingestion of lead in all other dietary sources at age 1 year, which fixes the endpoint of a phase-in beginning at age 3½ months. After age 1 year, the expression for early childhood lead intake merges with the more general expression for lead ingestion throughout life.

The Ryu *et al.* (1983) data (Fig. 3) allow dietary lead intake in early infancy to be quantified as a function of the lead concentration in milk or formula. Later, increasing variety in the diet precludes stipulation of a single observed relationship of lead intake to age. The simplest plausible relationship describing growth within a species is used instead: dependence of daily food and water intake on the 2/3 power of body weight (McMahon and Bonner, 1983). Marked changes in the lead content of diet or drinking water are modeled as abrupt changes in exposure.

TABLE 2

Comparison of Simulated Blood Lead Concentrations with Observed Blood Lead Ranges from Rabinowitz *et al.* (1985)

Simulated blood lead concentration, μg/dl	Observed blood lead range, μg/dl
3.9	<3.7
5.1	3.7–6.0
8.0	6.1–8.7
9.1	>8.7

Note. See Methods for details of simulation.

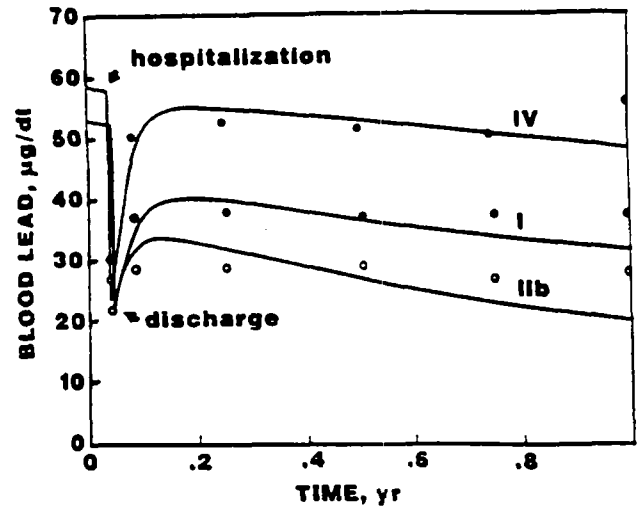

FIG. 6. Simulations for three subgroups from the Baltimore Lead Study (Chisholm *et al.*, 1985). Timing of hospitalization for chelation and of discharge are indicated. Time is expressed relative to timing of chelation. (I) Children discharged to old legally abated homes; (IIb) Children discharged to "lead-free" public housing; (IV) Children discharged to housing reported as abated but which presented previously unrecognized or newly developing lead hazards. Data points are geometric means of measurements in 93 (I), 15 (IIb), or 59 (IV) children. Curves are model simulations for CDUST = 5000 μg/g and CSOIL = 10,000 μg/g prior to chelation treatment and CDUST = 500 μg/g and CSOIL = 5000 μg/g (I), CDUST = 400 μg/g and CSOIL = 800 μg/g (IIb), and CDUST = 5000 μg/g and CSOIL = 10,000 μg/g (IV) after chelation treatment. These concentrations were selected on the basis of descriptions of the abatement procedures suggesting more pronounced reductions in interior than in exterior lead hazards. Other environmental sources of lead were as follows: air lead, 0.003 mg/m³; water lead, 0.005 mg/liter; oral intake of lead by children at age 1 year, 15 μg/day; intake of lead with food by adults, 50 μg/day; and year of birth, 1977.

Blood lead concentration data from the Glasgow Infant Diet Study (Lacey *et al.*, 1985) (Fig. 4) are not satisfactorily reproduced by the physiologically based model. The model, this version of which does not incorporate concentration-dependent absorption from the gastrointestinal tract, greatly overpredicts blood lead concentrations at the higher infant formula lead levels. Since formula lead concentrations were as high as 500 μg/liter, it is reasonable to surmise that dose-dependent fractional absorption was a major factor accounting for the discrepancy. Cutting fractional absorption to 1/3 of its low-exposure value brings predicted and observed blood lead concentrations into agreement at

the highest formula concentration modeled, 500 μg/liter. The very high levels of drinking water lead in the Glasgow study were found in low-pH water distributed through lead pipes and were unique to this region of western Scotland. The problem has since been corrected, and there should be little continuing need to model drinking water exposures of this magnitude. However, dose-dependent fractional absorption of lead from much smaller amounts in the gastrointestinal tract has recently been demonstrated in rats fed controlled amounts of lead either as soluble lead acetate or as pulverized mining waste soils (O'Flaherty *et al.*, 1994). That observation, together with the marked dose dependence of blood lead seen in the Glasgow study, suggests that modification of the physiologically based model to take into account dose-dependent gastrointestinal absorption in both rats and humans would be appropriate.

Fractional absorption of lead by children. The age dependence of fractional absorption of lead from the gastrointestinal tract is very poorly characterized. Alexander (1974) reported that fractional absorption from the gastrointestinal tract was as high as 53% in 8 healthy children up to 8 years old, consuming a free diet. Lead intake per unit body weight was highest in the single neonate in this series, and absorption and retention also tended to be higher in the younger children; but with the limited number of observations, experimental variability obscured any clear picture of age dependence of absorption. In the model, fractional absorption of lead from the gastrointestinal tract is set at 0.60 for the neonate, with a gradual decline to the adult level of 0.08 by age 10.

The magnitude of fractional uptake of inhaled lead in children is also not known, nor is it known to what extent it may depend on chemical form or particle size distribution (Knelson, 1974). An important factor determining inhalation exposure is respiration rate. Activity levels can vary greatly in children from time to time, and in general are higher per unit body weight than activity levels in adults. The simulations reported here assume 50% uptake of inhaled lead, the default value used for adults, and scale respiration rate from the rate in resting adults on the basis of the 2/3 power of body size alone. An appropriately higher respiration rate should be used in simulating lead kinetics in actively exercising children.

Excretion of lead by young children. Repeat lead balance studies in 12 infants ages 2 weeks to 2 years (Ziegler *et al.*, 1978) suggested that fecal endogenous lead excretion was about 2.8 times as great as urinary endogenous excretion. This value is not greatly different from the value 2.3 previously used for adults. In addition, the ratio of fecal to urinary excretion is highly variable from individual to individual (O'Flaherty, 1993). Consequently, the value of the ratio in adulthood was left unchanged in modeling the kinetics of lead in childhood.

Partitioning of lead between plasma and red cells in children. Much, although not all, lead binding in the red cell is to hemoglobins (Bruenger *et al.*, 1973; Ong and Lee, 1980a). Ong and Lee (1980b) observed a very strong binding of lead to fetal hemoglobin in samples of human cord blood. Experiments in which the α, β, and γ chains of fetal hemoglobin were separated and recombined *in vitro* demonstrated that the γ chain, unique to fetal hemoglobin, has a much greater affinity for lead than either the α or β chain of adult hemoglobin. Therefore, the idea that the relationship of red cell lead to plasma lead may be different in infants or young children and in adults is appealing.

No direct experimental evidence exists either to support or to refute this possibility. However, indirect evidence suggests that partitioning of lead between plasma and red cells may not in fact differ greatly between children and adults. Cavalleri *et al.* (1978) examined correlations between paired plasma and red cell lead concentrations in venous and cord blood in 75 women immediately after delivery. The best correlation in the data set was between the ratios of plasma lead to red cell lead in mothers and newborns (cord blood), indicating that at least some of the variation in measured plasma lead at specific total blood lead levels must be due to characteristic interindividual differences and that some of these differences are closely correlated between mother and child. It is not possible to determine precise relationships between maternal and fetal lead concentrations from the Cavalleri *et al.* (1978) data. Although the correlation lines of best fit between maternal and fetal measures suggest that fetal lead concentrations were higher than maternal lead concentrations at plasma lead concentrations below about 0.5 μg/dl, inspection of the scatter plots shows that lines of perfect correlation intersecting the origin would not be unreasonable fits to any of the three data sets (plasma lead, red cell lead, and ratio). Certainly the data do not suggest any marked systematic differences between the ratios of plasma and red cell lead in the newborns and in their mothers. Therefore, the expression that defines the plasma to red cell concentration ratio in the physiologically based adult lead kinetic model (O'Flaherty, 1993) was used in these simulations for infants and children as well.

Soil and dust ingestion. The expressions for soil and dust ingestion were designed to generate the age dependence of measured blood lead concentrations in the Cincinnati Prospective Lead Study. This age dependence is not readily generalizable. In the experience of some investigators, blood lead concentration does not peak at around age 2 years, but remains elevated through the next several years or even into adolescence (Kawai *et al.*, 1987; note also the persistently elevated blood lead concentrations in the Baltimore Lead Study (Fig. 6), compared with the predicted gradual blood lead decline). Many factors could contribute to continuation of high dust- and soil-related exposures into

later childhood. These include climatic factors (during what fraction of the year can the child play outdoors? how dry/dusty is the region?), social factors (how much of the time does the child play outdoors?), and exposure-related factors (are lead hazards limited to the area in and around the child's residence, or are they widely distributed throughout the neighborhood, including school playgrounds and interiors?) Other exposure sources may also be either age-dependent or dependent on the date (year). One implication of the rapidity with which blood lead responds to changes in current exposure in early childhood is that if blood lead concentration is to be modeled accurately as a function of age, then exposure must be known accurately as a function of age.

A data set that could not be satisfactorily reproduced by the physiologically based model is that of Yankel *et al.* (1977). These investigators measured blood lead concentrations in groups of children in the vicinity of a lead smelter. In a rural setting, with measured air lead concentrations around 0.0005 mg/m^3 and surface soil lead concentration only 300 μg/g, the "control" group in this study had mean blood lead concentrations of 25 μg/dl at age 2 and 17 μg/dl at age 9. It is necessary to invoke what would appear to be unreasonably high food and drinking water lead concentrations in order to generate such high blood lead concentrations in this exposure setting; note, for comparison, that the mean blood lead concentrations in the lowest exposure group in the Cincinnati Childhood Lead Study, whose environmental exposures were roughly comparable to these, did not exceed 10 μg/dl at any time. In addition, blood lead concentrations in the Yankel *et al.* study tended to remain elevated throughout early childhood before decreasing and then increasing again in adolescence. The reasons for the differences between the Yankel *et al.* data set and other longitudinal data sets are not immediately apparent.

Bone formation and resorption. Bone formation rate has historically been estimated by using calcium tracers, either stable or radioactive calcium isotopes or isotopes of elements that mimic the bone uptake behavior of calcium. Following a single intravenous dose of the tracer, the difference between the rate of loss of label from a soft-tissue pool that includes the blood and the rate of appearance of label in excreta is considered to be a measure of its one-way uptake into bone. This kinetic analysis has distinct limitations, since bone is not a well-mixed compartment as required by classical compartmental analysis, nor is it a sink for calcium tracers over even very short periods of time. Estimates of bone formation rate obtained by this technique are dependent on the length of time between tracer administration and final blood and excreta analyses. Nonetheless, of all the indicators of bone formation rate, this approximation of instantaneous uptake of calcium tracers by bone is both the most readily quantifiable and the most nearly representative of total bone formation activity. Therefore, it is the best available measure to use to model the impact of bone turnover on blood levels of those elements, such as lead, that mimic calcium kinetics.

Bone formation rate, estimated as the rate of calcium tracer uptake by bone (Fig. 1), increases during childhood, peaks, and then falls off sharply toward the relatively low level of formation associated with remodeling that persists throughout adulthood. The shape and temporal position of the peak are important determinants of the impact of the interaction between bone turnover rate and age at lead exposure on persistence of bone stores into adulthood. It is clear from the wide scatter of bone formation rates in subjects less than 20 years old that, at least at occasional time points or in particular individuals, bone formation rate can be very much greater than the average high rates associated with preadolescent growth. It is perhaps worth noting that the two exceptionally high points in Fig. 1 were for a boy and a girl both of whom weighed nearly twice as much as a standard adolescent of the same sex and age.

A number of other experimental measures or indices of bone formation and resorption have been identified. Among the more traditionally useful biochemical measures are plasma levels of the bone isoenzyme of alkaline phosphatase, for bone formation; and plasma acid phosphatase and urinary excretion of hydroxyproline, for bone resorption. Štěpán *et al.* (1985) examined these indices of bone formation and resorption in 2100 individuals greater than 1 year old. In general, the biochemical indices were found to be closely correlated with each other and with growth rate in children and adults. Elevated early levels persisted through adolescence, with low adult levels reached by the age of 25–30 years. Smaller peaks tended to occur shortly after birth, at age 6–7 years, and before the end of puberty, just prior to the rapid fall to adult levels.

A similar age dependence of plasma alkaline phosphatase activity was reported by Fleisher *et al.* (1977), with the additional observation that activity peaked at 11–12 years in girls and 13–14 years in boys. Yoneyama and Nagata (1980) linked urinary hydroxyproline excretion to the time of menarche in girls, showing that concentrations just before menarche, which marks the end of the growth spurt, were higher than concentrations just after. These patterns are consistent with the modeled net rate of deposition of bone calcium, which peaks at birth and at puberty (Fig. 7).

The link between bone mineralization and reproductive maturity implies that the age dependence of bone mineralization rate should be gender-specific. The age dependence of bone formation rate is not linked to gender in the current form of the model because the data are too sparse to allow differentiation of bone mineralization behavior on the basis of sex. For this reason, gender of the subjects is not indicated for the individual experimental observations in Fig.

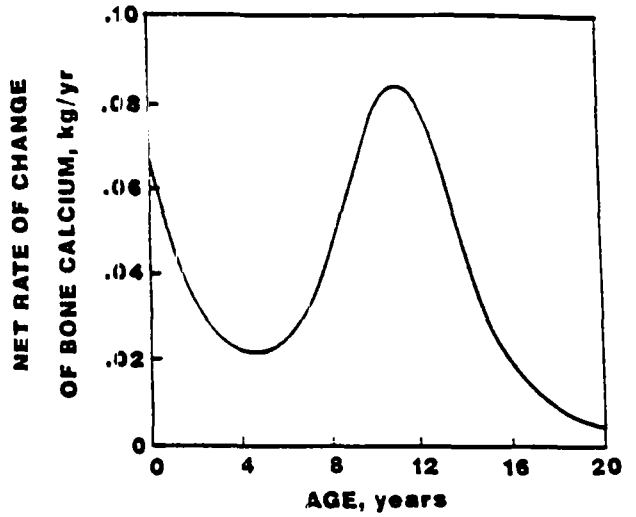

FIG. 7. Turnover rate of bone calcium as a function of age, as defined in the model.

1. More precise modeling will require a more complete data base.

It is reasonable to posit that the timing and magnitude of bone mineralization rate are also influenced by genetic and/or environmental factors. It is well established that bone mass varies with genetic makeup (Trotter *et al.*, 1960; Li *et al.*, 1989). In addition, Hui *et al.* (1985) demonstrated differences in bone mass and diameter of the radius among children and adults living in different areas of the United States (and coming from slightly different ethnic mixes). If such distinguishing differences were better characterized, they could be incorporated into the physiologically based model in order to simulate lead kinetic behavior for specific ethnic or geographically based population groups.

Turnover of bone calcium is as much as severalfold per year in infants and children through the adolescent growth spurt. This magnitude of turnover is entirely consistent with the requirement for intensive modeling to maintain the proper shape and configuration of growing bones as they increase in mass and shift in relative space. Not all bone participates consistently or equally in this modeling process, however. Some regions of bone turn over more rapidly than the average, while pockets of old (neonatal) bone persist throughout life. In addition, the rate of localized turnover does not necessarily decline with age. Instead, it appears most probable that it is the fraction of the skeleton undergoing active modeling that decreases with age in the growing child. Support for this concept is provided by the studies of Bryant and Loutit (1964) on the kinetics of strontium in children and adults. These investigators concluded, on the basis that the specific activity of bone strontium and dietary strontium (^{90}Sr/total Sr) remained in continuous equilibrium throughout the first several years of life even though dietary specific activity was changing at the time, that bone turnover was very rapid and was essentially complete during this period. In adolescents, strontium diet/bone specific activity equilibrium was not achieved. Accretion of new bone appeared to be the dominant process, with a comparatively low bone turnover (that is, a comparatively low resorption rate), as would be the case if localized high bone formation were taking place in a setting of largely low turnover or mature bone. The concept of increasing localization of active bone turnover during growth has been addressed by incorporating two bone tissue types into the childhood (growth) segment of the physiologically based model: a tissue engaged in active modeling, which accounts for total bone volume at birth but has disappeared by the time the skeleton has matured, and a tissue similar in its characteristics to mature bone, not present at birth but accounting for total bone volume at and after skeletal maturation. At present, the presence in the model of these two bone tissue types must be considered as offering more a framework for than a precise description of regionalization of active bone turnover, since their relative contributions to total bone turnover have necessarily been arbitrarily defined. One consequence of a continuous increase in the relative amount of mature bone during childhood is that the terminal rate of loss of lead from bone will be increasingly determined during growth by that bone fraction rather than by the actively modeling fraction.

Modeling blood lead concentrations in childhood. High bone turnover in early childhood implies that most of the lead acquired very early in life is not permanently fixed in the bone. It will be returned to the blood through bone resorption at some later time in childhood, when it will either be recycled to a region of forming bone, temporarily held in a soft tissue pool, or lost irreversibly by excretion. If exogenous lead sources are abruptly reduced or eliminated, the net rate of loss of lead from bone in childhood will be determined principally by the rate of bone resorption. Since fractional bone resorption rate is very high in infancy, it is to be expected that very early high bone lead burdens could be largely reversed by removing the young child to an environment where lead exposure is low. Table 3 gives model predictions for blood and bone lead concentrations at age 12 in a girl whose high childhood lead exposure was interrupted at various ages from 2 to 10 years. The simulations in Table 3 predict that were full abatement to be achieved, the accumulation of a large body burden of lead associated with early childhood lead exposure would be essentially fully reversible if intervention were sufficiently early, and reversible to a declining extent as the intervention occurred progressively later in childhood. Thus, while high bone formation rate in early childhood results in rapid uptake of circulating lead into mineralizing bone, bone lead is also lost rapidly in accordance with the high bone resorption rate. This is not true of adults, in whom bone turnover

mental exposure and the bioaccessibility/absorption interface between the environment and the individual must be characterized accurately if blood and bone lead are to be modeled accurately. The demands placed on a predictive model under these circumstances are very high. The current physiologically based model incorporates the principal anatomic and physiologic determinants of blood and bone lead concentration. Although the age dependences of some of these model features are poorly characterized at this time, the model provides a rational framework for interpreting the behavior of bone and blood lead in children and adults with widely varying current and past lead exposure. This is particularly important in early childhood, a period of great lability of both blood and bone lead during which current lead uptake is the key determinant of concentrations in both tissues.

APPENDIX

Ingestion of lead in dust and soil. The rates of ingestion of lead with dust and soil (RDUST, RSOIL, mg/day) are defined as the concentration of lead in the medium (CDUST, CSOIL, mg/g) multiplied by an age-dependent ingestion rate (MDUST, MSOIL, g/day). Thus,

RDUST, mg/day = (CDUST, mg/g)(MDUST, g/day) and

RSOIL, mg/day = (CSOIL, mg/g)(MSOIL, g/day).

MDUST and MSOIL are functions of age whose shapes were devised as described in the text (Methods). They are illustrated in Fig. 2.

Infant formula and food consumption. The concentration of lead in infant formula or mother's milk (CFMLA, mg/liter) is multiplied by the rate of ingestion of formula (DFMLAI, liters/year) by infants up to age 0.3 years (Ryu *et al.*, 1983) to obtain the rate of lead ingestion by infants in this age range (RFMLAI, mg/year):

RFMLAI, mg/year

= (CFMLA, mg/liter)(DFMLAI, liters/year).

This source of lead is phased out starting at age 0.3 years and terminating at age 1 year, by a linear decline in the rate of lead ingestion in formula (RFMLAB, mg/year):

RFMLAB, mg/year = RFMLAW, mg/year

− (RFMLAW, mg/year/0.7 years)((AGE − 0.3) year),

where RFMLAW is the rate of ingestion of lead in formula at age 0.3 years and AGE is given as fraction of a year.

Beginning at age 3½ months, ingestion of lead in foods and liquids other than formula (RSOLID, mg/year) is phased in as a linear increase to a value (RFOOD3, μg/day) for ingestion of lead in the diet by the 1-year-old child.

RSOLID, mg/year = ((AGE − 0.3) year)(365 days/year)

× (RFOOD3, μg/day)(0.001 mg/μg)/(0.7 years).

The rate of total lead ingestion in the diet by infants less than 1 year old (RFOODI, mg/year) is therefore

RFOODI, mg/year = RFMLAI, mg/year

+ RFMLAB, mg/year + RSOLID, mg/year.

The value of RFOODI at age 1 year becomes the starting point for the expression that links lead ingestion in food and drinking water throughout the remainder of the life span to the 2/3 power of body weight.

REFERENCES

Abrams, S. A., Esteban, N. V., Vieira, N. E., Sidbury, J. B., Specker, B. L., and Yergey, A. L. (1992). Developmental changes in children assessed using stable isotopes. *J. Bone Min. Res.* 7, 287–293.

Addiss, D. G., Schantz, P. M., Succop, P. A., Fried, J. A., Wilson, M., Roda, S., and Bornschein, R. L. (1991). *Incidence and Effect on Cognitive Function of Subclinical Toxocara Infection in Inner-City Children, Cincinnati.* Presented at the 1991 annual meeting of the American Society of Tropical Medicine and Hygiene.

Alexander, F. W. (1974). The uptake of lead by children in differing environments. *Environ. Health Perspect.* 7, 155–159.

Bauer, G. C. H., Carlsson, A., and Lindquist, B. (1957). Bone salt metabolism in humans studied by means of radiocalcium. *Acta Med. Scand.* 158, 143–151.

Bolger, P. M., Carrington, C. D., Capar, S. G., and Adams, M. D. (1991). Reductions in dietary lead exposure in the United States. In *Chemical Speciation and Bioavailability*, Vol. 3, pp. 31–36. Science and Technology Letters, Middlesex, UK.

Bornschein, R. B. (1994). Private communication. Data from the Cincinnati Lead Study, "Health Effects of Lead on Child Development," NIEHS-P01-ES01566.

Bornschein, R. L., Hammond, P. B., Dietrich, K. N., Succop, P., Krafft, K., Clark, S., Berger, O., Pearson, D., and Que Hee, S. (1985). The Cincinnati prospective study of low-level lead exposure and its effects on child development: Protocol and status report. *Environ. Res.* 38, 4–18.

Bronner, F., and Harris, R. S. (1956). Absorption and metabolism of calcium in human beings, studied with calcium-45. *Ann. NY Acad. Sci.* 64, 314–325.

Bronner, F., Richelle, L. J., Saville, P. D., Nicholas, J. A., and Cobb, J. R. (1963). Quantitation of calcium metabolism in postmenopausal osteoporosis and in scoliosis. *J. Clin. Invest.* 42, 898–908.

Bruenger, F. W., Stevens, W., and Stover, B. J. (1973). The association of ^{210}Pb with constituents of erythrocytes. *Health Phys.* 25, 37–42.

Bryant, F. J., and Loutit, J. F. (1964). The entry of strontium-90 into human bone. *Proc. R. Soc. London Ser. B* 159, 449–465.

Calabrese, E. J. (1994). Personal communication.

Cavalleri, A., Minoia, C., Pozzoli, L., Polatti, F., and Bolis, P. F. (1978). Lead in red blood cells and in plasma of pregnant women and their offspring. *Environ. Res.* 17, 403–408.

Chisholm, J. J., Jr., Mellits, E. D., and Quaskey, S. A. (1985). The relationship between the level of lead absorption in children and the age, type, and condition of housing. *Environ. Res.* 38, 31–45.

Choudhury, H., Peirano, W. B., Marcus, A., Elias, R., Griffin, S., and DeRosa, C. T. (1992). Utilization of uptake biokinetic (UBK) model to assess risk in contaminated sites. In *Superfund Risk Assessment in Soil Contamination Studies*, pp. 193–204. ASTM, Philadelphia, PA.

Christoffersson, J.-O., Schütz, S., Skerfving, S., Ahlgren, L., and Mattson, S. (198'). A model describing the kinetics of lead in occupationally exposed workers. In *In Vivo Body Composition Studies* (K. J. Ellis, S. Yasumura, and W. D. Morgan, Eds.), Chap. 5, pp. 335–347. Institute of Physical Sciences in Medicine, London.

Clark, S., Bornschein, R., Succop, P., Roda, S., and Peace, B. (1991). Urban lead exposures of children in Cincinnati, Ohio. *Chem. Speciation Bioavail.* 3, 163–171.

Drasch, C. A., and Ott, J. (1988). Lead in human bones: Investigations on an occupationally non-exposed population in southern Bavaria (F.R.G.). II. Children. *Sci. Total Environ.* 68, 61–69.

Fleisher, G. A., Eickelberg, E. S., and Elveback, L. R. (1977). Alkaline phosphatase activity in the plasma of children and adolescents. *Clin. Chem.* 23, 469–472.

Heaney, R. P., and Whedon, G. D. (1958). Radiocalcium studies of bone formation rate in human metabolic bone disease. *J. Clin. Endocrinol. Metab.* 18, 1246–1267.

Hui, S. L., Johnston, C. C., Jr., and Mazess, R. B. (1985). Bone mass in normal children and young adults. *Growth* 49, 34–43.

Kawai, M., Okamoto, Y., and Katagiri, Y. (1987). Variation of blood-lead levels with age in childhood. *Int. Arch. Occup. Environ. Health* 59, 91–94.

Knelson, J. H. (1974). Problem of estimating respiratory lead dose in children. *Environ. Health Perspect.* 7, 53–57.

Kosnett, M. J., Becker, C. E., Osterloh, J. D., Kelly, T. J., and Pasta, D. J. (1994). Factors influencing bone lead concentration in a suburban community assessed by noninvasive K X-ray fluorescence. *J. Am. Med. Assoc.* 271, 197–240.

Lacey, R. F., Moore, M. R., and Richards, W. N. (1985). Lead in water, infant diet and blood: the Glasgow Duplicate Diet Study. *Sci. Total Environ.* 41, 235–257.

Li, J.-Y., Specker, B. L., Ho, M., and Tsang, R. C. (1989). Bone mineral content in black and white children 1 to 6 years of age. *Am. J. Dis. Child.* 143, 1346–1349.

Mallon, R. P. (1983). *A Metabolic Model of Lead Kinetics Based upon Measured Organ Burdens during Chronic Exposure Experiments with Infant and Juvenile Baboons.* Ph.D. dissertation, New York University, University Microfilms International, Ann Arbor, MI.

Marcus, A. H. (1985). Multicompartment kinetic models for lead. II. Linear kinetics and variable absorption in humans without excessive lead exposure. *Environ. Res.* 26, 459–472.

McMahon, T. A., and Bonner, J. T. (1983). *On Size and Life*, pp. 51–57. Scientific American Books, New York.

Neer, R., Berman, M., Fisher, L., and Rosenberg, L. E. (1967). Multicompartmental analysis of calcium kinetics in normal adult males. *J. Clin. Invest.* 46, 1364–1379.

Nordberg, G. F., Mahaffey, K. R., and Fowler, B. A. (1991). Introduction and Summary. International workshop on lead in bone: Implications for dosimetry and toxicology. *Environ. Health Perspect.* 91, 3–7.

O'Flaherty, E. J. (1993). Physiologically based models for bone-seeking elements. IV. Kinetics of lead disposition in humans. *Toxicol. Appl. Pharmacol.* 118, 16–29.

O'Flaherty, E. J., Freeman, G. B., Johnson, J. D., Liao, S. C., and Bergstrom, P. D. (1994). Evaluating lead bioavailability data by means of a physiologically based lead kinetic model. Submitted for publication.

Ong, C. N., and Lee, W. R. (1980a). Distribution of lead-203 in human peripheral blood *in vitro*. *Br. J. Ind. Med.* 37, 78–84.

Ong, C. N., and Lee, W. R. (1980b). High affinity of lead for fetal hemoglobin. *Br. J. Ind. Med.* 37, 70–77.

Rabinowitz, M., Leviton, A., Needleman, H., Bellinger, D., and Waternaux, C. (1985). Environmental correlates of infant blood lead levels in Boston. *Environ. Res.* 38, 96–107.

Ryu, J. E., Ziegler, E. E., Nelson, S. E., and Fomon, S. J. (1983). Dietary intake of lead and blood lead concentration in early infancy. *Am. J. Dis. Child.* 137, 886–891.

Samuels, E. R., Meranger, J. C., Tracy, B. L., and Subramanian, K. S. (1989). Lead concentrations in human bones from the Canadian population. *Sci. Total Environ.* 89, 261–269.

Sherlock, J. C., and Quinn, M. J. (1986). Relationship between blood lead concentrations and dietary lead intake in infants: The Glasgow Duplicate Diet Study 1979–1980. *Food Add. Contam.* 3, 167–176.

Štěpán, J. J., Tesařová, A., Havránek, T., Jodl, J., Formánková, J., and Pacovský, V. (1985). *Clin. Chim. Acta* 151, 273–283.

Trotter, M., Broman, G. E., and Peterson, R. R. (1960). Densities of bones of white and Negro skeletons. *J. Bone Joint Surg. A* 42, 50–58.

U.S.EPA (1994). *Guidance Manual for the Integrated Exposure Uptake Model for Lead in Children.* National Technical Information Service (PB 93-963510).

Yankel, A. J., von Lindern, I. H., and Walter, S. D. (1977). The Silver Valley Lead Study: The relationship between childhood blood lead levels and environmental exposure. *J. Air Pollut. Control Assoc.* 27, 763–767.

Yoneyama, K., and Nagata, H. (1980). Urinary hydroxyproline and body dimensions of adolescent girls before and after menarche. *Hum. Biol.* 52, 107–114.

Ziegler, E. H., Edwards, B. B., Jensen, R. L., Mahaffey, K. R., and Fomon, S. J. (1978). Absorption and retention of lead by infants. *Pediatr. Res.* 12, 29–34.